

**The Urban Heat Island of Melbourne during
Heatwaves: Impacts of Future Urban Expansion
and Effectiveness of Green Infrastructure as
Mitigation Strategies**

Md Imran Hosen

B.Sc. Engg. (Civil), M.Sc. Engg. (Water)



A Thesis Submitted in Fulfillment of the Requirements for the
Degree of

Doctor of Philosophy

College of Engineering and Science, Victoria University, Australia
August 2018

Abstract

The city of Melbourne in southeast Australia experiences an Urban Heat Island (UHI) effect, which is exacerbated during heatwaves, and the latter are becoming more frequent, intense and longer in southeast Australia. In addition, Melbourne is the fastest growing city in Australia. Therefore, it is urgent to understand the dynamics of UHI and impacts of future urban expansion on the UHI during heatwaves. Based on these issues, there is a crucial need to investigate the effectiveness of potential mitigation strategies to minimize UHI effects during heatwaves. The overarching aim of the thesis is to investigate the impacts of future urban expansion on the UHI during heatwave events in Melbourne, and examine the effectiveness of different Green Infrastructure (GI) scenarios such as green/cool roofs, mixed forest (MF), mixed forest and grassland (MFAG), and mixed shrublands and grasslands (MSAG) in mitigating UHI effects.

The Weather Research and Forecasting (WRF) model coupled with the Single Layer Urban canopy Model (SLUCM) was used in simulating the UHI and heatwaves. Since the WRF model is known to be sensitive to the choice of physical parameterisation options, an initial sensitivity analysis of the model was conducted and the best-possible WRF configuration to simulate the UHI during heatwaves in Melbourne was determined, among a 27-member physics ensemble. This configuration was used throughout the rest of the thesis.

Urban expansion increased near surface UHI by 0.75 to 2.80 °C during the night but no substantial impacts during the day. Urban surfaces absorbed more solar heat during the day as compared to vegetated surfaces, and the absorbed heat was released slowly from evening to early morning. The storage heat in urban surfaces was the key driver in

increasing UHI during the night. Urban expansion did not substantially affect human health (HTC) comfort in existing and expanded urban areas.

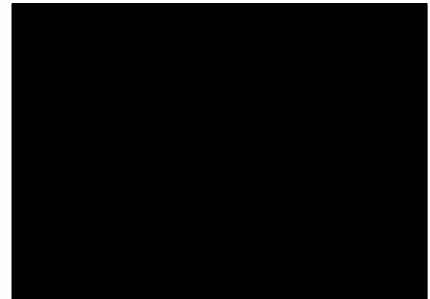
Green roofs showed good performance in reducing roof surface UHI (1 to 3.8 °C) and near surface UHI (0.3 to 1.1 °C) during the day but not during the night, while cool roofs showed higher reductions at the roof surface UHI (2.2 to 5.2 °C) and near surface UHI (0.5 to 1.6 °C) during the day. Green roofs increased evapotranspiration and provided shading, and consequently, increased Latent Heat (LH) and substantially decreased storage heat and sensible heat, and as a result, reduced the UHI. Cool roofs reflected a major portion of incoming solar radiation due to higher albedo, and reduced the sensible heat flux and storage heat, and these were the key drivers in reducing UHI during the day. In addition, both green and cool roofs showed good potential in improving HTC from extreme to very strong during the day.

Other GI scenarios such as MF, MFAG and MSAG were effective in reducing UHI effects and improving HTC during the night but no substantial reductions were occurred during the day. By increasing GI fractions from 20 to 50 %, the UHI was reduced by 0.6 to 3.4 °C for MF, 0.4 to 3.0 °C for MSAG and 0.6 to 3.7 °C for MFAG. The night time cooling was driven by reductions in storage heat as 20 to 50 % urban areas were replaced by GI, which would have led to even less radiation reaching the ground surface during the day due to their higher LAI and shade factor, and leading to lower storage heat.

As the green and cool roofs showed potential in reducing UHI effects during the day while urban vegetated patches showed effectiveness during the night, therefore, a combination of green/cool roofs and urban vegetated patches could be an optimal mitigation strategy in reducing UHI effects and improving HTC during both day and night.

Declaration

I, Md Imran Hosen, declare that the thesis by Publication entitled “The UHI of Melbourne during Heatwaves: Impacts of Future Urban Expansion and Effectiveness of Green Infrastructure as Mitigation Strategies” is not more than 100,000 words in length including quotes and excluding tables, figures, footnotes, bibliography and references. This thesis is my own research, except otherwise stated. The contents of the thesis have not been submitted, in whole or as a part, for any academic degree at any university or institution.



Dedication

The thesis and all the great works behind it are dedicated

To

My loving parents

Acknowledgements

I would like to express my sincere gratitude to my supervisors, Dr. Anne Ng, Dr. Jatin Kala and Dr. Shobha Muthukumaran for their heartiest support, constructive guidance and encouragement throughout my PhD study at Victoria University. Their review comments and feedbacks on my research and writing journal papers were very crucial for publishing journal articles and the successful completion of my PhD degree. They always made time for regular meeting and provided me proper guidance, when I asked for their help. I am grateful to them for keeping their faith on my ability and accepting me as one of their research students.

I owe my gratitude and sincere appreciation to my associate supervisor, Dr. Jatin Kala for his much constructive comments, discussions, ideas, encouragement and friendly attitude in supervision. I have been especially fortunate to work with such an erudite supervisor. His astute comments and suggestions in reviewing my journal and conference articles were greatly helpful to me. I believe this thesis would not have been made to its current form without his prudent supervision, proper direction, feedback and inspiration.

I am thankful to the Government of Australia and Victoria University for offering the full financial support through the International Postgraduate Research Scholarship (IPRS) scheme to conduct my PhD research at Victoria University. I also gratefully acknowledge the financial support provided by the Secomb Conference and Travel Fund and the College of Engineering and Science Conference Funding Scheme at Victoria University for attending two conferences within Australia. I am highly thankful to Stephanie Jacobs

and Carlo Jamandre for providing urban categories data for the city of Melbourne. Furthermore, data support by the Bureau of Meteorology (BoM) Australia, ECMWF (ERA-interim) data server (<http://apps.ecmwf.int/datasets/data/interim-full-daily/levtype=ml/>) and University of Wyoming (atmospheric sounding data) data server (<http://weather.uwyo.edu/upperair/sounding.html>), the creation of the ANUclim data funded by the Terrestrial Ecosystem Research Network (TERN) Ecosystem Modelling and Scaling Infrastructure (eMAST) Facility under the National Collaborative Research Infrastructure Strategy (NCRIS) 2013–2014 budget initiative of the Australian Government Department of Industry, the Australian Government Department of Environment in support of the National Carbon Accounting System, and the Australian National University are gratefully acknowledged.

I want to thank the respected faculty members of Water Resources Research Group, the officers and staff members of Graduate Research Center, Scholarship Unit and IT unit at Victoria University, who helped me out directly or indirectly throughout my PhD study. I would also like to thank my fellow PhD colleagues, friends, senior and younger brothers for their continuing support and encouragement.

Finally, I would like to express my heartiest love and gratitude to my family members for their kind love, endless mental support, generous prayers and sacrifice during my long journey, which was really an inspiration and a source motivation.

List of Publications

Journal Articles

1. **Imran, H.M.**, Kala, J., Ng, A. W. M., Muthukumaran, S. (2018). An evaluation of the performance of a WRF multi-physics ensemble for heatwave events over the city of Melbourne in southeast Australia. *Climate Dynamics*, 50 (7-8), 2553-2586. <https://doi.org/10.1007/s00382-017-3758-y>
2. **Imran, H.M.**, Kala, J., Ng, A. W. M., Muthukumaran, S. (2018). Effectiveness of Green and Cool Roofs in Mitigating Urban Heat Island Effects during a heatwave event in the city of Melbourne in southeast Australia. *Journal of Cleaner Production*. <https://doi.org/10.1016/j.jclepro.2018.06.179>
3. **Imran, H.M.**, Kala, J., Ng, A. W. M., Muthukumaran, S. (2018). Impacts of future urban expansion on urban heat island effects during heatwave events in the city of Melbourne in southeast Australia. *Quarterly Journal of the Royal Meteorological Society* (Submitted Revised Version after Addressing Reviewers' Comments).
4. **Imran, H.M.**, Kala, J., Ng, A. W. M., Muthukumaran, S. (2018). Effectiveness of vegetated patches as green infrastructure in mitigating urban heat island effects during a heatwave event in the city of Melbourne. *Weather and Climate Extremes* (Submitted Revised Version after Addressing Reviewers' Comments).

Conferences

1. **Imran, H.M.**, Kala, J., Ng, A. W. M., Muthukumaran, S. (2018). Mitigation of Urban Heat Island in the city of Melbourne: Green and Cool Roofs Strategies. AMOS-ICSHMO 2018 Conference, 5 – 9 February 2018. University of New South Wales, Kensington Campus, Sydney, Australia.
2. **Imran, H.M.**, Kala, J., Ng, A. W. M., Muthukumaran, S. (2017). Evaluating Three Planetary Boundary Layer Schemes in the WRF model for Urban Heat Island Assessment in Melbourne. AMOS/MSNZ Conference and ANZ Climate Forum, 7 - 10 February 2017. Australian National University, Canberra.

PART A:
DETAILS OF INCLUDED PAPERS: THESIS BY PUBLICATION

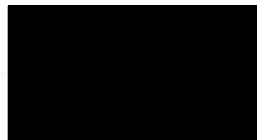
Please list details of each Paper included in the thesis submission. Copies of published Papers and submitted and/or final draft Paper manuscripts should also be included in the thesis submission

Item/ Chapter No.	Paper Title	Publication Status (e.g. published, accepted for publication, to be revised and resubmitted, currently under review, unsubmitted but proposed to be submitted)	Publication Title and Details (e.g. date published, impact factor etc.)
04	An evaluation of the performance of a WRF multi-physics ensemble for heatwave events over the city of Melbourne in southeast Australia	Published	Climate Dynamics (Year 2017) ISI and SCImago Journal Rank: Q1 Impact Factor: 3.77
05	Effectiveness of green and cool roofs in mitigating urban heat island effects during a heatwave event in the city of Melbourne in southeast Australia	Published	Journal of Cleaner Production (Year 2018) ISI and SCImago Journal Rank: Q1 Impact Factor: 5.65
06	Impacts of future urban expansion on urban heat island effects during heatwave events in the city of Melbourne in southeast Australia.	Currently Under Review	Quarterly Journal of Royal Meteorological Society (2018) ISI and SCImago Journal Rank: Q1 Impact Factor: 2.98
07	Effectiveness of vegetated patches as green infrastructure in mitigating urban heat island effects during heatwave in the city of Melbourne	Currently Under Review	Weather and Climate Extremes (2018) SCImago Journal Rank: Q1 Impact Factor: 2.42

Declaration by [candidate name]:

Md Imran Hosen

Signature:



Date: 05-05-2019

Table of Contents

Abstract	ii
Declaration	iv
Dedication	v
Acknowledgement	vi
List of Publications	viii
Details of Included Papers: Thesis by Publication	x
Table of Contents	xi
List of Tables	xiv
List of Figures	xv
Abbreviations	xvi

Chapter 1: Brief Introduction and Aims of Thesis

1.1 Research Background	1
1.2 Research Objectives	6
1.3 Scope of the Thesis	7
1.4 Research Significance and Innovation	8
1.5 Thesis Structure	10

Chapter 2: Literature Review

2.1 Introduction	11
2.2 The Urban Heat Island	11
2.3 Surface Energy Balance	14
2.4 Heatwaves and the UHI	17
2.5 Heatwaves and Human Health	22

2.6	Impact of Urbanization on the UHI	24
2.7	Mitigation Approaches of UHI Effects	26
2.7.1	Green Roofs	27
2.7.2	Cool Roofs	29
2.7.3	Urban Vegetation	31
2.8	Observational and Numerical Modelling Approaches in Studying the UHI....	33
2.9	Conclusions	37

Chapter 3: Methodology

3.1	Introduction	39
3.2	The WRF Model	39
3.2.1	Overall Description of the WRF Model	39
3.2.2	Domain Configuration	45
3.2.3	Input Reanalysis Data	46
3.2.4	Static Data of the WRF Model	48
3.3	Observational Data	48

Chapter 4: Sensitivity of the WRF Model to Physical Parameterization Options in Simulating the UHI and Heatwaves

4.1	Introduction	50
4.2	Declaration of Co-authorship and Co-contribution	51
4.3	An Evaluation of the Performance of a WRF Multi-Physics Ensemble for Heatwave Events over the City of Melbourne in Southeast Australia	53

Chapter 5: Green and Cool Roofs Mitigation Strategies in Reducing UHI Effects during Heatwave Event

5.1 Introduction	87
5.2 Declaration of Co-authorship and Co-contribution	88
5.3 Effectiveness of Green and Cool Roofs in Mitigating Urban Heat Island Effects during a Heatwave Event in the City of Melbourne in Southeast Australia	90

Chapter 6: Impacts of Future Urbanization on the UHI and Urban Meteorology during Heatwave Event

6.1 Introduction	103
6.2 Declaration of Co-authorship and Co-contribution	104
6.3 Impacts of Future Urban Expansion on Urban Heat Island Effects during Heatwave Events in the City of Melbourne in Southeast Australia	106

Chapter 7: Green Infrastructure Practices in Mitigating UHI Effects during Heatwave Event

7.1 Introduction	142
7.2 Declaration of Co-authorship and Co-contribution	143
7.3 Effectiveness of Green Infrastructure in Mitigating Urban Heat Island Effects during a Heatwave Event in the City of Melbourne in Southeast Australia	145

Chapter 8: General Discussion and Conclusions

8.1 General Discussion	181
8.2 Conclusions	186
8.3 Recommendations for Future Research	186

References	188
------------------	-----

List of Tables

Table 2.1	Number of hot days above 35 °C based on annual average summer temperature for long-term (1961 – 1990), short-term (2000-2009) and projected years of 2030 and 2070 for Australian capital cities	22
Table 2.2	Comparison of number of deaths caused by various natural hazards in Australia	23

List of Figures

Figure 2.1	Typical representation of the influence of urban surface on the boundary layer at regional scale. PBL and UBL represent planetary boundary layer and urban boundary layer, respectively	17
Figure 2.2	An example of typical persistent high that causes heatwave conditions over southeast Australia	18
Figure 2.3	Correlation between urban-rural temperature differences and population density for Melbourne	20
Figure 2.4	Trend of minimum temperatures during summer for Melbourne from 1910 to 2013 (BoM, Australia)	21
Figure 3.1	Interactions of various physical parameterizations of the WRF model	43
Figure 3.2	Schematic of the SLUCM	44
Figure 3.3	Location of modelling domains	46

Abbreviations

UHI	Urban Heat Island
UHI ₂	Near-surface Urban Heat Island
UHI _{sk}	Skin-surface Urban Heat Island
GI	Green Infrastructure
MF	Mixed Forest
MFAG	Mixed Forest and Grasslands
MSAG	Mixed Shrublands and Grasslands
WRF	Weather Research and Forecasting
SLUCM	Single Layer Urban canopy Model
HTC	Human Thermal Comfort
LH	Latent Heat
SH	Sensible Heat
G	Ground Storage Heat
RAMS	Regional Atmospheric Modelling System
GCM	Global Climate Model
BOM	Bureau of Meteorology
USEPA	United States Environmental Protection Agency
RCM	Regional Climate Models
NDVI	Normalized Difference Vegetation Index
LSM	Land Surface Model
NCEP	National Centre for Environmental Prediction
FNL	Final Operational Global Data Assimilation System

PBL	Planetary Boundary Layer
PBLH	Planetary Boundary Layer Height
SW	Shortwave
LW	Longwave
UTC	Coordinated Universal Time
LT	Local Time
MB	Mean Bias
MAE	Mean Absolute Error
RMSE	Root Mean Square Error
UTCI	Universal Thermal Climate Index
TKE	Turbulent Kinetic Energy
MSLP	Mean Sea Level Pressure
LAI	Leaf Area Index

Chapter 1

Brief Introduction and Aims of Thesis

1.1 Research Background

Urban growth can have a significant influence on the urban environment, climate and ecosystem across cities worldwide. Naturally vegetated surfaces are replaced by constructed artificial impervious surfaces, which alter the surface energy balance and hence impacts the urban environment and regional meteorology and climate (Liu et al., 2018; Morris et al., 2017; Yang et al., 2016). One of the consequences of urbanization is that urban areas experience higher temperatures as compared to surrounding rural areas, a phenomenon commonly referred to as the Urban Heat Island (UHI). This phenomenon was first observed in the early 19th century by Howard (1833), who recorded temperature differences between the city of London and surrounding rural areas, and recorded higher temperatures in the city. The concept of the UHI was expanded by Manley (1958) to describe this typical feature of urban climate, as the increase in temperature caused by artificial surfaces (man-made) resulting in a warm island, relative to the lower temperatures of the surrounding natural landscape.

The UHI occurs due to the radiative properties of impervious/urban surfaces, which leads to intensified heat accumulation and a higher temperature difference between urban and surrounding rural areas. The UHI can be easily distinguished by analyzing surface and air temperatures between urban and rural areas. The characteristics of UHI strongly depends

on the diurnal variations of incoming shortwave radiation. The urban surfaces store more heat during the day because of the higher thermal conductivity of construction materials and re-radiate this heat during the night. Urban areas are also characterized by lower wind speed because airflow is obstructed by urban morphological features (e.g., buildings) that reduce mixing and cooling effects. Low wind speed exacerbates UHI intensity while low clouds play more an effective role in limiting the effects of UHI as compared to high clouds during night (Oke, 1982). On the other hand, the rural surfaces cool rapidly during the night, and hence, the temperatures difference between urban and rural are highest during the evening and night.

The UHI effect is exacerbated during heatwaves and the combined effects of UHI and heatwaves are more intense than their individual effect (Li et al., 2015). Heatwaves can be broadly defined as very unusual and hot temperature conditions for a few consecutive days and the meteorological definition is commonly based on percentiles, being a period of at least three consecutive days, during which the daily maximum and minimum temperature exceeds the climatological 95th percentile for a particular region and day of year (Nairn and Fawcett, 2011). Recent studies have shown that the intensity and frequency of heatwaves are increasing globally (IPCC, 2012), and hence it is critical to better understand the interactions between UHI and heatwaves.

The UHI in combination with heatwaves can lead to a number of hazardous consequences, such as heat-related diseases and mortality (Zhou and Shepherd, 2010). Heatwaves are considered as the most severe natural hazard in southeast Australia especially during its hot summer, during which temperatures can peak above 40°C (e.g., 45.1 °C on 30 January 2009, 43.9 °C on 16 & 17 January 2014) (Victorian Auditor

General's Report, 2014). Urban residents are highly vulnerable during the heatwaves in Australia, with heatwaves leading to the highest mortality rates as compared to other natural hazards (Nicholls et al., 2008). For example, in the state of Victoria in southeast Australia, heatwaves triggered 374 and 167 excess deaths during January 2009 and 2014, respectively (Victorian Auditor General's Report, 2014).

The UHI and heatwaves have gained increasing attention by the general community, researchers, and policy makers worldwide. Australian cities are highly urbanized with 80% of the total population living in major cities (Australian Bureau of Statistics, 2011). The increased rate of urbanization is responsible for loss of vegetation and can negatively affect urban ecosystems. Pervious surfaces are replaced by higher thermal conductivity materials (e.g., concrete, bricks and bitumen). These artificial impervious surfaces absorb and store more heat during the day and emit that stored heat during the night, and this phenomenon is favourable to induce the UHI (Arnfield, 2003). The city of Melbourne has recently released its future urban expansion strategy titled "Plan Melbourne 2050" (more details can be found at: <http://www.planmelbourne.vic.gov.au/the-plan>). According to this plan, urban areas will substantially expand over the next 22 years. Therefore, there is an urgent need to better understand how future urban expansion may affect the UHI for the city of Melbourne. In addition, energy use is generally higher during summer (e.g. use of air conditioning, coolers, electric fans etc). Therefore, UHI and heatwaves as well as increased urban development are considered as prominent issues in southeast Australia (Victorian Department of Human Services, 2009), and there is an urgent need to investigate possible mitigation strategies in minimizing the adverse effects.

Several UHI mitigation strategies aiming at reducing UHI effects have been proposed in literature such as modification of urban geometry (Fahmy and Sharples, 2009; Pearlmutter et al., 1999) increasing emissivity and surface albedo (Golden and Kaloush, 2006; Sailor, 1995), increasing urban vegetation and surface shading (Sailor and Dietsch, 2007; Synnefa et al., 2008; Yaghoobian et al., 2010). A review of literature relevant to UHI mitigation strategies (Chapter 2) revealed that increasing the albedo (e.g., cool roofs, white paint) of urban environments and increased urban vegetation could be promising mitigation measures. Furthermore, several UHI mitigation studies have been conducted using Green Infrastructure (GI) scenarios in several cities (e.g. Stuttgart, Bremen, Dresden, Nurnberg and Berlin) of Germany (Baumueller and Baumueller, 2011), city of Adelaide in Australia (Razzaghmanesh and Razzaghmanesh, 2017) and the United Kingdom (Liverpool City Council's, 2012). These studies all showed that GI (e.g. urban trees, parks and green walls) scenarios substantially reduced the UHI, with green walls showing high effectiveness in reducing urban temperatures between 2 and 15 °C during the day (Razzaghmanesha and Razzaghmanesha, 2017).

GI can be defined as a network of natural and planted vegetation including street trees, urban forest, gardens, parks, wetlands, green walls, green and cool roofs (Foster et al., 2011). The increase in GI fractions in cities can be a sustainable mitigation strategy in reducing both air and surface temperatures (Bowler et al., 2010; Susca, 2012). Generally, urban temperature increases due to absorption of a higher amount of solar radiation by urban infrastructures during the day. Therefore, higher reflective materials (e.g., cool roofs) can minimize these effects by reflecting a higher proportion of incoming solar radiation, while GI scenarios reduce the effects of solar radiation by reflecting heat, providing shading and increasing evapotranspiration, and modifying patterns of wind

flow. Therefore, increasing the use of higher reflective materials (higher albedo) and implementing more GI scenarios in cities can be a potential and sustainable mitigating strategies in reducing UHI effects.

Several studies have been carried out in recent years to investigate the near-surface UHI using numerical climate models at various spatial scales (e.g., global/regional). Regional climate models such as the numerical Regional Atmospheric Modelling System (RAMS) (Walko et al., 2000) and National Center for Atmospheric Research model (MM5) (Grell et al., 1994) have been used to investigate the role of land use on the UHI (Georgescu et al., 2009; Grossman-Clarke et al., 2008). However, a limitation of these regional atmospheric models is that they were not able to explicitly resolve the combined effects of heat from natural (e.g. vegetation cover) versus artificial (e.g. road and building) sources, to characterize the UHI (Ooka, 2007). In the process of model development, this issue has been resolved in more advanced regional atmospheric models, such as the Weather Research and Forecasting (WRF) model (Skamarock et al. 2008), which has been coupled to the Single Layer Urban Canopy Model (SLUCM) (Kusaka et al., 2001; Chen et al., 2011), which is specifically designed for parameterizing the key physical processes within urban areas. The WRF-SLUCM model offers an ideal modelling platform for regional urban meteorology studies, and the model has been used extensively to investigate the UHI for several cities (Liu et al., 2018; Morris et al., 2017; Sharma et al., 2016; Yang et al., 2016).

1.2 Research Objectives

This thesis examines the potential of GI strategies (e.g., green/cool roofs, mixed forest (MF), mixed forest with grasslands (MFAG) and mixed shrublands and grasslands (MSAG) in mitigating UHI effects, as well as the impacts of future urban expansion for the city of Melbourne in southeast Australia, by using the coupled WRF-SLUCM model. The WRF model includes a number of physical parameterization options and the model is well documented to be sensitive to those physics options and these can vary based on the geographic and climatic conditions (Evans et al., 2012; Kala et al., 2015). Therefore, before using the coupled WRF-SLUCM model, it is essential to carry out sensitivity analysis of the model in simulating various climate variables related to the UHI. Hence, as the first part of this thesis, the sensitivity of the WRF-SLUCM model to its various parameterizations are carried out in simulating heatwaves using a multi-physics ensemble, by comparing the model outputs with observations. Having obtained an ideal model configuration, the WRF-SLUCM model is then used to investigate the effectiveness of different GI scenarios in mitigating UHI effects, as well as the impacts of planned future urban expansion on the UHI, for the city of Melbourne. Particular focus is given to understanding the physical processes and atmospheric mechanisms and drivers.

The specific objectives of this thesis are summarized as follows:

- I. Evaluation of the performance of the WRF model to simulate heatwave events over the city of Melbourne (Chapter 4).
- II. Evaluation of the effectiveness of green and cool roofs in mitigating UHI effects during heatwave event in the city of Melbourne (Chapter 5).
- III. Evaluation of the impacts of future urbanization on UHI effects during heatwave events in the city of Melbourne (Chapter 6).

- IV. Evaluation of the effectiveness of MF, MFAG and MSAG in mitigating UHI effects during heatwave event in the city of Melbourne (Chapter 7).

1.3 Scope of the Thesis

This thesis uses a case study approach by focusing on four of the most severe heatwave events to have affected the southeast of Australia over the past decades, to achieve the four aims described in the previous section. The thesis makes use of a single modelling tool, the WRF-SCLUM model. This methodology (discussed in more detail in Chapter 3), has inherent limitations, which limits the scope of the thesis as follows:

- While the sensitivity of WRF to different physical parameterizations is tested in Chapter 3, the thesis only uses a single urban canopy parameterization, i.e., the SLUCM, throughout the thesis. Other urban canopy parameterization schemes have been coupled to the WRF model, like for example, bulk and multi-layer UCM, but this thesis does not assess the sensitivity of WRF to different urban canopy schemes, as this is beyond the scope. The choice of using the SLUCM was based on the fact that it is the most widely used urban canopy scheme in WRF (e.g., Li et al., 2014; Morris et al., 2017; Sharma et al., 2016).
- The thesis uses case-study approach rather than long-term climate simulations, and hence the effects of natural climate variability are not assessed. This was deliberate, as the focus is the most severe heatwave events.
- The effects of future urban expansion are examined without considering future changes in climate. This thesis investigates how the UHI and urban meteorology would respond during different heatwaves in a hypothetical situation whereby future urban expansion in 2050 has already occurred.

- There are several different types of UHI mitigation strategies (e.g., modifying urban geometry, cool roads and walls (white painting on roads and walls), green walls, use of water bodies such as wetlands, minimizing anthropogenic heat etc), and it was not possible to comprehensively evaluate all of them. Based on a literature review (Chapter 2), this thesis only investigates the effectiveness of GI implementations including green/cool roofs, MF, MFAG and MSAG in mitigating UHI effects.

1.4 Research Significance and Innovation

The impacts of the UHI and increasing frequency and intensity of heatwaves pose a great challenge for adaptation and mitigation. The topic of heatwaves has gained significant attention, particularly in Australia and Europe, due to the public health hazards they pose, with 4000 deaths in Australia since 1800 (Victorian Department of Human Services, 2009), and 70000 deaths across western Europe in 2003 attributed to heatwaves (Robine et al., 2008). In addition, cities are experiencing rapid population growth, and these results in rapid urban expansion, which can exacerbate UHI effects. Therefore, there is an urgent need to assess the effectiveness of different UHI mitigation strategies, as well as the impacts of future urban expansion, for a city such as Melbourne, which experiences frequent heatwaves and is expanding rapidly. By examining the effectiveness of different UHI mitigation strategies, such as using green/cool roofs, MF, MFAG and MSAG, this thesis will provide valuable and timely information on what are the most effective UHI mitigation strategies, and to what extent these mitigation strategies need to be implemented. In addition, the thesis will provide important information for city planners

on the possible effects of future urban expansion and how these adverse effects can be minimized.

Energy consumption rises during heatwaves because of extensive use of air conditioners, electric fans and air coolers, and as a result, and this poses significant challenges to the energy sector (Reeves et al., 2010). In addition, air conditioners and coal fired power generation result in large amounts of greenhouse gas emissions. Implementing GI practices in urban areas is not only a potential solution in minimizing the effects of UHI during heatwaves, but it can also be an effective and appealing means in reducing greenhouse gas emissions by reducing energy use, as well as maintaining urban ecosystems, creating biodiversity habitat and delivering economic benefits. Therefore, the study outcomes will provide policy relevant information for city planners, engineers, stakeholders, local and national agencies for other cities for designing sustainable urban development strategy.

Heatwaves are one of the most important hazards in Australia because of their frequency and intensity, are expected to increase under future climate change (Cowan et al., 2014). Therefore, it is important to understand heatwave dynamics and processes to minimize the adverse impacts of heatwaves by investigating a number of mitigation strategies. It is also, important to understand how these mitigation strategies respond during heatwaves and what the mechanisms are. By examining the physical processes involved in heatwave dynamics in Southeast Australia and how these factors respond due to increased urbanization and various UHI mitigation approaches, this study will contribute to a deeper understanding and knowledge in this area. Finally, the results will be useful as a guideline for future research in other cities in Australia and different parts of the world, which experience similar climatic conditions.

1.5 Thesis Structure

This thesis is structured as a thesis by publications, divided into 8 chapters. The research background, objectives, scope and significance are presented in this chapter in Chapter 1. Chapter 2 summarize the literature review on the UHI, heatwaves, impacts of urbanization, and different UHI mitigation strategies, as well as UHI modelling approaches. Chapter 3 provides a general methodology, including a description of the WRF-SLUCM model, observational data sources and overall research design. Chapter 4 presents the evaluation of the sensitivity analysis of the WRF-SLUCM model in simulating the UHI and heatwaves for the city of Melbourne to determine the best WRF model configuration for Melbourne region, which is then used throughout the rest of the thesis. Chapters 5 evaluates the potential of green and cool roofs in mitigating UHI effects in the city of Melbourne. The potential impacts of future urban expansion are presented in Chapter 6. Chapter 7 assesses UHI mitigation strategies by using various GI practices including MF, MFAG and MSAG incorporating future urban expansion scenarios. Finally, Chapter 8 summarizes the main findings and recommends further research.

Chapter 2

Literature Review

2.1 Introduction

This chapter provides a detailed review of the UHI and its effects on the surface energy balance in sections 2.2 and 2.3, respectively. In sections 2.4 and 2.5, the UHI and heatwaves and their impacts on human health are presented. The effects of urbanization on the UHI are presented in section 2.6. Section 2.7 reviews the use of green and cool roofs, and GI as UHI mitigation strategies. Finally, section 2.8 reviews UHI modelling techniques and focuses on the importance in selecting the numerical models in UHI study.

2.2 The Urban Heat Island

The UHI is commonly defined as higher temperatures in urban areas as compared to rural areas. The UHI phenomenon can be classified according to different spatial scales. The UHI of individual features/blocks (including building and roads) at the neighbourhood scale is described as the temperature differences in the intra-city, and referred to as the micro-scale UHI. The local/regional scale UHI is described as variations of temperature across the entire urban and surrounding rural areas. The local/regional scale UHI is largely influenced by geographical and climatic conditions. Furthermore, the UHI can be measured at different heights within urban boundary layer. For instance, the surface UHI is calculated as the surface temperature differences (usually using the surface skin

temperature) between urban and rural areas. The pedestrian level UHI can be measured as the temperature differences between urban and rural areas at 2 m above the surface. The urban boundary layer UHI is defined as different atmospheric temperatures above the city, while the canopy layer UHI is defined as atmospheric temperatures differences between the ground surface and average building height of a city. The surface level and pedestrian level UHI have been the subject of many studies (Li et al., 2014; Morris et al., 2017; Sharma et al., 2016; Yang et al., 2016). The surface level UHI generally shows the highest intensity as compared to the pedestrian level UHI as the surface is directly heated by solar radiation (Li et al., 2014; Sharma et al., 2016). The UHI generally shows the highest intensity during anti-cyclonic conditions with clear skies and low wind speeds (Gedzelman et al., 2003; Morris et al., 2001). On the other hand, atmospheric warm fronts enhance mixing and turbulence, and consequently, minimize the differences between urban and rural temperatures, and reducing the intensity of UHI (Tumanov et al., 1999). Low winds exacerbate UHI effects while stronger winds significantly weaken the UHI (Morris et al., 2001).

There are many factors responsible to generate the UHI and many are related to the prevailing weather conditions. Stable weather conditions with smaller pressure gradients generally lead to more intense UHI due to lower winds. Temperature gradients become stronger when synoptic wind speeds are weaker, and as result a closed circulation pattern may form, associated with the UHI, which is characterized by a strong updraft motion over the center of the city, convergent flow near the ground surface and divergent flow aloft (Collier, 2006). Stronger wind speeds help to mix the air between urban and surrounding rural areas, and minimize temperature differences, and consequently, reduce UHI effects. Many cities in the mid-latitudes face a higher intensity of UHI during

summer months because of higher intensity of incoming solar radiation. In addition, regional climate variability and the frequency of synoptic conditions leading to extremely warm periods might also result in longer lasting UHI effects (Chandler, 1965).

Other factors affecting the UHI include urban geometry, types of urban land cover, anthropogenic heat emission and atmospheric pollution. The urban geometry and land use cover substantially affect the UHI cycle. For example, urban areas increase storage heat due to higher conductivity and heat absorption capacity by the construction materials and reduce wind speed because of higher roughness, and consequently, increase UHI effects particularly during the night (Chen and Frauenfeld, 2016; Coutts et al., 2008). The properties of different land-use types, such as albedo, shade factor and emissivity, play an important role in increasing sensible heat and decreasing latent heat flux, which drive the UHI during the day (Chen and Frauenfeld, 2016). The UHI has a clear diurnal and seasonal cycle (Gedzelman et al., 2003; Shepherd, 2005). The UHI has a lower intensity during the day, and is generally at its maximum intensity during the night. This is because of the stored heat during the day by the construction material and re-radiation of that stored heat during the night. Furthermore, cool islands can occur in urban areas especially during the day if most of the incoming solar radiation is absorbed by urban surfaces (Morris and Simmonds, 2000), i.e., most of the energy goes into increased ground heat flux, but in rural areas, most of the net radiation is transformed into sensible heat flux, which consequently results in rural temperatures being higher than urban temperatures.

An increasing trend in the UHI intensity has been documented for many cities and this is likely due to increased urbanization with an increasing population (He et al., 2007). However, establishing a specific and linear relationship between the UHI intensity and

population is not straightforward as the relationship between the UHI and population differs according to the geographic conditions of the cities (e.g., European and North American cities). Cities in tropical countries do not seem to fit into either range, because of differences in soil moisture between urban and rural areas. Ahmad and Hashim (2007) showed that soil moisture had the same effect on the UHI formation as natural vegetated surfaces.

2.3 Surface Energy Balance

To understand the UHI, it is important to understand the surface energy balance in urban areas because the modified partitioning of surface heat fluxes, due to urbanization, affects the atmospheric stability and thermodynamics properties of the boundary layer and mixing layer heights (Christen and Vogt, 2004).

The surface energy balance is as follows:

$$R_n = (1-r)S + L + Q_F = SH + LH + G \dots\dots\dots (2.1)$$

Where r and S are the albedo and total solar radiation incident on the surface, L is the net longwave radiation and Q_F is the anthropogenic heat added to the surface. The left part of the equation is the net energy input to the surface, i.e the net radiation. The right part represents the partitioning of the net radiation into sensible heat (SH), latent heat (LH) and the storage heat (G). The latter is defined as:

$$G = -k \frac{dT}{dZ} \dots\dots\dots (2.2)$$

Where, k is thermal conductivity, and dT/dZ is change in soil temperature with depth.

For vegetated surfaces, net radiation is partitioned mostly into SH and LE, and a smaller portion into G because of low thermal conductivity (k) of soil. On the other hand, the major portion of net radiation goes into G, rather than SH and LE, in urban areas due to much higher thermal conductivity of urban surfaces. The storage heat (G) in urban surfaces is controlled by the properties of construction materials such as heat capacities, thermal conductivities and density. The combined effect of these properties is represented by thermal inertia of a material, which describes the ability of a material to conduct and store heat energy during the day and re-radiate during the night (Mellon et al., 2000).

The energy balance is driven by net radiation, i.e. the net short wave and longwave radiation. Net radiation is converted into sensible, latent and ground/storage heat flux. Urban surfaces with lower albedo reflect a smaller amount of incoming shortwave radiation and absorb more solar radiation due to higher thermal conductivity materials, therefore, net radiation is higher in urban areas, and there is more energy available to be converted to sensible, latent and ground heat flux. With vegetated surfaces, more net radiation is partitioned into latent heat flux, rather than sensible heat flux, because of evaporation and transpiration.

Urbanization is one of the influential factors in altering the heat fluxes (storage heat, sensible and latent heat flux), and consequently, alters surface energy balance because of shading, trapping solar radiation and high thermal conductivity of construction materials. Soil moisture availability is another influential factor in controlling the surface energy balance. A surface covered by vegetation has higher potential of water retention while moisture is reduced in impervious surface due to surface runoff (Oke, 1982). Increased

soil moisture in vegetated areas substantially increases latent heat flux and reduces sensible heat flux.

Heat exchange within the urban canopy is mainly influenced by urban features such as density of buildings, height and width of buildings and roads and atmospheric conditions such as amount of turbulence (Coutts et al., 2007; Yang et al., 2016). The amount of stored heat by urban surfaces largely depends on the types and properties urban infrastructure (Coutts et al., 2007). Urban environment creates their own microclimate through the exchanges of energy, mass and momentum, and consequently, generates a distinctive urban boundary layer (Gunawardena et al., 2017). The radiative properties of any surface is the main driver in altering surface energy balance by distributing incoming shortwave and longwave solar radiation. In the absence of incoming shortwave radiation during the day, longwave radiation plays dominant role in driving the surface energy balance during the night. Impervious surfaces absorb a greater part of the incoming solar heat due to higher thermal conductivity and heat storage capacity during the day and results in warming the surface and near surface atmospheric layer because of re-radiation of stored heat during the night (Cheng and Chan, 2012; Coutts et al., 2007; Morris et al., 2017). Therefore, urban areas convert natural surfaces into heat reservoirs, and in addition, with building geometry, synoptic weather conditions and anthropogenic activities lead to increasing warming as compared to rural surroundings.

The urban heat budget is controlled by both horizontal and vertical transport of sensible heat flux from surface and urban canopy. Excessive surface warming during the day results in higher temperature and deeper convective mixed layer during the day. Figure 2.1 shows a typical influence of urban surfaces on the boundary layer structure at the

regional scale. The height of urban mixing layer varies due to convective effects which are controlled by the horizontal and vertical mixing and transport. Convective heat plumes are induced due to increased sensible heat flux from the urban surfaces caused by increased turbulence intensities in urban areas (Oke, 1982). The urban boundary layer can be lifted over the surrounding rural boundary layer, when an urban heat plume horizontally extends downwind of the city due to horizontal wind flow. As a result, temperature will not only increase in urban areas, but can extend the effect to surrounding rural areas based on the prevailing wind direction and speed (Voogt and Oke, 2003).

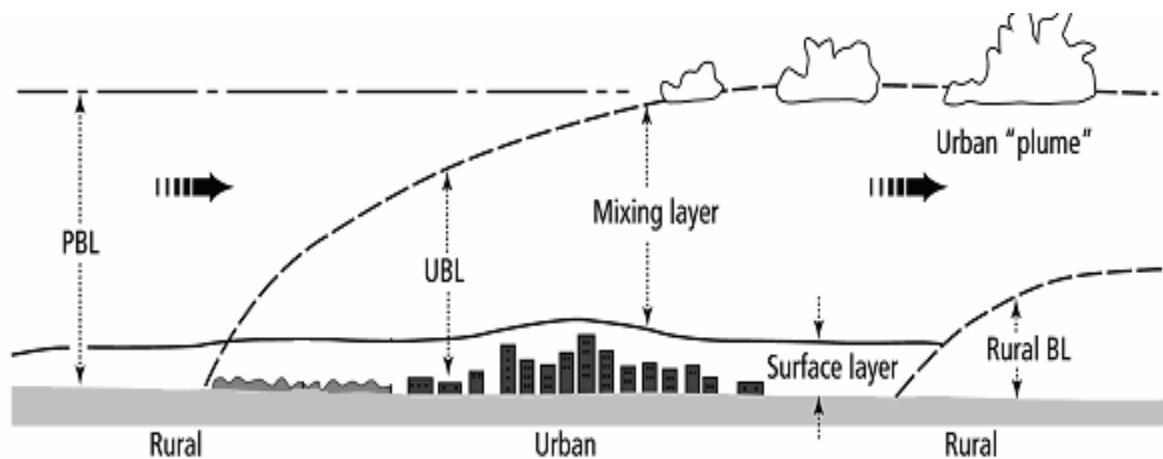


Figure 2.1 Typical representation of the influence of urban surface on the boundary layer at regional scale. PBL and UBL represent planetary boundary layer and urban boundary layer, respectively (Oke, 1997).

2.4 Heatwaves and UHI

Heatwaves in southeast Australia are largely driven by anticyclones (also known as high-pressure systems) (Perkins, 2015). Heatwaves typically occur when these anticyclones are stationary, in which case they are commonly referred to as a blocking-high, with a center of anomalously high-pressure (Coughlan, 1983). Conventional blocking-highs develop

when atmospheric winds in upper-level split due to meandering of the jet stream, which allows a region to be blocked from the zonal jet stream for several days (Pezza et al., 2012). As a result, poleward cooler air cannot mix with hotter air within this region, and consequently, warm air builds up. Other persistent highs occur at lower latitudes located 10° equatorward of the traditional blocking areas, where the subtropical ridge sits during summer (Perkins, 2015). These types of persistent highs are the main driving factors for numerous heatwaves over Australia (Marshall et al., 2014) (Figure 2.2). Pezza et al. (2012) have characterized the severe southeastern Australian heatwaves by slow-moving persistent-highs centered in the Tasman Sea as shown in Figure 2.3. Generally, heatwaves are due to persistent-highs located adjacent to the affected area, and advecting dry and hot air from the interior of the continent (Boschat et al., 2015; Marshall et al., 2014).

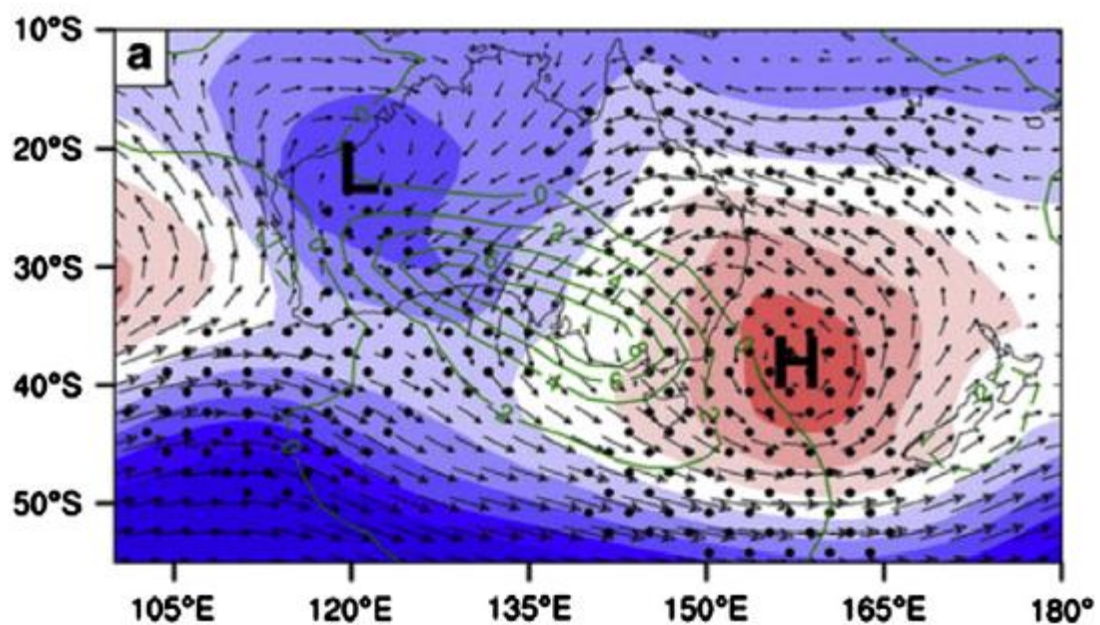


Figure 2.2 An example of typical persistent high that causes heatwave conditions over southeast Australia (Pezza et al., 2012).

Melbourne, the capital city of Victorian state in southeast Australia has been experiencing more frequent, longer, and intense heatwaves (Cowan et al, 2014). This includes extreme heatwaves in 2009 across southeastern Australia followed by another extreme heatwave in January 2014: a prolonged autumn heatwave for southeast Australia and intense summer heatwaves two of Australia's most significant heatwave events (BOM, 2014a; BOM, 2014b); and an exceptionally prolonged autumn warm spell over much of Australia in May 2014 (BOM, 2014c). The numbers of heatwaves, and their duration and intensity have increased over the last two decades over Australia, and especially in southeastern Australia (Steffen et al., 2014). In addition, the frequency, duration and intensity of heatwaves is expected to increase in the future, with heatwave duration expected to double by 2070 (Cowan et al., 2014).

The city of Melbourne also experiences UHI effects. A study by Torok et al. (2001) showed a positive correlation between UHI and population density for the city of Melbourne (Figure 2.3). Torok et al. (2001) reported that the city of Melbourne experienced a peak UHI of 7.1 °C in the city centre on the evening of 25 August 1992. There were sharp drops in temperature at the urban-rural boundary while the vegetation in parks showed a lower UHI effect (Figure 2.3). Furthermore, Coutts et al. (2008) and Coutts et al. (2016) investigated the UHI in Melbourne, and reported a substantial UHI intensity during the night (mean maximum UHI 4 °C). The UHI can be exacerbated during heatwaves according to Li and Bou-Zeid (2013). Heatwaves not only increase ambient temperatures, but also the temperature differences between urban and rural areas. Heatwaves in the city of Melbourne now start on average 17 days earlier, and the average intensity of a heatwave has increased by 1.5 °C, with the peak heatwave day likely to be 2

°C hotter than the long-term heatwave average (Steffen et al., 2014). Therefore, the UHI combined with heatwaves leads to higher warming than the UHI alone.

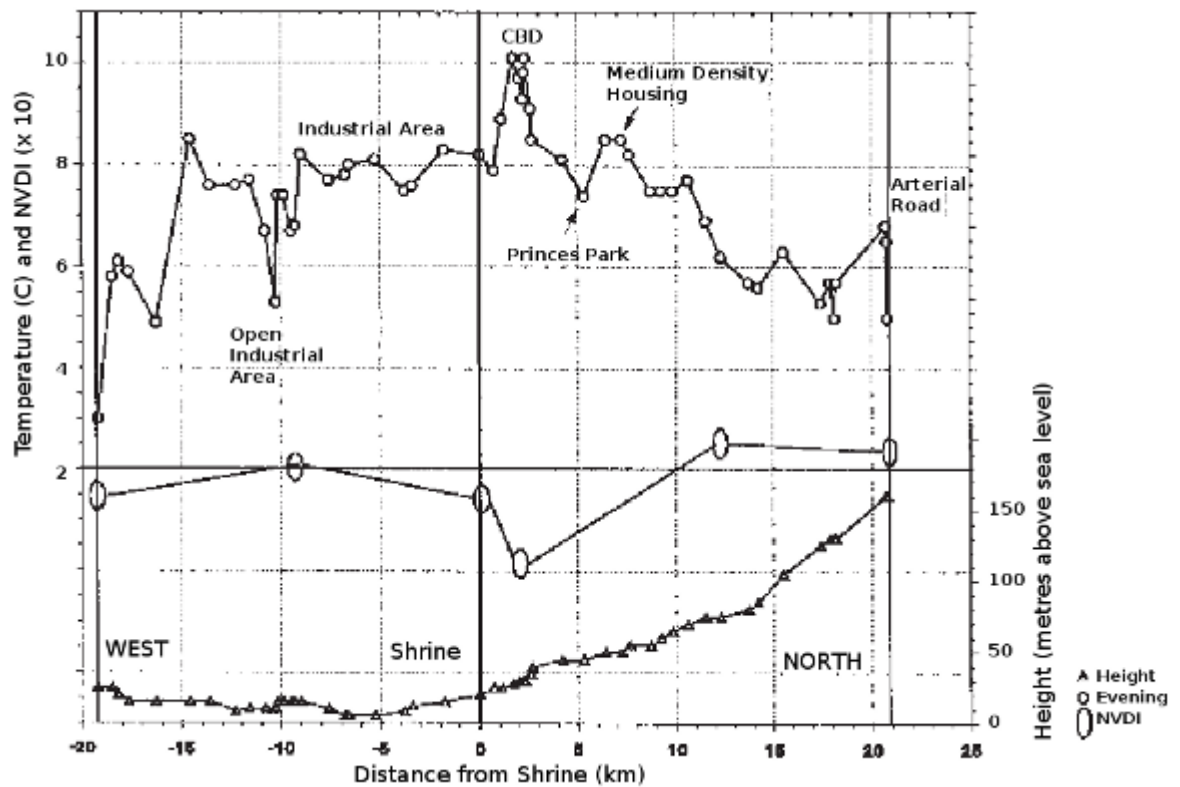


Figure 2.3 Correlation between urban-rural temperature differences and population density for Melbourne (Torok et al., 2001).

The Melbourne regional office of Bureau of Meteorology have kept accurate temperature records since 1910. Temperature records showed that a long term increase in the annual maximum and minimum temperatures over the city of Melbourne with linear trend of 0.08 °C and 0.14 °C per decade, respectively. The annual mean temperature for the city of Melbourne increased at a linear trend of 0.11 °C per decade from 1910 to 2013. This increasing trend also depends on the seasons, with the maximum temperature in each decade increasing by 0.06 °C for summer, 0.05 °C for spring and 0.11 °C for Autumn and

Winter. The minimum temperatures are increasing with a positive trend of 0.19 °C for summer, 0.16 °C for spring and 0.12 °C for Autumn and 0.08 °C for Winter. Long-term temperature data shows that minimum temperatures increase of 2 °C during summer and results in quicker warming nights (Figure 2.4).

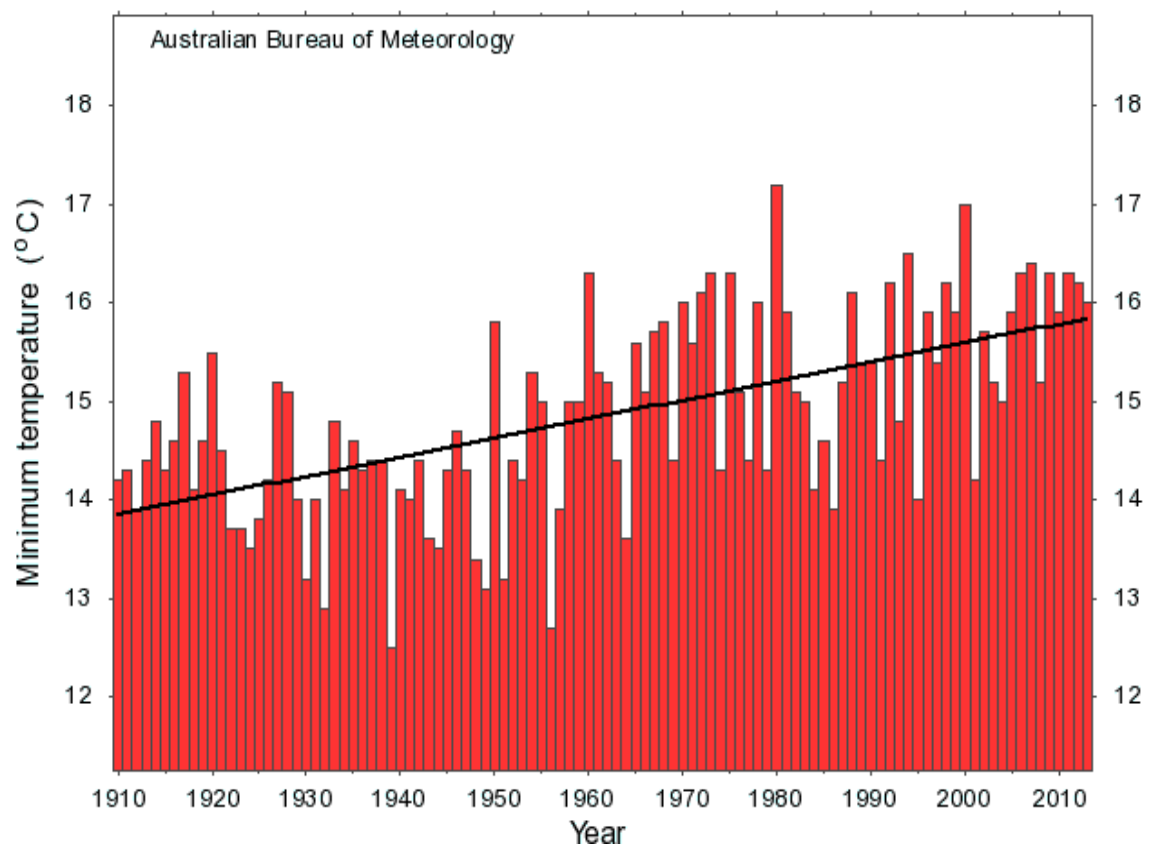


Figure 2.4 Trend of minimum temperatures during summer for Melbourne from 1910 to 2013 (BoM, Australia)

A comparison of increasing temperatures trends among different Australian cities is shown in Table 2.1. Temperatures are projected to increase by 1.0 to 2.5 °C and 2.2 to 5.0 °C by 2070 for low and high greenhouse gas emissions, respectively as compared to the

period 1980 to 1999 (Table 2.1). As a result, this increase temperature will increase the number of hot days and warm nights during summer.

Table 2.1 Number of hot days above 35 °C based on annual average summer temperature for long-term (1961 – 1990), short-term (2000-2009) and projected years of 2030 and 2070 for Australian capital cities (Steffen et al., 2014).

Cities in Australia	Long-term average (1961-1990)	Short-term average (2000-2009)	Projection for 2030	Projection for 2070 (low emission scenario)	Projection for 2070 (high emission scenario)
Melbourne	9.9	12.6	12 (11 - 13)	14 (12 - 17)	20 (15 - 26)
Sydney	3.4	3.3	4.4 (4.1 - 5.1)	5.3 (4.5 - 6.6)	8 (6 - 12)
Adelaide	17.5	25.1	23 (21 - 26)	26 (24 - 31)	36 (29 - 47)
Canberra	5.2	9.4	8 (7 - 10)	10 (8 - 14)	18 (12 – 26)
Darwin	8.5	15.7	44 (28 - 69)	89 (49 - 153)	227 (141 - 308)
Hobart	1.2	1.4	1.7 (1.6 - 1.8)	1.8 (1.7 - 2.0)	2.4 (2.0 - 3.4)

2.5 Heatwaves and Human Health

Heatwaves caused more hazards on human health than other natural disasters in Australia. Table 2.2 shows a comparison of fatality with other natural hazards in Australia. Heatwaves killed more people in Australia and accounted for 55.2 % of total natural hazard death for the period 1900 to 2011.

Table 2.2 Comparison of number of deaths caused by various natural hazards in Australia (Coates et al., 2014).

Natural Hazard	Number of Deaths (1900 – 2011)	% of Total Deaths
Extreme heat (Heatwaves)	4555	55.2
Flood	1221	14.8
Tropical Cyclone	1285	15.6
Bushfire	866	10.5
Lighting	85	1.0
Landslide	88	1.1
Wind Storm	68	0.8
Tornado	42	0.5
Hail Storm	16	0.2
Earthquake	16	0.2
Rain Strom	14	0.2

There are physiological limits to human heat, and when those limits are exceeded during extended heatwave periods, heat stress, and heat stroke and death may eventually occur (Sherwood and Huber, 2010). Generally, lower temperatures during the night helps physiological recovery of the human body during sleep. The increase in nocturnal temperatures in urban areas reduces physiological recovery and ambient temperatures above 23 °C during the night results in disturbance of sleep (Grunstein, 2013). The UHI causes night time human discomfort as the UHI is a nighttime phenomenon (Li and Bou-Zeid, 2013). For example, a heat alert system estimated that the daily mortality was about

15 – 17 % higher as compared to normal, for people 65 years old or more, when mean daily temperature exceed 30 °C (Nicholls et al., 2008). On the other hand, mortality was about 19 -21 % for the same group of people when night time temperatures (rather than the mean daily temperature) exceeded 24 °C (Nicholls et al., 2008). A report published by Englart (2015) showed that Ambulance service call outs rose by about 700 % during heatwaves in January 2014 when temperatures reached at 44 °C. Earlier in 2009 in Victoria, heatwaves caused 374 excess deaths followed by the historic Black Saturday bushfires which contributed to 173 deaths (Department of Human Services, 2009). Furthermore, the deaths related to extreme heat are projected to be higher especially for the city of Melbourne and Brisbane in Australia. According to Keating and Handmer (2013), extreme heat may cause an additional total 6214 deaths in Victoria by 2050. Based on projected impacts of heatwave on human health, there is high certainty that heatwaves will pose a significant health hazard for urban residents.

2.6 Impacts of Urbanization on the UHI

Increased urbanization and industrialization are the main driving factors for loss of vegetation and increased impervious surfaces. According to a population report of Population Reference Bureau (2005), half of the world population lives in urban areas and this number will increase to 60 % by 2030. Consequently, urbanization and industrialization will accelerate in the future. High thermal conductivity materials such as concrete, bricks and bitumen replace the pervious surfaces in urban areas. These materials absorb and store more heat during the day and emit heat at night, and this phenomenon is favourable in developing the UHI (Arnfield, 2003).

Urban expansion can often lead to adverse impacts on the urban environment including modification of regional and local urban meteorology. The decrease in surface albedo and increase in roughness due to urban expansion leads to increase in sensible heat and decrease in latent heat fluxes, and consequently, can affect temperature and humidity (Chen et al., 2016). Land use change in urban areas due to urbanization is an extreme type of land use change as urbanization dramatically alters the physical properties of land surface and affect its thermal radiative and aerodynamic character (Oke, 1987). Therefore, it is important to understand how urban expansion affects regional climate (Jin and Shepherd, 2005).

Rapid urbanization may further intensity the UHI, which substantially alters urban ecosystem and severely affects the human thermal comfort, particularly during summer and heatwave episodes (Rankin, 1959). Coutts et al. (2008) examined the impacts of urban expansion of the city of Melbourne according to Plan Melbourne 2030, and showed a higher intensity of the night time UHI especially in the expanded areas and activity centres. Another study examined the effect of new residential development and urban expansion on the fringes of the city of Sydney, and showed a stronger increase in minimum temperatures as compared to maximum temperatures (Argüeso et al., 2014). Recently, the city of Melbourne published the urban expansion strategy titled “Plan Melbourne 2050” to expand urban areas in surrounding suburbs to meet the future residential demand. As urban expansion substantially affects urban climate, therefore, it is urgent to examine the future urbanization impacts for the city of Melbourne based on Plan Melbourne 2050. However, no study yet to examine the impacts of future urbanization according to Plan Melbourne 2050.

2.7 Mitigation Approaches of UHI Effects

Considering the consequences of UHI effects, several studies have been conducted to characterize the near-surface UHI using numerical climate models. Furthermore, several UHI mitigation strategies aiming to reduce UHI effects have been proposed in the literature such as modification of urban geometry (Fahmy and Sharples, 2009; Pearlmutter et al., 1999), increasing emissivity and surface albedo (Golden and Kaloush, 2006; Morris et al., 2017; Sailor, 1995; Touchaei et al., 2016), increasing urban vegetation and surface shading (Razzaghmanesh et al., 2016; Razzaghmanesh and Razzaghmanesh, 2017; Sailor and Dietsch, 2007; Synnefa et al., 2008; Yaghoobian et al., 2010). Recent studies have shown that these mitigation strategies can reduce the UHI and hence provide important climatic benefits (Fintikakis et al., 2011; Santamouris et al., 2012).

Generally, urban areas have lower albedo due to darker surfaces and lower vegetation cover. Therefore, the use of higher reflective construction materials or coating (e.g., paint, whitening of roofs) or increasing vegetation cover are possible mitigation strategies in reducing temperatures over the urban areas. Mitigation of the effects of the UHI and heatwaves can be carried out by increasing urban vegetation, using higher albedo urban infrastructure, implementing water sensitive urban design and maintaining urban biodiversity. These mitigation approaches can be classified into four main categories as follows:

- ❖ Cooling by vegetation
- ❖ Cooling by increasing surface albedo of construction materials
- ❖ Cooling by sustainable urban infrastructures (e.g., orientation and windows of building)
- ❖ Cooling by anthropogenic heat reduction (e.g., heat exhaust from cooling systems, vehicles etc)

Among all these mitigation strategies, cooling by urban vegetation is a sustainable UHI mitigation strategy with multiple benefits (Ca et al., 1998; Eliasson, 1996; Rosenfeld et al., 1995; Rosenfeld et al., 1998; Spronken-Smith et al., 2000) while using higher albedo materials particularly on roofs has shown higher effectiveness in reducing the UHI intensity (Li et al., 2014; Sharma et al., 2016). Therefore, the current study focuses on UHI mitigation approaches using vegetation and reflective materials on roofs (e.g., green and cool roofs) and different types of urban vegetation.

2.7.1 Green Roofs

Green roof is defined as a partially or completely vegetated landscape installed on the roof of building including additional layers such as a growing medium, drainage layer and waterproof membrane (USEPA, 2008). Green roofs reduce solar radiation by shading and increasing evapotranspiration via transpiration during photosynthesis and soil evaporation (Authority Greater London, 2008). In summer, green roofs absorb 70 to 90 % energy from the sun by leaves during the photosynthesis process and the remaining energy is reflected back into the atmosphere (USEPA, 2008). Green roofs reduce a substantial amount of heat transferred from the roofs to the inside of buildings by shading and evapotranspiration. The roofs' vegetation also extends the life span of roofs by

providing protection from the UV radiation, adverse weather effects and temperature fluctuations (Oberndorfer et al., 2007). About 30 % green roofs has been shown to reduce the surface temperature by up to 1 °C in the Baltimore-Washington metropolitan area in the US, and the performance of green roofs was sensitive to increasing/decreasing in soil moisture (Li et al., 2014). This study also illustrated that the surface UHI during the peak temperature of the day was further reduced by 0.55 °C (when a soil moisture control limit was $0.45 \text{ m}^3 \text{ m}^{-3}$) and 0.27 °C (when a soil moisture control limit was $0.35 \text{ m}^3 \text{ m}^{-3}$). On the other hand, when the soil moisture was near the wilting point ($0.15 \text{ m}^3 \text{ m}^{-3}$) for dry conditions, the cooling benefit provided by green roofs due to soil moisture was almost completely eliminated.

Factors such as geographic location, roofs composition, solar exposure, growing medium and moisture content also influence temperature over green roofs (USEPA, 2008). A study reported that the 32 % green roofs can save 19200 MWh energy per year, and can store 80000 m^2 rainwater at roof level (Authority Greater London, 2008). A study was conducted by Rosenzweig et al. (2006) to investigate the UHI mitigation scenarios for the city of New York by using the regional climate model MM5. Although, their study did not explicitly represent buildings in the MM5 model, it assumed the presence of buildings through the boundary layer structure, which controls the heat and moisture transportation in the surface layer. Their study found that vegetation had greater impacts in reducing urban temperature than the urban geometry. They also reported that the 50 % green roofs covered with grass reduced urban surface temperatures up to by 0.1 to 0.8 °C. Banting et al. (2005) reported that green roofs covering a total area of 50 km^2 reduced local ambient air temperatures up to by 0.5 to 2 °C in Toronto in Canada. Wong et al. (2003) investigated the thermal benefits of green roofs through the field measurement data for

the tropical environment in Singapore and reported that the cooling effect of plants was responsible for the highest reduction (4.2 °C) in ambient air temperatures. In addition, green roofs in urban areas can retain storm water and pollutants from air. Consequently, retained storm water helps to reduce flash flood risks, generates a cooling effect and improves air quality and rainwater. This in turn protects against the entry of pollutants into lakes, ponds and rivers water during rainfall, and decreases the sewage load in the sewage networks (Manfred et al., 2002).

2.7.2 Cool Roofs

Cool roof is a roofing system that minimises solar adsorption and maximises solar reflectance and thermal emittance to stay cool in the sun (Akbari, 2008). Cool roofs have higher albedo (solar reflectance) and thermal emissivity. The materials of cool roofs can reflect 70 % of incoming solar radiation (Gartland, 2008). Several studies have investigated the temperature reduction due to increasing the albedo of cool roofs (e.g., Akbari et al., 2001; Synnefa et al., 2006), and report that for low albedo roofs, the maximum difference of temperatures can be as high as 50 °K between roof surface and surrounding air, and this difference can be lowered to 10 °K for high albedo roofs. Synnefa et al. (2006) investigated 14 different reflective coatings for thermal performance and optical properties. Temperature sensors, data logging systems and infrared thermography were used for their experimental study, which showed that cool coating reduced temperature by 4 °C during the day and 2 °C during night in summer conditions. Also, the analysis from their study showed that thermal performance of cool coatings and cool materials was affected by thermal reflectance during the day and by emissivity during the night.

Synnefa et al. (2008) measured the temperature differences between 10 conventionally pigmented coatings and 10 prototype cool colored coatings. The maximum temperature difference was 10.2 °C during the summer against the solar reflectance of 0.22 while the temperature difference was 1 °C during winter. Therefore, cool colored coatings avoid any heating penalty. The performance of five colors of thin layer asphalt was examined by Synnefa et al. (2011), who reported that the daily surface temperature fluctuation was 25 K for black asphalt and 8 K for colored thin layer asphalt. A review, on cool roofs in mitigating UHI effects and improving thermal comfort, revealed that the materials of cool roof decreased the flow of heat flux into the buildings and reduced the high temperatures (Santamouris et al., 2011). Some cool roof materials such as cool coatings (cementitious or elastomeric), cool shingle–ply roofing systems made by various materials and clay shingles with high albedo values were suggested by Gartland (2008). The smooth white coatings can increase the lifespan of cool roofs and albedo values from 0.04 to 0.80 as compared to roofs covered by black asphalt surface (Santamouris et al., 2011). Cool roofs require regularly cleaning and maintaining otherwise their reflectance will be reduced. For a white cool roof, solar reflectance reduced from 0.80 to 0.60 due to biomass and dust deposit (Levinson et al., 2005).

Recently, many studies have used Regional Climate Models (RCMs) for investigating the effectiveness of cool roofs in reducing the UHI (Li et al., 2014; Morris et al., 2017; Sharma et al., 2016; Touchaei et al., 2016; Yang et al., 2015). These studies report that cool roofs have great potential in reducing urban temperatures with maximum reductions of roof surface UHI by 7 °C in Chicago, USA (Sharma et al., 2016), 4 °C in Rome, Italy (Morini et al., 2016) and 3.5 °C in Baltimore-Washington, USA (Li et al., 2014).

Therefore, application of cool roofs at the city-scale can provide cooling benefits over larger areas for a city as compared to individual features/blocks.

2.7.3 Urban Vegetation

Near-surface urban temperatures can be reduced substantially by using urban vegetation. Urban vegetation increases latent heat flux and decreases storage heat via evapotranspiration and shading, and can therefore reduce the UHI. Besides, the urban vegetation allows more stormwater infiltration into the soil and increases soil moisture. Available soil moisture enhances evaporation rates and results in higher latent heat flux, consequently, reduces urban warming (Rizwan et al., 2008). A number of studies have focused on the potential of urban vegetation in countering UHI effects (Heisler et al., 1994; Taha et al., 1996; McPherson et al., 2005; Solecki et al., 2005).

Urban trees can be planted in two ways such as planting a tree directly in the ground or using cell structures, which facilitate the necessary space for full root development under a partial asphalt covering. Urban trees directly reflect or absorb solar radiation and reduce adjacent surface temperatures by shading during the day (Lee et al., 2013). Several studies investigated the potential of urban trees in reducing urban temperatures (Berry et al., 2013; Bowler et al., 2010; Lin and Lin, 2010; Souch and Souch, 1993). Urban trees can reduce urban air temperatures by 0.7 to 1.3 °C during early afternoon (Souch and Souch, 1993). Lin and Lin (2010) reported that air temperature was reduced by 0.64 to 2.52 °C under the tree canopy as compared to open space during midday. The cooling effect of trees largely depends on the size, species and characteristics of the trees (Georgi and Zafiriadis, 2006). The effect of urban trees has been investigated by many studies at the city-scale (Shashua-Bar and Hoffman, 2000; Takebayashi and Moriyama, 2009;

Wong and Yu, 2005). Their results showed that reductions of urban temperatures by urban trees ranged from 0.28 to 4 °C. At night, urban trees restrict longwave radiation loss and ventilation under the canopy and this can result in a warming effect in urban areas (Coutts et al., 2016).

Vegetation planted around a building can protect the building from solar radiation. Vegetation keeps the soil surrounding the building cooler, and reflects and diffuses solar radiation (Akbari et al., 2001). In park areas, the combined effects of evapotranspiration and shading can significantly reduce temperature and even create cool islands (Shashua-Bar and Hoffman, 2000). A study showed that average air temperatures in parklands were 4 °C lower than the inner city (Eliasson, 1996), whereas the cooling effect depends on the size of parks, types of vegetation and climatic conditions (Gago et al., 2013). Parklands not only keep parks cool but also the surrounding areas, and can reduce building cooling loads by up to 10 % (Yu and Hien, 2006). An investigation was carried out by Ca et al. (1998) to quantify the effect of parklands on summer climate in Tama of New York, and in a coastal metropolitan area in Japan. Their results indicated that parklands reduced temperatures by 1.5 °C in a busy commercial area at noon, and this led to reduced energy demand. They also proposed a park vegetation and shape index that can be used to quantify the cool island in park areas. Some studies reported that parklands are always cooler than spaces without any green cover (e.g., Hoyano, 1988; Parker, 1983). Furthermore, Yu and Hien (2006) and Cao et al. (2010) showed that parklands and green spaces reduced temperatures by 2 to 3 °C in summer and stabilized the temperatures fluctuation caused by building materials. However, cooling effect depends on the size of the parklands and solar radiation; but there is no linear relation between the cool islands and size of parklands (Cao et al., 2010; Eliasson, 1996).

2.8 Observational and Numerical Modelling Approaches in Studying the UHI

Estimation of UHI and the effects of urban expansion are not straightforward because UHI and urbanization effects are apparent at different scales (e.g., micro and local/regional scales). One possible method in estimating the UHI is by comparing observations from urban stations with data from near-by rural stations (Baker et al., 2002; Jáuregui, 2005). However, it is important to consider the effects of topography and natural features within the study area, and to ensure that there is no effect of the urban area on the rural stations (e.g., downwind of the city). An alternate method is to quantify urban effect by correlating historical temperature series data with the growth of a city (Philandras et al., 1999). Nevertheless, the problem is a comprehensive set of pre-urban measurements is not available for comparison, which would be required to distinguish station-by-station differences before and after urban expansion due to different weather pattern (Lowry 1998). Other experimental methods include transects (Unger et al., 2001), and the analysis of satellite derived temperature data (Lee, 1993) to investigate the UHI.

Furthermore, there are several methods to investigate the UHI and effect of urbanization. For instances, satellite measurements (Gallo et al., 1999) and population data (Easterling et al., 1997) haven been used in the USA. These two methods can be used to estimate different impacts of urbanization (Gallo et al., 1999). The effects of urbanization can also be analyzed by comparing trends between observed surface temperatures and reanalysis of global weather. Kalnay and Cai (2003), showed that the estimated averaged surface warming was 0.27 °C per century because of changes in urban and agricultural land use, and failure in accounting for agricultural land use effects could lead to the underestimation of the impact of land use changes. Recently, satellite imageries (e.g., related to meteorological and satellite thermal data) have been widely used to estimate a

normalized difference vegetation index (NDVI) to investigate the effect of land use changes (Romero et al., 1999). The NDVI can be used to estimate the UHI, as there is an inverse correlation between the NDVI and UHI for several cities. However, all these methods have inherent limitations, which make it difficult to estimate the different impacts of urban expansion on the UHI, and the effectiveness of different mitigation strategies. To overcome these difficulties, the numerical modelling approach is commonly used to examine the effects of land use change, particularly effect of urbanization on weather and climate at regional scales (Lamptey et al., 2005).

Numerical regional atmospheric models are commonly used to examine the influence of urbanization on weather and climate including temperatures, wind flow, precipitation and atmospheric boundary layer structure at a variety of spatial scales (e.g., regional and global) (Argüeso et al., 2014; Atkinson, 2003; Bornstein and Lin, 2000; Klaić et al., 2002; Li et al., 2014; Pino et al., 2004; Sharma et al., 2016). In these numerical models, the accurate representation of thermal and dynamic effects in the urban areas plays important role in the atmospheric boundary layer, which is very important for understanding and modelling the UHI. Micro-scale models resolve surface energy balance at the building scale, and these models are limited to studying urban meteorological conditions at very fine spatial scales of individual buildings. On the other hand, meso-scale models cannot resolve urban effects at building scale due to computational cost, and therefore require adopting an averaged building approach/parameterization (Martilli et al., 2002).

The parameterization of an urban canyon is difficult since urban surfaces are extremely heterogeneous and complex in nature. The main aspects that are required to be considered

in parameterizing urban effects are thermal properties of urban surfaces including trapping of radiation and shadowing effects, role of urban canopy on airflow and albedo effect due to radiation trapping between canyon walls (Piringer et al., 2002). However, the parameterization of urban surfaces can be done in many ways in meso-scale models (Masson, 2006). The first attempt to parameterize the urban surface in meso-scale model was a 1-D diagnostic UHI model (Myrup, 1969), which represented urban surface by its albedo, roughness, relative humidity and soil heat capacity. Over the years, 2-D and 3-D models were subsequently developed, and these have been reviewed by Craig and Bornstein (2001). All these first generation models considered zero building height in simulating urban effects, which leads to numerous limitations.

Recent attempts in parameterizing urban surfaces focus on the dynamic and thermodynamic properties of the urban surfaces (Masson, 2006). The dynamic properties of urban surfaces can be parameterized by adjusting roughness length or by introducing equations for turbulent kinetic energy for characterizing the drag generated by buildings. Thermodynamics effects of urban surfaces can be parameterized by using surface energy balance in different ways. One of the well-known and widely used approach is the Urban Canopy Model (UCM), which resolves surface energy budget for 3-D urban canopy using simplified urban geometry. This model computes individual energy budget for roofs, walls, roads and consider radiative interactions between walls and roads (Masson, 2006). The UCM can be single layer or multi-layers. In single layer models, the base of the atmospheric model is at roof level while buildings in multi-layer models influence several atmospheric levels (Martilli et al., 2002). The coupling of multi-layer models and atmospheric meso-scale models is complex because of direct interactions between meso-scale model and canopy scheme equations (Thompson et al., 2008). The Single Layer

Urban Canopy Model (SLUCM) has been used in a large number of meso-scale modeling studies in recent years for parameterizing urban surfaces for assessing urban effects on the urban meteorology and climate (e.g., Argüeso et al., 2014; Li et al., 2014; Sharma et al., 2016).

Numerical Regional Climate Models (RCMs) coupled with the SLUCM offer great opportunities to investigate urban weather and climate at large scales (e.g., mega-city and regional/meso-scales). The Single Layer Urban Canopy Model (SLUCM) has been coupled to the WRF model, which is one of the most widely used regional atmospheric modelling systems (e.g., Li et al., 2014; Liu et al., 2018; Morini et al., 2016; Sharma et al., 2016; Yang et al., 2015). All these studies report that the coupled SLUCM-WRF is a very effective modelling tool in studying urban meteorology at regional scale. The SLUCM in WRF parameterizes three-dimensional wall, roof and road surfaces (Grossman-Clarke et al., 2010; Kusaka and Kimura, 2004). Studies have shown that using the WRF model with the Noah land surface model and the SLUCM substantially improves the simulation of urban UHI (Kusaka and Kimura, 2004; Kusaka and Kimura, 2001). This coupled model includes improved configuration of urban thermodynamic and dynamic set up, which can consider thermal storage effects from natural (garden, street trees, park land) and artificial urban sources (building, road) (Kusaka et al., 2012).

Furthermore, the coupled WRF-SLUCM model offers a practical solution for assessing the cooling effects of green and cool roofs at the city scale with urban canopy parameterizations. The coupled WRF-SLUCM modelling systems has been widely used to investigate the effectiveness of green roofs for the UHI mitigation (e.g., Li et al., 2014; Liu et al., 2018; Sharma et al., 2016; Yang et al., 2016). A few studies have considered

only albedo adjustment and increased moisture availability rather than directly parameterized green roofs for detail physical processes. For example, Smith and Roebber (2011) investigated green roofs efforts in Chicago using the WRF-SLUCM model but did not directly parameterize the green roofs. Rather, they assumed a uniform increase of moisture availability and adjusted albedo within the entire urban domain at the roof level. A more efficient modelling approach for assessing the effectiveness of green roofs was applied by Li et al. (2014) in the Baltimore-Washington DC metropolitan area. They developed and used the Princeton UCM coupled with the WRF including well-tuned physical processes in the urban areas for investigating changes in surface and near surface UHI effects. Sharma et al. (2016) employed a physical based green roofs algorithm in the coupled WRF-UCM model, which was another practical solution for assessing green roofs impacts in reducing UHI effects. Therefore, the coupled WRF-SLUCM is an ideal tool not only for urban meteorology modelling but also an effective tool in evaluating the effectiveness of different UHI mitigation strategies at city scale.

2.9 Conclusions

This review presented a general overview on the UHI, heatwaves, impacts of increasing urbanization on the UHI, and various UHI mitigation strategies and modelling techniques. The major factors and their significance have been discussed on the formation, mitigation and modelling of the UHI. Although there are number of UHI mitigation strategies, the application of reflective materials on urban surfaces and increasing urban vegetation appear to be some of the most effective mitigation strategies in mitigating UHI effects. However, only few studies focus on the UHI mitigation strategies using particular types of urban vegetation such as urban forest/MF, MFAG and MSAG. In addition, the effectiveness of different mitigation strategies depends on their size of areas and

geographic and climatic conditions. Numerical models are commonly using urban weather and climate study, and the coupled WRF-SLUCM model is widely used for these purposes.

As outlined in Chapter 1, the aims of the thesis are to investigate impacts of future urban expansion on the UHI, and the effectiveness of green/cool roofs and GI scenarios in mitigating UHI effects in the city of Melbourne. This requires the use of a numerical atmospheric model as well as observational data-sets for model evaluation, and this is outlined in the next chapter.

Chapter 3

Methodology

3.1 Introduction

This Chapter describes the modelling tool and overall research methodology used in the thesis (please note that specific detailed methodology which is only relevant to particular chapters are provided in the publication which make up the chapter, for chapters 4 to 7). Section 3.2 presents a general overview of the meso-scale WRF-SLUCM model. A description of the different datasets used as part of the thesis and their sources is presented in section 3.3.

3.2. The WRF Model

3.2.1 Overall Description of the WRF Model

Regional Climate Models (RCMs) are used to dynamically downscale Global Circulation Models (GCMs) and re-analysis products from their relatively coarse resolutions of 150 to 250 km, down to much higher resolutions of 1 to 10 km. RCMs are modeling tools which can be used to examine changes in regional weather and climate, and these models can be used to investigate the effects of land-use changes, such as urban greening and urban expansion. RCMs solve the equations of energy, mass, momentum and humidity, and include parameterizations to account for processes, which cannot be resolved by solving fundamental equations (Hamdi and Schayes, 2005). One widely used RCM model is the advanced WRF meso-scale (Skamarock et al., 2005), which is a non-

hydrostatic mesoscale model designed for both research and operational use. The model allows for nesting to model resolutions of up to several hundred meters. The WRF model has been extensively used for urban climate/meteorology studies in different parts of the world (e.g., Argüeso et al., 2012; Li et al., 2014; Sharma et al., 2016). The model is driven with initial and lateral boundary conditions from reanalysis data, when the aim is to re-produce specific weather events from the past, or from GCMs, when the aim is to produce long-term current and future climate projections.

The WRF model explicitly resolves the state of atmospheric dynamics by using a series of mathematical equations of motion describing the flow of fluids. Atmospheric motions are determined based on solar radiation and interactions with earth surface including moisture, heat and momentum fluxes. The WRF-ARW dynamics solver was used to solve the fundamental equations, as it is the most commonly used dynamics solver in WRF. However, since the dynamics solver cannot explicitly resolve all processes, parameterization schemes are required. The WRF parameterization schemes includes the parameterization for the following physical processes: cloud microphysics, planetary boundary layer (PBL), convection, land surface and radiation (both longwave and shortwave). The WRF physics package offers multiple parameterization options for each physical process, and the user can customize the WRF model according to their needs (Rauscher et al., 2013).

The microphysics schemes parameterize the physical processes within a cloud. Small-scale atmospheric moisture, heat, and precipitation are included in this parameterization (Skamarock et al., 2008). Different microphysics schemes consider different water phase changes. For instance, the 6-class microphysics resolves rain snow, graupel, water vapor,

cloud water and ice while the 3-class microphysics only resolves water/ice, water vapor and rain/snow. In addition, the microphysics can be single moment or double moment to determine the physical traits of the precipitation in the cloud. Single moment schemes uses a single prediction equation for mass per precipitation type and a fixed distributed function for hydrometeor size while double moment schemes use a prediction equation to calculate hydrometeor concentrations per double-moment precipitation type (Lim and Hong, 2010). More complex microphysics schemes (e.g., the Thompson scheme, Thompson et al., 2008) are also available in the WRF model which requires substantial computation overhead and time.

Cumulus schemes are used to parameterize convective processes and the development of shallow clouds within a grid cell. Convective clouds and their associated effects are typically smaller than horizontal domain resolutions. Therefore, cumulus schemes are used to resolve vertical fluxes because of unresolved updrafts and downdrafts within the cloud (Arakawa, 2004; Mesinger and Arakawa, 1976). The Cumulus scheme also calculates motions surrounding the cloud (Arakawa, 2004). As the WRF model dynamical core can resolve convective processes less than 5 km horizontal resolution, the convective scheme is used for horizontal resolutions of 5 km or coarser.

The WRF model parameterizes both shortwave and longwave radiation. Radiation schemes include absorption, reflection and scattering by atmospheric gases and the surface. The outgoing shortwave radiation is calculated based on the surface albedo and cloud fractions (Skamarock et al., 2008). Longwave radiation schemes include either thermal or infrared radiation that is absorbed and emitted by atmospheric gases and land surface (Skamarock et al., 2008).

The PBL schemes play important role in the lower troposphere in parameterizing vertical fluxes of moisture, heat and momentum fluxes due to eddy transport in the atmospheric column (Hu et al., 2010). These schemes are used to calculate the flux profile within the boundary layer, which influence temperature, moisture, clouds and horizontal momentum. In addition, horizontal and vertical diffusion processes are also included in most PBL schemes. PBL schemes are typically classified as local or non-local closure schemes. A local closure scheme assumes that fluxes can move at the same level or neighbouring levels only. On the other hand, a non-local closure scheme assumes that fluxes can move within the entire vertical profile (Argüeso et al., 2012).

Land surface models (LSMs) parameterize the land surface processes by using information from surface layer, radiation, microphysics and cumulus schemes and combine them with data on land-surface properties (Skamarock et al., 2008). The heat and moisture fluxes computed by the LSM are used as a lower boundary layer condition to the PBL scheme. LSMs update land surface variables such as surface skin temperature, snow cover, canopy properties, soil temperature and moisture profiles (Skamarock et al., 2008). Finally, Figure 3.1 shows how all of the major physical processes interact with each other in the WRF model.

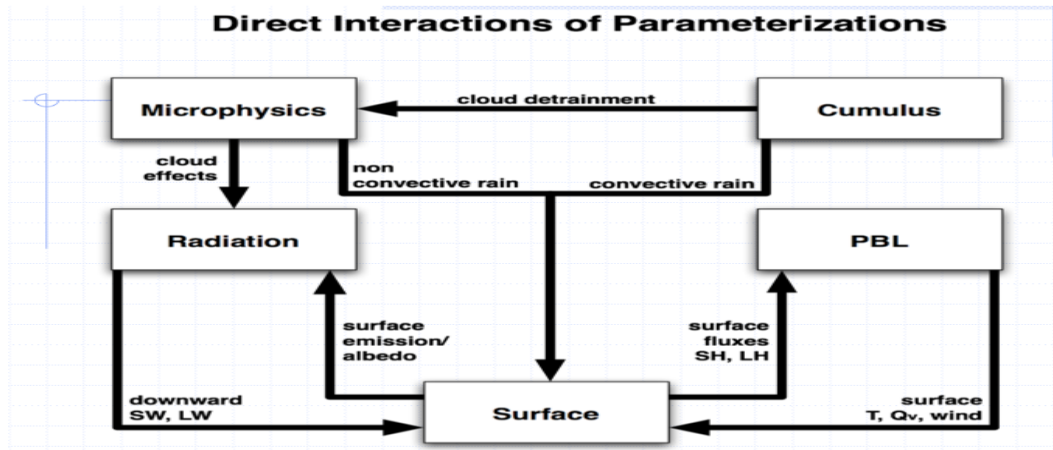


Figure 3.1 Interactions of various physical parameterizations of the WRF model (Dudhia, 2014)

For urban climate modeling, it is necessary to represent the complex physical processes associated with the exchange of heat, momentum and water vapor within the urban canopy, and these processes are not explicitly resolved by the LSM, thus requiring the need for explicit urban canopy schemes. To better represent the physical processes in urban areas, the Urban Canopy Model (UCM) in WRF offers three options; single layer UCM (SLUCM), Multi-layer Building Environment Parameterization (BEP) and Multi-layer Building Environment Model (BEM). These schemes are coupled with the Noah-LSM (Chen and Dudhia, 2001) in the WRF model. The coupled WRF-UCM model provides a more accurate simulation of atmospheric variables as compared to models that do not consider the effects of urban morphology (Lin et al., 2008). The SLUCM (Kusaka and Kimura, 2004; Kusaka et al., 2001) mainly improves the representation of lower boundary conditions and provides feedback for surface layer and PBL schemes (Kusaka et al., 2006). This thesis uses the SLUCM as the performance of this model is nearly equal to that of the multi-layer model for studying mesoscale heat islands (Kusaka and Kimura, 2004) and the model is commonly used in many urban climate studies (e.g.,

Argüeso et al., 2012; Lin et al., 2008; Liu et al., 2018; Sharma et al., 2016; Yang et al., 2016). The SLUCM has simplified urban geometry, which plays a key role in calculating the surface energy balance and wind shear in urban areas (Figure 3.2). The SLCUM includes a number of features such as canyon orientation, shading effect of building, shortwave and longwave radiation reflections, variations of azimuth angle, wind profile in canopy layer, anthropogenic heat and multi-layer heat transfer equations for roofs, walls and roads (Kusaka and Kimura, 2004). More specific details on the WRF-SLUCM is provided in Chapter 5.

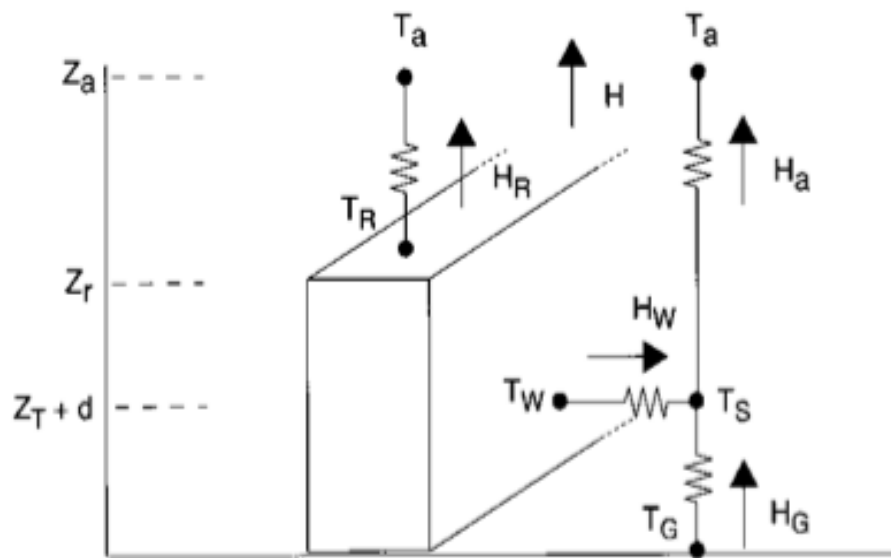


Figure 3.2 Schematic of the SLUCM. T_a is the air temperature at reference height Z_a , T_R is the building roof temperature, T_W is the building wall temperature, T_G is the road temperature, and T_S is the temperature defined at $Z_T + d$. H is the sensible heat exchange at the reference height. H_a is the sensible heat flux from the canyon space to the atmosphere, similarly, H_w is that from wall to the canyon space, H_G that from road to the canyon space, and H_R that from roof to the atmosphere (Kusaka et al., 2001).

3.2.2 Domain Configuration

The WRF model downscales GCMs or re-analysis data sets using the nested domains approach with increasing resolution. The model offers one-way and two-way nesting and common downscaling ratios are between 1:2 and 1:5. In one-way nesting, the parent domain passes information to the nested domain only. On the other hand, in two-way nesting, the parent domain provide boundary values for the nested domain, while the nested domain provides downscaled data back to its parent domain (Chen et al., 2011). In this thesis, two-way nested domain is used, which is a common approach in high resolution and short period simulations (e.g., Fallmann et al., 2014; Sharma et al., 2016). The parent domain is updated with information about small-scale processes from the inner nest, which improves model accuracy. The WRF model checks the reference state of each prognostic variable for ensuring that the coarse and finer grids are consistent at coincident points. The model also makes necessary adjustments if there is any discontinuities at the lateral boundaries (Skamarock et al., 2008).

Appropriate model configuration is important for obtaining the best results from the WRF for a particular application, since the model is highly sensitive to the physical parameterization options, input data, and domain size (Seth and Giorgi, 1998). The WRF model takes as input lateral boundary conditions from the driving re-analysis and any errors with this data will invariably propagate throughout the model (Kala et al., 2015). In addition, the size of the domains is chosen based on the information available in literature. Three two-way nested domains, with horizontal resolution of 18: 6: 2 km and 38 vertical layers is used in this thesis to simulate the heatwave events over the city of Melbourne (Figure 3.3). The extent of outer most domain cover a larger part of southeast

Australia while the 2nd domain covers major areas of the state of Victoria and the Tasman Sea. The inner most domain includes the city of Melbourne and surrounding rural areas.

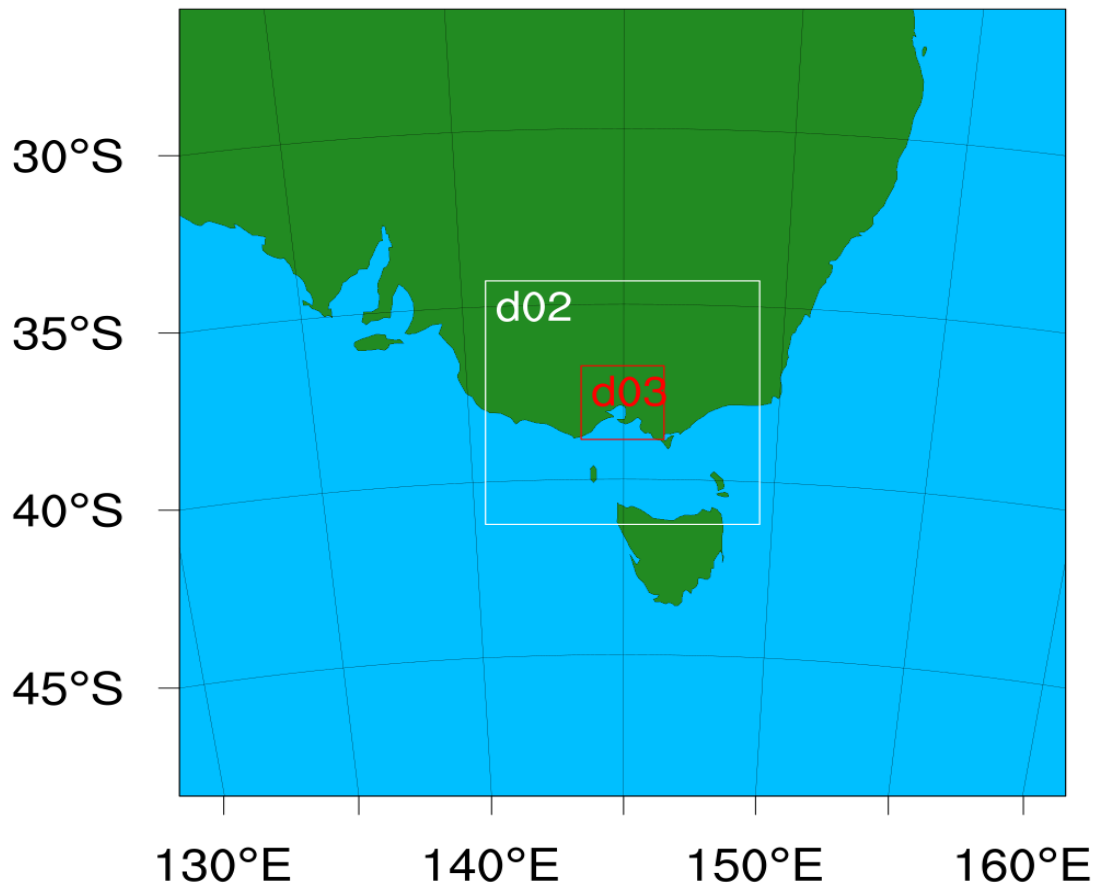


Figure 3.3 Location of modelling domains

3.2.3 Input Reanalysis Data

This thesis focuses on 4 of the worst heatwaves to have affected southeast Australia over the past decades. Hence, the WRF was driven with reanalysis rather than GCMs used for current and future climate projections. Re-analysis datasets are 3-dimensional gridded global assimilations of observational data assimilated in global numerical weather prediction models to better represent the state of the atmosphere at a particular point in

the past. Re-analysis data are considered as the near-perfect boundary conditions as these data are the best guess at representing the real state of the atmosphere at any one point in the past. The use of re-analysis data as initial and lateral boundary conditions as input the WRF model, allows the model output to be directly evaluated against observations. The most common reanalysis datasets are European Centre for Medium-Range Weather Forecasts ERA-interim (ERA-Int) (Dee et al., 2011), the National Centre for Environmental Prediction (NCEP) Final Operational Global Data Assimilation System (FNL), and the National Centre for Atmospheric Research/NCEP Reanalysis Data (NNRP) (Kalnay and Cai, 2003). ERA-interim is available at 1.5° and 0.75° resolutions and these data are available from 1980 to the present year. The FNL reanalysis datasets are available from 1999 to the present with 1° resolution. NNRP dataset are available from 1949 to the present year with 2.5° resolution. In this thesis, the ERA-interim data with 0.75° resolution is used as input to the WRF model since ERA-interim has been shown to better represent Australian climate as compared to other re-analysis data sets in the WRF (Kala et al., 2015). Finally, the WRF model was configured to update sea surface temperatures at a 6-hourly frequency using data from the ERA-interim. The ERA-interim included a large numbers of data sets including 3-D meteorological data (e.g., pressure, u, v, temperature, relative humidity, geopotential height), 3D soil data (e.g., soil temperature, soil moisture, soil liquid), 2D meteorological data (e.g., sea level pressure, surface pressure, surface u and v, surface temperature, surface relative humidity, input elevation) and 2-D meteorological optional data (e.g., sea surface temperature, physical snow depth, water equivalent snow depth) for representing the detailed weather and climatic conditions.

3.2.4 Static Data of the WRF Model

Besides the initial and boundary conditions data, the WRF model also requires information related to properties of the land surface such as topography, soil type and land use classification, which are static and do not change over time. These static data were obtained from the U.S. Geological Survey (Gesch et al., 1999) at 1 km resolution, which includes both 24-categories and 33-categories land use. Furthermore, the USGS 33-categories land use are modified in the WRF model based on Jackson et al. (2010) urban land category data for the city of Melbourne. In chapters 5 and 6, Jackson et al. (2010) urban data are used for classifying different urban land use types such as low-density, high-density and commercial/industrial areas for the city of Melbourne. Jackson et al. (2010) created a global urban dataset for the climate models for examining the potential effects of urbanization on the climate. For capturing the spatial variability in urban areas, the dataset represented three main urban properties such as spatial extent, urban morphology and thermal and radiative properties of building materials. This thesis used only the spatial extent of global urban dataset to define low-density, high-density and commercial/industrial areas for the city of Melbourne. Spatial extent of global urban data was derived based on density of population and calibrated over 33 regions (Jackson et al., 2010). Finally, the land use data was obtained from the Department of Agriculture and Water Resources, Australia (<http://www.agriculture.gov.au/abares/aclump/land-use/data-download>) and used to update USGS land use category.

3.3 Observational Data

The observational datasets were used to evaluate the WRF model in simulating atmospheric variables related to the UHI during heatwaves. The use of these datasets for evaluating the WRF model is discussed in detail in chapter 4. Hourly observational

datasets for temperature, wind speed and relative humidity at weather monitoring stations in Victorian state were used from the Australian Bureau of Meteorology (BoM). Daily gridded observed datasets for maximum and minimum temperatures at 1 km by 1 km resolution were obtained from the ANU Climate data-set (Chandler, 1965) (available online at: <http://dapds00.nci.org.au/thredds/catalog.html>). This dataset is an interpolation of station observations across the Australian continent and details of the algorithm can be found in Hutchinson et al. (2009) (Hutchinson et al., 2009). This observed gridded temperatures data was used to compute biases in the WRF model across the model domain. Atmospheric sounding data at 0000 and 1200 UTC for the weather station at Melbourne international airport was obtained from the website of the department of atmospheric science of Wyoming University (<http://weather.uwyo.edu/upperair/sounding.html>). Further details of use of these observational data-sets for evaluation are provided in Chapter 4.

Chapter 4

Sensitivity of the WRF Model to Physical Parameterization Options in Simulating the UHI and Heatwaves

4.1 Introduction

This chapter describes the model evaluation process by conducting a sensitivity analysis of the WRF model to different physical parameterization options for the Melbourne region. Sensitivity analyses are conducted in simulating the UHI and heatwaves over the city of Melbourne during four extreme heatwave events in 2000, 2006, 2007 and 2009. Different physical parameterization options are tested based on the literature and the performance in simulating various atmospheric variables is examined by comparing simulations against observations. Based on the overall best performance in simulating various atmospheric variables, the best WRF model configuration is determined, and this configuration is used for the rest of the chapters.

GRADUATE RESEARCH CENTRE

DECLARATION OF CO-AUTHORSHIP AND CO-CONTRIBUTION: PAPERS INCORPORATED IN THESIS BY PUBLICATION

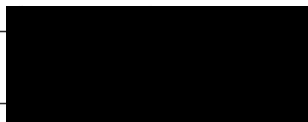
This declaration is to be completed for each conjointly authored publication and placed at the beginning of the thesis chapter in which the publication appears.

1. PUBLICATION DETAILS (to be completed by the candidate)

Title of Paper/Journal/Book:	An evaluation of the performance of a WRF multi-physics ensemble for heatwave events over the city of Melbourne in southeast Australia		
Surname:	Hosen	First name:	Md Imran
College:	College of Engineering & Science	Candidate's Contribution (%):	85 %
Status:			
Accepted and in press:	<input checked="" type="checkbox"/>	Date:	09-06-17
Published:	<input checked="" type="checkbox"/>	Date:	19-06-17

2. CANDIDATE DECLARATION

I declare that the publication above meets the requirements to be included in the thesis as outlined in the HDR Policy and related Procedures – policy.vu.edu.au.

	14-08-18
Signature	Date

3. CO-AUTHOR(S) DECLARATION

In the case of the above publication, the following authors contributed to the work as follows:

The undersigned certify that:

1. They meet criteria for authorship in that they have participated in the conception, execution or interpretation of at least that part of the publication in their field of expertise;
2. They take public responsibility for their part of the publication, except for the responsible author who accepts overall responsibility for the publication;
3. There are no other authors of the publication according to these criteria;
4. Potential conflicts of interest have been disclosed to a) granting bodies, b) the editor or publisher of journals or other publications, and c) the head of the responsible academic unit; and

5. The original data will be held for at least five years from the date indicated below and is stored at the following location(s):

College of Engineering and Science, Victoria University, Melbourne, Australia

Name(s) of Co-Author(s)	Contribution (%)	Nature of Contribution	Signature	Date
Dr. Anne Ng	5%	Review comments, Discussion on conceptual ideas		14/8/18
Dr. Shobha Muthukumaran	5%	Review comments, Discussion on conceptual ideas		14/8/18
Dr. Jatin Kala	5%	Critical review comments, Discussion on conceptual ideas		15/8/18

Imran, H.M., Kala, J., Ng, A.W.M. et al. An evaluation of the performance of a WRF multi-physics ensemble for heatwave events over the city of Melbourne in southeast Australia. *Clim Dyn* 50, 2553–2586 (2018). <https://doi.org/10.1007/s00382-017-3758-y>

The full-text of this article is subject to copyright restrictions, and cannot be included in the online version of the thesis.

The published version is available at: <https://doi.org/10.1007/s00382-017-3758-y>

Chapter 5

Green and Cool Roofs Mitigation Strategies in Reducing UHI Effects during Heatwave Event

5.1 Introduction

Having determined the ideal WRF model configuration in Chapter 4, this chapter examines the effectiveness of GI practices such as green and cool roofs in mitigating UHI effects and improving HTC for the city of Melbourne during one of the most severe heatwave events over southeast Australia in 2009. The effectiveness of green and cool roofs strategies in reducing UHI effects and improving HTC is examined for the existing urban areas for the Melbourne metropolitan areas, by conducting experiments with increasing fractions of green roofs, and increase albedo values for cool roofs. The effectiveness of green and cool roofs in mitigating UHI effects is analysed at city scale and the effectiveness of these strategies is also analysed separately for low-density, high-density, and commercial/industrial areas.

GRADUATE RESEARCH CENTRE

DECLARATION OF CO-AUTHORSHIP AND CO-CONTRIBUTION: PAPERS INCORPORATED IN THESIS BY PUBLICATION

This declaration is to be completed for each conjointly authored publication and placed at the beginning of the thesis chapter in which the publication appears.

1. PUBLICATION DETAILS (to be completed by the candidate)

Title of Paper/Journal/Book:	Effectiveness of Green and Cool Roofs in Mitigating Urban Heat Island Effects during a heatwave event in the city of Melbourne in southeast Australia		
Surname:	Hosen	First name:	Md Imran
College:	College of Engineering & Science	Candidate's Contribution (%):	85 %
Status:			
Accepted and in press:	<input checked="" type="checkbox"/>	Date:	16-06-2018
Published:	<input checked="" type="checkbox"/>	Date:	18-06-2018

2. CANDIDATE DECLARATION

I declare that the publication above meets the requirements to be included in the thesis as outlined in the HDR Policy and related Procedures – policy.vu.edu.au.

	
Signature	Date

3. CO-AUTHOR(S) DECLARATION

In the case of the above publication, the following authors contributed to the work as follows:

The undersigned certify that:

1. They meet criteria for authorship in that they have participated in the conception, execution or interpretation of at least that part of the publication in their field of expertise;
2. They take public responsibility for their part of the publication, except for the responsible author who accepts overall responsibility for the publication;
3. There are no other authors of the publication according to these criteria;
4. Potential conflicts of interest have been disclosed to a) granting bodies, b) the editor or publisher of journals or other publications, and c) the head of the responsible academic unit; and

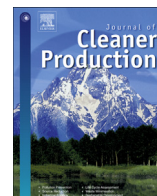
5. The original data will be held for at least five years from the date indicated below and is stored at the following location(s):

College of Engineering and Science, Victoria University, Melbourne, Australia

Name(s) of Co-Author(s)	Contribution (%)	Nature of Contribution	Signature	Date
Dr. Anne Ng	5%	Review comments, Discussion on conceptual ideas		14/8/18
Dr. Shobha Muthukumaran	5%	Review comments, Discussion on conceptual ideas		14/8/18
Dr. Jatin Kala	5%	Critical review comments, Discussion on conceptual ideas		15/8/18

This is the peer-reviewed published version of the following article:

H.M. Imran, J. Kala, A.W.M. Ng, S. Muthukumaran, Effectiveness of green and cool roofs in mitigating urban heat island effects during a heatwave event in the city of Melbourne in southeast Australia, *Journal of Cleaner Production*, Volume 197, Part 1, 2018, Pages 393-405, ISSN 0959-6526, <https://doi.org/10.1016/j.jclepro.2018.06.179>



Effectiveness of green and cool roofs in mitigating urban heat island effects during a heatwave event in the city of Melbourne in southeast Australia

H.M. Imran ^{a, c, *}, J. Kala ^b, A.W.M. Ng ^{a, c}, S. Muthukumaran ^{a, c}

^a College of Engineering and Science, Victoria University, Melbourne, Australia

^b Environmental and Conservation Sciences, School of Veterinary and Life Sciences, Murdoch University, Perth, Western Australia, Australia

^c Institute for Sustainable Industries & Livable Cities, Victoria University, Melbourne, Australia

ARTICLE INFO

Article history:

Received 1 February 2018

Received in revised form

5 June 2018

Accepted 16 June 2018

Available online 18 June 2018

Keywords:

UHI mitigation

Green & cool roofs

Coupled WRF-SLUCM

Thermal comfort

UTCI

ABSTRACT

This study evaluates the effectiveness of green and cool roofs as potential Urban Heat Island (UHI) mitigation strategies, and the impacts of these strategies on human thermal comfort during one of the most extreme heatwave events (27th - 30th January 2009) in the city of Melbourne in southeast Australia. The Weather Research and Forecasting model coupled with the Single Layer Urban Canopy Model including different physical parameterization for various types of roofs (conventional, green and cool roofs) is used to investigate the impacts of green and cool roofs. Results show that the maximum roof surface UHI is reduced during the day by 1 °C–3.8 °C by increasing green roof fractions from 30% to 90%, and by 2.2 °C–5.2 °C by increasing the albedo of cool roofs from 0.50 to 0.85. Cool roofs are more efficient than the green roofs in reducing the UHI with maximum differences of up to 1.4 °C. The reductions of the UHI vary linearly with the increasing green roof fractions, but slightly non-linearly with the increasing albedo of cool roofs. The maximum reductions in wind speed are 1.25 m s⁻¹ and 1.75 m s⁻¹ with 90% green and cool roofs (albedo 0.85) respectively. While previous studies report that the advection of moist air from rural areas is a key mechanism, this study shows that this is not the case for the extreme heatwave event due to the very dry and warm conditions, and instead, convective rolls play a more important role. This study also shows that initial soil moisture for green roofs does not have a substantial impact on the UHI. Finally, green roofs improve human thermal comfort by reducing the Universal Thermal Comfort Index by up to 1.5 °C and 5.7 °C for pedestrian and roof surface levels respectively, and by 2.4 °C and 8 °C for cool roofs for the same levels.

© 2018 Elsevier Ltd. All rights reserved.

1. Introduction

The increasing urban population is imposing a burden on the urban environment and climate. Urban dwellers are expected to contribute up to 70% of the world population by 2050 (O'malley et al., 2014). Vegetated surfaces are continuously being converted into urban and built surfaces to meet the increasing demand of the increasing urban population. This increased urbanization has substantial impacts by altering the surface energy balance, and consequently, affects the regional hydro-climatology (Song and Wang, 2015). One of the well-known urbanization effects on

urban climate is the Urban Heat Island (UHI), which results in higher temperatures in urban areas as compared to surrounding non-urban and nearby rural areas. Primarily, the UHI occurs due to human modifications of surface properties by using construction materials with lower albedos and higher specific heat capacity (e.g., bitumen on roads), reductions in vegetated areas, the emission of anthropogenic heat (e.g., via air conditioning). In addition, anthropogenic climate change is expected to result in more frequent incidents of climate extremes such as heatwaves in several parts of the globe (e.g., Cowan et al., 2014), and this poses additional threats to the urban environment (Field et al., 2014).

The definition of heatwave can be different according to different sectors. This paper refers to the meteorological definition which is based on percentiles (Perkins and Alexander, 2013), as at least three consecutive days during which the average of the

* Corresponding author. College of Engineering and Science, Victoria University, PO Box 14428, Melbourne, Victoria, Australia.

E-mail address: ihosen83@gmail.com (H.M. Imran).

maximum and minimum temperatures exceeds the climatological 95th percentile (Nairn and Fawcett, 2013). The UHI in combination with heatwave events severely affects human thermal comfort (HTC), ecosystems, the urban environment and the urban climate. The combination of UHI effects and heatwaves is becoming a very important issue in southeast Australia because of its hot summer season, with data from the Australian Bureau of Meteorology Melbourne regional office weather station showing that maximum temperatures reached up to 45.1 °C and 43.9 °C in January 2009 and 2014 respectively (Victorian Auditor General's Report, 2014). Australia is also expected to experience an overall increase in the duration, frequency, and intensity of heatwaves under future climate change (Cowan et al., 2014). Therefore, there is an urgent need to develop effective policies to make cities more resilient to anthropogenic impacts, such as heatwaves and the UHI.

Research on the mitigation of UHI effect has gained significant attention in recent years. A number of mitigation strategies in urban areas have been proposed in the literature, such as using more reflective construction materials (Morini et al. 2016, 2017; Touchaei et al., 2016), geometry of buildings (e.g., orientation, shape) (Guan et al., 2014), increasing urban vegetation fractions, and the use of green and cool roofs (Razzaghmanesha et al., 2016; Razzaghmanesha and Razzaghmanesha, 2017; Sharma et al., 2016; Li et al., 2014; Akbari et al., 2003). All these studies show that increasing the proportion of green spaces and higher albedo materials in urban areas have potential in mitigating UHI effects in cities. According to Akbari et al. (2003), green and cool roofs are effective strategies for mitigating UHI effects because of the substantial area covered by rooftops within cities. Both green and cool roofs reduce the UHI effects by reducing sensible heat flux, but the mechanism is different. Green roofs reduce sensible heat flux by providing shade and repartitioning available energy to increased latent heat flux via evapotranspiration. On the other hand, cool roofs reflect more incoming solar radiation due to higher albedo, and consequently, reduce sensible heat flux as a result of lower net radiation.

The effectiveness of green and cool roofs in mitigating UHI effects has been investigated based on different modeling techniques including building energy consumption (Rosenfeld et al., 1998; Wong et al., 2003) and hydrological budget (Carson et al., 2013; Sun et al., 2014) at different spatial scales. Several studies use regional climate models (RCMs) for investigating the effects of green and cool roofs on the urban environment at the synoptic scale (e.g., Synnefa et al., 2008; Millstein and Menon, 2011). In recent years, some studies have investigated the cooling effect of cool roofs by altering the albedo of urban areas by using RCMs (Morini et al., 2016, 2017; Touchaei et al., 2016; Taha 2008a, 2008b) and global climate models (GCMs) (e.g., Oleson et al., 2010; Irvine et al., 2011; Akbari et al., 2012). The relatively coarse resolution of GCMs does not allow for an accurate representation of landscape heterogeneity, and hence, the complex physical processes in the urban canopy cannot be resolved. RCMs, on the other hand, are useful tools in assessing the effectiveness of green and cool roofs in mitigating the UHI, as they are able to better resolve cities by using urban canopy parameterizations which include sub-grid scale effects.

Smith and Roebber (2011) used the Weather Research and Forecasting (WRF) model (Skamarock et al., 2005) coupled with single Urban Canopy Model (SLUCM) (Kusaka and Kimura, 2004), referred to as WRF-SLUCM, to investigate the effects of green and cool roofs on the urban climate of the city of Chicago in the US. They did not consider direct parameterizations for green roofs but adjusted the albedo for the entire urban domain neglecting the physical processes (e.g., additional moisture added by green roofs) relevant to green roofs. A more comprehensive study including

direct parameterizations of green and cool roofs has been conducted by Li et al. (2014) over the Baltimore–Washington DC metropolitan region in the USA during a heatwave event. They introduced a new urban parameterization model, the Princeton UCM (PUCM) coupled to the WRF model to assess changes in surface and near surface UHI and showed that soil moisture plays an important role in improving the performance of green roofs by controlling evaporation efficiency, consistent with previous studies (Sun et al., 2013). Several recent studies have assessed the effectiveness of green and cool roofs for UHI mitigation in city areas by using the coupled WRF-SLUCM model (Yang et al., 2015; Sharma et al., 2016). These latter have shown that green and cool roofs can substantially reduce roof surface temperature via a reduction in sensible heat flux. In addition, green and cool roofs alter the surface energy balance, which modifies the moisture and heat fluxes between the land surface and atmosphere, and weakens vertical mixing during the day, and hence, reduces the boundary-layer height (Miao et al., 2009; Sharma et al., 2016).

In Melbourne, and across southeast Australia, heatwaves have become more frequent in the last 20 years (Perkins-Kirkpatrick et al., 2016). The city of Melbourne has experienced the two most severe heatwave events in 2009 and 2014 in the past 10 years and these events have contributed significantly to increased mortality. According to the Victorian Auditor General's Report (2014), these two heatwaves have caused 374 and 167 excess deaths respectively, in the state of Victoria. The average annual number of days above 35 °C in the city of Melbourne is likely to double by 2030 and triple by 2070 (Climate Institute, 2013). Additionally, the average intensity of heatwave has increased by 1.5 °C with the peak heatwave day likely to be 2 °C warmer than the long-term heatwave average in the city of Melbourne (Steffen et al., 2014). Hence, there is a critical need to investigate UHI mitigation strategies, such as the use of green and cool roofs, for the city of Melbourne during heatwave events. Therefore, the present study investigates the effectiveness of green and cool roofs in mitigating UHI effects and explores the physical mechanisms/processes associated with these mitigation strategies during the heatwave event.

The WRF-SLUCM modeling system is used to evaluate the effectiveness of green and cool roofs in mitigating UHI effects in the city of Melbourne. Additional experiments are carried out with different initial soil moisture for green roofs to investigate the role of evapotranspiration in reducing the UHI. Furthermore, the paper focuses on the changes in boundary-layer dynamics as well as the effectiveness of green and cool roofs in improving the HTC, since UHI effects are exacerbated during heatwaves which increase heat-related illness and mortality. The key factors involved in improving HTC in urban areas during heatwave conditions are explored.

2. Methodology

2.1. Case study

This paper focuses on an extreme heatwave event lasting 3 days from the 27th to the 30th of January in 2009. This event was selected because it is one of the most severe heat waves in southeast Australia, which preceded the devastating Black Saturday bushfires in early February 2009 (Engel et al., 2013). This event occurred after a period of prolonged drought which is reported to have contributed up to 1 °C–3 °C to the heatwave event (Nicholls and Larsen, 2011), and antecedent soil moisture conditions have been shown to play an important role (Kala et al., 2015a).

2.2. WRF configuration

This study uses the WRFv3.8.1 model, which is a non-

hydrostatic RCM (Skamarock et al., 2008), which has been widely used for urban meteorology studies (e.g., Li and Bou-Zeid, 2014; Li et al., 2014; Yang et al., 2015; Sharma et al., 2016). The model was operated with three nested domains (d01, d02, and d03) as illustrated in Fig. 1(a) showing the three domains at 18 km, 6 km and 2 km resolution respectively. The second domain (d02) covers a large part of the state of Victoria while the innermost domain (d03) covers the Melbourne metropolitan area and surrounding rural areas. Following Imran et al. (2017), land-use categories from USGS were used to define the dominant land-use type for each grid cell. To obtain a more accurate representation of urban land-use, the global urban land-use dataset of Jackson et al. (2010) was used to represent the variability of urban categories in the modeling domain. The Jackson et al. (2010) data set represents four categories of urban areas (low-density urban, medium density urban, high-density urban and tall building areas) and properties such as urban morphology, urban extent, and radiative and thermal properties of building materials. In this study, we used the spatial extent of urban areas from Jackson et al. (2010) to re-classify all urban grid cells as either low-density urban, high-density urban, or commercial/industrial areas, as required by the SLUCM. The low and medium density urban areas of the Jackson et al. (2010) land-use

dataset were classified as low-density and high-density urban areas respectively, while the high-density urban areas and tall buildings were classified as commercial/industrial areas, as illustrated in Fig. 1(b). Such a re-classification allowed for a realistic representation of urban land-use categories for the region. Finally, non-urban land use categories were modified based on the Australian Land Use and Management Classification Version 7 (<http://www.agriculture.gov.au/abares/aclump/land-use/alum-classification>). The dominant land use categories across the model domain are shown in Fig. 1(b).

As part of configuring the WRF model, a user needs to specify the number of vertical atmospheric levels to be used. Following Imran et al. (2017), this study used 38 vertical levels from the surface to 50 hPa (top of the atmosphere), with levels more closely spaced close to the surface, so as to better resolve near surface atmospheric processes, and wider apart in the upper troposphere where high vertical resolution is not required. The WRF model offers multiple options for different physical parameterizations, including cloud microphysics (MP), planetary boundary layer (PBL), radiation, land surface model (LSM) and cumulus processes, and the model is well documented to be sensitive to the choice of physics options (e.g., Evans et al., 2012; Kala et al., 2015a). The choice of physical parameterizations was based on Imran et al. (2017) who investigated the sensitivity of WRF to different physical parameterizations and provided an ideal set-up for the simulation of heatwaves in southeast Australia. This includes: (a) the Noah LSM (Chen and Dudhia, 2001) coupled with the SLUCM (Chen and Dudhia, 2001; Liu et al., 2006; Chen et al., 2011), (b) the Mellor–Yamada–Janjic (MYJ) PBL scheme (Janjić, 1994), (c) the Thompson MP (Thompson et al., 2008), (d) the RRTMG shortwave and longwave radiation schemes (Iacono et al., 2008). No cumulus physics parameterization is used for the domain d03 as convection is resolved at 2 km resolution, while the Grell3D scheme (Grell and Dévényi, 2002) is used for the outer two domains d01 and d02. The interactions between these different physical parameterizations are illustrated in Fig. 2. For a more detailed description of the WRF model, we refer the reader to Skamarock et al. (2005), and for more details on WRF configuration, we refer the reader to WRF user's guide available online at http://www2.mmm.ucar.edu/wrf/users/docs/user_guide_V3/contents.html. The initial and boundary conditions for the WRF simulations were obtained from 6-hourly ERA-interim reanalysis product with $0.75 \times 0.75^\circ$ spatial resolution

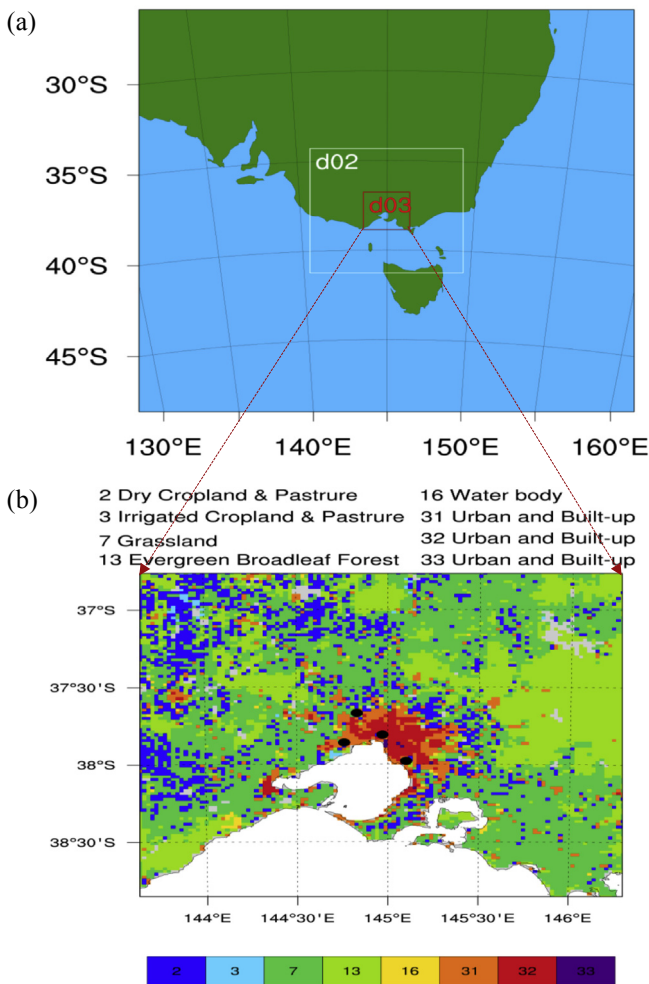


Fig. 1. (a) WRF domain configuration, d02 represents the second domain which has a resolution of 6 km, and d03 represents the innermost domain with a resolution of 2 km. (b) Dominant land use categories in the innermost domain (d03) with the locations of four weather stations (Black Circles) from the Australian Bureau of Meteorology, used for evaluation.

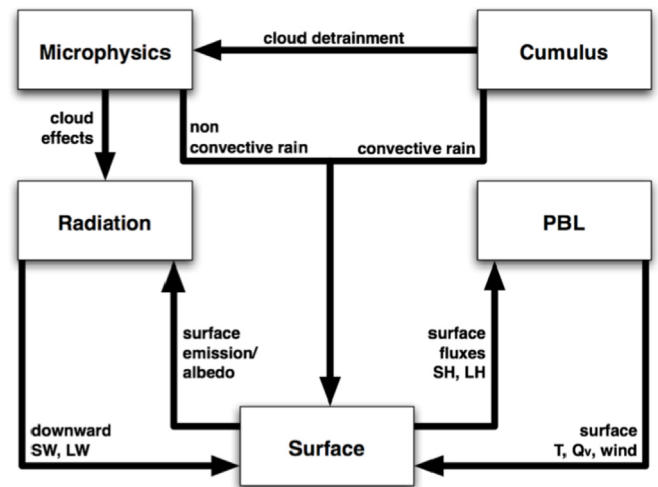


Fig. 2. Interactions between different physical parameterizations in the WRF model (Dudhia, 2014).

available from 1970 onwards (Dee et al., 2011). All analysis has been performed considering only the innermost domain (d03) for Melbourne metropolitan area.

2.3. Numerical set-up of green and cool roofs

The updated SLUCM incorporates various urban parameterizations for green and cool roofs (Chen et al., 2011). The SLUCM takes into consideration important properties of the urban canyon environment including solar azimuth angle, orientations of an urban canyon and the shadowing effects of buildings (Kusaka et al., 2001). The model diagnoses air temperature, skin temperature, wind speed, relative humidity and fluxes from all surfaces within the canyon. The SLUCM resolves air temperature at the top of the canyon exchanged with the lowest level of the atmosphere incorporating all factors within the urban canopy (Smith and Roebber, 2011).

Green roofs in the SLUCM consist of four different layers and a vegetation layer, and an urban irrigation algorithm is included. The total depth of the four layers is 50 cm including a 15 cm loam soil (5 cm top soil + 10 cm soil) layer for grassland, 15 cm growing medium layer, and 20 cm for concrete roof layer. In the SLUCM, the grid cells are treated as urban if the dominant land use category is classified as either low-density urban or high-density urban or commercial/industrial areas. When the SLUCM is used, an urban grid cell is further divided into an impervious and a grass-covered fraction as described by Chen et al. (2011). The grass fraction of the SLUCM represents urban parks and lawns and captures small scale variability inside the built terrain (Li et al., 2013). Fig. 3 shows a typical schematic diagram for impervious and vegetated fractions in the SLUCM for different roofs. Urban/built fraction includes buildings, roads, pavements and artificial built surfaces while vegetated fraction incorporates a cropland/grassland mosaic. The figure also illustrates energy fluxes for conventional, green and cool roofs.

The urban morphological properties used in this study are the same as the properties used in the default WRF model, except for

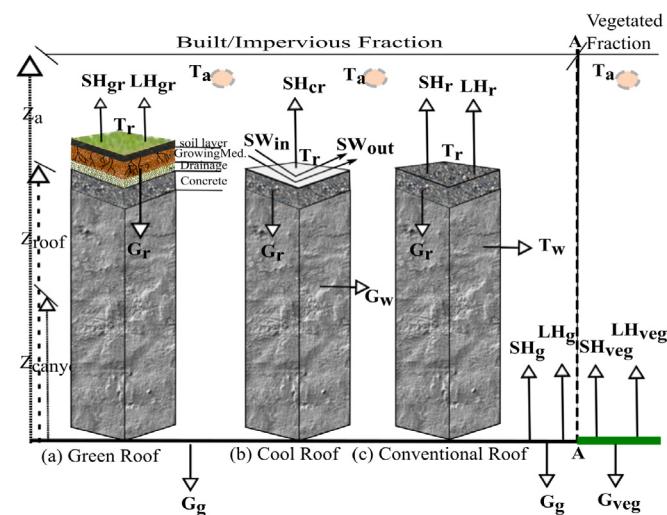


Fig. 3. A typical framework of an urban grid cell in the WRF-SLUCM. The SLUCM incorporates a built/impervious fraction (left side of line A-A) and another vegetated fraction (right side of boldly dotted line-A). The subscripts a, cr, g, gr, r, veg, and w represent air, cool roof, ground, green roof, conventional roof, vegetation and wall, respectively while the T, SH, LH, G and SW represent temperature, sensible heat flux, latent heat flux, storage heat and shortwave radiation. Finally, Z_{canyon} , Z_{roof} and Z_a represents street canyon height, rooftop height, and the first level of atmospheric model (adapted from Sharma et al., 2016).

the built/impervious fraction for low-density urban areas (Table 1). The SLUCM includes several parameters for each of the three urban categories, and the default parameters may not necessarily be representative for a particular city. Although the default impervious fraction in the WRF model is 0.50 for the low-density urban area, this study uses a 0.70 impervious fraction for the same area based on previous study by Coutts et al. (2007), who used urban fraction 0.71 for low-density areas for the city of Melbourne. Moreover, we found that the WRF model underestimated the near-surface temperature in our previous study (Imran et al., 2017). Therefore, an urban fraction of 0.50 for low-density urban areas appears to be too low, and hence this study uses a fraction of 0.70 to obtain more realistic simulations as compared to observations. The use of a higher urban fraction is also consistent with other studies whereby all urban areas were considered as high-density urban and assigned an urban fraction of 0.90 for all urban grid cells for the city of Sydney in Australia (Argueso et al., 2014).

2.4. Design of numerical experiments

Following Imran et al. (2017), simulations are carried out from the 27th to the 30th of January 2009 with the first 24 h considered as spin-up time and the remaining 72 h are used for analyses. Hourly outputs are used to assess the effectiveness of green and cool roofs for mitigating the UHI effects. The numerical experimental set-up using different roofs is shown in Table 2. The effectiveness of green and cool roof strategies in mitigating UHI effects are investigated by running experiments with increasing green roof fractions and roof-top albedo of the urban grid cells. The first experiment is for the conventional roofs (control) with an albedo of 0.20. This numerical experiment is designed as a standard coupled WRF-SLUCM model by updating only three urban categories (low density, high density and commercial/industrial areas) according to the Jackson et al. (2010) data-set for the city of Melbourne (Fig. 1(b)). The non-urban grid cells were not modified. The second numerical experiments are carried out to examine the effectiveness of cool roofs by using different albedo values of 0.50, 0.70 and 0.85. The third series of experiments are conducted to evaluate the effectiveness of green roofs employing different percentages of green roof fractions of 30%, 50%, 70% and 90%. The choice of these percentages was based on a study by Sharma et al. (2016) who showed that large percentages of green roof fractions are needed so as to result in noticeable effects of green roofs using the WRF-SLUCM. On the other hand, 100% cool roof is used for all cool roofs experiments as the default SLUCM does not have the functionality to alter the cool roof fraction, the idea being that the entire roof is painted or covered with reflective material. These reflective materials can be made of a highly reflective type of paint, a sheet covering, tiles or shingles. In the final numerical experiments, the cooling benefit of increased soil moisture in 50% green roofs is examined by using initial soil moisture of 0.30 and 0.40 $\text{m}^3 \text{m}^{-3}$ as compared to the default initial soil moisture of 0.15 $\text{m}^3 \text{m}^{-3}$ to examine the performance of green roofs under very dry conditions. The default initial soil moisture of green roofs is 0.20 $\text{m}^3 \text{m}^{-3}$. The rationale for using higher initial soil moisture was to investigate the effects of “once-off” irrigation at the start of the heat-wave event, and how long any subsequent cooling effects would last.

2.5. Outdoor HTC calculations

This study uses the UTCI index for representing the outdoor HTC by quantifying a physiological response based on meteorological input data. Although, there are several HTC indices such as the Discomfort Index, the approximate wet bulb globe temperature, and the Physiological Equivalent Temperature, for describing HTC,

Table 1

The urban properties for the three urban categories used by the SLUCM.

Properties/Parameters	Low-Density Urban	High-Density Urban	Commercial/Industrial
Built/Impervious fraction	0.70 (default 0.50)	0.90	0.95
Roof width (Rf)	8.3 m	9.4 m	10 m
Road width (Rd)	8.3 m	9.4 m	10 m
Roof fraction in built/impervious part [Rf/(Rf + Rd)]	50%	50%	50%
Roof fraction in whole urban grid	25%	45%	47.5%
Building Height	5 m	7.5 m	10 m

Table 2

Numerical experimental set-up.

Numerical Experiment	Type of roof	Albedo	Cool Roof Fraction	Green Roof Fraction	Initial Soil Moisture
Control	Conventional	0.2	–	–	–
Cool	Cool	0.50, 0.70 and 0.85	100%	–	–
Green	Green	–	–	30%, 50%, 70% and 90%	–
SMOIS	Green	–	–	50%	0.15, 0.30 and 0.40 m ³ m ⁻³

the UTCI is most widely used (Bröde et al., 2012a; Vatani et al., 2016).

The UTCI index is a widely accepted HTC index in representing bioclimatic conditions related to thermal stress under various climatic conditions which make this index more universal (Blazejczyk et al., 2012). The RayMan Pro 3.1 model is used for calculating the UTCI where the default clothing factor of 0.9 and activity rate of 80 W is used for a male of 35 years age. The UTCI index considers not only air temperature effects on the human body but also other climatic factors of wind speed, relative humidity and solar radiation (Johansson, 2006). The temperature, wind speed, relative humidity and solar radiation simulated by the WRF model are used as inputs in the RayMan model. The physical basis, abilities and limitations of RayMan have been discussed by Matzarakis et al. (2010). The UTCI index is classified into five categories as shown in Table 3 according to the scale proposed by Bröde et al. (2012b).

3. Results and discussion

3.1. Evaluation of the WRF model

The WRF model has been evaluated for the Melbourne region in our previous study (Imran et al., 2017), where we conducted an extensive sensitivity analysis of the WRF model to different physics options in simulating four heatwave events, including the case-study used in this paper. In our previous study (Imran et al., 2017), we compared WRF simulations against station and gridded surface observations as well as atmospheric soundings. We tested a number of physics options for each physical parameterization and evaluated the WRF model based on statistical analyses. In addition, we carried out an in-depth analysis of the physical processes associated during heatwaves and how these physical dynamics were simulated by the model. Finally, we showed that the WRF model was able to simulate the various climate variables the city of

Table 3

Universal Thermal Comfort Index (UTCI) range for different grades of human thermal perception and associated physiological stress (Bröde et al., 2012b).

UTCI (°C)	Physiological Stress
+9 to +26	no thermal stress
+26 to +32	moderate heat stress
+32 to +38	strong heat stress
+38 to +46	very strong heat stress
> +46	extreme heat stress

Melbourne during heatwave events. As additional evaluation for this paper, we compare the simulated hourly near-surface temperature (T2) and wind speed (10 m) against observations from four weather stations in the urban region from the Australian Bureau of Meteorology (black circles in Fig. 1(b)). The observed and simulated near-surface temperature and wind speed are averaged across the four weather stations. This is illustrated in Fig. 4 showing that the simulated temperature and wind speed were very close to observations, with relatively small differences between the model and observations. The WRF simulations captured the observed near surface and wind speed reasonably well, although the model had a tendency to simulate the increase in wind-speed slightly earlier than observed. Together with our previous evaluation (Imran et al., 2017), Fig. 4 shows that WRF performs satisfactorily and can be used for UHI studies, consistent with the existing literature (Sharma et al., 2014).

3.2. Diurnal cycles of sensible heat flux and UHI

Diurnal cycles of sensible heat flux, near-surface, and roof surface UHI are shown in Fig. 5 for the conventional roof (control), cool roof (albedo 0.85), and 90% green roof experiments. The Control simulation shows that the city of Melbourne is experiencing a near-surface UHI from 1.5 to 5.7 °C, and a roof-surface UHI from 3.0 to 11.0 °C, and the maximum UHI occurs in the evening. Diurnal variations of simulated near-surface and roof-surface UHI have

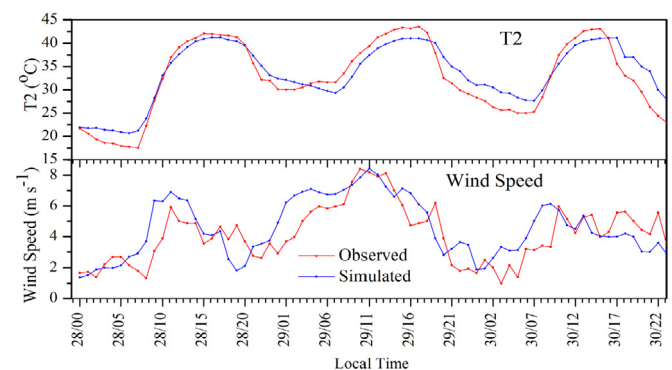


Fig. 4. Comparison of observed and simulated near-surface temperature (top) and wind speed (bottom) for 28–30 January 2009 at four BoM weather stations (black circle in Fig. 1(b)) in the urban areas. The mean from the four stations, and WRF outputs from the closest grid point to the stations are plotted.

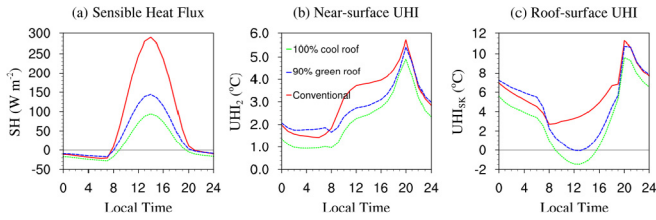


Fig. 5. Diurnal variations of (a) sensible heat flux ($W m^{-2}$), (b) near-surface UHI (UHI_2) ($^{\circ}C$) and (c) roof surface UHI (UHI_{sk}) from domain d03 averaged over 3 days (from 28th to 30th January 2009). Sensible heat flux results are averaged over urban grid points only and the UHI is the difference in near surface and roof surface temperature between urban and surrounding rural grid cells.

different hourly variations but reach their peak at the same time at 2000 local time while sensible heat flux reaches its peak at 1430 local time. The use of 90% green roof fraction results in lower sensible heat flux, near-surface and roof-surface UHI as compared to conventional roofs during the day while the cool roofs (albedo 0.85) result in the lowest sensible heat flux, near-surface and roof-surface UHI during both the day and night. The near-surface UHI shows an increasing trend during the day while the roof-surface UHI shows the opposite. Interestingly both green and cool roofs show maximum reductions during the day. Cool roofs with an albedo of 0.85 are more effective than 90% green roofs, with larger reductions in the sensible heat flux, near-surface and roof surface UHI. Although green roofs result in a slight warming during the early morning, cool roofs substantially reduce warming effects during both the day and night. It is noteworthy that both green and cool roofs are also effective in reducing sensible heat flux, near-surface and roof surface UHI, even when they reach their peaks.

3.3. Effectiveness of green roofs in mitigating UHI effects

Fig. 6 shows the energy balance of different green roof fractions in urban areas. Green roofs substantially reduce sensible heat flux, storage heat and net radiation, and increase latent heat flux. Increased green roof fractions (0%–90%) can reduce the daily peak sensible heat flux by up to $150 W m^{-2}$. Interestingly, green roofs especially 90% green roof fraction results in slightly higher sensible heat flux during the morning and late-night. The daily peak latent heat flux is higher by $70 W m^{-2}$ when 90% green roof fraction is used. The higher latent heat flux would be expected to result in

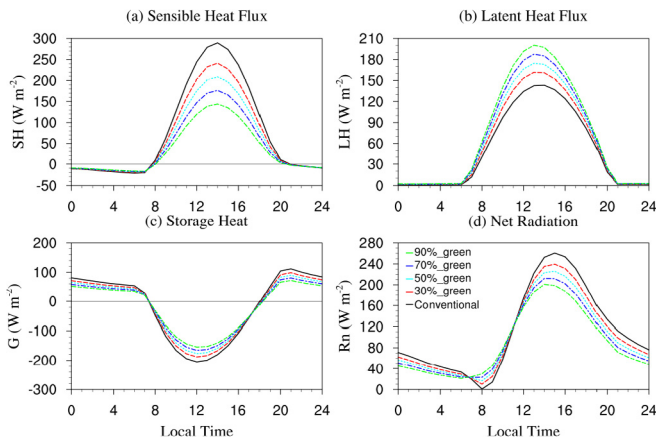


Fig. 6. Diurnal variation of (a) sensible heat flux (b) latent heat flux, (c) storage heat, and (d) net radiation, averaged only over urban grid points in domain d03 over 3 days (from 28–30 January in 2009), for experiments with 30%, 50%, 70% and 90% green roof fractions and the control.

larger reductions of roof surface temperature. This finding is reflected in Fig. 7 which shows that green roofs substantially reduce the roof surface UHI intensity during the day due to higher latent heat flux resulting from evapotranspiration. Although the differences in storage heat between green roof fractions and conventional roofs are small during early morning and late night, higher green roof fractions result in larger reductions of storage heat during the day. Usually, this energy is either stored into roofs and later released or conducted into the building indoor space and pumped back into the atmosphere by air conditioners (Li et al., 2014). Green roofs have relatively lower positive values of storage heat flux being released back into the atmosphere in the early morning and late night. On the other hand, green roofs show a higher reduction of storage heat being transferred to the buildings as compared to conventional roofs during the day. Net radiation is substantially reduced by the green roof fractions in the afternoon (1300–1800 local time). As reported by Sharma et al. (2016), this is most likely due to the slight increase in albedo by increasing green fractions.

The city-scale effectiveness (i.e., considering all urban grid cells in the metropolitan areas) of different green roof fractions in reducing the UHI is shown in Fig. 7 based on the ability of green roofs in reducing the maximum near-surface and roof surface UHI effects. The UHI is calculated as the difference between the urban and surrounding rural grid cells. The effectiveness of green roofs relative to conventional roofs in reducing the UHI is quantified as the difference of the UHI intensity between green roofs and conventional roofs ($UHI_{green} - UHI_{conventional}$). Fig. 7(a) and (b) show the diurnal changes of the UHI at the near-surface and roof surface levels respectively while 7(c) and 7(d) illustrate the relationship between green roof fractions and the reductions of the UHI, averaged over three diurnal cycles from 28–30 January in 2009. The use of green roofs in urban areas has a substantial cooling effect across the whole metropolitan area due to a reduction in sensible heat flux. Increasing the green roof fractions from 0% to 90% results in maximum reductions of the near-surface UHI from 0.30 to 1.15 $^{\circ}C$ and this occurs between 1200 and 1400 local time, while the maximum roof surface UHI reductions range from 1.0 to 3.8 $^{\circ}C$ and this occurs between 1300 and 1500 local time. Interestingly, both the near-surface and roof surface UHI reductions vary linearly with increasing green roofs fractions (Fig. 6(c) and (d)). The reductions of

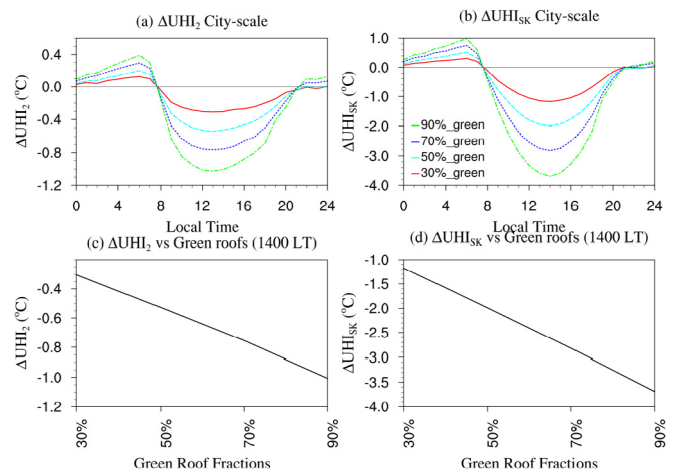


Fig. 7. Diurnal variations of (a) near-surface UHI (ΔUHI_2) and (b) roof surface UHI (ΔUHI_{sk}) reductions by using green roof fractions of 30, 50, 70, 90%. (c) and (d) are the corresponding reductions of near-surface and roof surface UHI effects when the reductions reach their maxima. The UHI has been averaged over urban grid points only in domain d03 over the 3 days (from 28–30 January in 2009).

roof surface UHI are substantially higher (0.70–2.65 °C) than the near-surface UHI during the day. This larger reduction of the roof surface UHI occurs due to higher evaporation and transpiration during photosynthesis during the day at the roof level. The lower reductions of the near-surface UHI is likely due to radiation effects (trapping solar radiation between buildings) inside the canopy. The building facades, impervious surfaces and heights between green roof and ground surfaces plays the important role in the dilution, dispersion and dissipation processes. On the other hand, the differences in near-surface UHI reductions among the green roof fractions are smaller than the reductions of the roof surface UHI.

Fig. 8 illustrates the effectiveness of different green roof fractions in mitigating the UHI effects for the three different urban categories (Fig. 1(b)) between the central business district and surrounding urban suburbs. The roof surface and near-surface UHI reductions are shown for low-density urban, high-density urban and commercial/industrial areas. These three urban categories have different urban properties for vegetated and impervious surfaces in the UCM (Table 1). Over the low-density urban area, the maximum reductions of the near-surface UHI intensities are 0.30, 0.50, 0.70 and 0.90 °C, and the roof surface UHI intensities are 1.0, 2.0, 2.7 and 3.5 °C during the day for green roof fractions of 30%, 50%, 70% and 90% respectively. High-density urban and commercial areas show reductions 0.40, 0.70, 1.0 and 1.4 °C for the near-surface UHI and 1.2, 2.5, 3.4 and 4.8 °C for the roof surface UHI by using the same percentages of green roof fractions. The high-density urban and commercial areas show higher reductions of the near-surface and roof surface UHI effects than the low-density urban area during the day. This finding shows that the application of green roofs can considerably reduce the roof surface and near-surface UHI effects in denser impervious areas due to the larger size of roof areas. Importantly, both the roof surface and near-surface UHI in the early morning (0200–0700 local time) are elevated as compared to conventional roofs at both the city-scale (Fig. 7) and the individual urban categories (Fig. 8) while there are no substantial differences during the night (2100–0200 local time). The roof surface and near-surface UHI are elevated by 1 °C and 0.40 °C respectively in the

early morning. According to Li et al. (2014), near-surface moisture in the low-density urban area is substantially increased due to evapotranspiration from surrounding larger size pervious area. As a consequence, a vapor pressure deficit over the low-density urban area reduces evapotranspiration, which helps to increase the temperature in the vegetated surface (Li et al., 2014). Overall, the warming effect at night is much lower as compared to the reductions in temperature during the day.

Fig. 9 shows the spatial differences in the roof surface UHI and wind speed at 10 m over the city of Melbourne by using 30%, 50%, 70% and 90% green roof fractions relative to conventional roofs, averaged from 1400 to 1800 local time over the 3 days simulation period. This time interval was chosen as it corresponds to the period when the roof surface temperature reaches its peak. Fig. 9 (top panel) shows that the 30% and 50% green roof fractions can reduce the roof surface UHI from 1 to 2 °C, while the 70% and 90% cool roof fractions can reduce the maximum UHI by 2–3 °C and 3–4 °C, respectively. The reductions in roof surface UHI increases with larger green roof fractions. Fig. 9 (bottom panel) also shows that green roofs have a smaller effect on wind speed as the reductions of wind speed by the green roof fractions are lower. Green roofs reduce the maximum wind speed by up to 0.25–1.25 m s⁻¹ by increasing green roof fractions from 30% to 90%. Interestingly, wind speed increases by up to 0.75 m s⁻¹ over offshore areas. This is likely related to changes in roughness due to the vegetation on green roofs. It is also noteworthy that the impacts of green roofs are not substantial in non-urban areas.

3.4. Effectiveness of cool roofs in mitigating UHI effects

The effectiveness of cool roofs in mitigating the UHI is assessed based on three numerical experiments by varying the albedo to 0.50, 0.70 and 0.85 for 100% cool roofs (the UCM model is designed for only 100% cool roofs). Fig. 10 shows changes in the surface energy balance due to increased albedo. Cool roofs reduce daily average sensible heat flux by up to 100, 170 and 220 W m⁻² by using the albedo values of 0.50, 0.70 and 0.85 respectively. Net radiation is also reduced by up to 100, 160 and 180 W m⁻² (~4 times) as compared to the conventional roofs by using the same albedo values during the day due to substantial amount of incoming solar radiation being reflected back to the atmosphere. Cool roofs are more effective in reducing net radiation and consequently, sensible heat flux, as compared to green and conventional roofs, especially during the day. Although green roofs transform net

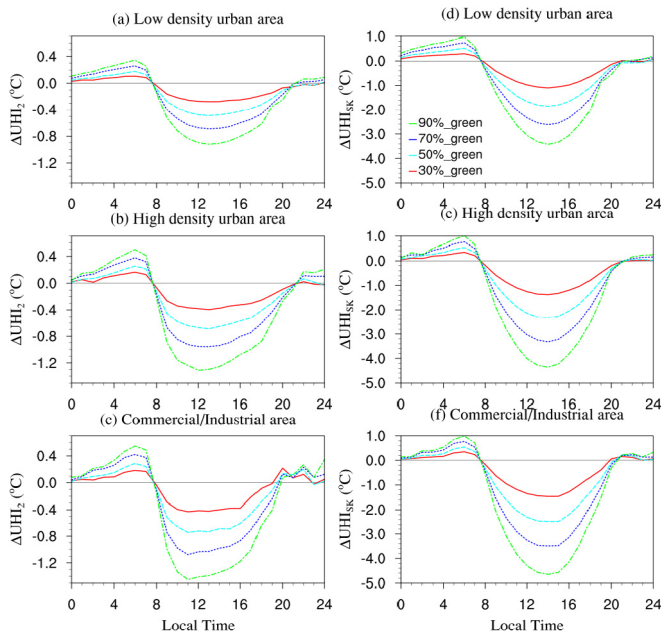


Fig. 8. The near-surface (left panel) and roof surface (right panel) UHI reductions for low density, high density, and commercial/Industrial urban categories by using 30%, 50%, 70% and 90% green roof fractions.

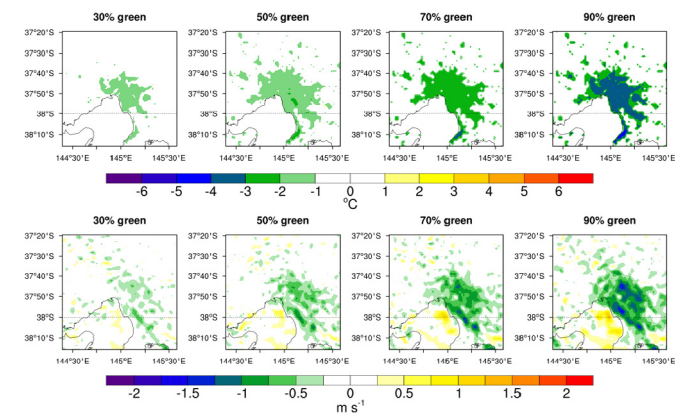


Fig. 9. Changes of roof surface UHI (upper panel) and wind speed at 10 m (bottom panel) by using 30%, 50%, 70% and 90% green roof fractions. All the results are averaged from 1400 to 1800 local time for the 3 days (from 28–30 January in 2009) over domain d03 when roof surface temperature reaches its peak.

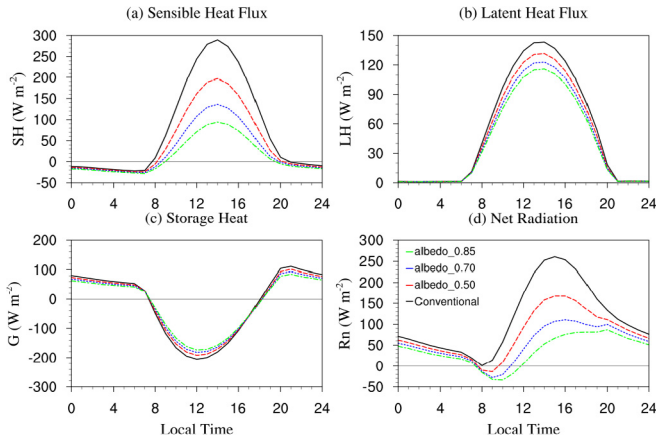


Fig. 10. Diurnal variation of (a) sensible heat flux (b) latent heat flux, (c) storage heat, and (d) net radiation, averaged only over urban grid points in domain d03 over 3 days (from 28–30 January in 2009), for experiments with albedo values of 0.5, 0.7, and 0.85 for cool roofs and the control.

radiation into latent heat flux due to evapotranspiration, the reduction in sensible heat flux is smaller as compared to the use of cool roofs. Interestingly, increasing albedo substantially reduces the latent heat flux in urban areas because of lower net radiation. In the UCM, 10% of urban grid cells are considered as a naturally vegetated surface. Therefore, the source of this latent heat flux must be from the naturally vegetated part of the urban grid cells. The reductions in storage heat of cool roofs are also similar to green roofs except in the morning (0700–1100 local time). However, the reductions of net reduction by cool roofs are considerably higher (120 W m^{-2}) than the green roofs during the day. The storage heat in the roofs re-radiates during the latter part of the day, or alternately, this heat can be transferred into the building indoor spaces and can increase the cooling energy demand for the air conditioners. Therefore, cool roofs and green roofs have the potential to reduce the cooling energy demand for buildings by reducing the storage heat, and consequently, reducing anthropogenic heat emissions in urban areas. Finally, cool roofs result in a substantial reduction in net radiation that is an important contributor in mitigating UHI effects. There are no substantial differences in the surface energy balance between cool and conventional roofs at night.

Fig. 11 shows the near-surface and roof surface UHI reductions by using albedo values of 0.85, 0.70 and 0.50, and the relationship

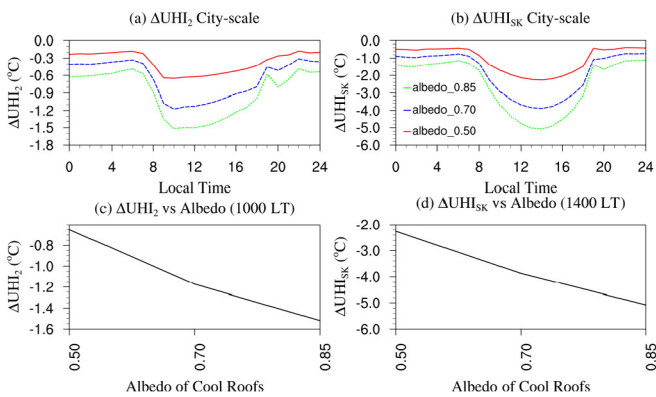


Fig. 11. Diurnal variations of (a) near-surface UHI (ΔUHI_2) and (b) roof surface UHI (ΔUHI_{sk}) reductions by using albedo values of 0.5, 0.7, and 0.85 for cool roofs. (c) and (d) are the corresponding reductions of near-surface and roof surface UHI effects when the reductions reach their maxima. The UHI has been averaged over urban grid points only in domain d03 over the 3 days (from 28–30 January in 2009).

between the albedo values and UHI reductions. The higher albedo of cool roofs substantially reduces the roof surface and near-surface UHI effects during the day. City-scale maximum reductions of the near-surface UHI reach up to 0.60, 1.1 and $1.5 \text{ }^\circ\text{C}$, while roof surface UHI reductions are 2.2, 3.8 and $5.2 \text{ }^\circ\text{C}$ by using albedos of 0.50, 0.70 and 0.85 respectively. Larger reductions of the roof surface UHI ($1 \text{ }^\circ\text{C}$) and the near-surface UHI ($0.50 \text{ }^\circ\text{C}$) are obtained by using cool roofs (albedo 0.85) as compared to 90% green roof fraction during the day (Fig. 7). The effectiveness of cool roofs in reducing UHI effects is drastically reduced (2/3) when the albedo is lowered from 0.85 to 0.50. Interestingly, a slight non-linear relationship is obtained between the UHI reductions and increasing albedo values of cool roofs (Fig. 11(c) and (d)) as compared to green roofs (Fig. 7(c) and (d)).

Fig. 12 shows the effectiveness of cool roofs in reducing both the roof surface and near-surface UHI effects for the different urban categories in the city center and surrounding low-density urban areas (Fig. 1 (b)). The reductions in the near-surface UHI are 0.50, 1.0 and $1.4 \text{ }^\circ\text{C}$ in the low-density urban areas during the day while the roof surface UHI reductions are 2.2, 3.6 and $5.0 \text{ }^\circ\text{C}$ by using albedos of 0.50, 0.70 and 0.85 respectively. During the day, cool roofs can reduce the near-surface UHI by 0.80, 1.5 and $2.2 \text{ }^\circ\text{C}$ and the roof surface UHI by 2.4, 4.2 and $5.8 \text{ }^\circ\text{C}$ in the high-density urban and commercial areas by using the same albedo. The cooling effect of cool roofs is larger in the high-density urban and commercial/industrial areas than the low-density urban area because of the larger roof areas (90–95%) in the high-density and commercial/commercial areas. When the albedo is reduced from 0.70 to 0.50 and 0.85 to 0.70, the cooling effects of cool roofs are reduced by up to $0.70 \text{ }^\circ\text{C}$ for near-surface temperature in both high-density urban and commercial areas, and $1.8 \text{ }^\circ\text{C}$ and $1.6 \text{ }^\circ\text{C}$ for the roof surface UHI in high-density urban and commercial areas, respectively. These results suggest that cool roofs may need a higher degree of maintenance for maintaining a high albedo by preventing dirt accumulation on the roof surfaces.

When considering all urban categories (Fig. 11) and each urban category separately (Fig. 12), a cool roof strategy results in larger

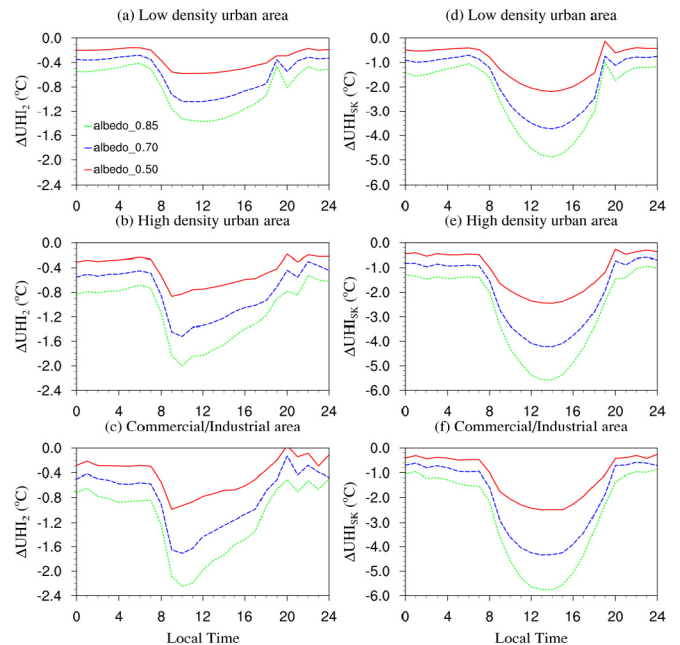


Fig. 12. Diurnal variation of the near-surface (left panel) and roof surface (right panel) UHI reductions for low density (a and b), high density (c and d) and commercial areas (e and f) by using albedo values of 0.50, 0.70 and 0.85 for cool roofs.

reductions of the roof surface and near-surface UHI effects in the early morning and the night as compared to using green roofs (Figs. 7 and 8). This finding suggests that cool roofs extend the daytime cooling effect into the night by reducing heat storage in the roofs during the day, which is consistent with the study of Li et al. (2014). A similar result has been reported by Georgescu et al. (2014), who have shown that cool roofs are more effective than green roofs in reducing the UHI.

In summary, it is notable that the substantial direct thermal impacts of green and cool roofs on roof surface temperature for both the city-scale and different urban categories happens during the afternoon (1200–1600 local time), which is nearly the same time when the daily roof surface temperature reaches its peak at 1500 local time (Fig. 5). On the other hand, the maximum direct thermal impacts of green and cool roofs for near-surface temperature occurs earlier between 900 and 1300 local time, but the near-surface temperature reaches its daily peak later at 1700 local time. Hence, the effectiveness of green and cool roofs in reducing the near surface temperature is limited as near surface temperatures are largely driven by properties of the land surface.

Fig. 13 shows the changes in roof surface UHI (upper panel) and the wind speed at 10 m (bottom panel) for different albedos with 100% cool roofs as compared to conventional roofs. Cool roofs can reduce the maximum roof surface UHI by up to 3, 4 and 5 °C in urban areas for albedos of 0.50, 0.70 and 0.85 respectively. The reductions of the roof surface UHI depends on the magnitude of the albedo, with higher albedo leading of higher amount of reflection of incoming shortwave radiation, and consequently, higher reductions of UHI effects. The reductions in wind speed by using cool roofs are also lower (0.5–1.75 m s⁻¹) in urban areas, but higher than the green roofs. On the other hand, cool roofs increase the wind speed (0.50–1.0 m s⁻¹) over offshore areas. As would be expected, the impacts of cool roofs in reducing the roof surface UHI and changing the wind speed are always higher in the center of the city.

3.5. Influence of initial soil moisture

All the simulations discussed so far use the WRF default initial soil moisture of 0.20 m³ m⁻³ for the green roofs. To investigate the effects of initial soil moisture, two additional simulations were

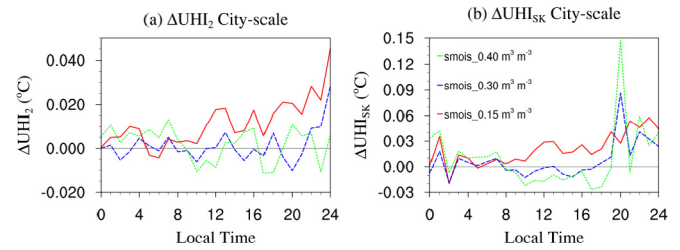


Fig. 14. Diurnal variations of (a) near-surface UHI (ΔUHI_2) and (b) roof surface UHI (ΔUHI_{sk}) as a function of green roof soil moisture (experiments with 50% green roof fraction). The UHI has been averaged over urban grid points only in domain d03 over the 3 days (from 28–30 January in 2009).

carried out by setting up initial soil moisture to 0.30 and 0.40 m³ m⁻³ for the experiment with 50% green roof fraction. An additional simulation was carried out using a lower initial soil moisture 0.15 m³ m⁻³ in order to examine the performance of 50% green roofs under dryer conditions. The impacts of initial soil moisture on green roofs are examined based on the ability of green roofs in reducing near-surface and roof surface UHI effects where the 50% green roof experiment is the control simulation. Fig. 14 shows that changing initial soil moisture conditions did not have a sustained effect on the UHI. Although the increased initial soil moisture in green roofs slightly reduces the near-surface UHI (maximum 0.015 °C) and the roof surface UHI (maximum 0.03 °C) during the day, the maximum near surface and roof surface UHI during the morning and night are elevated by up to 0.03 °C and 0.15 °C respectively as compared to the 50% green roofs. On the other hand, using drier initial soil conditions (0.15 m³ m⁻³) for green roofs increases warming effect during both the day and night. The near-surface UHI increases by up to 0.042 °C during the night while the roof surface UHI is elevated by up to 0.06 °C as compared to the 50% green roofs. Hence, the effect of initial soil moisture in green roofs is not substantial in reducing near-surface and roof surface UHI effects for this case study. This is likely due to the very hot and dry conditions quickly evaporating any excess soil moisture, consistent with the study by Kala et al. (2015b) who investigated the effects of higher initial soil moisture during the same heat-wave event.

3.6. Effects of green and cool roofs on boundary layer

Fig. 15 shows the changes in air temperature, winds (rotated to earth coordinates) and relative humidity in the boundary layer averaged over urban areas for 90% green roofs and cool roofs (albedo 0.85) as compared to conventional roofs over 3 days from 28–30 January in 2009. The maximum air temperature is reduced by up to 0.4 °C and 0.6 °C by using green and cool roofs respectively in the lower boundary layer during the day. Interestingly, the reduction in air temperature for cool roofs extends up to 1.8 km within the PBL, while the reduction for green roofs is only up to 0.9 km. The magnitude of the reduction in air temperature by cool roofs are higher by up to 0.2 °C as compared to green roofs. The maximum reduction in wind speed (1 m s⁻¹) occurs in the lower boundary layer for green and cool roofs during the late afternoon on the 28th and 30th January. However, the changes in wind speed are not substantial for the remaining hours in both lower and upper boundary layer as compared to conventional roofs. Furthermore, both green and cool roofs demonstrate no substantial changes in relative humidity as compared to conventional roofs in the lower boundary layer. This finding suggests that the changes in relative humidity as a result of evapotranspiration are not substantial because of the dry and hot conditions during the heatwave event.

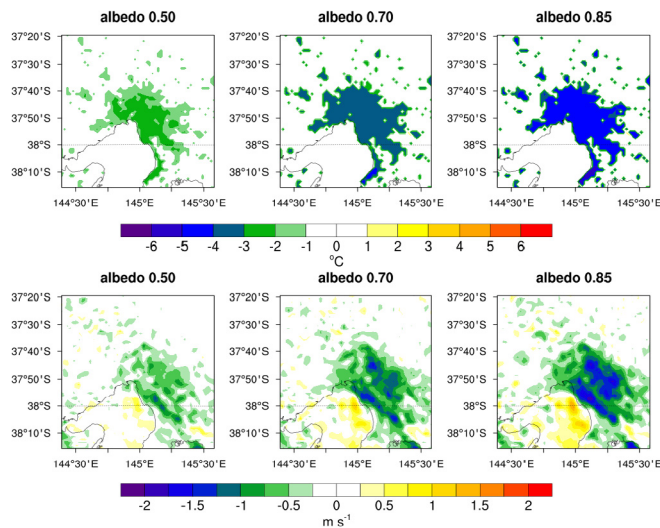


Fig. 13. Changes of roof surface UHI (upper panel) and wind speed at 10 m (bottom panel) by using albedo values 0.50, 0.70 and 0.85 for cool roofs. All the results are averaged from 1400 to 1800 local time for the 3 days (from 28–30 January in 2009) over domain d03 when roof surface temperature reaches its peak.

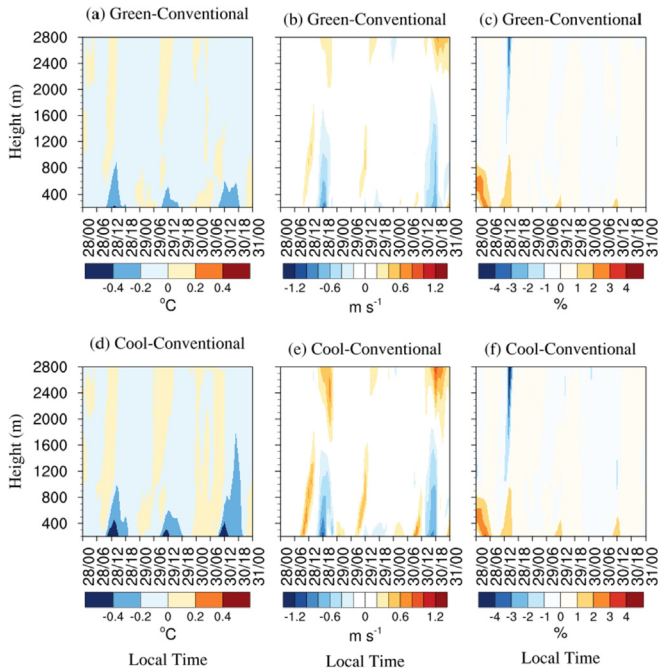


Fig. 15. The differences between green and conventional roofs (top) and cool and conventional roofs (bottom); (a) and (d) are the changes of air temperature; (b) and (e) are the changes of wind speed; (c) and (f) are the changes of relative humidity averaged over urban grid cells for green and cool roofs for the 3 days from 28–30 January.

This finding is not consistent with previous studies. For example, Li et al. (2014) report higher relative humidity in urban areas because of stronger advection of moist air from rural areas. Similarly, Sharma et al. (2016) report higher relative humidity for green roofs because of higher evapotranspiration and lower winds, and higher relative humidity for cool roofs due to the reduced temperature and moist cool air from surrounding rural areas. However, based on the analyses of vertical profiles of temperatures, winds and relative humidity of green and cool roofs, this study suggests that the advection of moist air from rural areas is unlikely to be the driving mechanism due to the extremely hot and dry conditions during the heatwave event. Another mechanism could be convective rolls due to heated urban surfaces and higher roughness of the urban areas.

To investigate the influence of convective rolls, it is useful to examine changes in the vertical wind component as well as turbulence. Vertical wind speeds are shown in Fig. 16(a)–(c) while Turbulent Kinetic Energy (TKE) are shown in Fig. 16(d)–(f) for conventional, 90% green roofs and cool roofs (albedo 0.85) over 3 days from 28–30 January in 2009. Finally, the planetary boundary layer heights (PBLH) are illustrated in Fig. 16(g) for the same experiments. The vertical wind speed, TKE and PBLH are important factors for indicating the strength of vertical mixing. Fig. 16(a) illustrates that the conventional roofs show stronger vertical wind speed on the 28th and 30th January, which indicates vertical transport of energy fluxes (e.g., latent and sensible heat fluxes) from surface to higher boundary layer. Furthermore, green and cool roofs (Fig. 16(b) and (c)) also indicate positive vertical wind speed with smaller reductions as compared to conventional roofs in most cases except on the 29th January which also indicates vertical transport of energy. Fig. 16(d) and (f) show that green and cool roofs result in a decrease in TKE from 0.2 to $1.5 \text{ m}^2 \text{ s}^{-2}$ during the day, while conventional roofs show the highest TKE ranging from 0.2 to $1.9 \text{ m}^2 \text{ s}^{-2}$. Both the vertical wind speed and the TKE results indicate that the conventional roofs result in stronger vertical mixing during the day as compared to green and cool roofs, which show

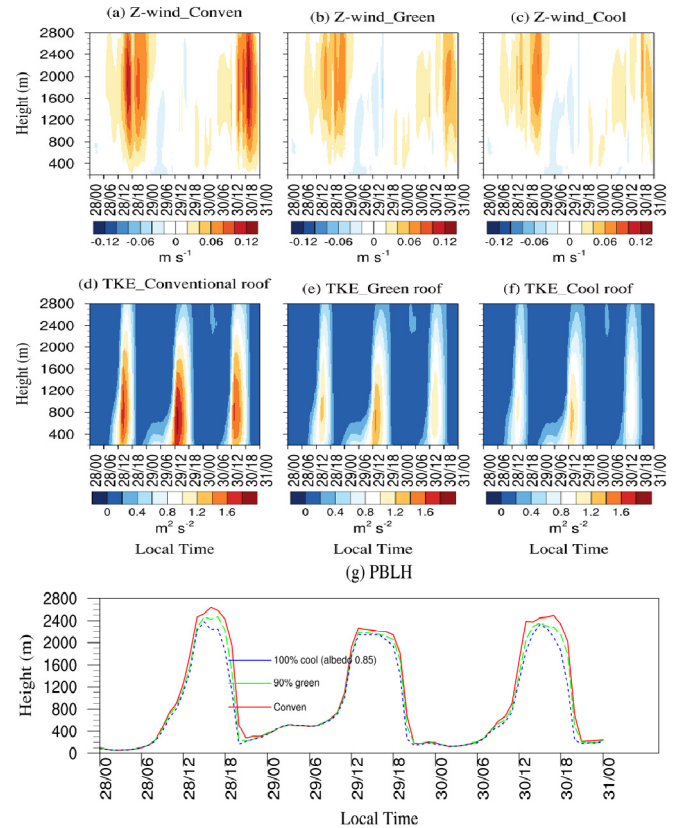


Fig. 16. Vertical wind speed for (a) conventional roofs, (b) 90% green roofs and (c) cool roofs with the albedo of 0.85. TKE for (d) conventional roofs, (e) green roofs (f) cool roofs. Temporal variations of PBLH for (g) conventional, green and cool roofs.

reductions in the vertical wind speed and TKE. The prevalence of vertical mixing in all experiments is due to the strong surface heating during the heatwave event. These findings are consistent with the reduction in sensible heat fluxes by green and cool roofs (Figs. 6(a) and 10(a)). Green roofs reduce PBLH by up to 180 m as compared to conventional roofs while cool roofs reduce the maximum PBLH by 300 m over urban areas (Fig. 16(g)). In general, lower sensible heat flux reduces vertical mixing and reduces vertical wind speed, and consequently, the PBLH is shallower. Fig. 16(b) and (c) illustrate that green and cool roofs slightly reduce vertical wind speeds, and consequently, generate lower PBLH due to lower sensible heat flux. Similar results have been obtained by Georgescu (2015) and Sharma et al. (2016), who have shown that lower sensible heat flux generated by green and cool roofs leads a reduction in vertical mixing and the lower PBLH.

Li et al. (2014) reported that the advection of moist air from rural to urban areas occurs due to weaker vertical mixing over urban areas, and consequently, the atmosphere beyond a given height over urban areas is not affected by surface conditions. The much weaker vertical mixing further enables the development of stronger advection. However, this study did not obtain stronger advection of moist air from rural areas (Fig. 15(c) and (f)) and this is most likely because of the considerable vertical mixing for green and cool roofs over urban areas (Fig. 16(b) and (c)). In general, vertical mixing helps to develop horizontal convective rolls over urban areas. As a result, the urban atmosphere is strongly affected by the surface conditions in urban areas during heatwave events. Fig. 16(a)–(f) suggest that the heated surfaces in the urban areas are the main influencing factor for controlling vertical wind speed and TKE that enhances in developing larger convective rolls over urban

areas. According to (Miao et al., 2009), the development of convective rolls is enhanced when the vertical wind speed is stronger. Based on the vertical wind speed and TKE analyses for green and cool roofs, the result indicates the stronger influence of convective rolls on the urban atmosphere during heatwave conditions. This is another important finding of this study as compared to previous studies, which reported that the synoptic or mesoscale wind plays an important role for the advection of moist air from rural areas into urban areas (Li et al., 2014; Sharma et al., 2016).

3.7. Effects of green and cool roofs on human thermal comfort

Fig. 17 shows the control (top panel) and changes in human thermal stress via UTCI index at pedestrian and roof-surface levels (middle and bottom panels). The improvement in HTC is smaller at pedestrian level/near-surface (2 m) for both green and cool roofs. However, the HTC is noticeably improved by reducing of the UTCI index at roof-surface level during the day. For pedestrian level UTCI, using 50% and 90% green roofs result in reductions of the maximum UTCI by up to 0.60 °C and 1.5 °C during the day, respectively, while cool roofs with albedos of 0.50 and 0.85 lead to reductions in the maximum UTCI by 1 °C and 2.4 °C respectively. At roof-surface level, the maximum reductions of the UTCI are 2.8 °C and 5.7 °C by using 50% and 90% green roofs, and 3.2 °C and 8 °C by using an albedo of 0.50 and 0.85 for cool roofs, respectively. Green and cool roofs are very effective in reducing the UTCI index from extreme (UTCI > 46 °C) to very strong (UTCI > 38 °C) at roof-surface level during the day according to the classification presented in Table 3. Interestingly, cool roofs always result in a higher UTCI reduction than the green roofs, while 90% green roofs and cool roofs with an albedo of 0.85 show almost similar reductions of the UTCI. It is noteworthy that at night, cool roofs also reduce the UTCI while green roofs increase the UTCI, but the changes are small. Cool roofs are more efficient than green roofs in improving HTC during the day because of higher reflection of incoming solar radiation. Green and cool roofs substantially improve the HTC at rooftop-podium level as compared to the pedestrian level as the temperature

reductions are much higher at the roof-surface level than the near surface. This finding suggests that green and cool roofs result in smaller changes to the pedestrian level HTC due to the additional reflective radiation from building facades and impervious surfaces at the surface. This is expected as green and cool roofs are unlikely to affect the energy balance at pedestrian level due the considerable distance between roof-surface and near-surface levels, and consequently, this result in only minor improvements for the pedestrian level HTC. It is also noteworthy that green and cool roofs are able to reduce heat stress, even when very strong and extreme heat stress occurs at pedestrian and roof surface level respectively during the day. Furthermore, the differences in wind speed and relative humidity between conventional and green and cool roofs are small (Fig. 15), but the differences in sensible heat and latent heat fluxes are substantial (Figs. 6 and 10) for green roofs while the differences in sensible flux are higher for cool roofs. Therefore, the sensible and latent heat fluxes play a key role in controlling HTC for green roofs while sensible heat flux is the key driving factor in improving HTC for cool roofs during heatwave.

4. Conclusions

Heatwave events exacerbate UHI effects, and the frequency and intensity of heatwaves are increasing in southeast Australia. Therefore, it is critical to investigate the effectiveness of mitigation strategies such as the use of green and cool roofs. To address this important question, this study evaluates the effectiveness of green and cool roofs in mitigating UHI effects and improving HTC in the city of Melbourne during an extreme heatwave event from the 27th to 30th of January 2009 using the WRF-UCM model.

The UHI reductions vary linearly with the increasing green roof fractions, but slightly non-linear with the increasing albedo of cool roofs. The roof surface UHI is reduced from 1.15 °C to 3.8 °C when green roof fractions are increased from 30% to 90%. Furthermore, cool roofs result in maximum reductions of the roof surface UHI ranging from 2.2 to 5.2 °C by increasing the albedo from 0.50 to 0.85, which is a larger reduction by approximately 1.4 °C as compared to 90% green roofs. The impacts of green and cool roofs varied for the different urban categories with reductions of the roof surface UHI by green roofs ranging from 1 to 3.5 °C in low-density urban areas, and 1.2–4.6 °C in the high-density urban and the commercial/industrial areas. Similarly, the reductions due to cool roofs ranged from 2.2 to 5.0 °C in the low-density urban areas, and 2.4–5.8 °C in the high-density urban and the commercial/industrial areas. The high density and commercial/industrial areas experienced larger UHI reductions because of larger areas of cool roofs. Furthermore, increasing soil moisture did not have a substantial influence in reducing UHI effects. However, soil moisture deficit on green roofs can exacerbate the UHI effects during both the day and night.

The green roofs and cool roofs not only alter the surface energy balance and reduce the UHI effects but also influence the boundary layer up to 2.5 km. The decrease in sensible flux due to the green and cool roofs reduces vertical mixing and the PBLH, and consequently, reduces the air temperature. However, the changes in wind speed and relative humidity are not substantial in the lower boundary layer during the day. Green and cool roofs decrease the sensible heat flux and consequently reduce vertical mixing, the depth of boundary layer and temperatures over urban areas in the lower atmosphere, which reduces UHI effects. Cool roofs reflect the incoming solar radiation, and consequently, decrease the sensible heat flux and reduce UHI effects. Green roofs provide heat transfer benefits via evapotranspiration. Nonetheless, green roof approach has a limitation particularly in the early morning because of increased UHI effects. This problem might be overcome by applying

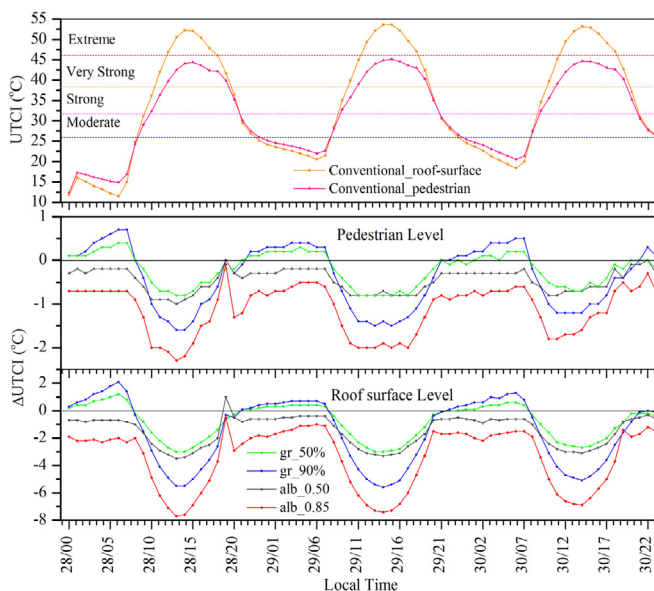


Fig. 17. Hourly time series of HTC in pedestrian and roof-surface levels for conventional roofs (top). The changes of HTC in near-surface (middle) and roof surface (bottom) levels for green and cool roofs. HTC effects represented by the UTCI index. All results are averaged over only urban grid points in domain d03 for the 3 days (from 28–30 January in 2009).

an optimal strategy including the appropriate mix of vegetation on green roofs and cool roofs, and this requires further study.

Green and cool roofs substantially improve HTC at the roof surface level but this effect is much smaller at the pedestrian level. Both green and cool roofs are effective in improving HTC by reducing the UTCI index from extreme ($UTCI > 46^{\circ}\text{C}$) to very strong ($UTCI > 38^{\circ}\text{C}$) at roof surface level although the improvement of HTC at pedestrian level is not substantial. Interestingly, green and cool roofs show their potential in reducing thermal stress during the day when the worst (very strong to extreme) thermal stress occurs. This finding reflects the potential of green and cool roofs in reducing heat related illness and offering comfortable recreational and amenity spaces for the urban dwellers.

Our results also indicate that the physical processes/mechanisms involved in altering boundary layer structure and reducing UHI effects interact differently based on the characteristics of heatwave conditions as compared to regular summer days and geographical locations for green and cool roofs. Based on the analyses of vertical profiles of air temperature, wind and relative humidity, this study suggests that the advection of moist air from rural areas is unlikely to be the driving mechanism in boundary layer dynamics due to the extremely hot and dry conditions during the heatwave event. Furthermore, the study investigates the influence of convective rolls by examining the changes in the vertical wind component and TKE, which indicates the stronger influence of convective rolls on the urban boundary layer dynamics during heatwave conditions because of heated urban surfaces.

Finally, the study has some important inherent limitations which are important to discuss. While our study shows that cool and green roofs have potential to reduce UHI effects, implementing 90% green roofs, and having 100% of roofs with high albedos of up to 0.85 is not likely to be practically feasible across an entire city. The aim of this study was to investigate the maximum response, and this provides useful information, however, this does not necessarily translate to practical implementation. Additionally, the WRF-SLUCM model has inherent limitations in how buildings are represented in the model, for example, extensive (depth < 150 mm) versus intensive (depth > 150 mm) roofs and pitched versus flat roofs may have different effects on the surface energy balance, and this cannot be resolved by the model. Nonetheless, this study provides useful findings on the maximum expected response due to cool and green roofs at the large scale, and these findings are relevant for other cities which experience similar weather conditions during summer.

Acknowledgements

Data support by the Bureau of Meteorology (BoM) Australia and ECMWF (ERA-interim) data server (<http://apps.ecmwf.int/datasets/data/interim-full-daily/levtype=ml/>) are gratefully acknowledged. Authors also acknowledge Stephanie Jacobs and Carlo Jamandre for providing urban categories data (Jackson et al. (2010)) for the city of Melbourne. Jatin Kala is supported by an Australian Research Council Discovery Early Career Researcher Award (DE170100102). The comments from two anonymous reviewers helped to improve this manuscript. All of this assistance is gratefully acknowledged.

References

Akbari, H., Matthews, H.D., Donny, S., 2012. The long-term effect of increasing the albedo of urban areas. *Environ. Res. Lett.* 7 (2), 024004.
 Akbari, H., Shea Rose, L., Taha, H., 2003. Analyzing the land cover of an urban environment using high-resolution orthophotos. *Landsc. Urban Plann.* 63 (1), 1–14.
 Argueso, D., Evans, J.P., Fita, L., 2014. Temperature response to future urbanization and climate change. *Clim. Dynam.* 42 (7), 2183–2199. <https://doi.org/10.1007/s00382-013-1789-6>.

Blazejczyk, K., Epstein, Y., Jendritzky, G., Staiger, H., Tinz, B., 2012. Comparison of UTCI to selected thermal indices. *Int. J. Biometeorol.* 56 (3), 515–535.
 Bröde, P., Fiala, D., Blazejczyk, K., Holmér, I., Jendritzky, G., Kampmann, B., Tinz, B., Havenith, G., 2012a. Deriving the operational procedure for the universal thermal climate index (UTCI). *Int. J. Biometeorol.* 56 (3), 481–494.
 Bröde, P., Krüger, E.L., Rossi, F.A., Fiala, D., 2012b. Predicting urban outdoor thermal comfort by the Universal Thermal Climate Index UTCI—a case study in Southern Brazil. *Int. J. Biometeorol.* 56 (3), 471–480.
 Carson, T.B., Marasco, D.E., Culligan, P.J., McGillis, W.R., 2013. Hydrological performance of extensive green roofs in New York City: observations and multi-year modeling of three full-scale systems. *Environ. Res. Lett.* 8 (2), 024036.
 Chen, F., Duhdia, J., 2001. Coupling an advanced land surface—hydrology model with the penn state—NCAR MM5 modeling system. Part II: preliminary model validation. *Mon. Weather Rev.* 129 (4), 587–604.
 Chen, F., Kusaka, H., Bornstein, R., Ching, J., Grimmond, C.S.B., Grossman-Clarke, S., Loridan, T., Manning, K.W., Martilli, A., Miao, S., Sailor, D., Salamanca, F.P., Taha, H., Tewari, M., Wang, X., Wyszogrodzki, A.A., Zhang, C., 2011. The integrated WRF/urban modelling system: development, evaluation, and applications to urban environmental problems. *Int. J. Climatol.* 1 (2), 273–288.
 Climate Institute, 2013. Infrastructure Interdependencies and Business-level Impacts Report. The Climate Institute, 2013. <http://www.climateinstitute.org.au/articles/publications/infrastructure-interdependenciesand-business-level-impacts.html>.
 Coutts, A., Beringer, J., Tapper, N., 2007. Impact of increasing urban density on local climate: spatial and temporal variations in the surface energy balance in Melbourne, Australia. *J. Appl. Meteor. Climatol.* 46, 477–493. <https://doi.org/10.1175/JAM2462.1>.
 Cowan, T., Purich, A., Perkins, S., Pezza, A., Boschat, G., Sadler, K., 2014. More frequent, longer, and hotter heat waves for Australia in the twenty-first century. *J. Clim.* 27 (15), 5851–5871.
 Dee, D.P., Uppala, S.M., Simmons, A.J., Berrisford, P., Poli, P., Kobayashi, S., Andrae, U., Balmaseda, M.A., Balsamo, G., Bauer, P., Bechtold, P., Beljaars, A.C.M., Van De Berg, L., Bidlot, J., Bormann, N., Delsol, C., Dragani, R., Fuentes, M., Geer, A.J., Haimberger, L., Healy, S.B., Hersbach, H., Hólm, E.V., Isaksen, I., Kållberg, P., Köhler, M., Matricardi, M., McNally, A.P., Monge-Sanz, B.M., Morcrette, J.J., Park, B.K., Peubey, C., De Rosnay, P., Tavolato, C., Thépaut, J.N., Vitart, F., 2011. The ERA-Interim reanalysis: configuration and performance of the data assimilation system. *Quarterly. J. Roy. Meteorol. Soc.* 137, 656 553–597.
 Duhdia, J., 2014. A history of mesoscale model development. *Asia-Pacific J. Atmos. Sci.* 50, 121–131. <https://doi.org/10.1007/s13143-014-0031-8>.
 Engel, C.B., Lane, T.P., Reeder, M.J., Reznay, M., 2013. The meteorology of black Saturday. *Quarter. J. Roy. Meteorol. Soc.* 139 (672), 585–599.
 Evans, J.P., Ekström, M., Ji, F., 2012. Evaluating the performance of a WRF physics ensemble over South-East Australia. *Clim. Dynam.* 39 (6), 1241–1258.
 Field, C.B., Barros, V.R., Mach, K., Mastrandrea, M., 2014. Climate change 2014: impacts, adaptation, and vulnerability. In: Working Group II Contribution to the IPCC 5th Assessment Report—technical Summary, p. 76.
 Georgescu, M., 2015. Challenges associated with adaptation to future urban expansion. *J. Clim.* 28 (7), 2544–2563.
 Georgescu, M., Morefield, P.E., Bierwagen, B.G., Weaver, C.P., 2014. Urban adaptation can roll back warming of emerging megapolitan regions. *Proc. Natl. Acad. Sci. Unit. States Am.* 111 (8), 2909–2914.
 Grell, G.A., Dévényi, D., 2002. A generalized approach to parameterizing convection combining ensemble and data assimilation techniques. *Geophys. Res. Lett.* 29 (14), 38–1–38–4.
 Guan, H., Soebarto, V., Bennett, J., Clay, R., Andrew, R., Guo, R., Gharib, S., Bellette, K., 2014. Response of office building electricity consumption to urban weather in Adelaide. *South Australia Urban Climate* 1, 42–55.
 Iacono, M.J., Delamere, J.S., Mlawer, E.J., Shephard, M.W., Clough, S.A., Collins, W.D., 2008. Radiative forcing by long-lived greenhouse gases: calculations with the AER radiative transfer models. *J. Geophys. Res.* 113, D13 n/a–n/a).
 Imran, H.M., Kala, J., Ng, A.W.M., Muthukumar, S., 2017. An evaluation of the performance of a WRF multi-physics ensemble for heatwave events over the city of Melbourne in southeast Australia. *Clim. Dynam.* 50 (7–8), 2553–2586.
 Irvine, P.J., Ridgwell, A., Lunt, D.J., 2011. Climatic effects of surface albedo geo-engineering. *J. Geophys. Res.* 116, D24 n/a–n/a).
 Jackson, T.L., Feddema, J.J., Oleson, K.W., Bonan, G.B., Bauer, J.T., 2010. Parameterization of urban characteristics for global climate modeling. *Ann. Assoc. Am. Geogr.* 100 (4), 848–865.
 Janjić, Z.I., 1994. The step-mountain eta coordinate model: further developments of the convection, viscous sublayer, and turbulence closure schemes. *Mon. Weather Rev.* 122 (5), 927–945.
 Johansson, E., 2006. Influence of urban geometry on outdoor thermal comfort in a hot dry climate: a study in Fez. Morocco. *Build. Environ.* 41 (10), 1326–1338.
 Kala, J., Andrys, J., Lyons, T.J., Foster, I.J., Evans, B.J., 2015a. Sensitivity of WRF to driving data and physics options on a seasonal time-scale for the southwest of Western Australia. *Clim. Dynam.* 44 (3), 633–659.
 Kala, J., Evans, J.P., Pitman, A.J., 2015b. Influence of antecedent soil moisture conditions on the synoptic meteorology of the Black Saturday bushfire event in southeast Australia. *Quarter. J. Roy. Meteorol. Soc.* 141, 3118–3129. <https://doi.org/10.1002/qj.2596>.
 Kusaka, H., Kimura, F., 2004. Thermal effects of urban canyon structure on the nocturnal heat island: numerical experiment using a mesoscale model coupled with an urban canopy. *Model J. Appl. Meteorol.* 43 (12), 1899–1910.

- Kusaka, H., Kondo, H., Kikegawa, Y., Kimura, F., 2001. A simple single-layer urban canopy model for atmospheric models: comparison with multi-layer and slab models. *Boundary-Layer Meteorol.* 101 (3), 329–358.
- Li, D., Bou-Zeid, E., 2014. Quality and sensitivity of high-resolution numerical simulation of urban heat islands. *Environ. Res. Lett.* 9 (5), 055001.
- Li, D., Bou-Zeid, E., Oppenheimer, M., 2014. The effectiveness of cool and green roofs as urban heat island mitigation strategies. *Environ. Res. Lett.* 9 (5), 055002.
- Li, D., Bou-Zeid, E., Barlage, M., Chen, F., Smith, J.A., 2013. Development and evaluation of a mosaic approach in the WRF-Noah Framework. *J. Geophys. Res.: Atmos.* 118 (11) <https://doi.org/10.1002/2013JD020657>, 918–11, 935.
- Liu, Y., Chen, F., Warner, T., Basara, J., 2006. Verification of a mesoscale data-assimilation and forecasting system for the Oklahoma city area during the joint urban 2003 field project. *J. Appl. Meteorol. Climatol.* 45 (7), 912–929.
- Matzarakis, A., Rutz, F., Mayer, H., 2010. Modelling radiation fluxes in simple and complex environments: basics of the RayMan model. *Int. J. Biometeorol.* 54 (2), 131–139.
- Miao, S., Chen, F., Lemone, M.A., Tewari, M., Li, Q., Wang, Y., 2009. An observational and modeling study of characteristics of urban heat island and boundary layer structures in Beijing. *J. Appl. Meteorol. Climatol.* 48 (3), 484–501.
- Millstein, D., Menon, S., 2011. Regional climate consequences of large-scale cool roof and photovoltaic array deployment. *Environ. Res. Lett.* 6 (3), 034001.
- Morini, E., Touchaei, A.G., Rossi, F., Cotana, F., Akbari, H., 2017. Evaluation of Albedo Enhancement to Mitigate Impacts of Urban Heat Island in Rome (Italy) Using WRF Meteorological Model Urban Climate. <https://doi.org/10.1016/j.juclim.2017.08.001> (in press).
- Morini, E., Touchaei, A.G., Castellani, B., Rossi, F., Cotana, F., 2016. The impact of albedo increase to mitigate the urban heat island in terni (Italy) using the wrf. *Model Sustain.* 8, 999.
- Nairn, J., Fawcett, R., 2013. Defining Heatwaves: Heatwave Defined as a Heat Impact Event Servicing All Community and Business Sectors in Australia. The Centre for Australian Weather and Climate Research. Accessed 22 Nov 2016. http://www.cawcr.gov.au/technical-reports/CTR_060.pdf.
- Nicholls, N., Larsen, S., 2011. Impact of drought on temperature extremes in Melbourne, Australia. *Aust. Meteorol. Oceanogr. J.* 61 (2), 113–116.
- O'malley, C., Piroozfarb, P. A. E., Farr, E.R.P., Gates, J., 2014. An investigation into minimizing urban heat island (UHI) effects: a UK perspective. *Energy Procedia* 62 (Suppl. C), 72–80.
- Oleson, K.W., Bonan, G.B., Feddema, J., 2010. Effects of white roofs on urban temperature in a global climate model. *Geophys. Res. Lett.* 37 (3) n/a-n/a.
- Perkins-Kirkpatrick, S.E., White, C.J., Alexander, L.V., Argüeso, D., Boschat, G., Cowan, T., Evans, J.P., Ekström, M., Oliver, E.C.J., Phatak, A., Purich, A., 2016. Natural hazards in Australia: heatwaves. *Climatic Change* 1–14. <https://doi.org/10.1007/s10584-016-1650-0>.
- Rosenfeld, A.H., Akbari, H., Romm, J.J., Pomerantz, M., 1998. Cool communities: strategies for heat island mitigation and smog reduction. *Energy Build.* 28 (1), 51–62.
- Perkins, S.E., Alexander, L.V., 2013. On the measurement of heat waves. *J. Clim.* 26, 4500–4517.
- Razzaghmanesha, M., Razzaghmanesha, M., 2017. Thermal performance investigation of a living wall in a dry climate of Australia. *Build. Environ.* 112, 45–62.
- Razzaghmanesha, M., Beechama, S., Salemi, T., 2016. The role of green roofs in mitigating Urban Heat Island effects in the metropolitan area of Adelaide, South Australia. *Urban For. Urban Green.* 15, 89–102.
- Sharma, A., Conry, P., Fernando, H.J.S., Alan, F.H., Hellmann, J.J., Chen, F., 2016. Green and cool roofs to mitigate urban heat island effects in the Chicago metropolitan area: evaluation with a regional climate model. *Environ. Res. Lett.* 11 (6), 064004.
- Sharma, A., Fernando, H.J., Hellmann, J., Chen, F., 2014. Sensitivity of WRF model to urban parameterizations, with applications to Chicago metropolitan urban heat island. ASME 2014 4th Joint US-European Nuclear Engineering Division Summer Meeting 14 Environ. Res. Lett. 11 (2016), 064004 (American Society of Mechanical Engineers) p V01DT28A002.
- Skamarock, W.C., Klemp, J.B., Dudhia, J., Gill, D.O., Barker, D.M., Wang, W., Power, J.G., 2005. A Description of the Advanced Research WRF Version 2. NCAR Technical Note, NCAR/TND468 + STR. National Center for Atmospheric Research, Boulder.
- Skamarock, W.C., Klemp, J.B., Dudhia, J., Gill, D.O., Barker, D.M., Duda, M.G., Huang, X.-Y., Wang, W., Powers, J.G., 2008. A Description of the Advanced Research WRF Version 3. NCAR Technical Note NCAR/TN-475 + STR. National Center for Atmospheric Research, Boulder.
- Smith, K.R., Roebber, P.J., 2011. Green roof mitigation potential for a proxy future climate scenario in Chicago, Illinois. *J. Appl. Meteorol. Climatol.* 50 (3), 507–522.
- Song, J., Wang, Z.-H., 2015. Interfacing the urban land-atmosphere system through coupled urban canopy and atmospheric models. *Boundary-Layer Meteorol.* 154 (3), 427–448.
- Steffen, W., Lesley, H., Sarah, P., 2014. Heatwaves: Hotter, Longer, More Often – Climate Council. <https://www.climatecouncil.org.au/uploads/9901f6614a2cac7b2b888f55b4dff9cc.pdf>.
- Sun, T., Bou-Zeid, E., Ni, G.-H., 2014. To irrigate or not to irrigate: analysis of green roof performance via a vertically-resolved hygrothermal model. *Build. Environ.* 73 (Suppl. C), 127–137.
- Sun, T., Bou-Zeid, E., Wang, Z.-H., Zerba, E., Ni, G.-H., 2013. Hydrometeorological determinants of green roof performance via a vertically-resolved model for heat and water transport. *Build. Environ.* 60 (Suppl. C), 211–224.
- Synnefa, A., Dandou, A., Santamouris, M., Tombrou, M., Soulakellis, N., 2008. On the use of cool materials as a heat island mitigation. *Strat. J. Appl. Meteorol. Climatol.* 47 (11), 2846–2856.
- Taha, H., 2008a. Episodic performance and sensitivity of the urbanized MM5 (uMM5) to perturbations in surface properties in Houston Texas. *Boundary-Layer Meteorol.* 127 (2), 193–218.
- Taha, H., 2008b. Meso-urban meteorological and photochemical modeling of heat island mitigation. *Atmos. Environ.* 42 (38), 8795–8809.
- Thompson, G., Field, P.R., Rasmussen, R.M., Hall, W.D., 2008. Explicit forecasts of winter precipitation using an improved Bulk microphysics scheme. Part II: implementation of a new snow parameterization. *Mon. Weather Rev.* 136 (12), 5095–5115.
- Touchaei, A.G., Akbari, H., Tessum, C.W., 2016. Effect of increasing urban albedo on meteorology and air quality of Montreal (Canada) - episodic simulation of heat wave in 2005. *Atmos. Environ.* 132, 188–206.
- Vatani, J., Golbabaie, F., Dehghan, S.F., Yousefi, A., 2016. Applicability of Universal Thermal Climate Index (UTCI) in occupational heat stress assessment: a case study in brick industries. *Ind. Health* 54 (1), 14–19.
- Victorian Auditor General's Report, 2014. Heatwave Management: Reducing the Risk to Public Health. <http://www.audit.vic.gov.au/publications/20141014-Heatwave-Management/20141014-Heatwave-Management.pdf>.
- Wong, N.H., Cheong, D.K.W., Yan, H., Soh, J., Ong, C.L., Sia, A., 2003. The effects of rooftop garden on energy consumption of a commercial building in Singapore. *Energy Build.* 35 (4), 353–364.
- Yang, J., Wang, Z.-H., Chen, F., Miao, S., Tewari, M., Voogt, J.A., Myint, S., 2015. Enhancing hydrologic modelling in the coupled weather Research and forecasting-urban modelling system. *Boundary-Layer Meteorol.* 155 (1), 87–109.

Chapter 6

Impacts of Future Urbanization on the UHI and Urban Meteorology during Heatwave Event

6.1 Introduction

Chapter 5 investigated the effectiveness of green and cool roofs in mitigating the UHI of Melbourne using current urban land use. However, the population is increasing rapidly in Melbourne, which is leading to an increase in urbanization in surrounding suburbs of the city of Melbourne. In 2017, the city of Melbourne released the urban expansion strategy under the vision of Plan Melbourne 2050. According to Plan Melbourne 2050 urban expansion strategy, urban areas will substantially expand particularly West, North, and South-Eastern part of the city. The expanded urban areas could exacerbate the effects of UHI, and consequently can decrease the HTC. Hence, this Chapter examines the potential impacts of future urban expansion (based on the Plan Melbourne 2050) on the UHI, HTC and urban meteorology for the city of Melbourne during the same four heatwave events that considered in chapter 4.

GRADUATE RESEARCH CENTRE

DECLARATION OF CO-AUTHORSHIP AND CO-CONTRIBUTION: PAPERS INCORPORATED IN THESIS BY PUBLICATION

This declaration is to be completed for each conjointly authored publication and placed at the beginning of the thesis chapter in which the publication appears.

1. PUBLICATION DETAILS (to be completed by the candidate)

Title of Paper/Journal/Book:	Impacts of future urban expansion on urban heat island effects during heatwave events in the city of Melbourne in southeast Australia		
Surname:	Hosen	First name:	Md Imran
College:	College of Engineering & Science	Candidate's Contribution (%):	85 %
Status:	Currently Under Review		
Accepted and in press:	<input type="checkbox"/>	Date:	<input type="text"/>
Published:	<input type="checkbox"/>	Date:	<input type="text"/>

2. CANDIDATE DECLARATION

I declare that the publication above meets the requirements to be included in the thesis as outlined in the HDR Policy and related Procedures – policy.vu.edu.au.

	14-08-2018
Signature	Date

3. CO-AUTHOR(S) DECLARATION

In the case of the above publication, the following authors contributed to the work as follows:

The undersigned certify that:

1. They meet criteria for authorship in that they have participated in the conception, execution or interpretation of at least that part of the publication in their field of expertise;
2. They take public responsibility for their part of the publication, except for the responsible author who accepts overall responsibility for the publication;
3. There are no other authors of the publication according to these criteria;
- 4.* Potential conflicts of interest have been disclosed to a) granting bodies, b) the editor or publisher of journals or other publications, and c) the head of the responsible academic unit; and

5. The original data will be held for at least five years from the date indicated below and is stored at the following location(s):

College of Engineering and Science, Victoria University, Melbourne, Australia

Name(s) of Co-Author(s)	Contribution (%)	Nature of Contribution	Signature	Date
Dr. Anne Ng	5%	Review comments, Discussion on conceptual ideas		14/8/18
Dr. Shobha Muthukumaran	5%	Review comments, Discussion on conceptual ideas		14/8/18
Dr. Jatin Kala	5%	Critical review comments, Discussion on conceptual ideas		15/8/18

This is the pre-peer reviewed version of the following article: Imran, HM, Kala, J, Ng, AWM, Muthukumaran, S. Impacts of future urban expansion on urban heat island effects during heatwave events in the city of Melbourne in southeast Australia. *Q J R Meteorol Soc.* 2019; 145: 2586– 2602, which has been published in final form at <https://doi.org/10.1002/qj.3580>. This article may be used for non-commercial purposes in accordance with Wiley Terms and Conditions for Use of Self-Archived Versions.

Impacts of Future Urban Expansion on Urban Heat Island Effects during Heatwave Events in the City of Melbourne in Southeast Australia

H. M. Imran^{1,3,4}, J. Kala², A. W. M. Ng^{1,4}, and S. Muthukumaran^{1,4}

¹College of Engineering and Science, Victoria University, Melbourne, Australia

²Environmental and Conservation Sciences, Murdoch University, Perth, Western Australia

³Institute of Water and Environment, Dhaka University of Engineering & Technology, Gazipur, Bangladesh

⁴Institute for Sustainable Industries & Livable Cities, Victoria University, Melbourne, Australia

Abstract

The city of Melbourne in southeast Australia is planning to substantially expand urban areas by the year 2050 and this expansion has the potential to alter the Urban Heat Island (UHI), i.e., higher temperatures in urban areas as compared to surrounding rural areas. Moreover, Melbourne has been experiencing more frequent heatwaves for last two decades, and the intensity and duration of heatwaves is expected to increase in the future, which could exacerbate the UHI. This study evaluates the potential impacts of future urban expansion on the urban meteorology in southeast Australia during four of the most severe heatwave events during the period of 2000 to 2009. Urban expansion is implemented as high density urban with a high urban fraction of 0.9 to investigate the maximum possible impacts. Simulations are carried out using the Weather Research and Forecasting model coupled with the Single Layer Urban Canopy Model with current land use and future urban expansion scenarios. Urban expansion increases the near-surface (2 m) UHI (UHI_2) by 0.75 to 2.80 °C and the skin-surface UHI (UHI_{sk}) by 1.9 to 5.4 °C over the expanded urban areas during the night, with no changes in existing urban areas. No substantial changes in the UHI_2 and UHI_{sk} occur during the day over both existing and expanded urban areas. This is largely driven by changes in the storage heat flux, with an increase in storage heat at night, and a decrease during the day, i.e., excess storage heat accumulated during the day is released at night, which causes slower decrease of near surface temperature and increase in the UHI. Urban expansion did not affect human health (HTC) comfort in existing urban areas and there were no marked differences in HTC between existing and expanded urban areas.

¹Correspondence to: H.M. Imran, College of Engineering and Science, Victoria University, PO Box 14428, Melbourne, Victoria, Australia.
Phone: +61399195041
Fax: +61399194139
E-mail: ihosen83@gmail.com

Keywords: Urban expansion, Urban Heat Island, coupled WRF-SLUCM model, Human Thermal Comfort

1. Introduction

Changes in land cover due to increased urbanization can substantially affect the urban environment and climate (Seto and Shepherd, 2009). One of the well-documented effects of urbanization is the Urban Heat Island (UHI); i.e., higher temperatures in urban areas as compared to surrounding rural areas, particularly during the night (Arnfield, 2003). Urban expansion has the potential to further enhance UHI effects (e.g., Argüeso et al., 2014; Liu et al., 2018; Yang et al., 2016; Morris et al., 2017; Pauleit et al., 2005) and hence, understanding the impacts of future urban expansion on the UHI is very important. A number of features such as building fabric, building form, thermal properties of construction materials, synoptic condition & wind flow and anthropogenic heat lead to generate the UHI in urban areas (Oke et al., 1991; Harman and Belcher, 2006). The UHI is driven by the higher thermal heat capacity and heat storage of urban infrastructure and reduced evapotranspiration due to the loss of vegetation and increase in impermeable surfaces. The UHI results in higher air temperatures at screen level in urban areas that can contribute to heat-related illnesses including heart disease, which can lead to mortality, particularly during summer, and these effects can be exacerbated during heatwaves in Australia (Department of Infrastructure and Regional Development, 2013). For example, a total 4555 people's death were attributed to extreme heat over the period 1900 to 2011 in Australia, which is 55.2% of total natural hazard deaths (Coates et al., 2014). In addition, higher temperatures in urban areas also affect urban ecosystems as well as human thermal comfort and increase the rate of energy consumption (Block et al., 2012).

Melbourne is the fastest growing city in Australia and according to Plan Melbourne 2050, the urban area is expected to expand into surrounding suburban regions (more details about plan Melbourne is available at <http://www.planmelbourne.vic.gov.au/the-plan>). The urbanization rate in the Melbourne metropolitan areas is increasing rapidly with the projected population of Melbourne expected to increase from 3.5 million and reach 8 million by 2056 (Australian Bureau of Statistics, 2008). Moreover, studies predict more frequent and longer lasting heatwaves over eastern Australia (Perkins et al., 2016), and UHI effects are likely to be most pronounced during such events (Liu et al., 2018). The rapid expansion of urban areas is

continuing within the metropolitan area, which will play an important role in the development of this city in future.

Coutts et al. (2008) investigated the impacts of long-term urban planning strategies according to Plan Melbourne 2030, on the local climate and above canopy UHI during the Austral summer for the month of January in 2004 (current urban scenario) and 2030 (future urban scenario) in the city of Melbourne by using The Air Pollution Model (TAPM) (Hurley, 2000). They showed that the urban expansion according to plan Melbourne 2030, would likely lead to a more intense UHI during the night, with effects during the day being less significant. An earlier study by Coutts et al., (2007) examined the impacts of urban density on the surface energy balance for the city of Melbourne and showed that increasing urban fractions led to higher nocturnal temperatures. A number of studies have used climate models for urbanization-related climate studies at different spatial scales (global, regional) (Liao et al., 2014; Wang et al., 2012; Wang et al., 2015; Zhao et al., 2013), and these studies also report higher near-surface air temperature due to increased urbanization. However, the impacts of urban expansion during heatwave events are largely unknown.

The impacts of urbanization on the UHI can be investigated from meteorological observations as well as remote sensing data. However, a number of atmospheric models now include explicit urban canopy schemes which incorporate complex urban parameterizations and this can be a useful tool in sustainable urban planning. Hence, numerical weather and climate models are increasingly used to assess the impacts of urbanization (both current and future) on weather and climate at global and regional scales (e.g., Chen et al., 2014). A commonly used numerical modeling tool is the Weather Research and Forecasting (WRF) (Skamarock et al. 2005) coupled to the Single Layer Urban Canopy Model (SLUCM) model (Kusaka et al., 2001), which has been used to investigate the response of urban meteorology to land use changes, including urbanization, in major metropolitan cities such as Guangzhou, China (Meng et al., 2011), New York USA (Holt and Pullen, 2007), and Sydney in eastern Australia (Argüeso et al., 2014).

Careful urban planning can be a useful mitigation strategy in reducing the adverse impacts of urbanization and improving urban climate and human health (Stone et al., 2010). According to Adachi et al. (2014), a compacted city has a higher potential to increase the mean UHI effects as compared to a sparse city. Changes in urban structures vary between different cities

and the mitigation of heat-related risks varies according to different urban structures (Frolking et al., 2013; Oke, 1981). Therefore, the impacts of future urbanization at the city and neighborhood scales need to be included in urban design and development plans. The aim of this study is to investigate the impacts of increased urbanization according to plan Melbourne 2050 on the urban meteorology during heatwave events. The study focuses on the physical mechanisms, which play key roles in affecting key atmospheric variables as a result of urban expansion. Although this study is limited to one particular city, the overall principles will be relevant elsewhere for other cities, which experience a similar climate.

2. Methodology

2.1 Plan Melbourne Urban Planning Strategy/Projections

The Victorian Government has introduced an urban planning strategy titled ‘Plan Melbourne 2050’ to accommodate the increasing population. The Plan Melbourne 2050 urban expansion data can be obtained from the Environment, Land, Water and Planning Department of the Victoria State Government (<http://www.planmelbourne.vic.gov.au/maps>). This plan describes the future shape of the city of Melbourne over the next 33 years, with the new wave of urban growth expected to spread to the outer-suburban especially in the west, north, and southeast of the city (Fig. 1c).

The anticipated urban development could affect Melbourne’s built and natural environment and could potentially increase UHI effects if urban development is not planned in a careful manner. The city of Melbourne has already faced several extreme heatwave events, during which maximum temperatures reached 45.1°C and 43.9°C during 2009 and 2014 respectively. During summer, prevailing anticyclonic conditions can lead to heatwaves which bring dry and warm air over the city, which exacerbates urban temperatures (Nairn and Fawcett, 2013; Nicholls and Larsen 2011). Summer heatwaves can lead to temperatures in excess of 35 °C, while the mean UHI intensity is estimated at 3.56°C in the early morning (6 a.m.), during these heatwave events in Melbourne (Morris and Simmonds, 2000). However, the UHI intensity can be much higher than the mean UHI under optimal conditions such as clear skies and low winds. A maximum UHI of 7.1°C has been observed in the central business district of Melbourne at 9 p.m. (local time) from an automobile transect carried out in 1992 (Torok et al., 2001).

2.2. Case Studies

The study investigates the impacts of urban expansion during severe heatwave events as heat stress is more likely during such events. Following Imran et al. (2018b), who evaluated the WRF model coupled to the SLUCM, in simulating heat waves events over southeast Australia, this study focuses on four heatwave events which were the most severe over the city of Melbourne during the period of 2000 to 2009. These events occurred in 2000 (2nd to 4th February), 2006 (20th to 22nd January), 2007 (16th to 18th February) and 2009 (28th to 30th January). Event-4 was the most severe among these four heatwave events. It led to the Black Saturday bushfires (one of the largest bushfire events in Australia's history that led to a large number of fatalities) in early February 2009 (Engel et al., 2013).

2.3. WRF model set-up and experiments

This WRF model is commonly used for urban meteorology studies (e.g., Argüeso et al., 2014; Chen, et al., 2014; Morris, et al., 2017; Sharma et al., 2016) and the version used in this study is WRFv3.8.1. The model was used to simulate the four heatwave events with present urban land-use (control simulations) and experiments were carried using the 2050 urban land-use scenarios over the city of Melbourne in southeast Australia. The initial and boundary conditions were obtained from 6-hourly ERA-interim reanalysis data (Dee et al., 2011). Three two-way nested domains with horizontal grid resolutions of 18, 6 and 2 km were used (Fig. 1a). The innermost domain (D03) mainly covers the city of Melbourne and surrounding rural areas. A total of 38 vertical levels were used, closely spaced in the boundary layer and further apart in the upper atmosphere. Following Imran et al., (2018a), the first 24 hours of the simulation period are considered as spin-up time and the remaining 72 hours simulations are used for analyses.

The choice of physics parameterizations was based on Imran et al. (2018b), who conducted an extensive sensitivity analysis of WRF to different physics options in simulating the same four heatwave events over the city of Melbourne. Imran et al. (2018b) evaluated a number of physics options by comparing WRF simulations against station, gridded and atmospheric sounding observations. In addition, they carried out an analysis of the physical processes and dynamics associated during the four heatwave events and showed that the WRF model is able to simulate various climate variables (e.g. temperature, relative humidity, wind speed) and UHI over the city of Melbourne. This choice of physical parameterizations includes the Thompson microphysics scheme (Thompson et al., 2008), the RRTMG shortwave and

longwave radiation schemes (Iacono et al., 2008), the MYJ Planetary Boundary Layer (PBL) scheme (Janjic 1994), the Monin-Obukhov surface layer scheme, the Noah land-surface model (Chen and Dudhia, 2001) and the Grell-3d cumulus scheme (Grell and Dévényi, 2002). No cumulus scheme was used for the innermost domain because of a resolution of 2 km is sufficient to resolve convection. We do not carry out model evaluation in this paper, as extensive evaluation is documented in Imran et al. (2018b) for the same 4 heatwave events, as well as Imran et al. (2018a) who conducted further comparisons of WRF-SLUCM winds and temperature against station observations for the most severe event out of the 4 case studies.

The SLUCM was used to parameterize the physical urban processes, which represent energy and momentum exchange between urban surfaces (e.g., roofs, walls, and roads) and the atmosphere (Kusaka et al., 2001). The default representation of urban land-use in WRF was replaced by the Jackson et al. (2010) urban dataset for representing the current spatial distribution of low-density, high-density and commercial/industrial areas in the city of Melbourne. The Jackson et al. (2010) data is a global dataset of four urban categories (low-density urban, medium-density urban, high-density urban and tall building areas) and also includes properties of urban extent, urban morphology, and thermal and radiative properties of building materials. It is specifically designed for use in urban meteorology and climatological studies. The four urban categories from the Jackson et al. (2010) urban land use data were converted into the three categories (low-density, high-density and commercial/industrial) based on the 24-USGS land use categories, as used by the SLUCM in the WRF model. We note that other land use databases can be used in WRF, e.g., MODIS. Our choice of the USGS database is based on our previous studies (Imran et al 2018a, 2018b) which showed that WRF was able to adequately simulate the heatwave events when compared against meteorological stations in the urban area. The low and medium density urban categories of the Jackson et al. (2010) land-use dataset were classified as low and high-density urban areas respectively, while the high-density urban areas and tall buildings were classified as commercial/industrial areas, as illustrated in Fig. 1(b). These re-classifications allow for a realistic representation of urban land-use categories for this city. Only urban grid cells were modified and the remaining grid cells were kept the same as the default WRF land use data. Fig. 1(b) shows the current distribution of urban land-use and Fig. 1(c) shows the future urban expansion scenario based on Plan Melbourne 2050. Following the previous study by Argueso et al. (2014), who investigated the impacts of future urban expansion in the

city of Sydney in eastern Australia using WRF-SLUCM, all future urban expansion (Fig. 1(c)) was classified as high density urban. A similar approach has been used to investigate the impacts of future climate change and urban expansion for US cities using the coupled WRF-SLUCM model (Krayenhoff et al., 2018).

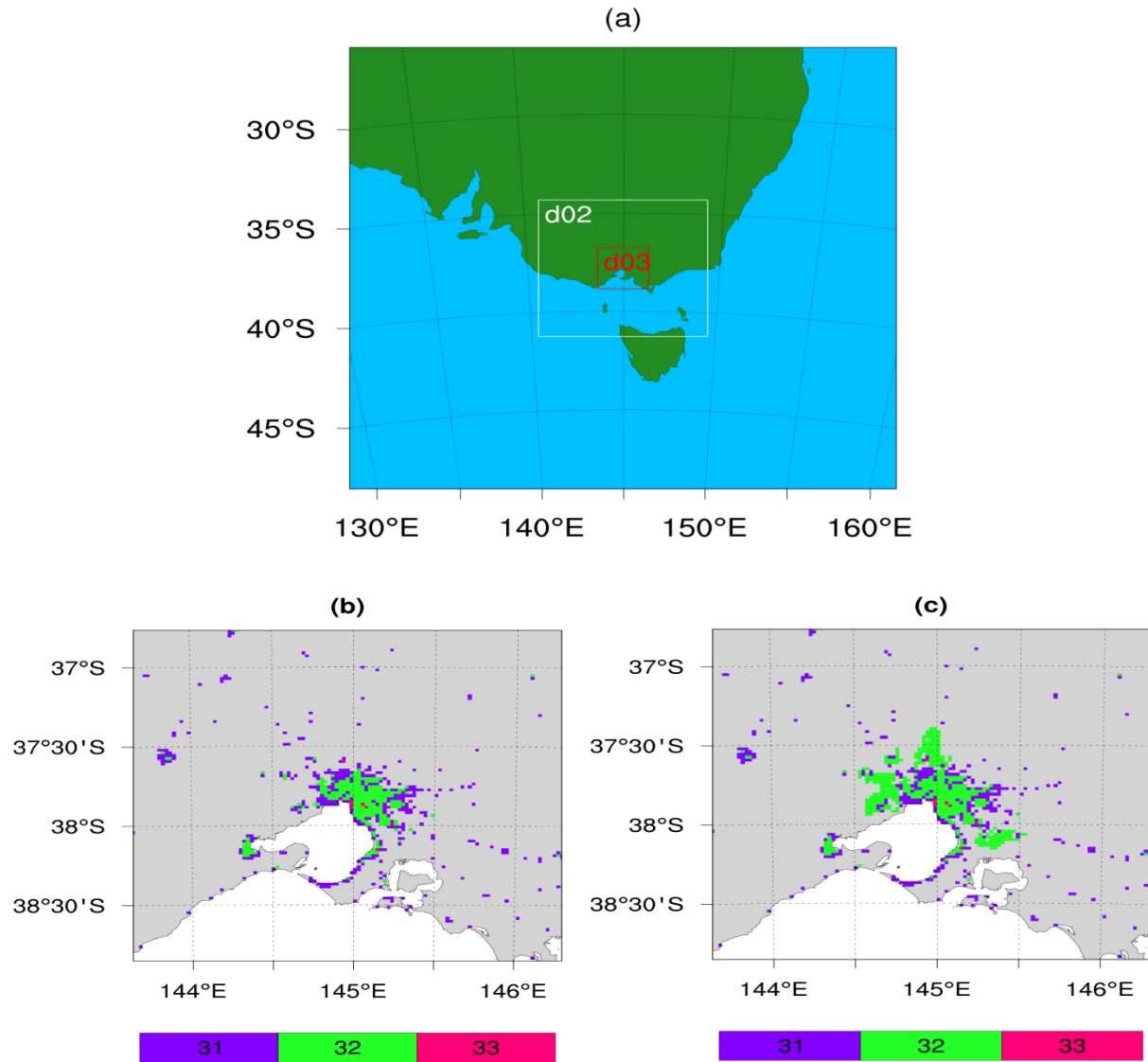


Fig. 1. (a) Model nested domain configuration (the boundary represents the outer domain with a resolution of 18 km, and d02 and d03 denote the boundaries of the two inner nested domains, with resolutions of 6 km and 2 km respectively), (b) current distribution of urban land-use, (c) high-density urban expansion according to Plan Melbourne 2050. The numbers 31, 32 and 33 represent the low-density urban, high-density urban and commercial/industrial areas, respectively.

The urban morphological properties for all simulations use the default set-up in the WRF model except urban fraction for low-density urban areas (Table 1) which was increased from 0.5 to 0.7. Default urban fractions are included in the SLUCM for three urban categories, which may not necessarily be representative for a specific city. Using urban fractions of 0.50 and 0.70 showed that the results were more realistic when using an urban fraction of 0.7 for low-density urban areas and this is consistent with a study focusing on the UHI in Melbourne by Coutts et al. (2007), who derived urban fractions using Geographic Information System and aerial photography. Following Coutts et al. (2007), other studies also have used same urban fraction 0.70 for low-density urban areas in evaluating UHI effects in the city of Melbourne (Jacobs et al., 2017; Jacobs et al. 2018; Imran et al., 2018a). The use of higher urban fraction as compared to default values is also consistent with other studies which have used WRF-SLUCM for UHI studies for cities in China (Chen and Frauenfeld, 2016), and city of Sydney in southeast Australia (Argueso et al., 2014).

Table 1. Urban properties for low-density, high-density and commercial/industrial areas used by the SLUCM in WRF.

Properties/Parameters	Low-Density Urban	High-Density Urban	Commercial/Industrial
Built/Impervious fraction	0.70 (default 0.50)	0.90	0.95
Roof width (Rf)	8.3 m	9.4 m	10 m
Road width (Rd)	8.3 m	9.4 m	10 m
Roof fraction in built/impervious part [Rf/(Rf + Rd)]	50 %	50 %	50 %
Roof fraction in whole urban grid	25 %	45 %	47.5 %
Building Height	5 m	7.5 m	10 m

2.4. Numerical Experiments

The impacts of urban expansion are explored by incorporating high-density urban expansion over the rural areas based on the proposed urban expansion strategy of the Plan Melbourne 2050. A total of 8 numerical simulations were conducted: 4 control experiments with current urban land use (Fig. 1(b)), and 4 experiments with high-density urban expansion according to plan Melbourne 2050 (Fig. 1(c)). All simulations used the same initial and boundary conditions from ERA-Interim re-analysis.

2.5. Human Thermal Comfort (HTC) Calculation

This study also examines the impacts of urban expansion on the pedestrian level (approximated as above 2 m from ground level) HTC characterized by the UTCI index (Bröde et al., 2012). Although there are a number of indices used to calculate the HTC (e.g., the Discomfort Index, the approximate wet bulb globe temperature, and the Physiological Equivalent Temperature), the UTCI has been used in calculating HTC index in several studies (e.g., Coutts et al., 2016; Vatani et al., 2016). The UTCI is a physiological response index in representing human-bioclimate conditions and their relevance to human thermal stress under different climatic conditions, which makes this index universal in nature, and it represents the temporal variability of thermal conditions better than other indices (Blazejczyk et al., 2012). In this study, the radiation and human-bioclimate model Rayman Pro version 3.1 (Matzarakis et al., 2010; Matzarakis et al., 2007) is used for calculating the UTCI index. The UTCI takes into consideration not only the effect of air temperature, but also wind speed, relative humidity, and incoming solar radiation (Johansson, 2006). These variables were taken from the WRF outputs at pedestrian level at 2 m except incoming solar radiation at surface level as input data to the Rayman model. The latter also requires several human thermal parameters, and a default activity factor of 0.80 W and clothing factor of 0.90 for a male of 35 years of age were used. Different values of the UTCI correspond to different physiological stresses as illustrated in Table 2 (Bröde et al., 2012). It should be noted that there are some limitations and assumptions when computing indices such as the UTCI from model outputs. Wind speed at 2 m has to be interpolated from 10 m, as models typically diagnose winds at 10 m for evaluation purposes. Additionally, the calculation assumes a person is always sunlit, which is not realistic in urban environments. Finally, temperatures at 2 m from models such as WRF are diagnosed using Monin-Obukhov similarity over a flat surface. In urban areas, given the complexity of urban surfaces, this diagnosed temperature, does not truly represent air temperature at an elevation of 2 m, but rather should be interpreted as a diagnostic representative near-surface urban air temperature (Li and Bou-Zeid 2013).

Table 2.Scale of Universal Thermal Comfort Index (UTCI) for different grades of human thermal perception and associated physiological stress (Bröde et al., 2012)

UTCI (°C)	Physiological Stress
+9 to +26	no thermal stress
+26 to +32	moderate heat stress
+32 to +38	strong heat stress
+38 to +46	very strong heat stress
> +46	extreme heat stress

2.6. Brief Meteorology of the four Heatwave Events

Fig. 2 shows the mean daily mean sea level pressure (MSLP), wind speed with direction at 10 m and potential temperature at 850 hPa from the outermost domain, Fig. 1(a). All four events were characterized by a strong anti-cyclone to the east, and an approaching cold-front from the south-west (top panel). The anticyclone resulted in the advection of hot and humid air from north and north-east (middle and bottom panels). This north/north-easterly wind-flow resulted in very hot conditions throughout the lower atmosphere (bottom panel), with potential temperatures reaching a maximum of 310 to 312 °K during event-4 over large parts of southeast Australia.

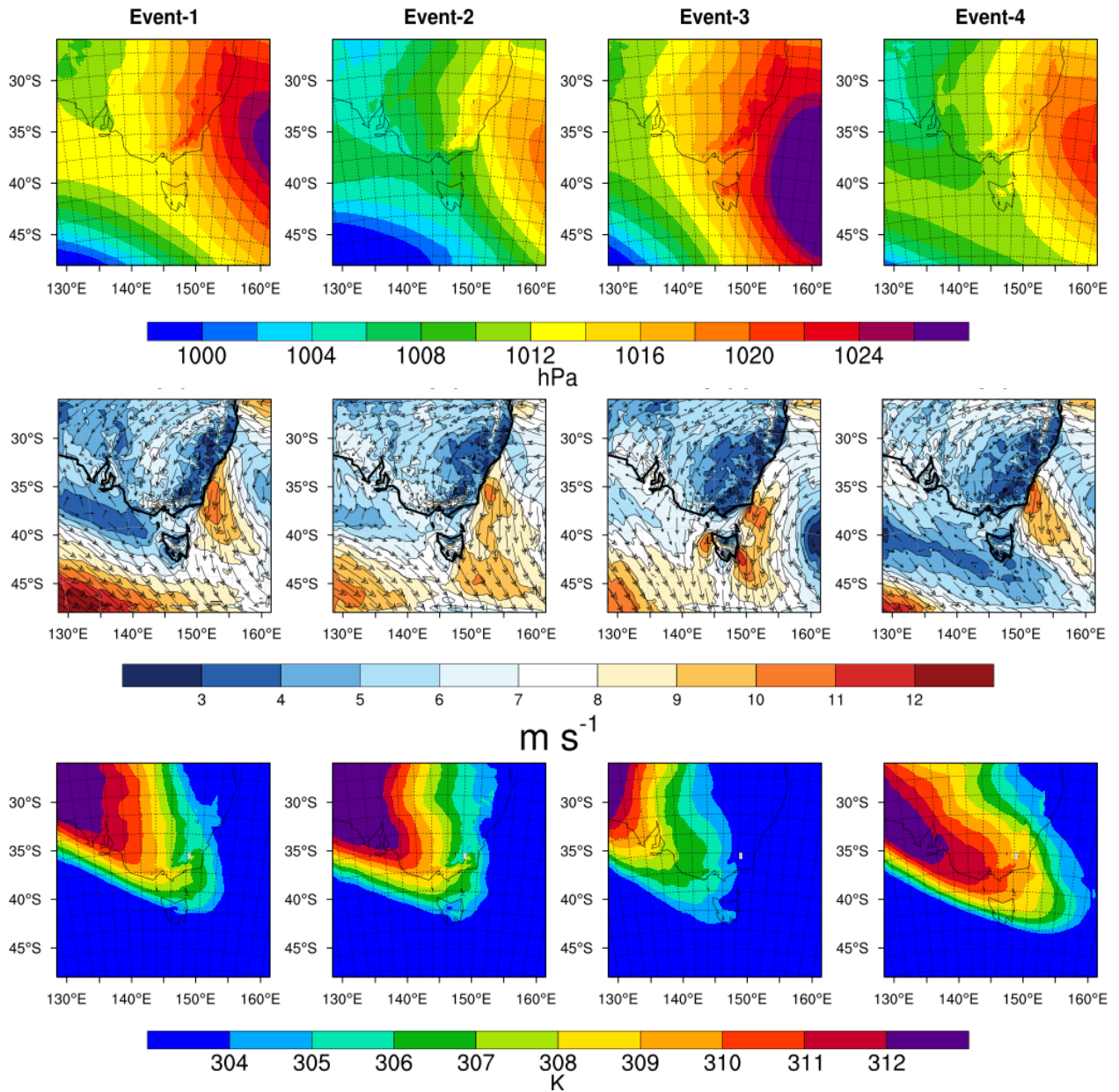


Fig. 2. Mean Sea Level Pressure (top panel), wind speed (colored contours) and direction (middle panel) and potential temperature at 850 hPa (bottom panel) for the four heatwave events averaged over 72 hours, from the outermost domain (Fig. 1).

3. Results

3.1. Impacts of high-density urban expansion on the surface energy balance

The diurnal cycle of the surface energy balance is shown in Fig. 3 for the control (solid lines) and experiments (dotted lines) with urban expansion, averaged over urban grid cells only. Urban expansion results in higher sensible heat flux during both the day and night for all events. The differences range from 70 to 80 W m^{-2} during the evening between 1800 and 1900 local time while early morning peaks range from 22 to 35 W m^{-2} for the four events.

Urban expansion results in a large reduction of latent heat flux for all events, with the maximum reduction occurring at 1300 local time, and varying between 100 and 140 W m^{-2} among the four events, which is a much larger change in magnitude as compared the increase in sensible heat flux. The reduction in latent heat flux and higher thermal capacity of urban surfaces lead to enhanced storage heat for all events (Fig. 3(c)). A positive sign of storage heat indicates the flow of heat from the surface to atmosphere and vice-versa for negative storage heat. Urban expansion results in maximum reduction in storage heat of 90 W m^{-2} for the four events at 1200 local time, while the storage heat increases nearly 50 and 70 W m^{-2} during the morning and the night, respectively.

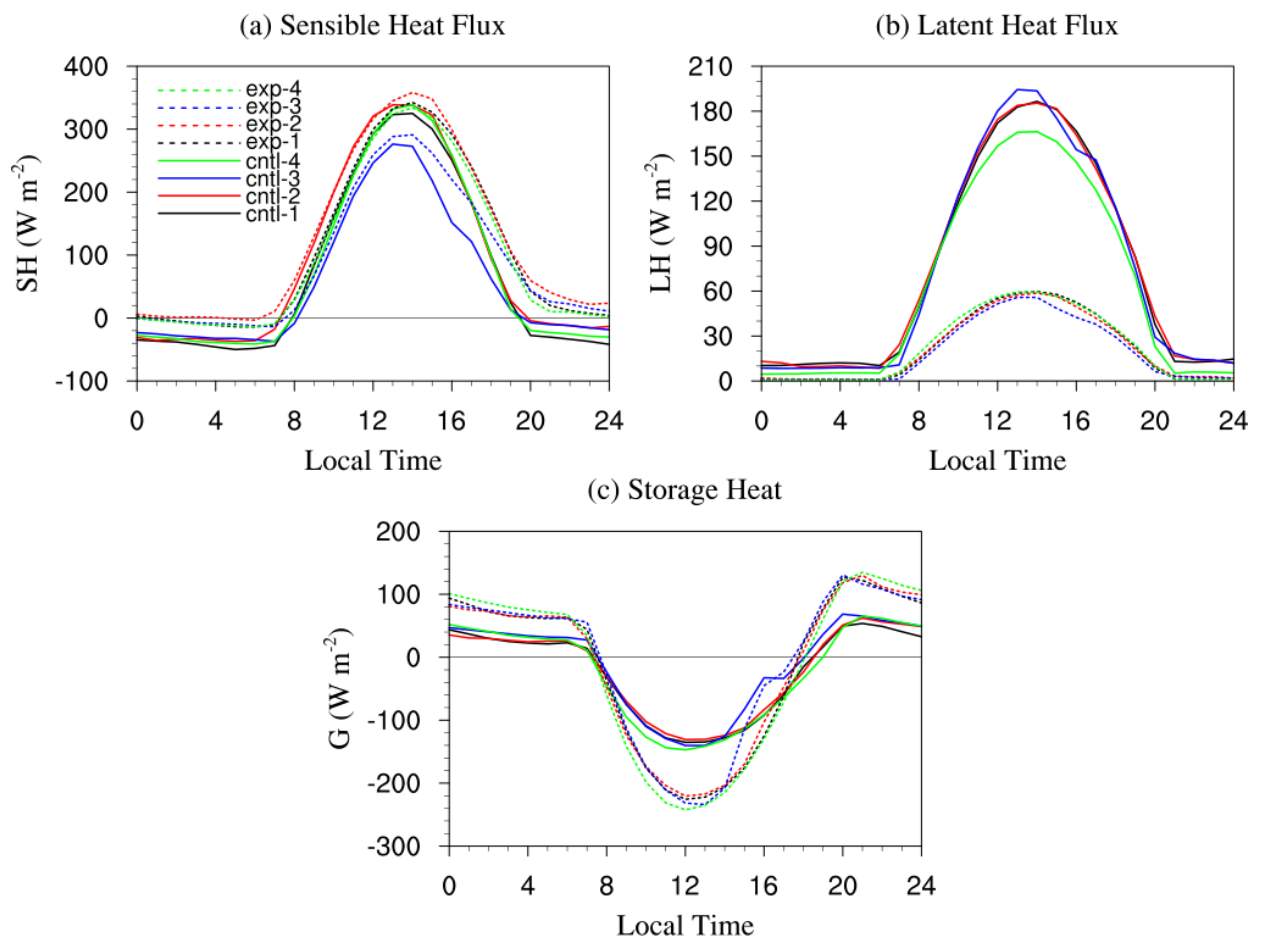


Fig. 3. Diurnal cycle of the surface energy balance for control simulations (solid lines) and experiments (dotted lines) for the four heatwave events, averaged over expanded urban grid cells only (Fig. 1(c)).

The spatial changes (experiment minus control) in daily mean sensible and latent heat fluxes are shown in Fig. 4 (note that daily mean changes in storage heat are not shown in Fig. 4, but

discussed in more detail in later in the paper in Fig. 10 as changes are of opposite sign during the day and night and hence shown separately). The increase in sensible heat flux ranges from 50 to 70 $W m^{-2}$ in the western part of the city of Melbourne for the four events while areas to the north and southeastern parts of the city show an increase between 20 and 40 $W m^{-2}$. The latent heat flux reductions range from 50 to 70 $W m^{-2}$ in the most areas over the expanded areas in the western and southeastern part of the city of Melbourne. The areas to the north show reductions in latent heat flux of 30 to 50 $W m^{-2}$. Urban expansion results in slightly smaller changes in sensible and latent heat fluxes during event-4 as compared to all other events. This is likely due to this heatwave event being the driest and hottest of all four events. For events-2 and 3, the changes in sensible and latent heat fluxes extend to surrounding non-urban areas and this is further explored in section 4).

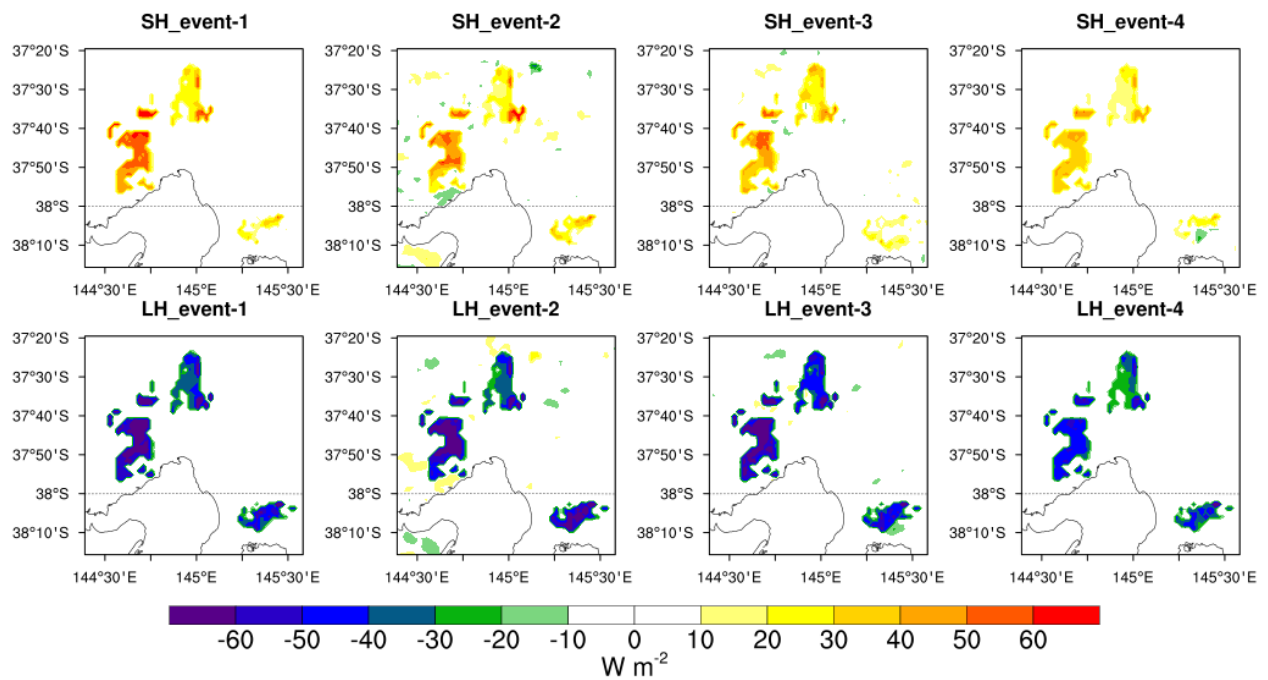


Fig. 4. Changes (experiment minus control) in daily mean sensible (SH, top panels) and latent fluxes (LH, bottom panels) due to urban expansion for the four events, averaged over 72 hours.

3.2. Impacts of high-density urban expansion on the near-surface and skin-surface UHI

Fig. 5 (a) and (b) show the influence of urban expansion on the near-surface urban heat island (UHI_2) and skin-surface urban heat island (UHI_{sk}) at the city-scale (averaged over original and expanded urban grid cells across the domain), and Fig. 5 (c) and (d) show the same variables but averaged over the expanded urban areas only (Fig. 1(c)). Urban expansion

increases the UHI_2 and UHI_{sk} at city scale and over expanded urban areas. The maximum UHI intensity for near-surface and skin-surface is highest during the night at both the city-scale and over expanded urban areas. At the city-scale, UHI_2 increases by 0.20 to 0.35 °C during the morning and 0.10 to 0.50 °C during the night while UHI_{sk} increases by 0.10 to 0.40 °C and 0.10 to 0.50 °C during morning and night respectively. Furthermore, UHI_2 increases by 1.2 to 2 °C during the morning and 1 to 2.8 °C during the night over the expanded urban areas, but such large changes are not observed at the city scale. The effect of urban expansion is greater on the UHI_{sk} as compared to the UHI_2 , with the UHI_{sk} ranging from 2.2 to 4.1 °C during the morning and 2 to 5.4 °C during the night over expanded urban areas only. Interestingly, event-4 showed the highest change in UHI_2 and UHI_{sk} during both morning and the night at both the city-scale and over expanded areas likely due to the drier and more severe heatwave characteristics among four heatwave events. All events showed a lower change in UHI_2 and UHI_{sk} between 0900 and 1600 local time over expanded urban areas only.

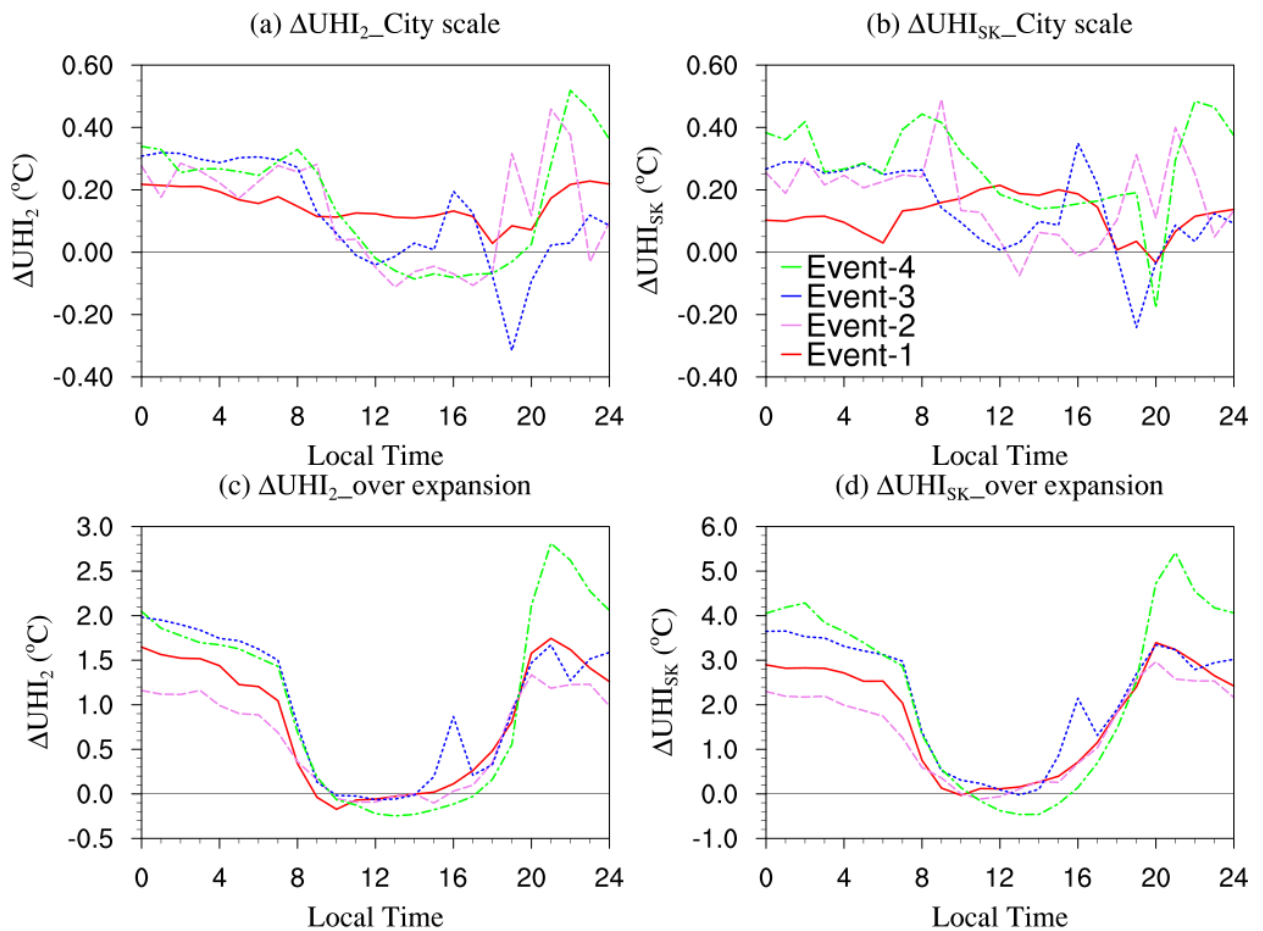


Fig. 5. Changes in diurnal (a) UHI_2 (UHI at 2 m above the ground) and (b) UHI_{sk} (surface UHI) averaged over all urban grid cells (original plus expanded), and (c) UHI_2 and (d) UHI_{sk} averaged over the expanded urban areas only (Fig. 1(c)).

The spatial changes (experiment minus control) in mean near-surface (T_2) and skin-surface (T_{sk}) temperatures are shown in Figs. 6 and 7 respectively averaged over three different time intervals 0200 to 0600 (before sunrise), 1000 to 1400 (when the change in UHI_2 and UHI_{sk} is minimum) and 2000 to 2400 local time (when the change in UHI_2 and UHI_{sk} is maximum) for the four events. T_2 increases between 1.0 and 3.0 °C before sunrise, and 1.0 and 4.5 °C from evening to midnight, while events 3 and 4 show the warmest conditions as compared to events 1 and 2 (Fig. 6). No substantial changes in T_2 are evident during the day (middle row) for all four events. The increases in T_{sk} (Fig. 7) are higher than T_2 , ranging between 1.0 and 7.0 °C for all the four events before sunrise, and between 2000 and 2400 local time when the maximum changes in UHI_2 and UHI_{sk} occurs. Similar to changes in T_2 , changes in T_{sk} are not substantial during the day. It is also important to note that the high-density urban expansion extends the change in T_2 and T_{sk} to the surrounding areas before sunrise, and from evening to midnight. Event-4 shows the highest change in T_2 and T_{sk} due to high-density urban expansion as compared to other three events before sunrise and after sunset. The changes in mean T_2 and T_{sk} during these 3 time periods were largely driven by changes in the minimum T_2 and T_{sk} over these periods, rather than the mean (Supplementary Figures S1 and S2).

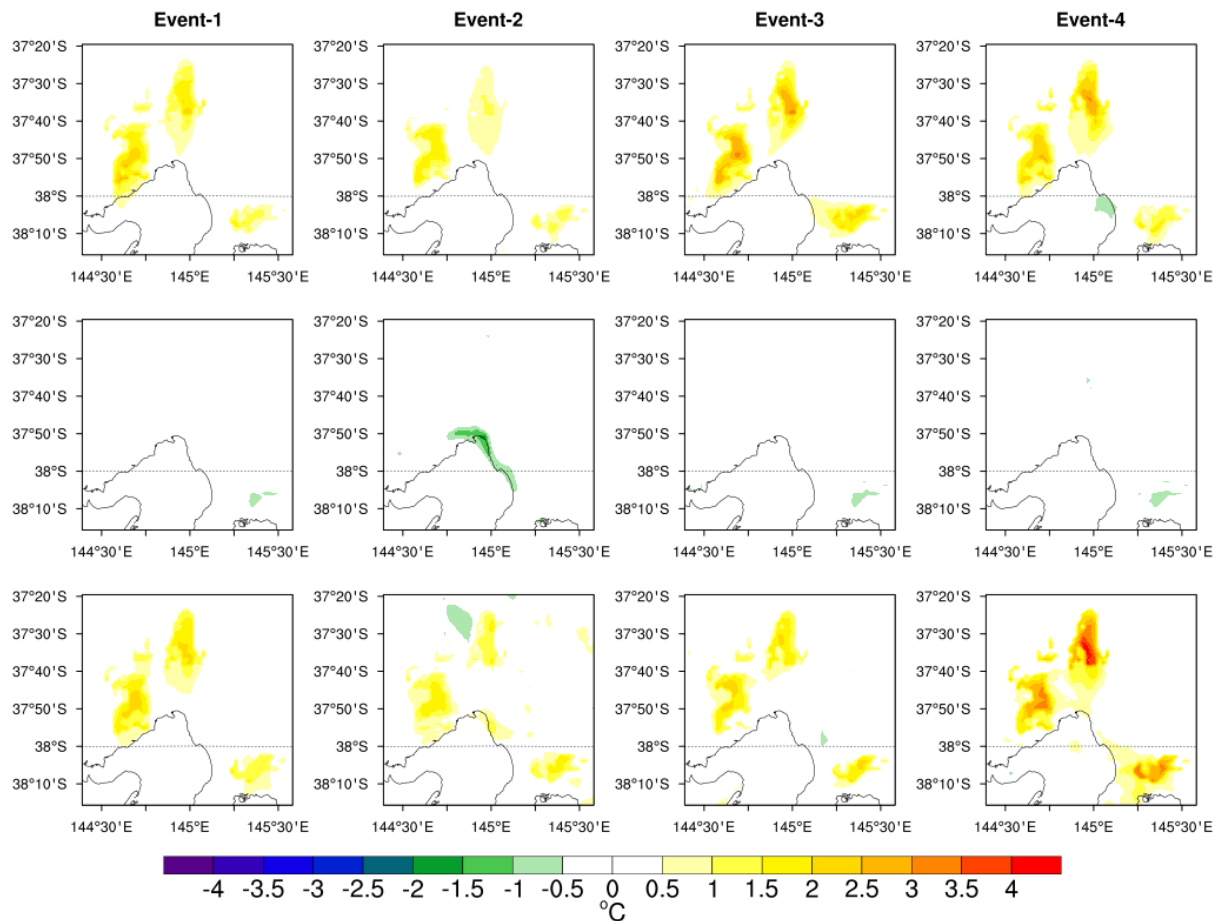


Fig. 6. Changes (experiment minus control) in mean T_2 (experiment minus control) due to urban expansion for the four events. Top row shows the results before sunrise (0200 to 0600 local time), middle row shows results when the effect of ΔUHI_2 is minimum (1000 to 1400 local time), and bottom row shows the results when the effect of ΔUHI_2 is maximum (2000 to 2400 local time).

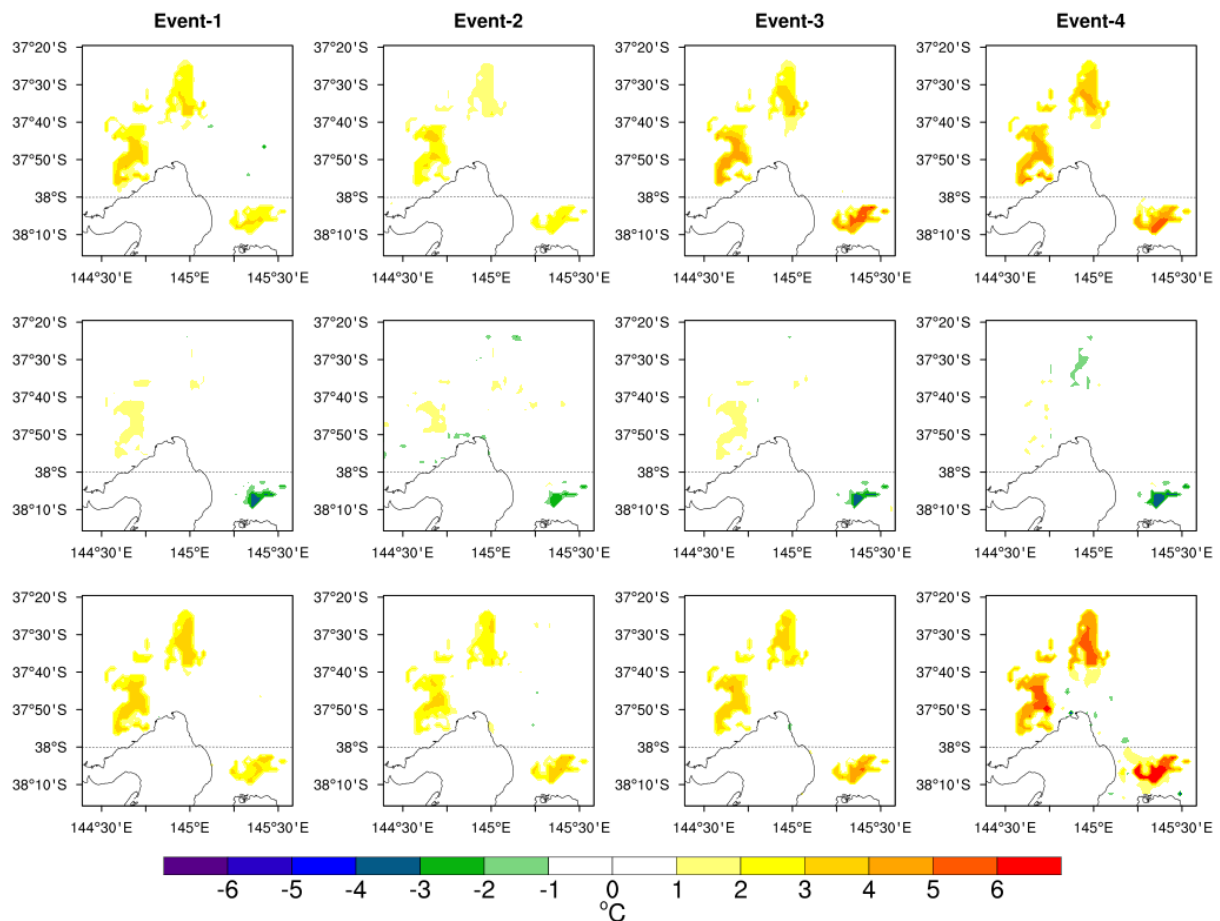


Fig. 7. Changes in mean T_{sk} (experiment minus control) due to urban expansion for the four events. Top row shows the results before sunrise (0200 to 0600 local time), middle row shows results when the effect of ΔUHI_{sk} is minimum (1000 to 1400 local time), and bottom row shows the results when the effect of ΔUHI_{sk} is maximum (2000 to 2400 local time).

The spatial distributions of changes in mean storage heat flux, wind speed at 10 m and relative humidity at 2 m averaged over the different times (before sunset, during the day and after sunset) are shown in Figs. 8, 9 and S_3 (supplementary figure) respectively. These were examined to help explore the physical processes and dynamics associated with the causes of higher intensity of the UHI_2 and UHI_{sk} during the morning and night. Upward storage heat flux (positive storage heat) increases from 20 to 60 $W m^{-2}$ before sunrise and 40 to 80 $W m^{-2}$ during the evening for all events. On the other hand, downward/absorbed storage heat flux (negative storage heat) increases from 50 to 100 $W m^{-2}$ during the day for all events. The magnitude of increased storage heat is higher during the evening as compared to increased storage heat before sunrise. The changes in T_2 and T_{sk} are therefore largely driven by the

changes in storage heat flux. During the day, urban expansion results in more heat storage, which is released at night. Since there were no changes in wind direction, but only in wind speed, Fig. 9 shows the changes of wind speed (experiment minus control), and the wind barbs show the wind direction for the experiments only. The wind was predominantly northerly during both the day and night for all events, with wind speed reductions from 1.0 to 4.0 m s⁻¹ especially during the day. The reductions of wind speed were slightly higher during the day as compared to reductions of wind speed before sunrise and evening time.

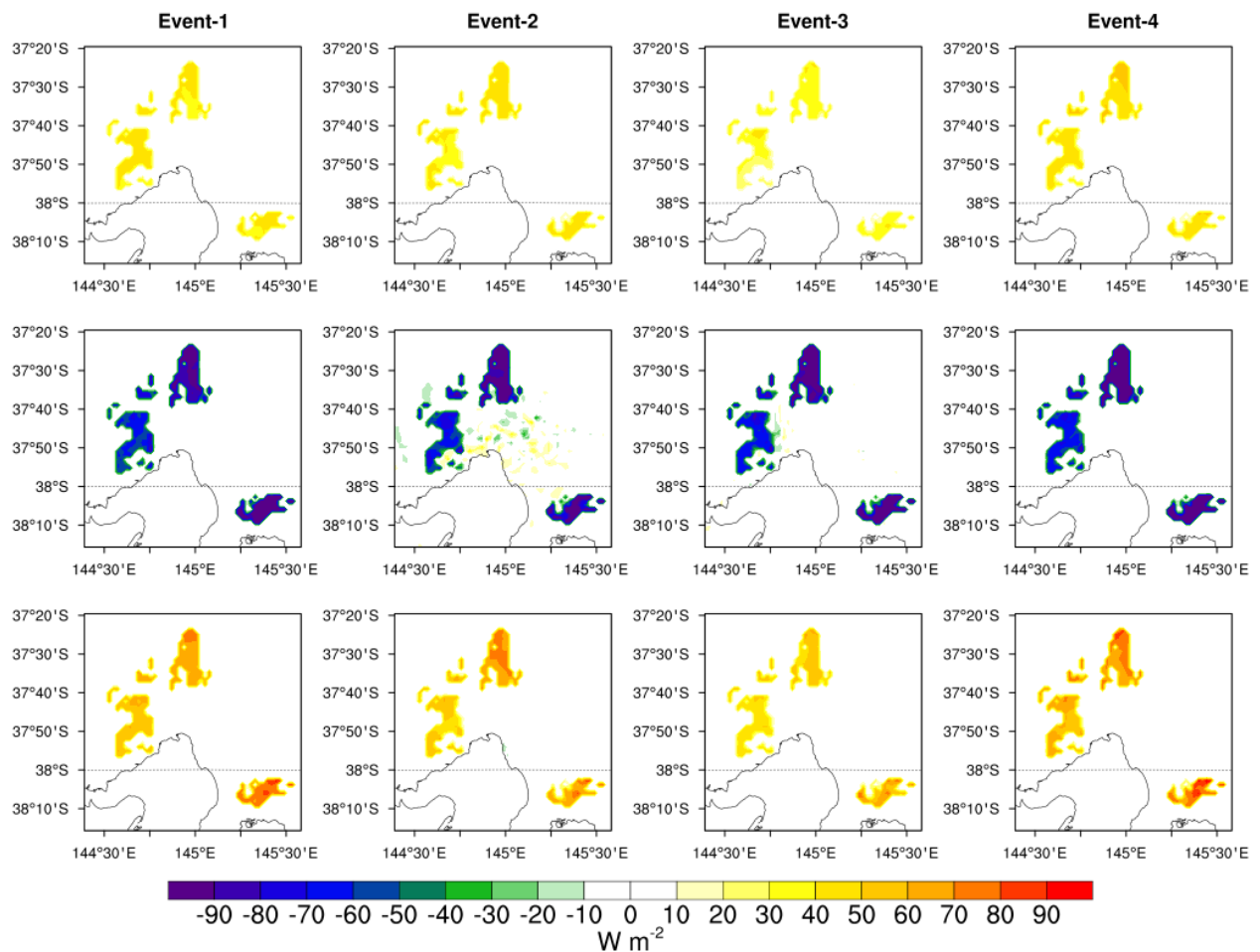


Fig. 8. Changes in storage heat (experiment minus control) due to urban expansion for four events. Top row shows the results before sunrise (0200 to 0600 local time), middle row shows results when the ΔUHI_2 and ΔUHI_{sk} is minimum (1000 to 1400 local time), and bottom row shows the results when the ΔUHI_2 and ΔUHI_{sk} is maximum (2000 to 2400 local time).

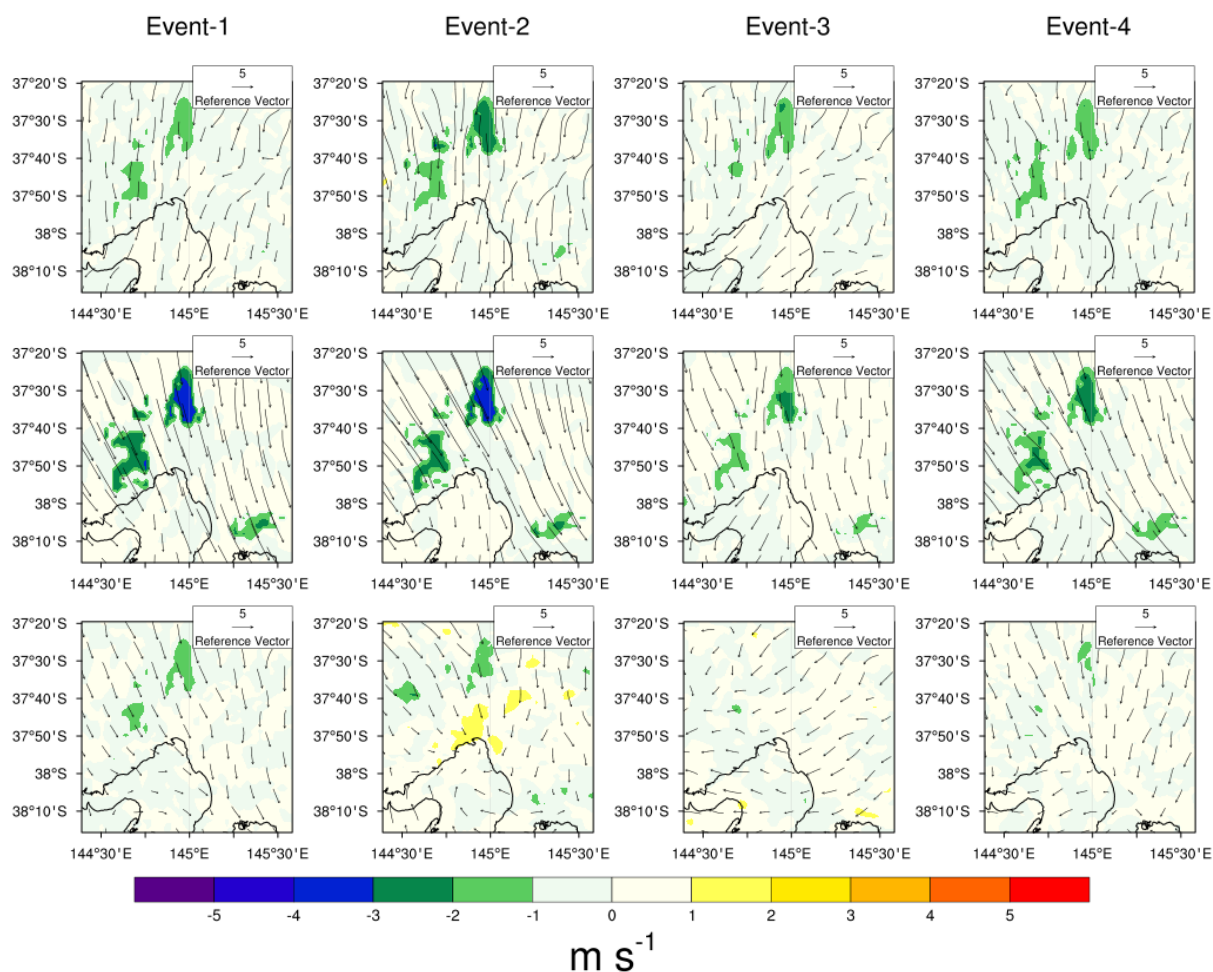


Fig. 9. Wind direction from the experiment only as shown by the wind vectors and changes in wind speed (experiment minus control) due to urban expansion for four events shown as filled color contours. The top row shows results before sunrise (0200 to 0600 local time), middle row shows results when the ΔUHI_2 and ΔUHI_{sk} are minimum (1000 to 1400 local time), and bottom row shows results when the ΔUHI_2 and ΔUHI_{sk} is maximum (2000 to 2400 local time).

3.3 Impacts of Urban Expansion within the Boundary Layer

The planetary boundary layer plays an important role in the transport and mixing of fluxes of heat and moisture. The changes in potential temperature within the boundary layer are shown in Fig. 10. Urban expansion increases the potential temperatures between 0.4 and 1.4 °C in the lower PBL (<300 m) between the evening and morning for all events, and potential temperature decreases from 0.2 to 1.0 °C in the upper PBL (>300 m) both during day and night, especially for events 2 and 4. Event 2 showed the largest changes within the boundary layer as compared to all other events, showing that the magnitude of the response to future urban expansion depends on the event, especially within the middle and upper boundary

layer. Changes in PBL height were small (not shown), and only showed a slight increase during both the day and night, peaking in the evening.

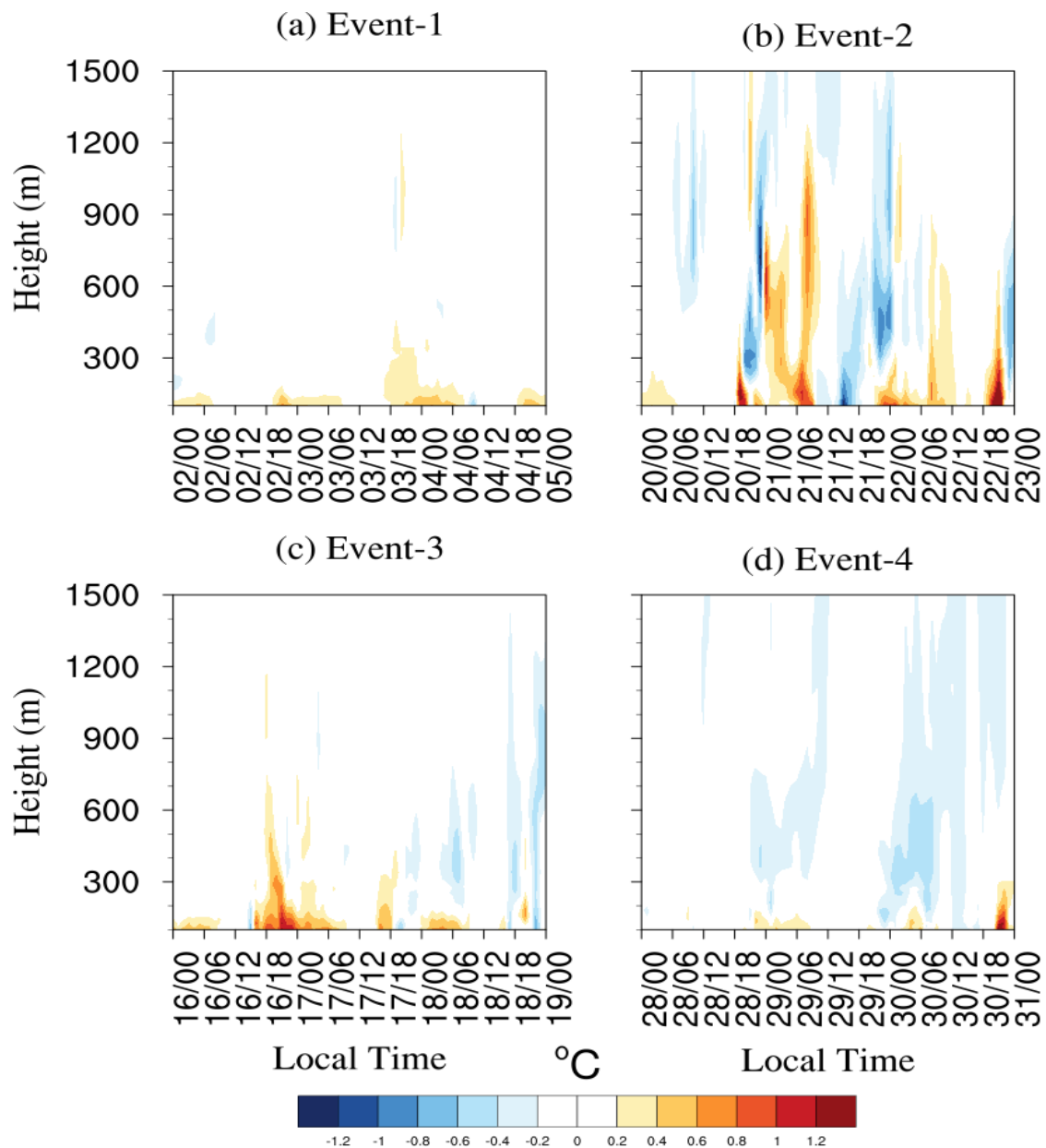


Fig. 10. Changes (experiment minus control) in hourly potential temperatures within the planetary boundary layer for (a) Events-1, (d) Events-2, (c) Events-3 and (d) Events-4, averaged over all urban grid cells in the expanded urban areas only.

Figs. 11 and S₄ (supplementary figure) are similar to Fig. 10 but show the effect of urban expansion on wind speed within the boundary layer. Urbanization results in a reduction in wind speed from 0.8 to 2.0 m s⁻¹ in the lower boundary layer (<300 m) for all the events mostly during the night because wind was obstructed by the higher roughness (0.50) of urban structures as compared to the roughness of replaced vegetated surfaces particularly dry

cropland and grassland (0.05 to 0.12). In the upper boundary layer (>300 m) wind speed increases from 0.8 to 2.5 m s⁻¹ especially for events-2 and 3. This increase in wind speed in the upper boundary occurs likely due to increased pressure gradient because of the decrease in temperature in the upper layer.

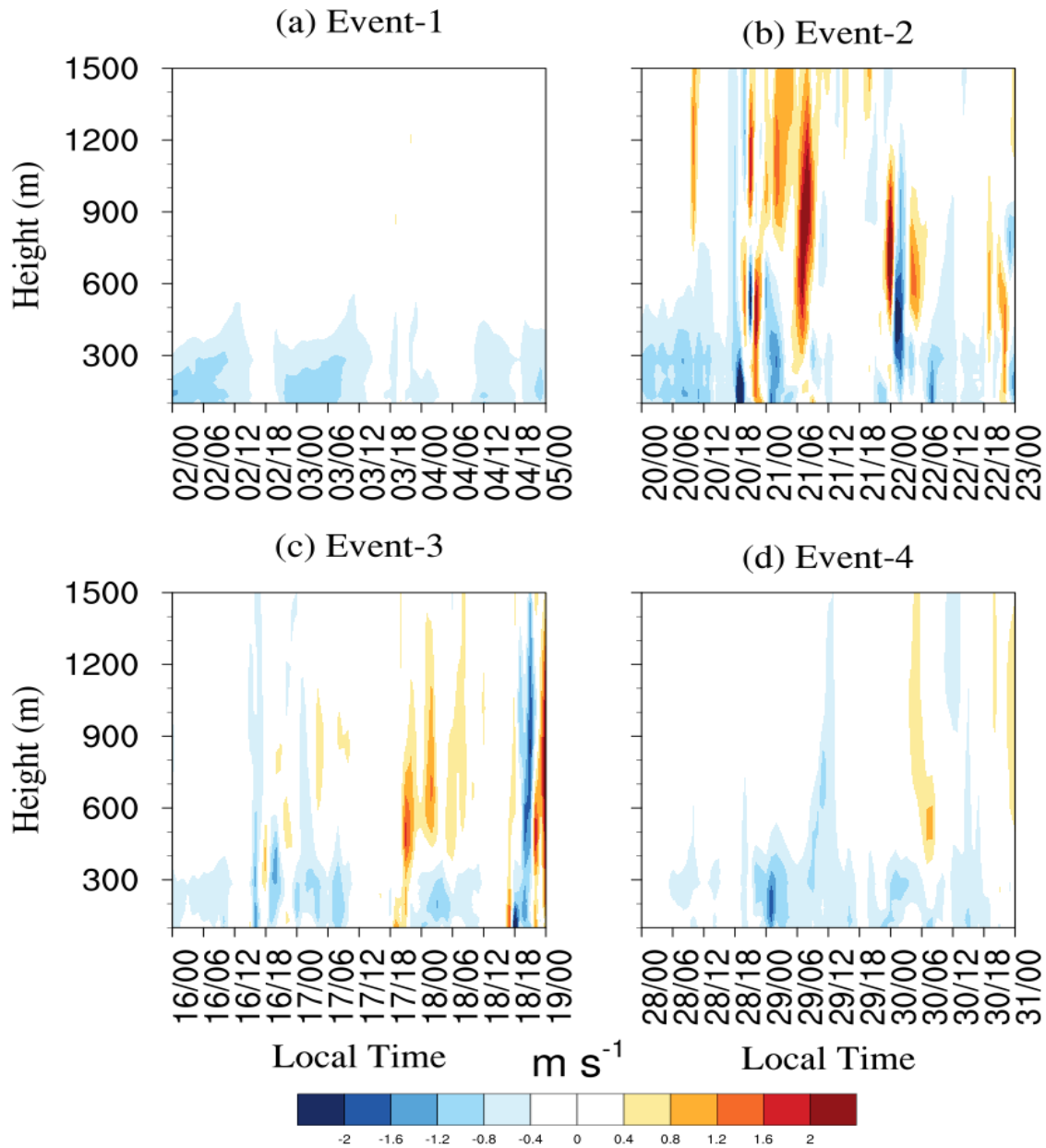


Fig. 11. Changes (experiment minus control) in hourly wind speed within the planetary boundary layer for (a) Events-1, (d) Events-2, (c) Events-3 and (d) Events-4, averaged over all urban grid cells in the expanded urban areas only.

3.4. Impacts on Human Thermal Comfort

The hourly variations in human thermal comfort (HTC) at pedestrian level (approximated as 2 m above ground level) for the four events are assessed over 3 days. The HTC is represented by the UTCI index. The higher UTCI index indicates a decrease in HTC and vice-versa. Fig 12 (top) shows the hourly variation in the UTCI for the 4 events for the control experiment showing that strongest heat stress occurs between midday and afternoon, and event-4 showed the most severe HTC. We next examined the difference in UTCI between existing and expanded urban areas, and existing areas. The differences were small (+1 to -1 °C, not shown), showing that urban expansion does not have a strong influence on the UTCI in existing urban areas. We also examined the difference in UTCI between the expanded urban area and existing urban area as shown in Fig. 12 (bottom). The expanded urban area has slightly lower UTCI (1 to 2.5 °C) between 10.00 and 17.00 local time as compared to existing urban areas, but higher UTCI between 1 and 5 °C from evening to morning (1800 to 1000 local time), when the UTCI is generally at it's lowest. For event-4, the most severe event, the increase in UTCI during this period can change the HTC from moderate to strong, but overall, this increase does not lead to marked changes in HTC.

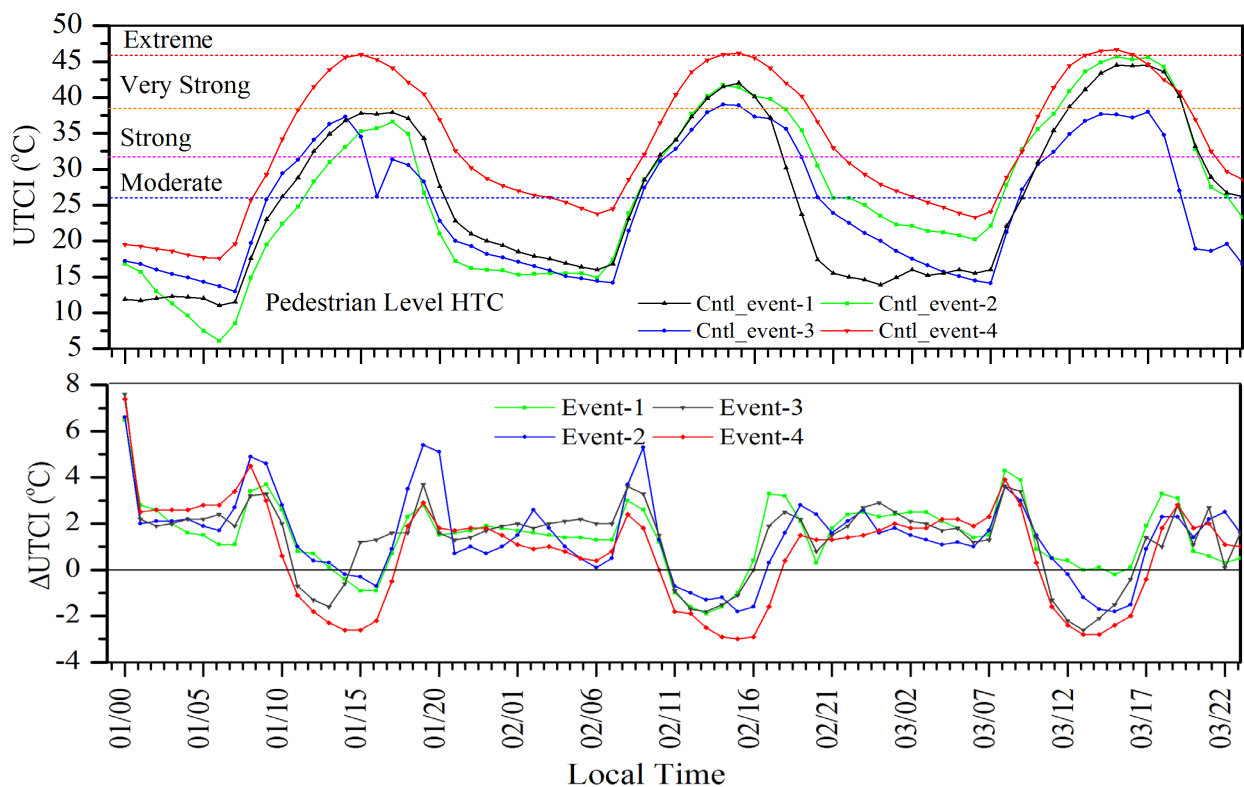


Fig. 12 Hourly variation in pedestrian level UTCI from the control simulations for 3 days (top), and changes (expansion minus existing urban areas) in hourly UTCI (bottom).

4. Discussion and Conclusions

Previous studies have investigated the impacts of future urbanization in the city of Melbourne and other Australia cities (Coutts et al. 2008, Argüeso et al., 2014), however, no studies have investigated the impacts of future urbanization on the UHI during heatwave events, when health impacts are likely to be the most severe. Additionally, these studies were based on older policies, namely, plan Melbourne 2030, and the release of plan Melbourne 2050 calls for an updated assessment of the impacts of future urbanization. Our results show that urban expansion substantially affects the surface energy balance by converting vegetated surfaces to impervious surfaces, which limits the availability of soil moisture and evapotranspiration, and affects the partitioning of surface heat fluxes by increasing sensible heat flux and decreasing latent heat flux. Liu et al. (2018) and Argüeso et al. (2014) report similar results in their studies, and showed that urban expansion leads to a substantial increase in sensible heat flux and decrease in latent heat flux. Urban surfaces lead to an increase in sensible heat flux during the day as compared to vegetated surfaces because of a lack of evapotranspiration and trapping of solar radiation within the urban canopy. As the urban expansion replaces vegetated surfaces to impervious urban surfaces, the reduction in evapotranspiration and soil moisture reduces the latent heat flux especially during the day. Hence, sensible heat flux increases and latent heat flux decreases over the expanded urban areas (Fig. 3a, 3b). The increase in sensible heat flux and decrease in latent heat flux were generally higher in the western part of the city (Fig. 4), because the western suburbs of the Melbourne city are climatologically drier and less densely forested as compared to east suburbs (Jacobs et al., 2018). Therefore, the land cover and climatic conditions appear to play an important role on reduction in latent heat flux and increase in sensible flux. However, these changes in sensible and latent heat fluxes do not influence the UHI directly, but the storage heat flux plays a more important role.

There was a substantial increase in storage heat over the expanded urban areas but no change in the surrounding areas. Absorption of solar radiation by the urban surfaces increases the storage heat during the day as compared to vegetated surfaces due to higher conductivity and heat storage capacity of the construction materials (Liu et al., 2018; Li et al., 2015; Morris et al., 2017). As a result, negative storage heat flux (from the atmosphere to surface) increases during the day while positive storage heat (from the surface to atmosphere) increases between evening and morning. All 4 heat-wave events showed the same overall response, i.e., enhanced storage heat in urban surfaces during the day, because of extreme hot and dry

weather conditions, which is released at night. Event-4 being the most severe, showed the largest response overall. Since the incoming solar radiation is more intense during heatwaves as compared usual summer days (Liu et al., 2018; Wang, et al., 2017), higher urban fraction of urban surfaces absorb and store more solar heat, and consequently, intensify the nocturnal UHI_2 and UHI_{sk} (Fig. 5). The stored heat is slowly released during the night until morning (Liu et al., 2018; Wang et al., 2017; Coutts et al., 2007), and therefore, urban expansion intensifies the nocturnal UHI_2 and UHI_{sk} (Fig. 5), and also leads to a substantial increase in mean near-surface (Fig. 6), skin surface (Fig. 7) temperatures, and minimum near-surface (Fig. S₁) and skin-surface (Fig. S₂) temperatures during the night particularly from evening until morning.

It is noteworthy that there were no substantial UHI effects during the day. The likely reason is that both urban and vegetated surfaces were heated by intense solar radiation with drier weather condition due to heatwaves during the day, which dominated the fluxes over urban and vegetated areas and reduced the thermal difference between these two areas (Liu et al., 2018). Another important finding of this study is that increases in the mean temperature before sunrise, between 1000 to 1400 and 2000 to 2400 were driven by changes in the minimum between these time intervals. Dry and hot inland winds from the north (inland) to the south (Ocean) extend the UHI_2 beyond expanded areas, although there was an overall reduction in wind speed near the surface. The changes in wind speed are unlikely to have a large impact on the T_2 and T_{sk} as the reductions in wind speed were fairly small for all events.

Urban expansion had a substantial influence on the potential temperature within the lower boundary layer particularly during the evening and night due to higher heat storage by the urban surfaces. The increase in potential temperatures decreased with the increasing PBL height, which is consistent with Yang et al. (2016), who showed lower potential temperature with increasing PBL height due to urbanization.

Urban expansion did not affect the HTC in existing urban areas, and differences in the UTCI between the existing and expanded urban areas were not large enough to change the HTC, except for the most severe event from evening to morning, when the UTCI is low. It is noteworthy that the hourly variations of the UTCI indices follow the variations of diurnal cycles of the UHI_2 and, which is driven by the increase in storage heat. Therefore, storage heat due to urbanization plays a crucial role in decreasing HTC during the night.

Finally, this study has some limitations, which need to be discussed. The impacts of future climate change on the future urban expansion are not considered as the simulations including urban expansion are driven with the ERA-interim reanalysis data since this study is based on real case studies. Future warming is likely further exacerbate UHI effects if there is no mitigation, and therefore, the effects of future urban expansion are likely to be underestimated in this study. For example, Krayenhoff et al. (2018) showed the combination of urban expansion and future climate change is likely to increase summertime urban warming by 1-6 K in the afternoon and 3-8 K at night by the end of the century. These ranges of warming are larger than our results for increases in near surface temperature due to urban expansion alone. We also acknowledge the use of constant urban fractions, road fractions, building heights etc, for each of the 3 urban categories is unlikely to be truly representative of the city of Melbourne. This study evaluated the impacts of high-density urban expansion using a constant urban fraction for all future expansion, to investigate the maximum possible response, rather than the expected response. Offline simulations with the Noah land surface model for the city of Houston, USA, have shown that explicitly specifying the urban fraction for each grid-cell, as opposed to using constant values for each urban land use category, yielded more accurate simulations of the surface radiative temperature (Monaghan et al. 2014). Therefore, future studies should investigate the use of spatially varying urban properties versus constant values.

Acknowledgements

Data support by the Bureau of Meteorology (BoM) Australia, ECMWF (ERA-interim) data server (<http://apps.ecmwf.int/datasets/data/interim-full-daily/levtype=ml/>) and the Environment, Land, Water and Planning Department of the Victoria State Government (<http://www.planmelbourne.vic.gov.au/maps>) and are gratefully acknowledged. The authors also acknowledge Stephanie Jacobs and Carlo Jamandre for providing urban categories data (Jackson et al. (2010)) for the city of Melbourne. Jatin Kala is supported by an Australian Research Council Discovery Early Career Researcher Award (DE170100102).

References

- Adachi, S. A., Kimura, F., Kusaka, H., Duda, M. G., Yamagata, Y., Seya, H., Aoyagi, T. (2014). Moderation of Summertime Heat Island Phenomena via Modification of the Urban Form in the Tokyo Metropolitan Area. *Journal of Applied Meteorology and Climatology*, 53(8), 1886-1900. doi: 10.1175/jamc-d-13-0194.1
- Argüeso, D., Evans, J. P., Fita, L., & Bormann, K. J. (2014). Temperature response to future urbanization and climate change. *Climate Dynamics*, 42(7), 2183-2199. doi: 10.1007/s00382-013-1789-6
- Arnfield, A. J. (2003). Two decades of urban climate research: a review of turbulence, exchanges of energy and water, and the urban heat island. *International Journal of Climatology*, 23(1), 1-26. doi: doi:10.1002/joc.859
- Australian Bureau of Statistics (2008). ABS 3222.0 Population projections, Australia 2006 to 2101, viewed 7 August 2018:
<<http://www.abs.gov.au/Ausstats/abs@.nsf/Latestproducts/3222.0>>.
- Blazejczyk, K., Epstein, Y., Jendritzky, G., Staiger, H., & Tinz, B. (2012). Comparison of UTCI to selected thermal indices. *International Journal of Biometeorology*, 56(3), 515-535. doi: 10.1007/s00484-011-0453-2
- Block, A. H., Livesley, S. J., & Williams, S. J. (2012). Responding to the Urban Heat Island: A Review of the Potential of Green Infrastructure.
<http://www.vcccar.org.au/sites/default/files/publications/VCCCAR%20Urban%20Heat%20Island%20-WEB.pdf>
- Brode, P., Fiala, D., Błazejczyk, K., Holmer, I., Jendritzky, G., Kampmann, B., Tinz, B., Havenith, G. (2012). Deriving the operational procedure for the universal thermal climate index (UTCI). *Int. J. Biometeorol.* 56 (3), 481e494. doi: 10.1007/s00484-011-0454-1
- Chen, F., & Dudhia, J. (2001). Coupling an Advanced Land Surface–Hydrology Model with the Penn State–NCAR MM5 Modeling System. Part I: Model Implementation and Sensitivity. *Monthly Weather Review*, 129(4), 569-585. doi: 10.1175/1520-0493(2001)129<0569:caalsh>2.0.co;2
- Chen, F., Yang, X., & Zhu, W. (2014). WRF simulations of urban heat island under hot-weather synoptic conditions: The case study of Hangzhou City, China. *Atmospheric Research*, 138, 364-377. doi: <https://doi.org/10.1016/j.atmosres.2013.12.005>

- Chen, L., & Frauenfeld, O. W. (2016). Impacts of urbanization on future climate in China. *Climate Dynamics*, 47(1), 345-357. doi: 10.1007/s00382-015-2840-6
- Coates, L., Haynes, K., O'Brien, J., McAneney, J., & de Oliveira, F. D. (2014). Exploring 167 years of vulnerability: An examination of extreme heat events in Australia 1844–2010. *Environmental Science & Policy*, 42, 33-44. doi: <https://doi.org/10.1016/j.envsci.2014.05.003>
- Coutts, A. M., Beringer, J., & Tapper, N. J. (2007). Impact of increasing urban density on local climate: spatial and temporal variations in the surface energy balance in Melbourne, Australia. *Journal of Applied Meteorology and Climatology*, 46(4), 477-493.
- Coutts, A. M., Beringer, J., & Tapper, N. J. (2008). Investigating the climatic impact of urban planning strategies through the use of regional climate modelling: a case study for Melbourne, Australia. *International Journal of Climatology: A Journal of the Royal Meteorological Society*, 28(14), 1943-1957.
- Coutts, A. M., White, E. C., Tapper, N. J., Beringer, J., & Livesley, S. J. (2016). Temperature and human thermal comfort effects of street trees across three contrasting street canyon environments. *Theoretical and Applied Climatology*, 124(1), 55-68. doi: 10.1007/s00704-015-1409-y
- Dee, D. P., Uppala, S. M., Simmons, A. J., Berrisford, P., Poli, P., Kobayashi, S., . . . Vitart, F. (2011). The ERA-Interim reanalysis: configuration and performance of the data assimilation system. *Quarterly Journal of the Royal Meteorological Society*, 137(656), 553-597. doi: doi:10.1002/qj.828
- Department of Infrastructure and Regional Development (2013). Australian State of the Cities 2013. Chapter 4 Sustainability Australian Government
<http://www.infrastructure.gov.au/infrastructure/pab/soac/>
- Engel, C. B., Lane, T. P., Reeder, M. J., & Rezný, M. (2013). The meteorology of Black Saturday. *Quarterly Journal of the Royal Meteorological Society*, 139(672), 585-599. doi: doi:10.1002/qj.1986
- Frolking, S., Milliman, T., Seto, K. C., & Friedl, M. A. (2013). A global fingerprint of macro-scale changes in urban structure from 1999 to 2009. *Environmental Research Letters*, 8(2), 024004
- Grell, G. A., & Dévényi, D. (2002). A generalized approach to parameterizing convection combining ensemble and data assimilation techniques. *Geophysical Research Letters*, 29(14), 38-31-38-34. doi: doi:10.1029/2002GL015311

- Harman, I. N., & Belcher, S. E. (2006). The surface energy balance and boundary layer over urban street canyons. *Q.J.R. Meteorol. Soc.*, *132*, 2749-2768. doi:10.1256/qj.05.185
- Holt, T., & Pullen, J. (2007). Urban Canopy Modeling of the New York City Metropolitan Area: A Comparison and Validation of Single- and Multilayer Parameterizations. *Monthly Weather Review*, *135*(5), 1906-1930. doi: 10.1175/mwr3372.1
- Hurley, P. (2000). Verification of TAPM meteorological predictions in the Melbourne region for a winter and summer month. *Australian Meteorological Magazine*, *49*(2), 97-107.
- Iacono, M. J., Delamere, J. S., Mlawer, E. J., Shephard, M. W., Clough, S. A. & Collins, W. D. (2008). Radiative forcing by long-lived greenhouse gases: Calculations with the AER radiative transfer models. *Journal of Geophysical Research: Atmospheres*, *113*(D13). doi: doi:10.1029/2008JD009944
- Imran, H. M., Kala, J., Ng, A. W. M., & Muthukumaran, S. (2018a). Effectiveness of green and cool roofs in mitigating urban heat island effects during a heatwave event in the city of Melbourne in southeast Australia. *Journal of Cleaner Production*, *197*, 393-405. doi: <https://doi.org/10.1016/j.jclepro.2018.06.179>
- Imran, H. M., Kala, J., Ng, A. W. M., & Muthukumaran, S. (2018b). An evaluation of the performance of a WRF multi-physics ensemble for heatwave events over the city of Melbourne in southeast Australia. *Climate Dynamics*, *50*(7), 2553-2586. doi: 10.1007/s00382-017-3758-y
- Jackson, T. L., Feddema, J. J., Oleson, K. W., Bonan, G. B., & Bauer, J. T. (2010). Parameterization of urban characteristics for global climate modeling. *Annals of the Association of American Geographers*, *100*(4), 848-865.
- Jacobs, S. J., Gallant, A. J., Tapper, N. J., & Li, D. (2018). Use of cool roofs and vegetation to mitigate urban heat and improve human thermal stress in Melbourne, Australia. *Journal of Applied Meteorology and Climatology*(2018).
- Jacobs, S. J., Gallant, A. J. E., & Tapper, N. J. (2017). The Sensitivity of Urban Meteorology to Soil Moisture Boundary Conditions: A Case Study in Melbourne, Australia. *Journal of Applied Meteorology and Climatology*, *56*(8), 2155-2172. doi: 10.1175/jamc-d-17-0007.1
- Janjic, Z. (1994). The step-mountain eta coordinate model: Further developments of the convection, viscous sublayer, and turbulence closure schemes (Vol. 122:5).
- Johansson, E. (2006). Influence of urban geometry on outdoor thermal comfort in a hot dry climate: A study in Fez, Morocco. *Building and environment*, *41*(10), 1326-1338.

- Krayenhoff, E. S., Moustaoui, M., Broadbent, A. M., Gupta, V. & Georgescu, M. (2018). Diurnal interaction between urban expansion, climate change and adaptation in US cities. *Nat. Clim. Chang.* 8, 1097–1103.
- Kusaka, H., Kondo, H., Kikegawa, Y., & Kimura, F. (2001). A simple single-layer urban canopy model for atmospheric models: Comparison with multi-layer and slab models. *Boundary-layer meteorology*, 101(3), 329-358.
- Li, D., Sun, T., ., Liu, M., Yang, L., Wang, L.,& Gao, Z. (2015). Contrasting responses of urban and rural surface energy budgets to heat waves explain synergies between urban heat islands and heat waves. *Environmental Research Letters*, 10(5), 054009.
- Li, D., & Bou-Zeid, E. (2013). Synergistic interactions between urban heat islands and heat waves: The impact in cities is larger than the sum of its parts. *Journal of Applied Meteorology and Climatology*, 52(9), 2051-2064.
- Liao, J., Wang, T., Wang, X., Xie, M., Jiang, Z., Huang, X., & Zhu, J. (2014). Impacts of different urban canopy schemes in WRF/Chem on regional climate and air quality in Yangtze River Delta, China. *Atmospheric Research*, 145-146, 226-243. doi: <https://doi.org/10.1016/j.atmosres.2014.04.005>
- Liu, X., Tian, G., Feng, J., Ma, B., Wang, J., & Kong, L. (2018). Modeling the Warming Impact of Urban Land Expansion on Hot Weather Using the Weather Research and Forecasting Model: A Case Study of Beijing, China. *Advances in Atmospheric Sciences*, 35(6), 723-736. doi: 10.1007/s00376-017-7137-8
- Matzarakis, A., Rutz, F., & Mayer, H. (2007). Modelling radiation fluxes in simple and complex environments—application of the RayMan model. *International Journal of Biometeorology*, 51(4), 323-334. doi: 10.1007/s00484-006-0061-8
- Matzarakis, A., Rutz, F., & Mayer, H. (2010). Modelling radiation fluxes in simple and complex environments: basics of the RayMan model. *International Journal of Biometeorology*, 54(2), 131-139. doi: 10.1007/s00484-009-0261-0
- Meng, W. G., Zhang, Y.X., Li, J.N., Lin, W.S., Dai, G.F., & Li, H.R. (2011). Application of WRF/UCMin the simulation of a heat wave event and urban heat island around Guangzhou. *Journal of Tropical Meteorology*, 17(3), 257-267. doi: 10.3969/j.issn.1006-8775.2011.03.007
- Monaghan, A. J., Hu, L., Brunzell, N. A., Barlage, M., & Wilhelmi, O. V. (2014). Evaluating the impact of urban morphology configurations on the accuracy of urban canopy model temperature simulations with MODIS. *J. Geophys. Res. Atmos.*, 119, 6376–6392, doi:10.1002/2013JD021227

- Morris, C. J. G., & Simmonds, I. (2000). Associations between varying magnitudes of the urban heat island and the synoptic climatology in Melbourne, Australia. *International Journal of Climatology*, 20(15), 1931-1954. doi: doi:10.1002/1097-0088(200012)20:15<1931::AID-JOC578>3.0.CO;2-D
- Morris, K. I., Chan, A., Morris, K. J. K., Ooi, M. C. G., Oozer, M. Y., Abakr, Y. A., Al-Qrimli, H. F. (2017). Impact of urbanization level on the interactions of urban area, the urban climate, and human thermal comfort. *Applied Geography*, 79, 50-72. doi: <https://doi.org/10.1016/j.apgeog.2016.12.007>
- Nairn, J., & Fawcett, R. (2013). Defining heatwaves: heatwave defined as a heat impact event servicing all community and business sectors in Australia. The Centre for Australian Weather and Climate Research. http://www.cawcr.gov.au/technical-reports/CTR_060.pdf. Accessed 22 Nov 2016
- Nicholls, N., & Larsen, S. (2011). Impact of drought on temperature extremes in Melbourne, Australia. *Australian Meteorological and Oceanographic Journal*, 61(2), 113-116.
- Oke, T. R. (1981). Canyon geometry and the nocturnal urban heat island: Comparison of scale model and field observations. *J. Climatol.*, 1: 237-254. doi:10.1002/joc.3370010304
- Oke, T. R., Johnson, G. T., Steyn, D. G. and Watson, I. D. (1991). Simulation of surface urban heat islands under 'ideal' conditions at night. Part 2: Diagnosis of causation. *Boundary-Layer Meteorol.*, 56; 339–358.
- Harman, I. N., & Belcher, S. E. (2006). The surface energy balance and boundary layer over urban street canyons. *Q. J. R. Meteorol. Soc.*, 132; 2749–2768. doi: 10.1256/qj.05.185
- Pauleit, S., Ennos, R., & Golding, Y. (2005). Modeling the environmental impacts of urban land use and land cover change—a study in Merseyside, UK. *Landscape and Urban Planning*, 71(2), 295-310. doi: <https://doi.org/10.1016/j.landurbplan.2004.03.009>
- Perkins-Kirkpatrick, S., White, C., Alexander, L., Argüeso, D., Boschat, G., Cowan, T., Phatak, A. (2016). Natural hazards in Australia: heatwaves. *Climatic Change*, 139(1), 101-114.
- Seto, K. C., & Shepherd, J. M. (2009). Global urban land-use trends and climate impacts. *Current Opinion in Environmental Sustainability*, 1(1), 89-95. doi: <https://doi.org/10.1016/j.cosust.2009.07.012>
- Sharma, A., Conry, P., Fernando, H. J. S., Alan, F. H., Hellmann, J. J., & Chen, F. (2016). Green and cool roofs to mitigate urban heat island effects in the Chicago metropolitan

- area: evaluation with a regional climate model. *Environmental Research Letters*, 11(6), 064004.
- Skamarock, W. C., Klemp, J. B., Dudhia, J., Gill, D. O., Barker, D. M., Wang, W., & Powers, J. G. (2005). A description of the advanced research WRF version 2: National Center For Atmospheric Research Boulder Co Mesoscale and Microscale Meteorology Div.
- Stone, B., Hess, J. J., & Frumkin, H. (2010). Urban Form and Extreme Heat Events: Are Sprawling Cities More Vulnerable to Climate Change Than Compact Cities? *Environmental Health Perspectives*, 118(10), 1425-1428. doi: 10.1289/ehp.0901879
- Thompson, G., Field, P. R., Rasmussen, R. M. & Hall, W. D. (2008). Explicit Forecasts of Winter Precipitation Using an Improved Bulk Microphysics Scheme. Part II: Implementation of a New Snow Parameterization. *Monthly Weather Review*, 136(12), 5095-5115. doi: 10.1175/2008mwr2387.1
- Torok, S. J., Morris, C. J. G., Skinner, C., & Plummer, N. (2001). *Urban heat island features of southeast Australian towns* (Vol. 50).
- Vatani, J., Golbabaie, F., Dehghan, S. F., & Yousefi, A. (2016). Applicability of Universal Thermal Climate Index (UTCI) in occupational heat stress assessment: a case study in brick industries. *Industrial Health*, 54(1), 14-19. doi: 10.2486/indhealth.2015-0069
- Wang, J., Feng, J., Yan, Z., Hu, Y., & Jia, G. (2012). Nested high-resolution modeling of the impact of urbanization on regional climate in three vast urban agglomerations in China. *Journal of Geophysical Research: Atmospheres*, 117(D21). doi: doi:10.1029/2012JD018226
- Wang, J., Yan, Z., Quan, X.-W., & Feng, J. (2017). Urban warming in the 2013 summer heat wave in eastern China. *Climate Dynamics*, 48(9), 3015-3033. doi: 10.1007/s00382-016-3248-7
- Wang, X., Sun, X., Tang, J., & Yang, X. (2015). Urbanization-induced regional warming in Yangtze River Delta: potential role of anthropogenic heat release. *International Journal of Climatology*, 35(15), 4417-4430. doi: doi:10.1002/joc.4296
- Yang, L., Niyog, D., Tewari, M., Aliaga, D., Chen, F., Tian, F., & Ni, G. (2016). Contrasting impacts of urban forms on the future thermal environment: example of Beijing metropolitan area. *Environ. Res. Lett.* 11 034018. doi:10.1088/1748-9326/11/3/034018
- Zhao, C., Jiang, Q., Sun, Z., Zhong, H., & Lu, S. (2013). Projected Urbanization Impacts on Surface Climate and Energy Budgets in the Pearl River Delta of China. *Advances in Meteorology*, 2013, 10. doi: 10.1155/2013/542086

Supplementary Material

Figs. S₁ and S₂ are similar Figs 6 and 7, except that they show changes in minimum T_2 and T_{sk} , respectively, rather than the mean. The increase in minimum T_2 ranges from 0.5 to 3.0 °C before sunrise and 0.5 to 4.5 °C during the evening (2000 to 2400 local time) for all four events. There are no substantial effects of urban expansion on minimum T_2 during the day. Furthermore, the increase in minimum T_{sk} ranges from 1.0 to 6.0 °C before sunrise and 1.0 to 7.0 °C from the evening to midnight. Similar to minimum T_2 , no substantial change in T_{sk} occurs during the day. The urban expansion extends the effects of minimum T_2 and T_{sk} in surrounding non-urban areas especially for events 3 and 4. In addition, the increase in minimum T_{sk} is also higher than the minimum T_2 for all events. It is noteworthy that the event 4 shows a higher increase of minimum T_2 and T_{sk} as compared to other three events. There were no substantial changes in maximum T_2 and T_{sk} (not shown). The changes in T_2 and T_{sk} are highest in the center of the expanded urban areas, with the most severe heatwave event (event 4) showing the largest increase.

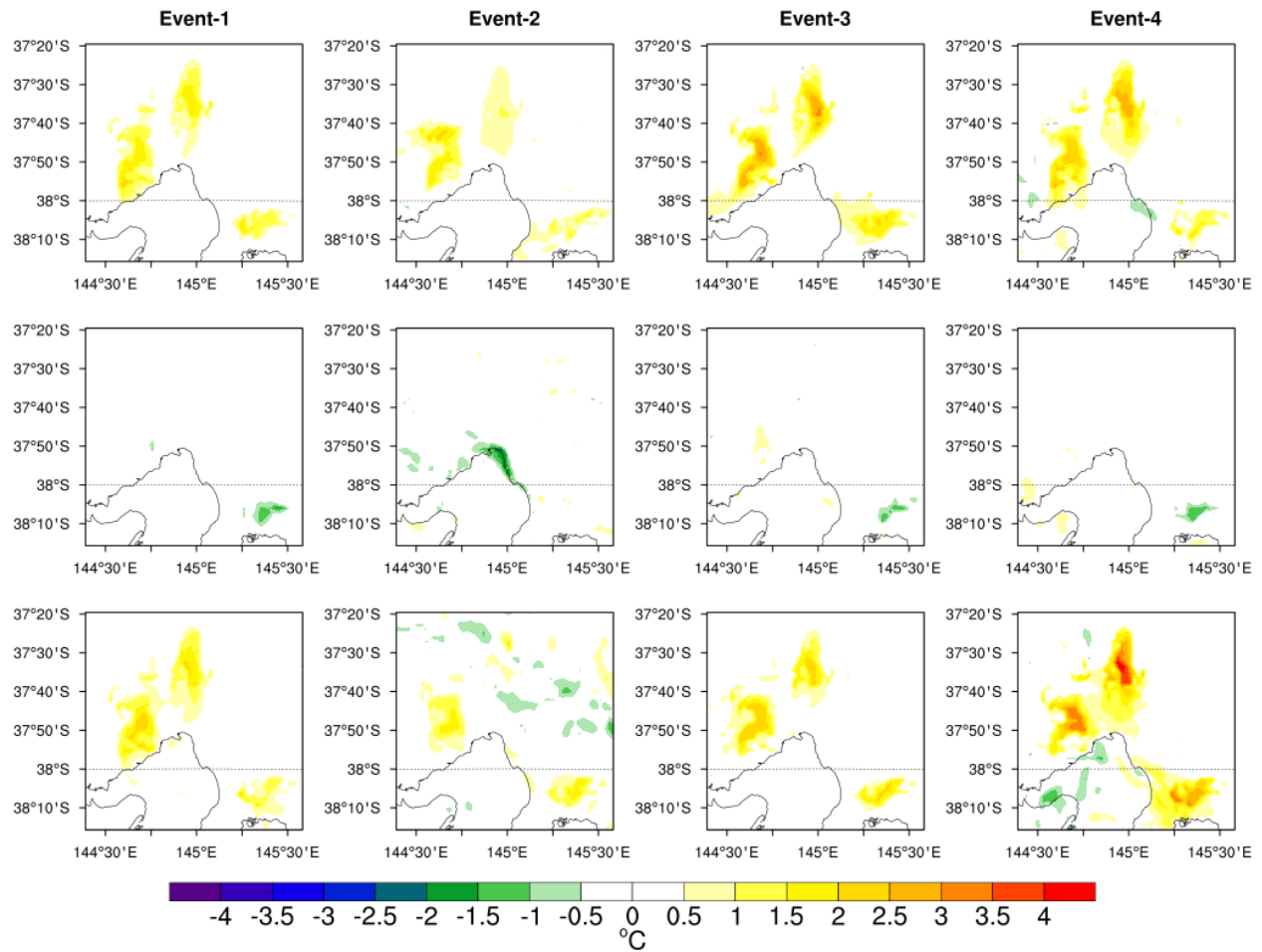


Fig. S1. Changes in minimum T_2 (experiment minus control) due to urban expansion for four events. Top row shows the results before sunrise (0200 to 0600 local time), middle row shows results when the ΔUHI_2 is minimum (1000 to 1400 local time), and bottom row shows the results when the ΔUHI_2 is maximum (2000 to 2400 local time).

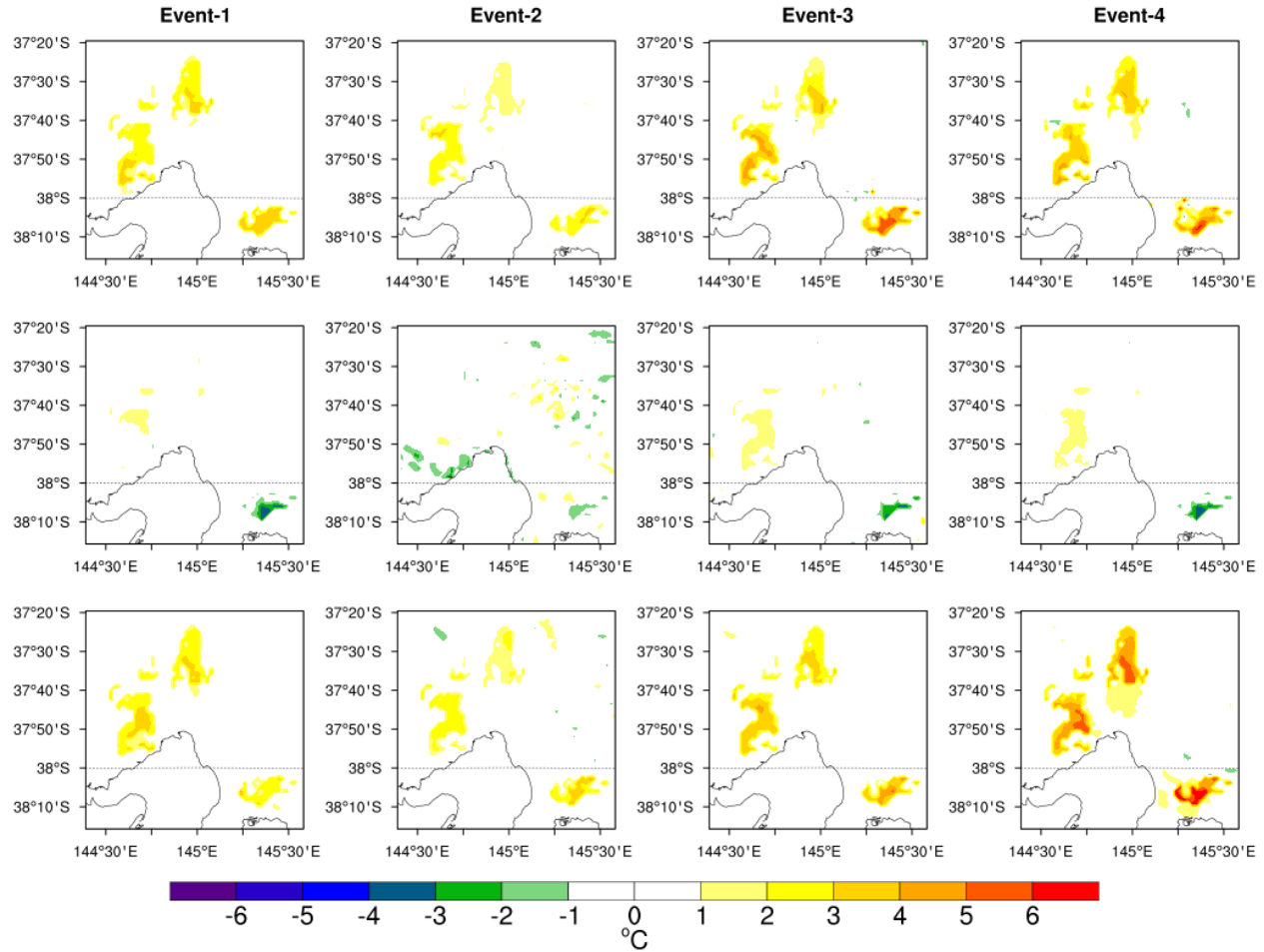


Fig. S₂. Changes in minimum T_{sk} (experiment minus control) due to urban expansion for four events. Top row shows the results before sunrise (0200 to 0600 local time), middle row shows results when the ΔUHI_{sk} is minimum (1000 to 1400 local time), and bottom row shows the results when the ΔUHI_{sk} is maximum (2000 to 2400 local time).

Near-surface relative humidity is reduced due to urban expansion with reductions ranging from 1 to 11 % before sunrise, 1 to 10 % during the evening, and there were no substantial changes in relative humidity during the day for all events (Fig. S₃). It is noteworthy that the reductions in relative humidity extend to surrounding non-urban areas especially before sunrise and after sunset for all events. Relative humidity increases slightly over the coastal areas for event 4 before sunrise and for event 2 during the day while events 2 and 3 show an increase in relative humidity over both coastal and surrounding non-urban areas after sunset. Since evapotranspiration is shut-down at night, the reductions in relative humidity must be due to the

increase in temperature as warmer air can hold more moisture, which would result in lower relative humidity.

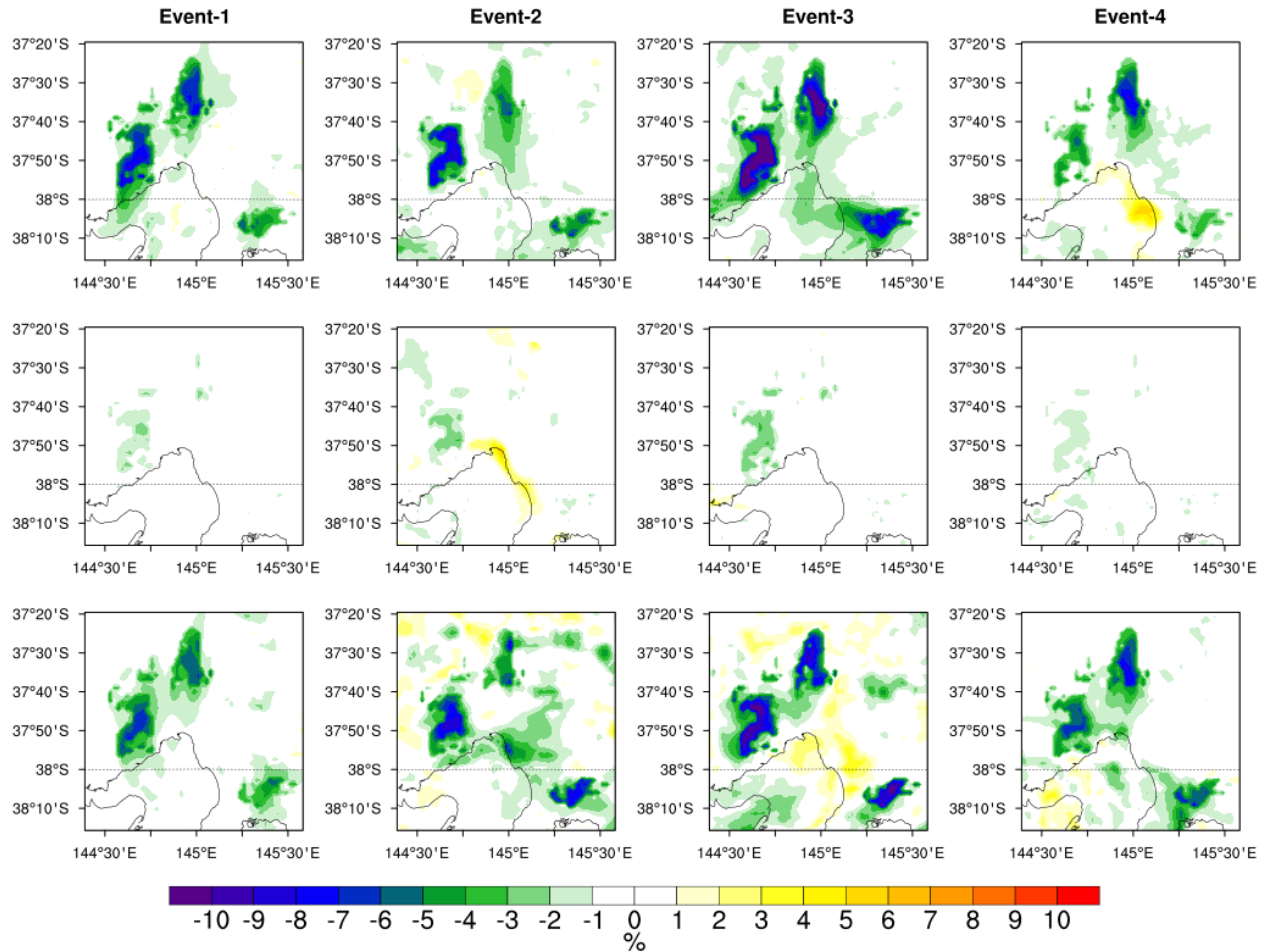


Fig. S3. Changes in relative humidity (experiment minus control) due to urban expansion for four events. Top row shows the results before sunrise (0200 to 0600 local time), middle row shows results when the ΔUHI_2 and ΔUHI_{sk} is minimum (1000 to 1400 local time), and bottom row shows the results when the ΔUHI_2 and ΔUHI_{sk} is maximum (2000 to 2400 local time).

Furthermore, relative humidity decreases from 2 to 6 % especially in the lower boundary layer (<200 m), accompanied by an increase in relative humidity of 2 to 7 % in the upper boundary layer (>300m) (Fig. S4). Urban expansion results in a larger influence on relative humidity for events-2 and 3 as compared to events-1 and 4, showing that the magnitude of the response can be quite varied depending on the event. The increase in relative humidity in the upper boundary layer (Fig. S4) occurs because of decrease in temperature in the same layer.

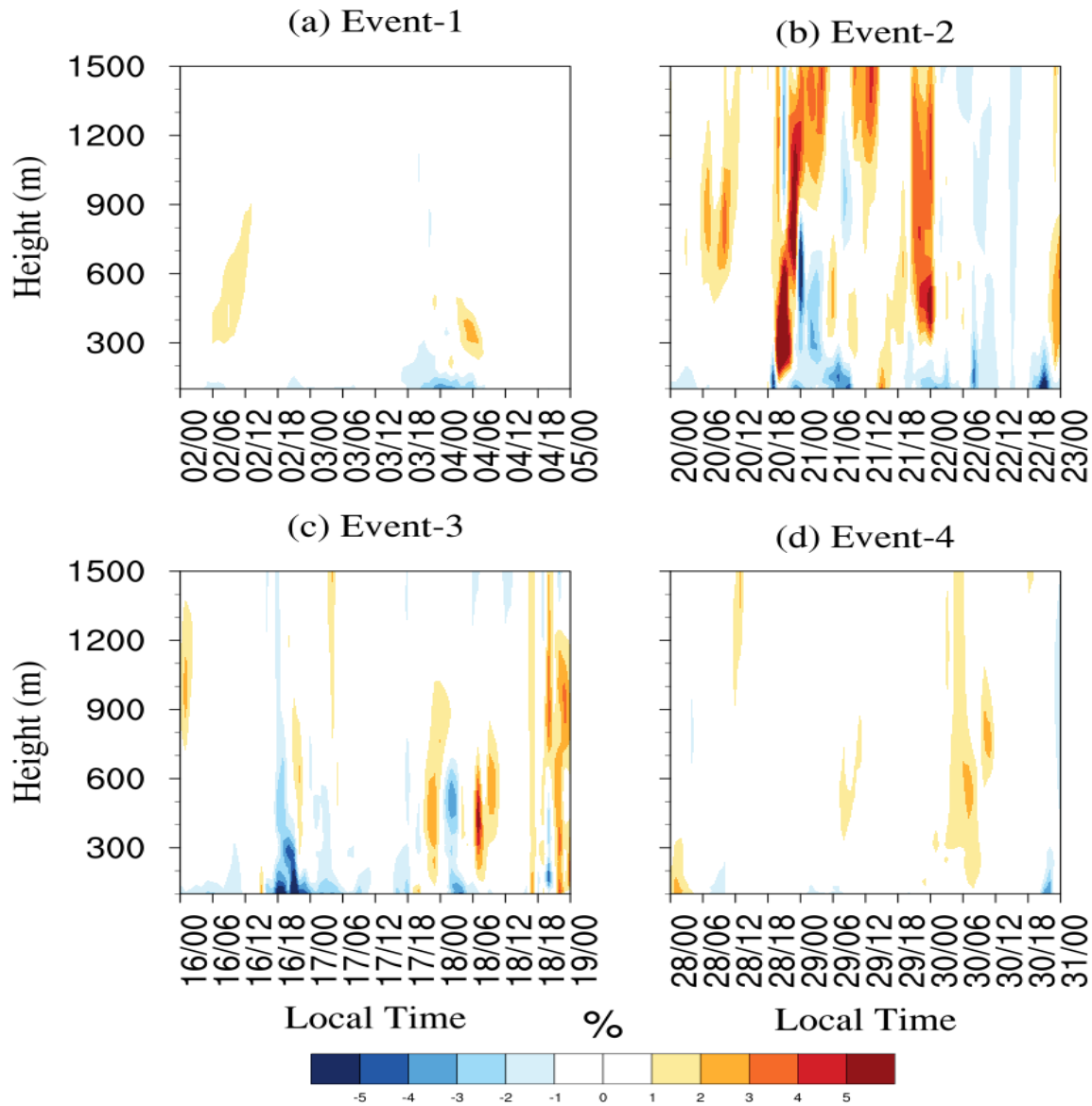


Fig. S4. Changes (experiment minus control) in hourly relative humidity within planetary boundary layer for (a) Events-1, (d) Events-2, (c) Events-3 and (d) Events-4, averaged over all urban grid cells in the expanded urban areas only.

Chapter 7

Green Infrastructure Practices in Mitigating UHI Effects during Heatwave Event

7.1 Introduction

This chapter examines the effectiveness of different vegetated patches as GI practices in reducing UHI effects by increasing fractions of different vegetated patches from 20 to 50 %. This chapter further builds on chapter 6, by running simulations with future urban expansion scenarios based on Plan Melbourne 2050 urban expansion strategy to examine the effectiveness of possible UHI mitigation strategies to minimize the impacts of future urbanization. We note that Chapter 5 investigated the effectiveness of green and cool roofs but did not include future urban expansion, as the data from Plan Melbourne 2050 was not available at the time that these simulations were carried out. Similar to Chapter 5, this chapter also investigates the potential of different vegetated patches/GI scenarios in improving HTC.

GRADUATE RESEARCH CENTRE

DECLARATION OF CO-AUTHORSHIP AND CO-CONTRIBUTION: PAPERS INCORPORATED IN THESIS BY PUBLICATION

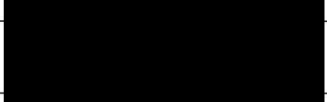
This declaration is to be completed for each conjointly authored publication and placed at the beginning of the thesis chapter in which the publication appears.

1. PUBLICATION DETAILS (to be completed by the candidate)

Title of Paper/Journal/Book:	Effectiveness of green infrastructure in mitigating urban heat island effects during heatwave in the city of Melbourne in southeast Australia		
Surname:	Hosen	First name:	Md Imran
College:	College of Engineering & Science	Candidate's Contribution (%):	85 %
Status:	Currently Under Review		
Accepted and in press:	<input type="checkbox"/>	Date:	<input type="text"/>
Published:	<input type="checkbox"/>	Date:	<input type="text"/>

2. CANDIDATE DECLARATION

I declare that the publication above meets the requirements to be included in the thesis as outlined in the HDR Policy and related Procedures – policy.vu.edu.au.

	14-08-2018
Signature	Date

3. CO-AUTHOR(S) DECLARATION

In the case of the above publication, the following authors contributed to the work as follows:

The undersigned certify that:

1. They meet criteria for authorship in that they have participated in the conception, execution or interpretation of at least that part of the publication in their field of expertise;
2. They take public responsibility for their part of the publication, except for the responsible author who accepts overall responsibility for the publication;
3. There are no other authors of the publication according to these criteria;
4. Potential conflicts of interest have been disclosed to a) granting bodies, b) the editor or publisher of journals or other publications, and c) the head of the responsible academic unit; and

5. The original data will be held for at least five years from the date indicated below and is stored at the following location(s):

College of Engineering and Science, Victoria University, Melbourne, Australia

Name(s) of Co-Author(s)	Contribution (%)	Nature of Contribution	Signature	Date
Dr. Anne Ng	5%	Review comments, Discussion on conceptual ideas		14/8/18
Dr. Shobha Muthukumaran	5%	Review comments, Discussion on conceptual ideas		14/8/18
Dr. Jatin Kala	5%	Critical review comments, Discussion on conceptual ideas		15/8/18

This is the pre-peer reviewed version of the following article: H.M. Imran, J. Kala, A.W.M. Ng, S. Muthukumaran, Effectiveness of vegetated patches as Green Infrastructure in mitigating Urban Heat Island effects during a heatwave event in the city of Melbourne, *Weather and Climate Extremes*, Volume 25, 2019, 100217, ISSN 2212-0947, <https://doi.org/10.1016/j.wace.2019.100217>

Effectiveness of Vegetated Patches as Green Infrastructure in Mitigating Urban Heat Island Effects during a Heatwave Event in the City of Melbourne

H. M. Imran^{1,3}, J. Kala², A. W. M. Ng^{1,4}, and S. Muthukumar^{1,4}

¹College of Engineering and Science, Victoria University, Melbourne, Australia

²Environmental and Conservation Sciences, Murdoch University, Perth, Western Australia

³Institute of Water and Environment, Dhaka University of Engineering & Technology, Gazipur, Bangladesh

⁴Institute for Sustainable Industries & Livable Cities, Victoria University, Melbourne, Australia

Abstract

The city of Melbourne in southeast Australia experiences frequent heatwaves and their frequency, intensity and duration are expected to increase in the future. In addition, Melbourne is the fastest growing city in Australia and experiencing rapid urban expansion. Heatwaves and urbanization contribute in intensifying the Urban Heat Island (UHI) effect, i.e., higher temperatures in urban areas as compared to surrounding rural areas. The combined effects of UHI and heatwaves have substantial impacts on the urban environment, meteorology and human health, and there is, therefore, a pressing need to investigate the effectiveness of different mitigation options. This study evaluates the effectiveness of urban vegetation patches such as mixed forest (MF), combination of mixed forest and grasslands (MFAG), and combination of mixed shrublands and grasslands (MSAG) in reducing UHI effects in the city of Melbourne during one of the most severe heatwave events. Simulations are carried out by using the Weather Research and Forecasting (WRF) model coupled with the Single Layer Urban Canopy Model (SLUCM). The fractions of vegetated patches per grid cell are increased by 20 %, 30 %, 40 % and 50 % using the mosaic method of the WRF model. Results show that by increasing fractions from 20 to 50 %, MF reduces near surface (2 m) UHI (UHI_2) by 0.6 to 3.4 °C, MSAG by 0.4 to 3.0 °C, and MFAG by 0.6 to 3.7 °C during the night, but there was no cooling effect for near surface temperature during the hottest part of the day. The night-time cooling was driven by a reduction in storage heat. Vegetated patches partitioned more net radiation into latent heat flux via evapotranspiration,

¹ Correspondence to: H.M. Imran, College of Engineering and Science, Victoria University, PO Box 14428, Melbourne, Victoria, Australia.
Phone: +61399195041
Fax: +61399194139
E-mail: ihosen83@gmail.com

with little to no change in sensible heat flux, but rather, a reduction in the storage heat flux during the day. As the UHI is driven by the release of stored heat during the night, the reduced storage heat flux results in reductions in the UHI. The reductions of the UHI₂ varied non-linearly with the increasing vegetated fractions, with larger fractions of up to 50 % resulting in substantially larger reductions. MF and MFAG were more effective in reducing UHI₂ as compared to MSAG. Vegetated patches were not effective in improving HTC during the day, but a substantial improvement of HTC was obtained between the evening and early morning particularly at 2100 local time, when the thermal stress changes from strong to moderate. Although limited to a single heatwave event and city, this study highlights the maximum potential benefits of using vegetated patches in mitigating the UHI during heatwaves and the overall principles are applicable elsewhere.

Keywords: UHI mitigation, Urban Vegetation, Heatwave, WRF-SLUCM

1. Introduction

Urbanization results in increased runoff and decreased infiltration of water due to impervious surfaces. The higher thermal conductivity of construction materials in urban areas increases the absorption of solar radiation and reduced vegetation cover limits evapotranspiration. These changes in the surface energy balance can have impacts on near-surface air temperature, humidity, winds and atmospheric convection (Liu et al., 2018; Morris et al., 2017). A well-documented impact of urbanization is the Urban Heat Island (UHI), defined as higher temperatures in city areas as compared to surrounding rural areas (Howard, 1833). In addition, the intensity of the UHI is amplified during heatwaves (Li et al., 2015; Zhao et al., 2018). From a meteorological context, a heatwave is usually defined as very unusual hot conditions for at least three consecutive days, during which the mean of minimum and maximum temperatures exceeds the climatological 95th percentile (Nairn and Fawcett, 2013). The combination of UHI and heatwaves can severely affect urban meteorology, environment, energy demand and human health (Liu et al., 2018).

The higher temperatures in urban areas increases energy demand for cooling systems and water demand for urban landscape irrigation (Yu and Hien, 2006). The increased energy demand can also cause higher ambient temperatures via the use of air conditioners for building cooling systems (Ohashi et al., 2007). The UHI and heatwaves further amplify heat-

related diseases and mortality (Mirzaei and Haghghat, 2010; Nicholls et al., 2008). For example, between 35,000 and 50,000 people are estimated to have died in Europe because of heat-related diseases during heatwaves in 2003 (Harlan et al., 2006). This threat is also important in Australia, with 374 and 167 additional human deaths during heatwaves in the state of Victoria in southeast Australia in 2009 and 2004 respectively (Victorian Auditor General's Report, 2014). The threats imposed by the UHI and heatwaves are very important in southeast Australia because of its hot summer, and these threats are likely to get worse in the future with projections that the intensity, frequency and duration of heatwaves in Australia will increase (Cowan et al., 2014).

The city of Melbourne, the capital of Victorian state of Australia, has been facing frequent heatwaves for the last two decades (Perkins-Kirkpatrick et al., 2016). For example, maximum temperatures of up to 45.1 °C and 43.9 °C were recorded in January 2009 and 2014 respectively (Victorian Auditor General's Report, 2014). In addition, the rate of urbanization is increasing rapidly to accommodate the increasing population. It is estimated that the population of the city of Melbourne will increase by 1.5 to 3.5 million by 2056 (Australian Bureau of Statistics, 2008). Hence, urban expansion will continue to meet the residential demands for the increasing population. Recently, the Victorian government released “Plan Melbourne 2050”, a policy document which provides projections of future urbanization and recent studies have shown that this future urban expansion could increase the nocturnal near-surface UHI by 0.75 to 2.80 °C over the expanded urban areas during heatwaves in the city of Melbourne (Imran et al., 2018c). Therefore, impacts of the UHI, especially during heatwave events, must be minimized to make the city more resilient and livable.

A number of studies, including observational, modelling, or both, focusing on the micro to the meso-scale, have investigated the effectiveness of using different mitigation strategies to reduce the UHI in various cities. These strategies include increasing urban vegetation (Bowler et al., 2010; Coutts et al., 2016; Fallmann et al., 2013; Oliveira et al., 2011; Rizwan et al., 2008) ; use of water bodies (Hathway and Sharples, 2012; Theeuwes et al., 2013; Žuvela-Aloise et al., 2016) and changing the size and geometry of urban infrastructures (Ali-Toudert and Mayer, 2007; Middel et al., 2014). Adding more urban trees, parks, gardens, wetlands, and green roofs within urban areas, is generally referred to as the implementation of Green Infrastructure. The GI strategy is generally regarded as a sustainable strategy in mitigating UHI effects due to their multiple functionality and benefits for the urban

environment such as increasing biodiversity and improving air quality in urban areas (Akbari et al., 2001). Initially, GI was defined as floodways, wetlands and parks, which provide water infiltration and flood control facilities (McMahon and Benedict, 2000). More recently, the definition has been expanded to include a variety of environmental and sustainability goals through a network of natural and planted vegetation such as street trees, parklands, rain gardens, community gardens, wetlands, green and cool roofs, and green walls (Foster et al., 2011). However, there is limited information about the potential of GI in mitigating UHI effects particularly during heatwaves when different GI scenarios are applied at the city scale. In addition, there is a pressing need to examine to what extent these mitigation strategies should be implemented to obtain substantial cooling benefits to mitigate UHI effects during heatwaves.

Increasing the areas of green spaces in urban areas can be an effective strategy to mitigate UHI effects by modifying the surface energy balance of the city by reducing storage heat in urban surfaces (Jacobs et al., 2018) and increasing evapotranspiration (Loughner et al., 2012). These two mechanisms play a key role in reducing UHI effects. Urban surfaces have higher thermal conductivity than vegetated surfaces, and store more heat during the day, which is later released at night. Hence, by decreasing the surface area of urban surfaces, and increasing the area of vegetated surfaces, storage heat is reduced during the day, leading to cooling at night. Another effect of vegetation on urban surfaces is direct shading by vegetation on urban surfaces, which also results in lower storage heat, and consequently, night-time cooling. Additionally, vegetated surfaces transform more of the net radiation to latent heat, rather than sensible heat, due to the evapotranspiration processes, and consequently, reduce urban temperatures. The size of green areas and their spacing play an important role in obtaining the optimum cooling benefit for the surrounding environment. Honjo and Takakura (1990) investigated the spatial extent of cooling effects of green areas based on their size. They reported that cooling effect extended to almost 300 m and 400 m, when the sizes of green areas were 100 m² and 400 m² respectively. Shashua-Bar and Hoffman (2000) used an empirical model to investigate the cooling effect of wooded sites using a combination of trees and urban green areas. They showed that the partially shaded areas by the tree canopy was the main driving factor for controlling air temperature within green areas, while tree characteristics and geometry played a limited role.

Urban vegetation also plays significant role in improving human thermal comfort within cities (Coutts et al., 2016; Shashua-Bar et al., 2010). Coutts et al. (2016) investigated the effects of street trees in reducing air temperature and improving Human Thermal Comfort (HTC) within individual streets at the micro-scale in the city of Melbourne in southeast Australia, and showed that urban trees are effective in reducing daytime Universal Thermal Climate Index (UTCI) during summer, whereby the thermal stress is reduced from very strong (UTCI>38 °C) to strong (UTCI 32 °C). Furthermore, Jacobs et al. (2018) investigated the effectiveness of increasing urban vegetation, cool roofs and a combination of both strategies in reducing UHI effects and human thermal stress in the city of Melbourne using the Princeton Urban Canopy model (Wang et al., 2013) coupled with the WRF model. In their study, the percentage of urban grass was increased to evaluate the effectiveness of urban vegetation in reducing UHI intensity. Jacobs et al. (2018) report that urban vegetation is effective in mitigating UHI effects during the night due to lower ground/storage heat flux, with minimal cooling during the day, while cool roofs are more effective during the day but the combination of urban vegetation and cool roofs provides the maximum cooling benefit. Green and cool roofs have also been shown to reduce the UHI and improve the HTC particularly during the day, in the city of Melbourne during heatwaves (Imran et al., 2018a). Although all these studies provide highly valuable information on the effectiveness of different UHI mitigation strategies, the effects of implementing different GI components such as mixed forest, shrublands and grasslands, and their combined effects in reducing UHI effects and improving HTC for the city of Melbourne during heatwave events need further investigation. In addition, given the impacts of future urban expansion in Melbourne on the UHI (Imran et al. 2018c), there is a need to investigate the effectiveness of different GI components in reducing UHI impacts during heatwaves under future urban expansion scenarios. By implementing different types of urban vegetation/GI components, this study further builds on Imran et al. (2018c) by examining the effectiveness of different areas of vegetated patches within urban grid cells in reducing UHI effects due to urban expansion. The aim of this study is to evaluate the effectiveness of different types of urban vegetated patches, such as mixed forest, mixed forest with grasslands and mixed shrublands with grasslands in mitigating UHI effects and improving HTC at a city scale (meso-scale) during one of the most severe heatwave events, using the latest future urban expansion scenario for the city, as per the “Plan Melbourne 2050” urban expansion strategy. Simulations are carried out by increasing fractions of vegetated patches within urban grid cells to investigate the maximum possible cooling benefits that can be obtained.

2. Methodology

2.1. Model Configuration

Numerical weather and climate models are effective and commonly used in urban meteorology studies. One of the most widely used models is the Weather Research and Forecasting (WRF) model, which has been used in numerous urban meteorology studies (Li et al., 2014; Imran et al., 2018a; Jacobs et al., 2017; Jacobs et al., 2018; Li et al., 2015; Liu et al., 2018; Morris et al., 2017; Sharma et al., 2016). This study uses the Weather Research and Forecasting (WRFv3.8.1) model with the Advanced Research WRF (ARW) dynamics solver (Skamarock et al., 2008).

The WRF model was operated using three nested domains (d01, d02 and d03) at 18, 6 and 2 km horizontal resolution respectively, as illustrated in Fig. 1(a). The largest domain (d01) includes a larger part of southeast Australia and the second domain (d02) covers major part of Victorian State. The innermost domain covers the Melbourne metropolitan and surrounding rural areas. The dominant land use categories for each grid cell are derived from the 24-USGS land use classification. Furthermore, the urban grid cells were modified based on the Plan Melbourne 2050 urban expansion strategy (more details about plan Melbourne at <http://www.planmelbourne.vic.gov.au/the-plan>). Such re-classification of urban land use represents the future urban expansion for the city of Melbourne. Following Imran et al. (2018c) who investigated the impacts of future urbanization on the UHI during heatwaves in Melbourne, all urban expansion was set to high-density urban. This is also consistent with other studies, which have investigated the impacts of future urban expansion for other Australian cities (e.g., Argüeso et al., 2014). The dominant land use classification for the innermost domain are shown in Fig. 1(b). 38 vertical levels were used (model top at 50 hPa), spaced closer together near the surface, and wider apart in the upper atmosphere. Initial and boundary conditions were from 6-hourly ERA-interim reanalysis, which has a spatial resolution of 0.75×0.75 degrees (Dee et al., 2011).

The WRF model offers a number of physics options for each physical parameterization including the Land Surface Model (LSM), Planetary Boundary Layer (PBL), cumulus parameterization, short and longwave radiation (SW and LW) and microphysics (MP), and the model is known to be sensitive to selection of different physics options (e.g., Evans et al.,

2012; Imran et al., 2018b; Kala et al., 2015a). This study uses the physics options suggested by Imran et al. (2018b), who conducted an extensive sensitivity analyses of the different physical parameterizations of the WRF model in simulating the UHI during heatwaves for the city of Melbourne, including the heatwave event in this study. By evaluating an ensemble of WRF simulations against station, gridded and sounding observations, Imran et al. (2018b) provide an ideal WRF set-up for simulating the UHI during heatwaves. This set-up has been used and further evaluated by Imran et al. (2018a), who investigated the effectiveness of green and cool roofs as UHI mitigation strategies during heatwaves in Melbourne. Hence this study uses the same set-up, which includes: unified Noah LSM (Chen and Dudhia, 2001), the Thompson MP scheme (Thompson et al., 2008), the Mellor-Yamada-Janjic PBL scheme (Janjic, 1994), the RRTMG SW and LW schemes (Iacono et al., 2008), the Monin-Obukhov similarity scheme for the surface-layer and the Grell-Devenyi scheme (Grell and Dévényi, 2002) scheme for cumulus convective parameterization. The cumulus scheme is only used for the two outermost domains d01 (18 km) and d02 (6 km) as the innermost domain, d03 (2 km) is at a sufficiently high resolution to resolve convection.

Additionally, WRF was operated with the unified Noah LSM coupled with the Single Layer Urban Canopy Model (SLUCM) (Chen and Dudhia, 2001; Chen et al., 2011; Liu et al., 2006) with the mosaic option. The SLUCM calculates fluxes for the urban surfaces within a grid cell, and incorporates parameterization of physical processes involved in the exchange of heat, momentum and water vapor in the urban environment by considering shadowing effects from buildings, reflection of shortwave and longwave radiation, wind profile in the canopy layer and a multilayer heat transfer equation for roofs, walls, and road surfaces (Kusaka and Kimura, 2004; Kusaka et al., 2001). On the other hand, the Noah LSM calculates fluxes for the vegetated portion of the grid cell. Thus, the coupled Noah-LSM and the SLUCM complete the urban surface energy balance by calculating fluxes from both the vegetated portion and built/impervious portion of urban areas. However, an important limitation of WRF-SLUCM is that the model does not resolve direct interactions between vegetation and urban surfaces, such as the shading effects of vegetation on buildings facades and roads, whereas more sophisticated urban canopy models resolve such effects (e.g., Lee and Park 2008; Lemonsu et al., 2012; Krayenhoff et al., 2013; Redon et al., 2017). Since the aim of this paper is to investigate the effects of relatively large portions of urban grid cells being completely converted to vegetation, rather than the implementation of vegetation within individual urban canyons, direct shading of urban surfaces by vegetation is not the key

mechanism, and hence this limitation is reasonable given the aims. We note that we do not show any model evaluation in this paper since extensive model evaluation against observations for the same heatwave event, using the same WRF version and configuration has already been carried by Imran et al. (2018b), and additional model evaluation is also provided in Imran et al. (2018a). Both studies showed that WRF was able to simulate the UHI and heatwave conditions well.

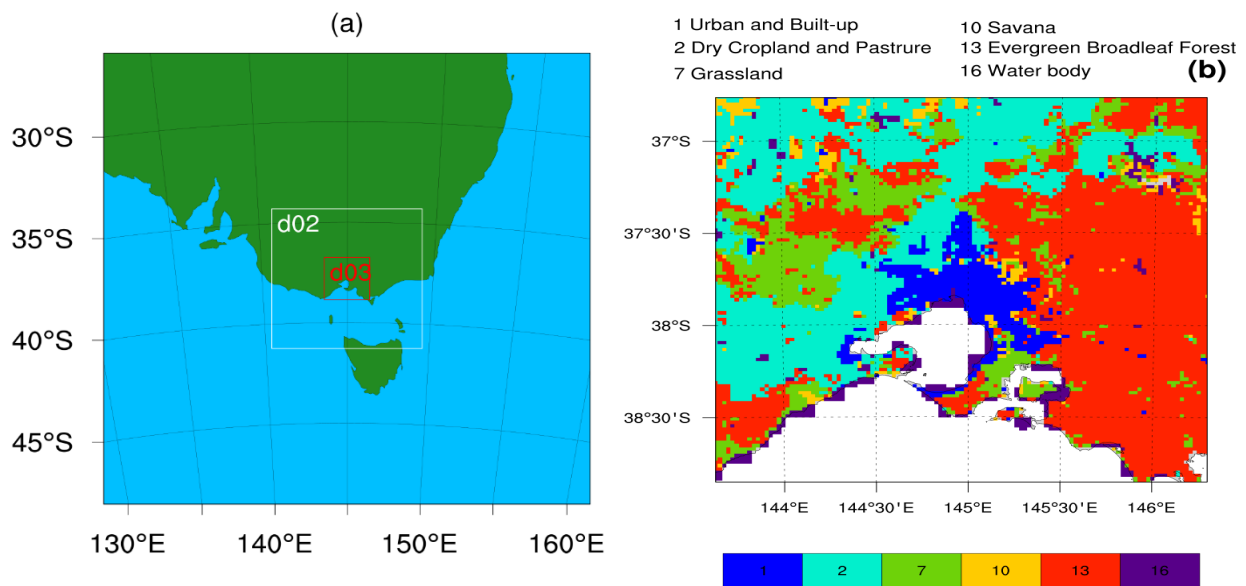


Fig. 1. (a) WRF domain configuration, where d02 and d03 represent second and innermost domains with resolution 6 km and 2 km, respectively, (b) Dominant land use classification in the innermost domain (d03) incorporating future urban expansion according to Plan Melbourne 2050.

The Noah LSM in WRF can be operated by using either dominant land-use types or a mosaic approach. When using dominant land-use types, the whole grid cell represents only one land use category. On the other hand, when mosaic approach is used, a grid cell can be subdivided into multiples tiles, to represent different land use categories within a single grid cell. This method is ideal to investigate the effects of converting relatively large portions of urban grid cells to vegetation. Moreover, recent studies by Sharma et al. (2017) have showed that use of the mosaic approach in WRF to represent sub-grid scale variations in land use improved simulation of the UHI for the city of Chicago in the USA. The mosaic approach allows a user to introduce different land use types into individual grid cells. To investigate the effectiveness

of different vegetated patches in mitigating UHI effects, the mosaic approach was used, with two tiles per grid cell for MF and MSAG and three tiles per grid cell for MFAG (more details in section 2.2). When the mosaic approach is used, the SLUCM is used only for the urban tile instead of the whole grid cell, and the Noah LSM is used for the vegetated portion.

2.2. Numerical Experiments

Following our recent work which examined the effectiveness of green and cool roofs in mitigating UHI effects in Melbourne during a heatwave event (Imran et al., 2018a), we focus on one of the most severe heatwave events, which occurred from the 27th to 30th January 2009. All simulations were conducted for four days and the first 24 hours were considered as spin-up time, following our previous study (Imran et al., 2018a). This heatwave event occurred after a long of period of drought (Nicholls and Larsen, 2011), and antecedent soil moisture conditions played an important role (Kala et al., 2015b). To examine the effectiveness of different types of GI scenarios, a portion of each urban grid cell is replaced with different types of vegetated patches, namely, MF, MSAG and MFAG by using the Mosaic option. MF is a combination of different trees such as evergreen broadleaf/needleleaf trees and deciduous broadleaf/needleleaf trees. The city of Melbourne's urban forest strategy is that urban forest will be no more than 5% of any tree species, no more than 10% of any genus and no more than 20% of any one family (Melbourne (Vic.) Council, 2011). Therefore, this study uses the mixed type of vegetation, which includes mixed forest, shrublands and grasslands. To evaluate the potential city-scale effects of the proposed vegetated patches, comparisons are made between the control run (includes both current urban land use and future urban expansion) and experiments (includes different vegetated patches implemented into all urban grid cells). For all simulations, the urban and built areas are modified following Imran et al. (2018c) based on the Plan Melbourne 2050 urban expansion strategy and increasing fractions of each vegetated patch (Table 1) are incorporated into all urban grid cells (includes current urban and 2050 urban expansion). All these simulations were carried out by increasing the land-use fraction within all urban grid cells by 20%, 30%, 40% and 50%, as summarized in Table 1, and Table 2 summarizes key properties of the different plant functional types. It should be noted that urban surfaces in the SLUCM are assigned an urban fraction (Chen et al 2011), e.g., 0.9 for high density urban as used in this study. The rest is assumed to be grass, and the minimum and maximum LAI for the urban category in Table 2 refers to the 0.1 grass fraction. The shade factors in Table 2 refer to direct shading on the

ground by the different vegetation types or urban grid cells. It is important to note that these shade factors do not represent shading of vegetation on urban surfaces and vice-versa as this is not resolved by the model.

Table 1. Design of numerical experiments for different vegetated patches

Vegetated Patches	Urban Fraction (%)	Fraction of Vegetated Patch (%)	Combinations
Control (Urban)	100	-	Urban/Impervious areas
MF (Mixed Forest)	80	20	20% Mixed forest
	70	30	30% Mixed forest
	60	40	40% Mixed forest
	50	50	50% Mixed forest
MSAG (Mixed Shrublands and Grasslands)	80	20	20% Mixed shrublands and grasslands
	70	30	30% Mixed shrublands and grasslands
	60	40	40% Mixed shrublands and grasslands
	50	50	50% Mixed shrublands and grasslands
MFAG (Mixed Forest and Grasslands)	80	20	10% Mixed forest + 10% Grasslands
	70	30	15% Mixed forest + 15% Grasslands
	60	40	20% Mixed forest + 20% Grasslands
	50	50	25% Mixed forest + 25% Grasslands

Table 2. Different properties of urban area and vegetated patches in the WRF model

Urban/Vegetated Patches	Shade Factor	Minimum LAI	Maximum LAI	Minimum Albedo	Maximum Albedo
Urban	0.10	1.00	1.00	0.15	0.15
Mixed Forest (MF)	0.80	2.80	5.50	0.17	0.25
Mixed Shrubland/Grassland (MSAG)	0.70	0.60	2.60	0.22	0.30
Mixed Forest and Grassland (MFAG)	0.80	0.52	2.90	0.19	0.23

2.3. Pedestrian Level HTC Calculation

Following Imran et al. (2018a) and Imran et al. (2018c), this study uses the Universal Thermal Comfort Index (UTCI) index in quantifying the pedestrian level (2 m) HTC, via the UTCI index. The UTCI index is used to assess how different vegetated patches improve the HTC in the city of Melbourne. The UTCI index calculates a physiological response based on meteorological and several human thermal parameters and represents human bioclimatic conditions and their relevance to human thermal stress. The UTCI index is used in representing human thermal stress under various climatic conditions (Blazejczyk et al., 2012;

Vatani et al., 2016), which makes this index widely used. Temperature, relative humidity and solar radiation simulated by the WRF model were used as meteorological input and a default clothing factor of 0.90 and activity rate of 80 W for a male of 35 years are used as human thermal parameters. All these variables were used as input to the bioclimatic model RayMan Pro 3.1 (Matzarakis et al., 2007, 2010) to calculate the UTCI index. The HTC is classified as five categories based on the ranges of the UTCI index (Bröde et al., 2012) as shown in Table 3.

Table 3. Universal Thermal Comfort Index (UTCI) range for different grades of human thermal perception and associated physiological stress (Bröde et al 2012)

UTCI (°C)	Physiological Stress
+9 to +26	no thermal stress
+26 to +32	moderate heat stress
+32 to +38	strong heat stress
+38 to +46	very strong heat stress
> +46	extreme heat stress

3. Results

3.1. Diurnal Variations of the UHI

Before investigating the effects of different vegetated patches on the UHI, it is useful to first analyze the diurnal variation of the UHI from the control simulation to first understand its temporal evolution. Additionally, since the Plan Melbourne policy aims to increase vegetation cover by 40 % by 2040, we also include results from 40 % increase experiments. This is illustrated in Fig. 2, showing the hourly variation of the near surface (2 m) (UHI_2) and skin surface UHI (UHI_{sk}). The UHI_2 and UHI_{sk} are computed as the difference between urban and surrounding rural areas. The effectiveness of vegetated patches relative to urban areas in reducing the UHI_2 and UHI_{sk} is estimated as the difference of the UHI_2 and UHI_{sk} , respectively between the experiment (with different fractions of vegetated patches within urban grid cells) and control (only urban) ($UHI_{veg} - UHI_{urban}$). The control simulation shows the UHI_2 ranges from 1.0 to 5.9 °C and UHI_{sk} ranges from 2.0 to 11.0 °C. The UHI_2 and UHI_{sk} reach their peaks at 1900 and 2000 local time, respectively. The intensity of UHI_{sk} is higher than the UHI_2 especially between the evening and early morning. The intensity of UHI_{sk} is lower during the day as compared to the night, since the urban surfaces emit less

heat during the day due to higher thermal conductivity of construction materials. On the other hand, urban surfaces re-radiate stored heat and result in higher skin-surface temperatures during the night. Vegetated patches reduce the UHI_2 and UHI_{sk} from evening to morning and no cooling effect is obtained during the day while the maximum UHI_2 and UHI_{sk} occurred at 1900 and 2000 local time, respectively.

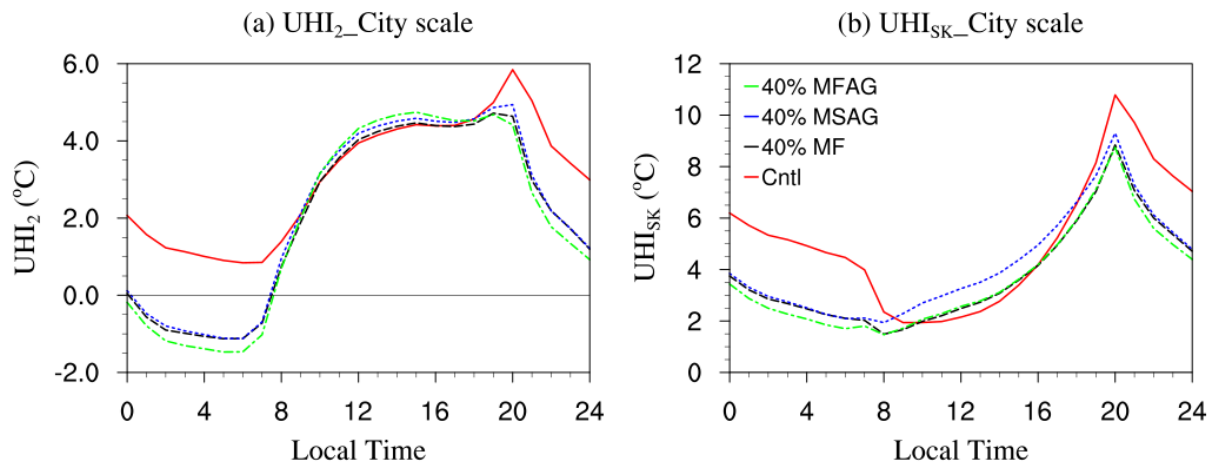


Fig. 2. Diurnal variations of near surface (UHI_2) and skin-surface (UHI_{sk}) UHI averaged over the urban grid cells only across domain d03 over 3 days (28 to 30 January 2009), for the control simulation, and 40% MF, MSAG and MFAG experiments.

3.2 Reductions of the UHI by Different % of Vegetated Patches

Having examined the diurnal variation of the UHI_2 and UHI_{sk} from the control simulation and 40% experiments, we now examine the changes in the UHI_2 and UHI_{sk} with different percentages of vegetated patches within urban grid cells. This is illustrated in Fig. 3 showing the city-scale impacts of vegetated patches on the UHI_2 and UHI_{sk} averaged over three diurnal cycles from 28 to 30 January 2009 by using their fractions 20%, 30%, 40% and 50% (Table 1). The changes in UHI_2 and UHI_{sk} are calculated as the differences between the experiments and the control.

Fig 3. shows that MF was effective in reducing the UHI_2 and UHI_{sk} from the night to morning (Fig. 3a and 3b). The UHI_2 shows smaller changes (<0.5 °C) as compared to UHI_{sk} . The reductions of UHI_2 and UHI_{sk} increase with increasing fractions of MF. The UHI_2 reductions range from 0.6 to 3.4 °C during the night when the fraction of MF increases from 20% to 50% while the reductions of UHI_{sk} range from 0.8 to 4.2 °C. Although the UHI_{sk} increases slightly during the day (between 1000 and 1700 local time), there is no substantial

increase in the UHI_2 . Both the UHI_2 and UHI_{sk} show maximum reductions at around 2100 local time. MSAG reduces the UHI_2 from 0.4 to 3.0 °C, and the UHI_{sk} from 0.8 to 3.7 °C between the evening and early morning (Fig. 3c and 3d). It is noteworthy that MSAG shows more warming at the skin surface between 1000 and 1700 local time with an increase in the UHI_{sk} between 0.3 and 1.0 °C, but there are no substantial changes in UHI_2 . MFAG shows slightly higher effectiveness in reducing UHI effects during night as illustrated in Fig. 3e and 3f showing that increasing fractions of MFAG from 20 to 50% can reduce the UHI_2 by 0.6 to 3.7 °C, and UHI_{sk} by 1.0 to 4.4 °C from evening to early morning. The maximum reduction occurs at 2100 local time, similar to the experiments with MF and MSAG.

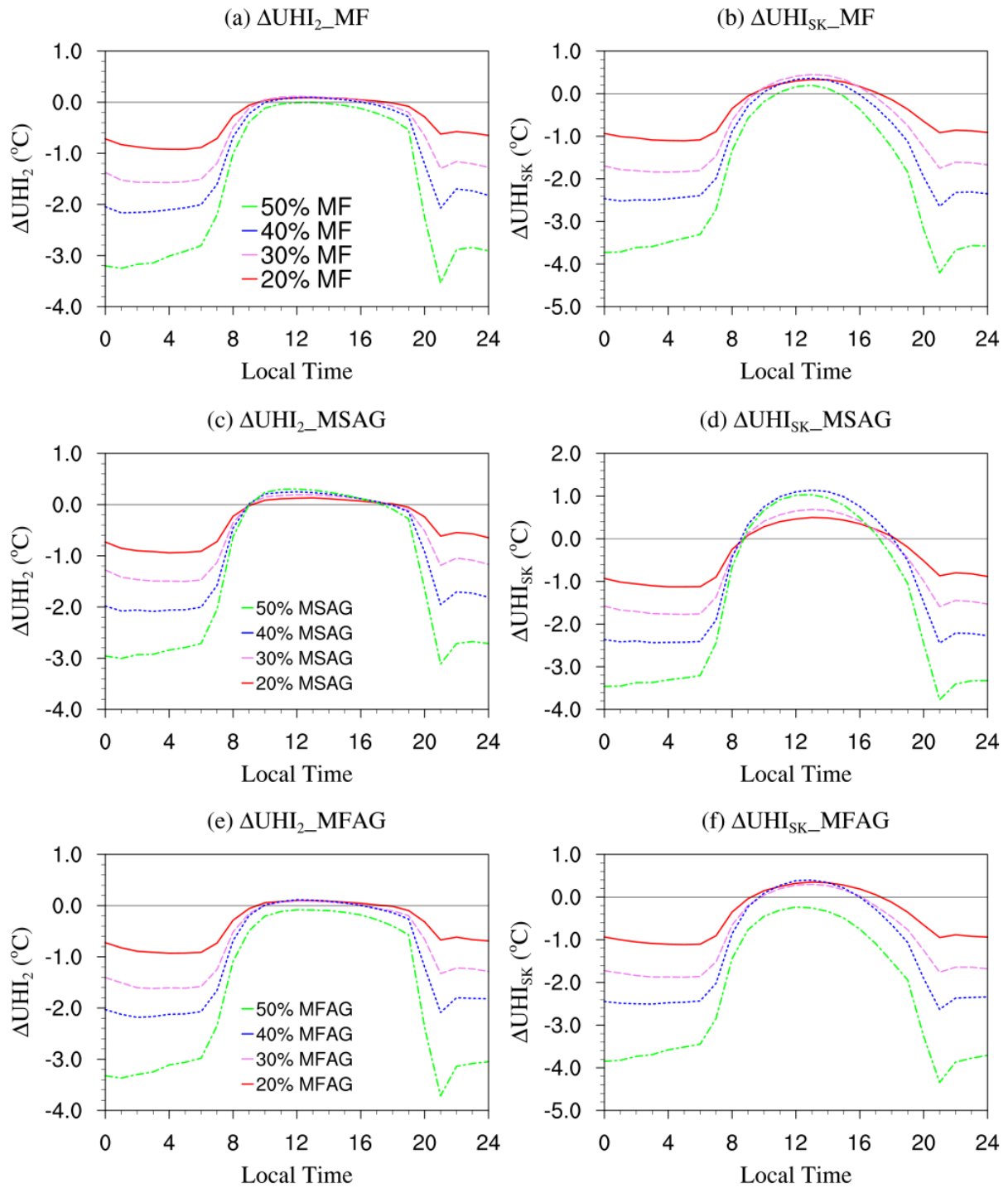


Fig. 3. Hourly changes (experiment minus control) in UHI_2 (left column) and UHI_{sk} (right column) for (a) and (b) MF, (c) and (d) MSAG and (e) and (f) MFAG by using their fractions 20%, 30%, 40% and 50%. The UHI_2 and UHI_{sk} have been averaged over urban grid cells only over 3 days from 28 to 30 January 2009

Fig. 4 shows the relationship between reductions in the UHI_2 and UHI_{sk} as a function of different vegetated fractions when the maximum UHI_2 and UHI_{sk} reductions occurs at 2100 local time. There are non-linear relationships between the reductions of both UHI_2 and UHI_{sk} and increasing vegetated fractions. Much larger reductions in the UHI_2 and UHI_{sk} occur when vegetated fractions increases more than 40%. MFAG show the highest reductions in UHI_2 and UHI_{sk} while the MSAG show the lowest reductions. The reductions of UHI_2 and UHI_{sk} by MF are slightly lower as compared to MFAG.

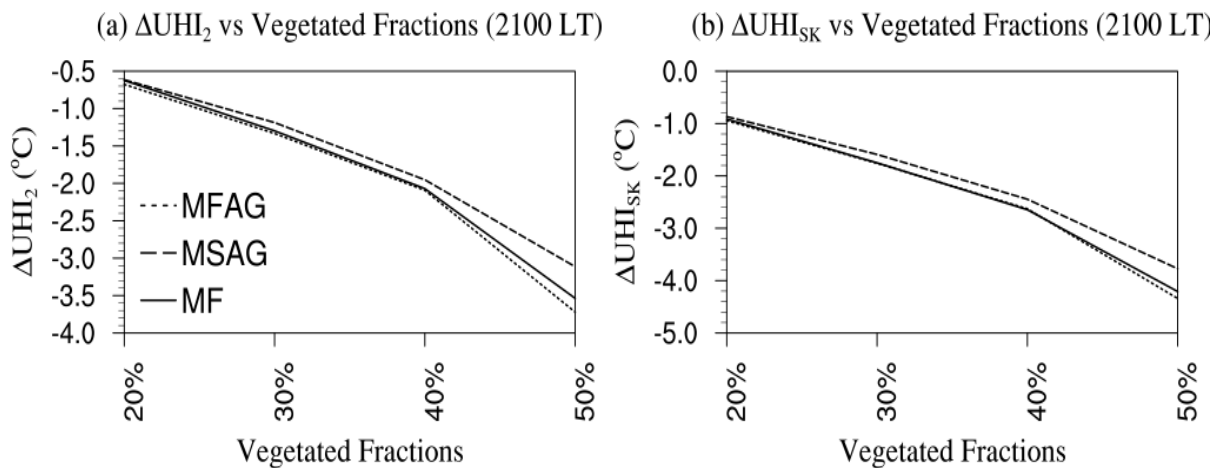


Fig. 4 Change in (a) UHI_2 and (b) UHI_{sk} as a function of % vegetated patches when the reductions reach their maxima (2100 local time). The UHI_2 and UHI_{sk} have been averaged over 3 days over 28 to 30 January 2009.

3.3. Influence of Different % of Vegetated Patches on the Surface Energy Balance

To better understand the drivers of the changes in Figs. 3 and 4, we next examine the changes in the surface energy balance, as illustrated in Fig.5 showing the sensible (SH), latent (LH) and ground/storage (G) heat fluxes for the control and all experiments (Table 1). MF and MFAG do not show substantial changes in SH except for 50 % MF and MFAG, which show reductions in SH between 20 and 40 $W m^{-2}$ during midday as compared to the control. Interestingly, all fractions of MSAG slightly increase SH (by approximately 10 $W m^{-2}$) during the day particularly at midday. By increasing vegetated fractions from 20 to 50 %, LH increases by 20 to 120 for MF, 5 to 50 for MSAG and 20 to 130 $W m^{-2}$ for MFAG during the day. It is noteworthy that the MF and MFAG show a higher increase in LH during the day as compared to MSAG. It is also noteworthy that there was a larger increase of LH for 20 to 30 %, lower increase of LH for 30 to 40 % and abruptly higher increase of LH for 50%

vegetated patches. Storage heat increases by 20 to 80 for MF, 20 to 60 for MSAG and 20 to 80 W m^{-2} for MFAG by increasing vegetated fractions from 20 to 50%. All fractions of vegetated patches show a similar diurnal cycle of storage flux. A positive sign of storage heat during the night indicates heat fluxes flow from the surface to the atmosphere and vice-versa for negative storage heat during the day. The daytime reductions in storage heat flux are higher as compared to the nighttime reductions as less heat is stored during the day to be released during the night. The maximum reductions of storage heat occur at 1200 local time. MF and MFAG show higher reductions in storage heat and higher increases in LH as compared to MSAG. There were no changes in downwelling shortwave radiation and small reductions (less than 10 W m^{-2}) in downwelling longwave radiation between late night and early morning (not shown). In summary, vegetated patches substantially alter the surface energy balance by increasing LH and decreasing storage heat with relatively small changes in downwelling longwave and SH.

Fig. 3 showed that vegetated patches reduce the maximum UHI_2 and UHI_{sk} at 2100 local time and this is related to reductions in storage heat during the day. By replacing part of an urban grid cell with vegetation, the storage heat flux is reduced, as urban surfaces have higher thermal conductivity than vegetated surfaces. Additionally, a higher proportion of vegetation in urban grid cells leads to partitioning of net radiation into LH due to evapotranspiration but there were no substantial reductions in SH. The reduced storage heat in urban surfaces during the day which is released after sunset, leads to a cooling effect by the vegetated patches from evening to morning. On the contrary, MSAG show a slight warming effect during midday because of the slight increase in sensible flux at that time. Vegetated patches have little influence in reducing the UHI_2 during the day despite the fact that there is an increase in LH during this time. This is due to the fact that the increase in latent heat flux is not accompanied by a decrease in sensible heat flux, but rather changes in the ground heat flux. With little to no change in sensible heat flux, there are little to no changes in temperature during the day.

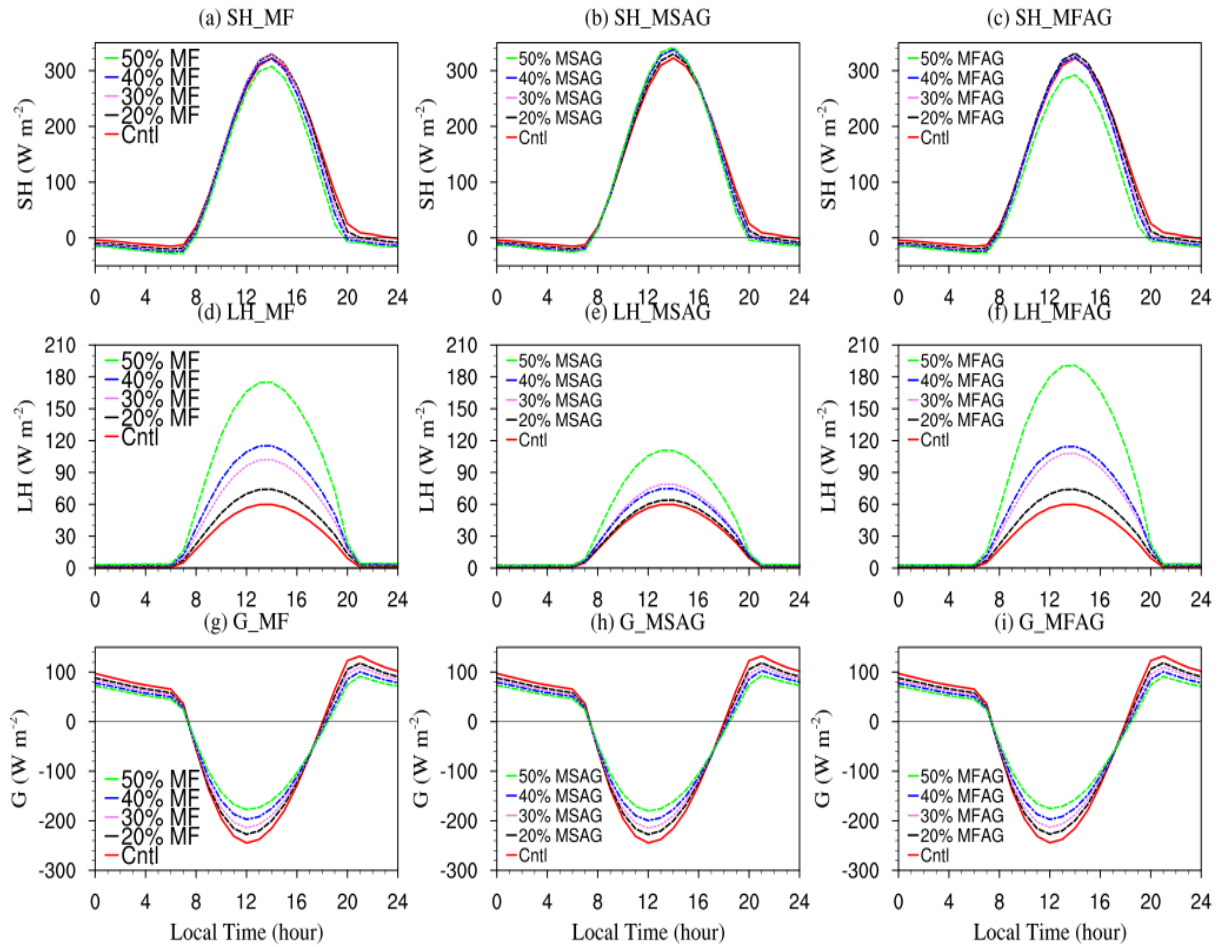


Fig. 5. Surface energy balance for MF (left column), MSAG (middle column) and MFAg (right column) for all experiments including the control simulation (Table 1), averaged over urban grid cells only in d03 (Fig. 1) over 3 days from 28 to 30 January 2009.

3.4. Spatial Changes due to Different Vegetated Patches

Having examined changes averaged over urban grid cells, we now examine the spatial changes across the domain. This is illustrated in Fig. 6 showing the spatial changes (experiments minus control) in mean T_2 when maximum reductions in the UHI occur (averaged from 2100 to 0400 local time from 28 to 30 January 2009) as a function of increasing fractions of vegetated patches. By increasing vegetated fractions from 20 to 50%, reductions in T_2 range from 0.5 to 5.0 °C for MF, 0.5 and 4.5 °C for MSAG, and 0.5 to 5.5 °C for MFAg. It is noteworthy that although the reduction ranges of mean T_2 are nearly similar for MF and MSAG, MFAg show higher reductions over larger areas. The highest reduction in the T_2 occurs in the center of the city. The non-linearity of the reduction in temperature with increasing fractions of vegetated patches shown earlier in Fig. 4 is further

reflected in Fig. 6 showing the much larger reductions with 50 % scenarios as compared to lower percentages.

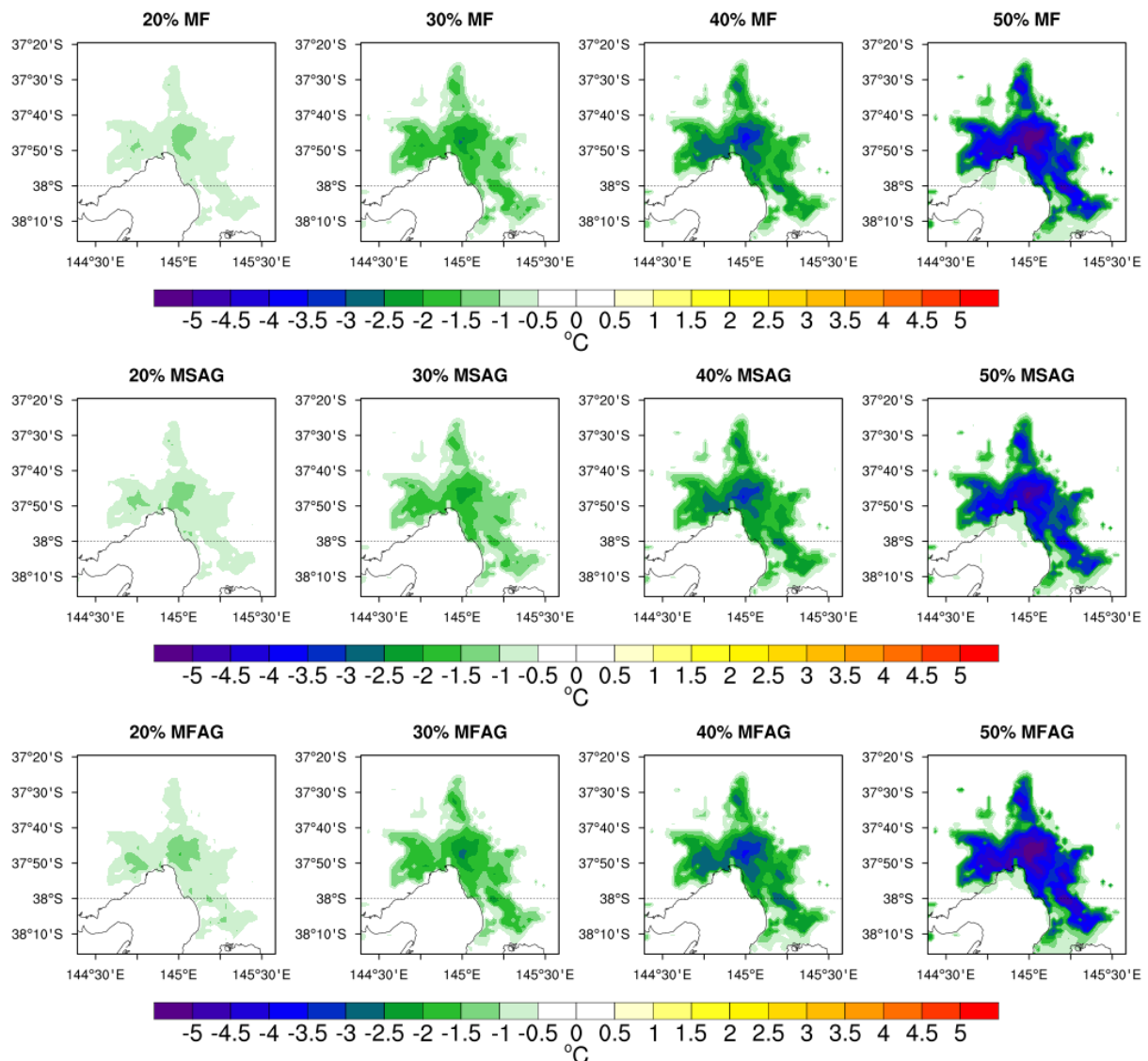


Fig. 6. Changes in T_2 (experiment minus control) by using 20 %, 30 %, 40 % and 50 % vegetated patches averaged from 2100 to 0400 (when maximum UHI_2 reduction occurs) local time over 3 days from 28 to 31 January 2009.

Fig. 7 shows the changes in storage heat for increasing proportions of different vegetated patches averaged over the same period used for Fig. 6. The reductions in storage heat ranges from 5 to 35 $W m^{-2}$ by increasing the fractions from 20 to 50 % of MF and MSAG while the decrease in storage heat ranges from 5 to 40 $W m^{-2}$ for MFAG by increasing the same fractions. MFAG and MF are slightly more effective in reducing the storage heat over larger areas as compared to MSAG.

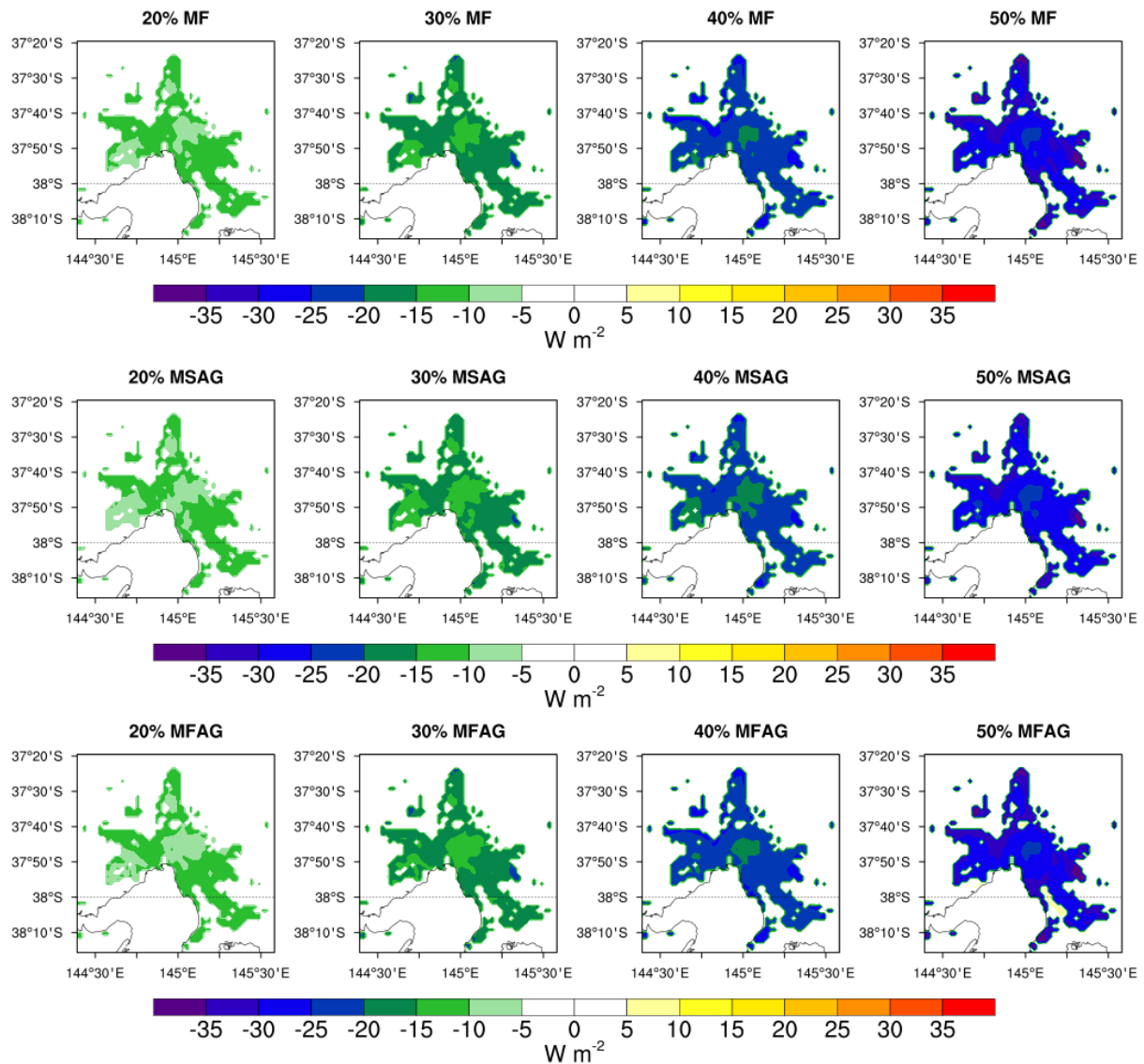


Fig. 7. Changes in storage heat (experiment minus control) for MF (upper), MSAG (middle) and MFAG (bottom) by using fractions 20%, 30%, 40% and 50%. All the results are averaged from 2100 to 0400 local time for the 3 days (28 to 30 January 2009) when maximum UHI₂ reductions occurred.

The effects of the vegetated patches on the spatial distribution of relative humidity (2 m) and wind speed (10 m) are shown in Figs. 8 and 9 respectively, averaged over the same period used for Fig. 6. The 20 % MF, MSAG and MFAG experiments do not substantially increase the relative humidity as there are no substantial reductions of T_2 (Fig. 6). Increasing the fractions of vegetated patches from 30 to 40 %, leads to increases in relative humidity by 2 to 8 % for MF, MSAG and MFAG. The 50 % MF, MSAG and MFAG experiments show

substantial increases in relative humidity ranging from 4 to 14 % because of larger reductions in T_2 (Fig. 6). The increases in relative humidity by MF and MFAG are higher as compared to MSAG. 50 % vegetated patches lead to the highest increase in relative humidity over the urban areas as compared to other fractions. The increase in relative humidity is a direct result of the changes in temperature as where were no changes in mixing ratio. There were no substantial changes in relative humidity during the day (from 1100 to 1400 local time, not shown), when vegetated patches caused a slight warming effect.

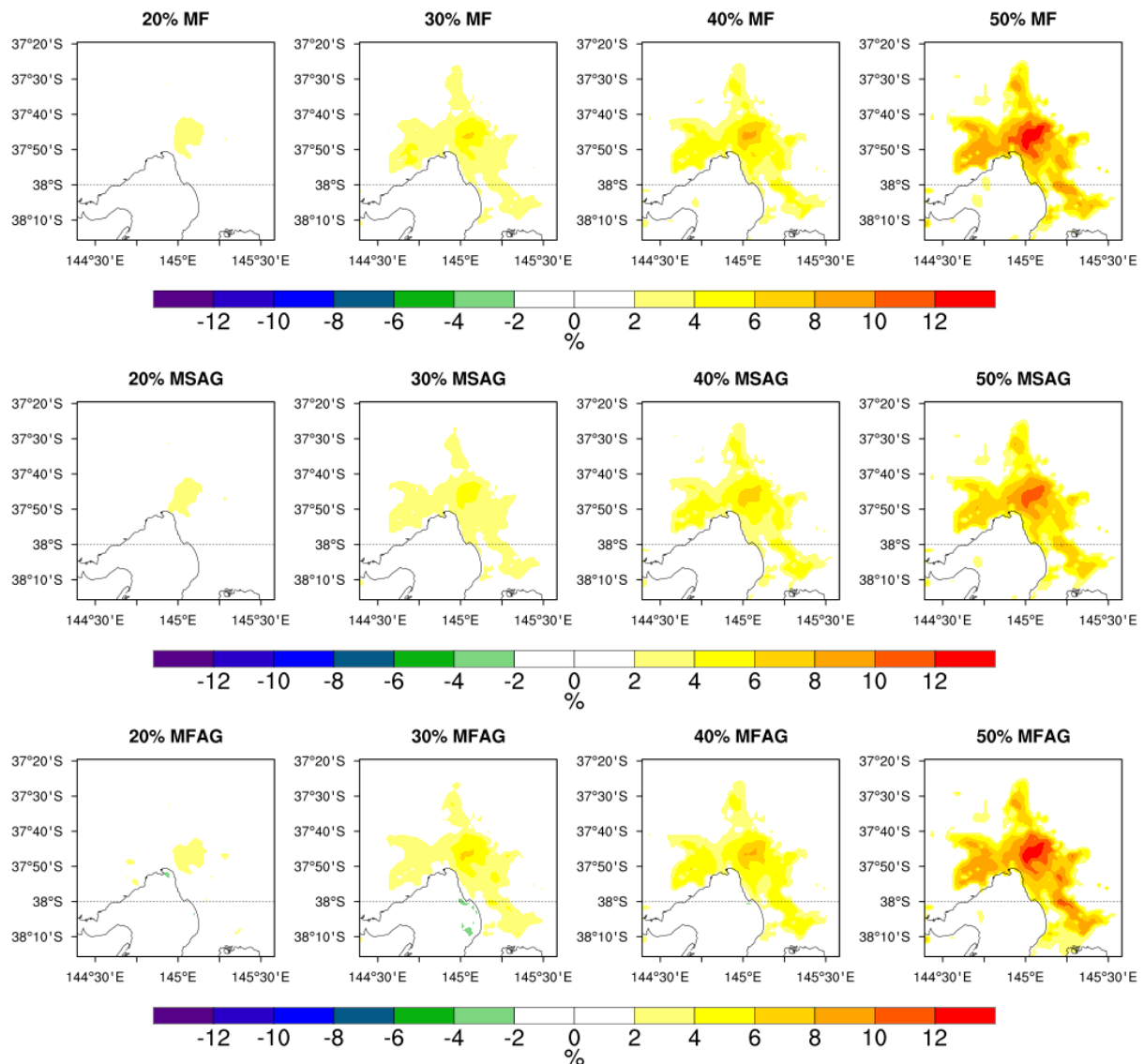


Fig. 8. Changes in relative humidity (experiment minus control) for MF (upper), MSAG (middle) and MFAG (bottom) by using fractions 20%, 30%, 40% and 50%. All the results are averaged from 2100 to 0400 local time for the 3 days (28 to 30 January 2009) when maximum UHI_2 reductions occur.

Fig. 9 shows the changes in wind speed (experiments minus control) due to implementation of different fractions of vegetated patches in the urban areas. The wind direction from the experiments is overlaid on the changes in wind speed, as there were no substantial changes in wind direction due to the implementation of vegetated patches. Wind speed ranges between 5 and 7 m s^{-1} over urban areas for control experiment (not shown). The reductions in wind speed range from 0.25 to 1.25 m s^{-1} by increasing fractions of vegetated patches from 20 to 50 %.

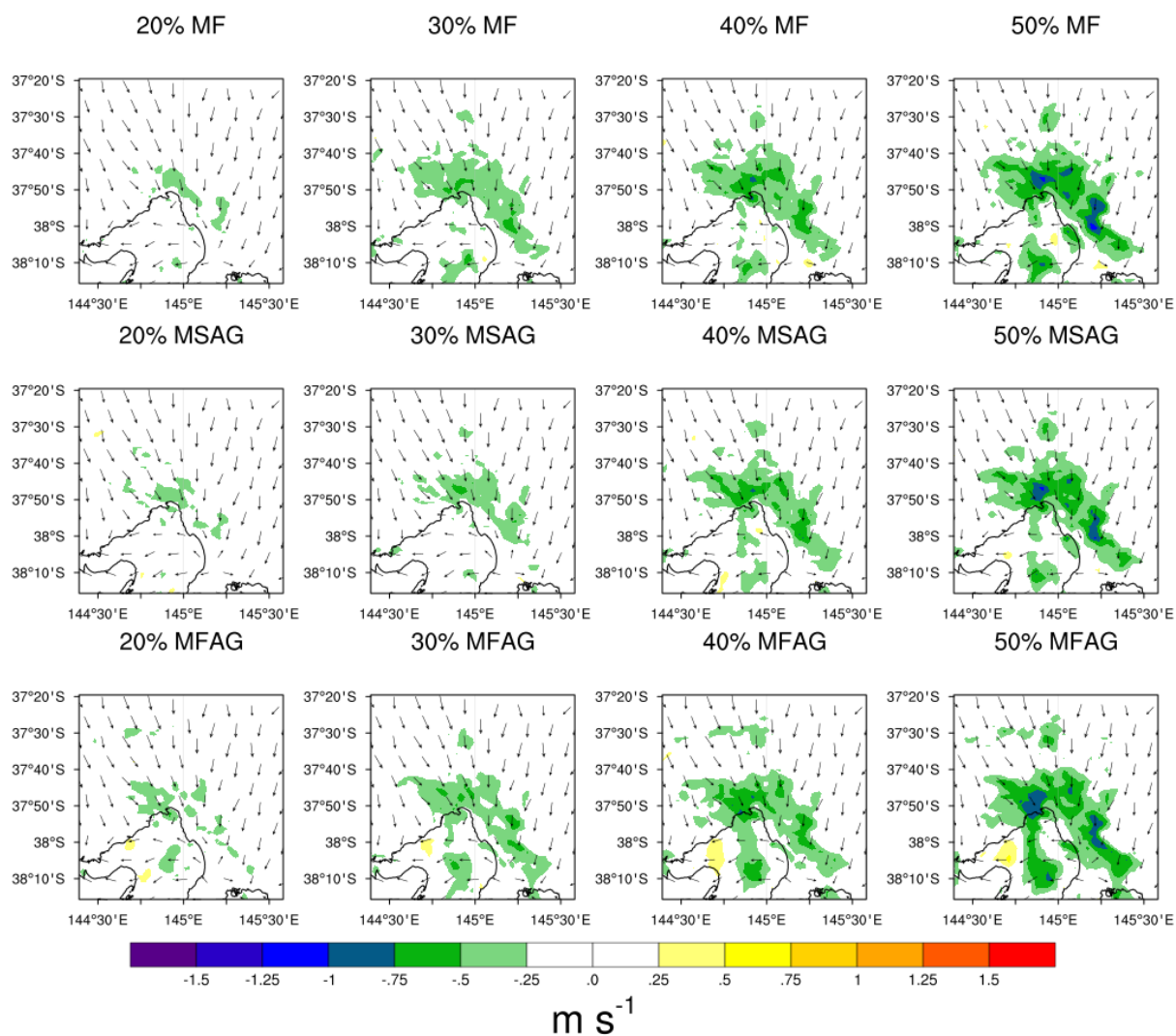


Fig. 9. Wind direction (only for experiments) and changes in wind speed (experiments minus control) for MF (upper), MSAG (middle) and MFAG (bottom) by using their fractions 20%, 30%, 40% and 50%. All results are averaged from 2100 to 0400 local time for the 3 days (28 to 30 January 2009) when maximum UHI_2 reductions occur.

Furthermore, changes in the boundary layer structure, e.g., vertical profiles of air temperatures, wind speed, relative humidity, vertical wind component and turbulent kinetic energy were examined, but these did not show substantial changes and are therefore not shown. Vegetated patches did not substantially influence vertical mixing within the boundary layer during the heatwave event.

3.5 Changes in Human Thermal Comfort (HTC)

Fig. 10 shows the HTC via the UTCI index for the control simulation (Fig. 10 (a)) and the changes in HTC for 40 % (Fig. 10(b)) and 50 % (Fig. 10(c)) vegetated patches as these vegetated fractions showed the largest changes in UHI_2 and UHI_{sk} . A lower UTCI index indicates higher HTC and vice-versa. The results illustrate that increasing vegetated patches in urban areas improves the HTC from evening to night in the urban areas. MF and MFAG increase HTC by reducing the UTCI index from 3.2 to 4.8°C during the night by using 40 to 50% vegetated patches, while MSAG reduces UTCI index from 1.7 to 2.5°C. The maximum improvement in HTC occurs during the evening (2100 local time), when the maximum UHI_2 and UHI_{sk} reductions occur. No substantial improvement of HTC is obtained during the day (between 1000 to 1700 local time) especially when very strong human discomfort occurs. Therefore, vegetated patches are not able to improve HTC when stronger heat stress occurs. In addition, MSAG slightly deteriorate the HTC by increasing the UTCI index by 0.50 °C due to slightly higher sensible heat flux during the day (Fig. 10b, 10c). MF and MFAG show similar effectiveness in improving HTC (reducing UTCI) while MSAG show lower effectiveness as compared to MF and MFAG.

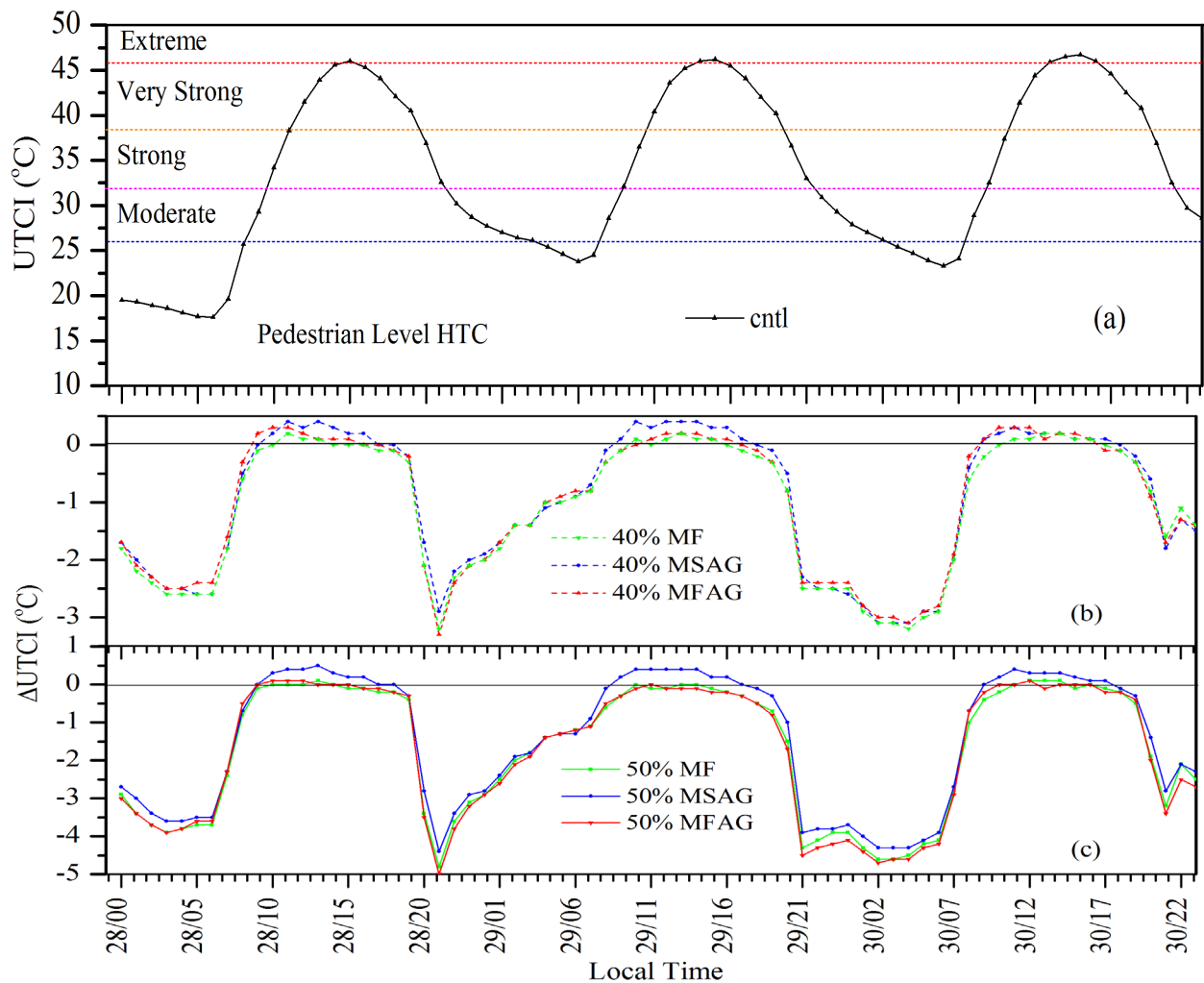


Fig. 10. (a) Hourly time series of the UTCI index at pedestrian level for the control simulation. (b) Changes in UTCI (experiment minus control) at pedestrian level for 40 % and (c) 50 % vegetated patches. All results are averaged over only urban grid cells across domain d03 for the 3 days over 28 to 30 January 2009

4. Discussion

This study examined the potential of different vegetated patches in urban areas in reducing UHI effects due to future urban expansion in the city of Melbourne during an extreme heatwave event. Although MF, MFAG and MSAG substantially increased latent heat flux and decreased storage heat during the day (Fig. 5), no substantial reductions of the UHI_2 and UHI_{sk} occurred during the day, as there was little to no change in sensible heat flux (Fig. 3). Rather there was a slight warming effect in the skin surface temperature between 1000 and 1700 local time which is likely due to the rapid release of terrestrial radiation and trapping of solar heat from MSAG, MFAG and MF as compared to a slower release from the urban

surfaces as reported by Papangelis et al. (2012), who found similar warming effects over open vegetated urban green surfaces due to faster release of terrestrial radiation. Additionally, the heatwave event considered in this study resulted in very hot and dry conditions, and therefore, vegetated surfaces would like have become warmer as compared to usual summer days during the day. The key driver in substantial reduction of the UHI_2 and UHI_{sk} between evening and early morning was the storage heat flux, and this result is consistent with Jacobs et al. (2018). The higher the reductions of storage heat (Fig. 7), the higher the reductions of the UHI_2 and UHI_{sk} (Fig. 6). The main driver of the reduction in storage heat was the lower urban fraction with increasing fractions of vegetated patch implementation (Table 1).

A number of studies report daytime cooling of the near surface air temperature by increasing urban vegetation (e.g., Lee and Park 2008; Loughner et al., 2012; Coutts et al., 2016) due to shading and evapotranspiration, but this study found no such cooling during the day. The urban canopy models and experiments used for those studies considered shading effects of urban vegetation over buildings, roads and walls, which was the main driving mechanism in reducing day time temperatures in urban areas. In this study, vegetation is implemented as patches using the mosaic approach, i.e., entire portions of urban grid cells are converted to vegetated surfaces, rather than the implementation of vegetation which urban canyons whereby the shading effect of individual trees on buildings would be a key factor. The nighttime cooling was driven by a reduction in storage heat by the urban surfaces during the day as the higher fractions of urban areas were replaced by vegetated surfaces (e.g., MF, MFAG and MSAG). MF and MFAG showed higher cooling effect as compared to MSAG since MF and MFAG had a lower storage heat. This lower storage heat is likely due to the higher shade factor and LAI as compared to MSAG, which would have led to even less radiation reaching the ground surface during the day, leading to lower storage heat. Similar findings have been reported by other studies (Kumar and Kaushik, 2005; Lin and Lin, 2010). Several studies have shown that leaf color (e.g., light green leaves) and LAI of plants are the most important factors in driving the cooling effect (Kumar and Kaushik, 2005; Lin and Lin, 2010; Rey, 1999; Tanaka and Hashimoto, 2006), with light-green leaves being more effective in reflecting solar radiation as compared to darker-green leaves and higher LAI of plants provides more cooling benefits via evapotranspiration. This study suggests that higher LAI and shade factor (on the ground) for MF and MFAG as compared to MSAG (Table 2) leads to higher reductions of the UHI_2 and UHI_{sk} . Although, the cooling effect of MF, MFAG and MSAG depend on other factors (e.g., leaf thickness, texture of trees), which are beyond the

scope of this study. There was a slight warming effect at skin-surface level due to increasing vegetated patches particularly for MSAG at 1200 local time because of a slight increase in sensible heat. MSAG resulted in higher SH flux due their lower LAI and shade factor (Table 2) as compared to MF and MFAG. Lower LAI would have allowed more solar radiation to reach the surface, and given the very dry soil conditions during the heatwave, more solar radiation reaching the surface would have enhanced SH, and consequently led to a slight warming effect on skin surface temperature. Furthermore, increased vegetation patches showed minimal cooling effect for near surface temperature during the hottest part of the day similar to Jacobs et al. (2018).

Although previous studies showed that the cooling effect of parks extended to surrounding built-up areas (Papangelis et al., 2012; Yu and Hien, 2006) due to cooler air advection over the parks and downwind into the urban areas (Papangelis et al., 2012), this study did not show noticeable cooling effects beyond urban areas when different types of vegetated patches were used (Fig. 6). The reason was likely due to very dry air flowing from heated interior during the heatwave event, which limited cooling effects to surrounding areas. The relationship between the UHI reductions and increased fractions of vegetated patches was non-linear, with 50 % vegetated patches resulting in much larger cooling benefits than lower fractions. This was most likely due to the reductions of wind speeds (Fig. 9) for 50 % as compared to other vegetated fractions. The higher vegetated fractions led to weaker winds particularly in the center of the city. These weaker winds would have promoted stagnation rather than advection of the cooler air, leading to more cooling in the city center (Fig. 6), where the reductions of wind speeds were higher (Fig. 9). Furthermore, MF and MFAG showed higher effectiveness in reducing UHI effects as compared to MSAG (Fig. 6) because of lower storage heat (Fig. 7), which is likely due to the higher shade factor and LAI (Table 2).

Earlier studies have shown that MFAG can result in reductions of air temperature by 5 °C in the city of Washington and Baltimore, USA (Loughner et al., 2012), and 2.5 °C due to MF in Athens, Greece (Papangelis et al., 2012) during the night, due to lower storage heat in the areas of MFAG and trees during the day and unobstructed and rapid release of this stored heat during the night. Loughner et al. (2012) showed that MFAG reduced neighborhood air temperature by 1 °C during the day because of advection of cooler air due to sea-breeze while Papangelis et al. (2012) reported the reduction of maximum day time temperature by 4.1 °C

for MF due to the combined effects of tree shading and evapotranspiration, and sea-breeze. Although this study showed cooling benefits from different vegetated patches during the night, there were no cooling effects during the day as no substantial reductions in SH occurred during this time.

Several studies have shown that changes in wind speed and direction were another driver in influencing the variability of air temperature as these variables play important role in influencing vertical mixing (Lin and Lin, 2010; Loughner et al., 2012; Park et al., 2012). This study did not show substantial reductions in wind speed for 20 and 30 % vegetated patches (Fig. 9). However, the moderate reductions of wind speed (ranging from 0.50 to 1.25 m s⁻¹), particularly in the center of the city for 40 and 50 % vegetated patches, could have had an influence on cooling in the center of the city. Vegetated patches were not effective in improving HTC during the day and the reason was most likely due to increased relative humidity during the same time (Fig. 10). However, HTC substantially improved during the night due to vegetated patches because of the reductions of storage heat (Figs. 5 and 7).

5. Conclusions

The study investigated the effectiveness of MF, MSAG and MFAG as vegetated patches in reducing UHI effects in the city of Melbourne in southeast Australia using the mesoscale WRF model coupled with the SLUCM during a severe heatwave event. A future urbanization scenario was implemented based on the Plan Melbourne 2050 urban expansion strategy. Experiments were carried out by increasing the percentage of vegetated patches from 20 to 50% within all urban grid cells by using the mosaic approach in WRF. All vegetated patches led to reductions in the UHI₂ and UHI_{sk} and thereby improved HTC from evening to early morning. The reductions of UHI₂ and UHI_{sk} were higher when the fractions of vegetated patches were increased, but substantially higher when 50% was used, and the cooling effects were more intense in the center of the city. The application of different vegetated patches substantially altered the surface energy balance by substantially reducing storage heat and increasing latent heat flux, with the storage heat flux being the key driver in reducing UHI effects.

MF and MFAG were more effective in reducing UHI effects as compared to MSAG. On the other hand, MSAG resulted in slight warming during midday because of increased sensible

heat flux due to lower LAI and shade factor. The effectiveness of different vegetated patches in reducing UHI effects was not substantial during the day as there were no changes in sensible heat flux. In addition, considerable reductions in wind speed were obtained for only 40 and 50 % vegetated patches especially in the center of the city, and therefore, the cooling effects due to implementing vegetated patches stagnate in the center of the city. In addition, vegetated patches also improved HTC particularly during the night when substantial reductions of UHI occurred. Based on overall results, the findings of this study suggests that the urban greening strategy, released by the city of Melbourne to increase urban vegetation cover from 22 to 40 % by 2040, could help to achieve a more thermally comfortable, sustainable and livable urban environment.

Finally, this study has some limitations that need to be discussed. Direct interactions between vegetation and urban surfaces are not accounted for in our model. In reality, shading effects of vegetation at the edges of vegetated patches on urban surfaces would likely result in even lower storage heat flux. Hence the cooling effects reported in this study are likely to be under-estimated. The study quantified the effectiveness of different vegetated patches in mitigating UHI effects including future urban scenarios but without considering future warming which would be expected by 2050. Reductions in the UHI via vegetated patches could be lower if there is substantial future warming. This study also assumed that vegetated patches are implemented within all urban grid cells rather than only within the future projected urban expansion area. It is unlikely that up to 40 to 50% vegetated patches can be practically implemented across the entire city. Hence, this study only provides estimates of the maximum possible benefits, rather than practical benefits considering the challenges of implementing vegetated patches at such large scales. It should also be noted that this study does not include anthropogenic heat emissions during the simulations, such as heat from air conditioning units.

Acknowledgements

Data support by the Bureau of Meteorology (BoM) Australia and ECMWF (ERA-interim) data server (<http://apps.ecmwf.int/datasets/data/interim-full-daily/levtype=ml/>) are gratefully acknowledged. Jatin Kala is supported by an Australian Research Council Discovery Early Career Researcher Award (DE170100102).

References

- Akbari, H., Pomerantz, M. and Taha, H. (2001). Cool surfaces and shade trees to reduce energy use and improve air quality in urban areas. *Solar Energy*, 70(3), 295-310. doi: [https://doi.org/10.1016/S0038-092X\(00\)00089-X](https://doi.org/10.1016/S0038-092X(00)00089-X)
- Ali-Toudert, F. and Mayer, H. (2007). Effects of asymmetry, galleries, overhanging façades and vegetation on thermal comfort in urban street canyons. *Solar Energy*, 81(6), 742-754. doi: <https://doi.org/10.1016/j.solener.2006.10.007>
- Argüeso, D., Evans, J. P., Fita, L. and Bormann, K. J. (2014). Temperature response to future urbanization and climate change. *Climate Dynamics*, 42(7), 2183-2199. doi: 10.1007/s00382-013-1789-6
- Australian Bureau of Statistics (2008). ABS 3222.0 Population projections, Australia 2006 to 680 2101, viewed 7 August 2018: 681 <<http://www.abs.gov.au/Ausstats/abs@.nsf/Latestproducts/3222.0>>.
- Blazejczyk, K., Epstein, Y., Jendritzky, G., Staiger, H. and Tinz, B. (2012). Comparison of UTCI to selected thermal indices. *International Journal of Biometeorology*, 56(3), 515-535. doi: 10.1007/s00484-011-0453-2
- Bowler, D. E., Buyung-Ali, L., Knight, T. M. and Pullin, A. S. (2010). Urban greening to cool towns and cities: A systematic review of the empirical evidence. *Landscape and Urban Planning*, 97(3), 147-155. doi: <https://doi.org/10.1016/j.landurbplan.2010.05.006>
- Bröde, P., Fiala, D., Błażejczyk, K., Holmér, I., Jendritzky, G., Kampmann, B., . . . Havenith, G. (2012). Deriving the operational procedure for the Universal Thermal Climate Index (UTCI). *International Journal of Biometeorology*, 56(3), 481-494. doi: 10.1007/s00484-011-0454-1
- Chen, F. and Dudhia, J. (2001). Coupling an Advanced Land Surface–Hydrology Model with the Penn State–NCAR MM5 Modeling System. Part I: Model Implementation and Sensitivity. *Monthly Weather Review*, 129(4), 569-585. doi: 10.1175/1520-0493(2001)129<0569:caalsh>2.0.co;2

- Chen, F., Kusaka, H., Bornstein, R., Ching, J., Grimmond, C. S. B., Grossman-Clarke, S., . . . Zhang, C. (2011). The integrated WRF/urban modelling system: development, evaluation, and applications to urban environmental problems. *International Journal of Climatology*, 31(2), 273-288. doi: doi:10.1002/joc.2158
- Coutts, A. M., White, E. C., Tapper, N. J., Beringer, J. and Livesley, S. J. (2016). Temperature and human thermal comfort effects of street trees across three contrasting street canyon environments. *Theoretical and Applied Climatology*, 124(1), 55-68. doi: 10.1007/s00704-015-1409-y
- Cowan, T., Purich, A., Perkins, S., Pezza, A., Boschat, G. and Sadler, K. (2014). More Frequent, Longer, and Hotter Heat Waves for Australia in the Twenty-First Century. *Journal of Climate*, 27(15), 5851-5871. doi: 10.1175/jcli-d-14-00092.1
- Dee, D., Uppala, S., Simmons, A., Berrisford, P., Poli, P., Kobayashi, S., . . . Bauer, P. (2011). The ERA-Interim reanalysis: configuration and performance of the data assimilation system, QJ Roy. Meteor. Soc., 137, 553–597.
- Evans, J. P., Ekström, M. and Ji, F. (2012). Evaluating the performance of a WRF physics ensemble over South-East Australia. *Climate Dynamics*, 39(6), 1241-1258. doi: 10.1007/s00382-011-1244-5
- Fallmann, J., Emeis, S. and Suppan, P. (2013). Mitigation of urban heat stress - a modelling case study for the area of Stuttgart. *Die Erde*, 144(3-4), 202-216. doi: 10.12854/erde-144-15
- Foster, J., Lowe, A. and Winkelmann, S. (2011). The value of green infrastructure for urban climate adaptation. *Center for Clean Air Policy*, 750, 1-52.
- Grell, G. A. and Dévényi, D. (2002). A generalized approach to parameterizing convection combining ensemble and data assimilation techniques. *Geophysical Research Letters*, 29(14), 38-31-38-34. doi: doi:10.1029/2002GL015311
- Harlan, S. L., Brazel, A. J., Prashad, L., Stefanov, W. L. and Larsen, L. (2006). Neighborhood microclimates and vulnerability to heat stress. *Social Science & Medicine*, 63(11), 2847-2863. doi: <https://doi.org/10.1016/j.socscimed.2006.07.030>

- Hathway, E. A. and Sharples, S. (2012). The interaction of rivers and urban form in mitigating the Urban Heat Island effect: A UK case study. *Building and Environment*, 58, 14-22. doi: <https://doi.org/10.1016/j.buildenv.2012.06.013>
- Honjo, T. and Takakura, T. (1990). Simulation of thermal effects of urban green areas on their surrounding areas. *Energy and Buildings*, 15(3), 443-446. doi: [https://doi.org/10.1016/0378-7788\(90\)90019-F](https://doi.org/10.1016/0378-7788(90)90019-F)
- Howard, L. (1833). The climate of London, vols. I–III. *London: Harvey and Dorton*.
- Iacono, M. J., Delamere, J. S., Mlawer, E. J., Shephard, M. W., Clough, S. A. and Collins, W. D. (2008). Radiative forcing by long-lived greenhouse gases: Calculations with the AER radiative transfer models. *Journal of Geophysical Research: Atmospheres*, 113(D13). doi: [doi:10.1029/2008JD009944](https://doi.org/10.1029/2008JD009944)
- Imran, H. M., Kala, J., Ng, A. W. M. and Muthukumaran, S. (2018a). Effectiveness of green and cool roofs in mitigating urban heat island effects during a heatwave event in the city of Melbourne in southeast Australia. *Journal of Cleaner Production*, 197, 393-405. doi: <https://doi.org/10.1016/j.jclepro.2018.06.179>
- Imran, H. M., Kala, J., Ng, A. W. M. and Muthukumaran, S. (2018b). An evaluation of the performance of a WRF multi-physics ensemble for heatwave events over the city of Melbourne in southeast Australia. *Climate Dynamics*, 50(7), 2553-2586. doi: [10.1007/s00382-017-3758-y](https://doi.org/10.1007/s00382-017-3758-y)
- Imran, H. M., Kala, J., Ng, A. W. M. and Muthukumaran, S. (2018c). Impacts of Future Urban Expansion on Urban Heat Island Effects during Heatwave Events in the City of Melbourne in Southeast Australia. *Quarterly Journal of the Royal Meteorological Society* (Submitted).
- Jacobs, S. J., Gallant, A. J. and Tapper, N. J. (2017). The Sensitivity of Urban Meteorology to Soil Moisture Boundary Conditions: A Case Study in Melbourne, Australia. *Journal of Applied Meteorology and Climatology*, 56(8), 2155-2172.
- Jacobs, S. J., Gallant, A. J., Tapper, N. J. and Li, D. (2018). Use of cool roofs and vegetation to mitigate urban heat and improve human thermal stress in Melbourne, Australia.

Journal of Applied Meteorology and Climatology, 0(0), null. doi: 10.1175/jamc-d-17-0243.1

Janjic, Z. (1994). *The step-mountain eta coordinate model: Further developments of the convection, viscous sublayer, and turbulence closure schemes* (Vol. 122:5).

Kala, J., Andrys, J., Lyons, T. J., Foster, I. J. and Evans, B. J. (2015a). Sensitivity of WRF to driving data and physics options on a seasonal time-scale for the southwest of Western Australia. *Climate Dynamics*, 44(3), 633-659. doi: 10.1007/s00382-014-2160-2

Kala, J., Evans, J. P. and Pitman, A. J. (2015b). Influence of antecedent soil moisture conditions on the synoptic meteorology of the Black Saturday bushfire event in southeast Australia. *Quarterly Journal of the Royal Meteorological Society*, 141(693), 3118-3129. doi: doi:10.1002/qj.2596

Krayenhoff, E.,S., Christen, A., Martilli, A., Oke, T.R. (2013). A Multi-layer Radiation Model for Urban Neighbourhoods with Trees. *Boundary-Layer Meteorol* 151, 139–178. <https://doi.org/10.1007/s10546-013-9883-1>

Kumar, R. and Kaushik, S. (2005). Performance evaluation of green roof and shading for thermal protection of buildings. *Building and Environment*, 40(11), 1505-1511.

Kusaka, H. and Kimura, F. (2004). Coupling a Single-Layer Urban Canopy Model with a Simple Atmospheric Model: Impact on Urban Heat Island Simulation for an Idealized Case. *Journal of the Meteorological Society of Japan. Ser. II*, 82(1), 67-80. doi: 10.2151/jmsj.82.67

Kusaka, H., Kondo, H., Kikegawa, Y. and Kimura, F. (2001). A Simple Single-Layer Urban Canopy Model For Atmospheric Models: Comparison With Multi-Layer And Slab Models. *Boundary-Layer Meteorology*, 101(3), 329-358. doi: 10.1023/a:1019207923078

Lee, S.H. and Park, S.U. (2008). A Vegetated Urban Canopy Model for Meteorological and Environmental Modelling. *Boundary-Layer Meteorol* 126, 73–102. <https://doi.org/10.1007/s10546-007-9221-6>

- Lemonsu, A., Masson, V., Shashua-Bar, L., Erell, E., Pearlmutter, D. (2012). Inclusion of vegetation in the Town Energy Balance model for modelling urban green areas. *Geoscientific Model Development* 5, 1377–1393. <https://doi.org/10.5194/gmd-5-1377-2012>
- Li, D., Bou-Zeid, E. and Oppenheimer, M. (2014). The effectiveness of cool and green roofs as urban heat island mitigation strategies. *Environmental Research Letters*, 9(5), 055002.
- Li, D., Sun, T., Liu, M., Yang, L., Wang, L. and Gao, Z. (2015). Contrasting responses of urban and rural surface energy budgets to heat waves explain synergies between urban heat islands and heat waves. *Environmental Research Letters*, 10(5), 054009.
- Lin, B.-S. and Lin, Y.-J. (2010). Cooling Effect of Shade Trees with Different Characteristics in a Subtropical Urban Park. *HortScience*, 45(1), 83-86.
- Liu, X., Tian, G., Feng, J., Ma, B., Wang, J. and Kong, L. (2018). Modeling the Warming Impact of Urban Land Expansion on Hot Weather Using the Weather Research and Forecasting Model: A Case Study of Beijing, China. *Advances in Atmospheric Sciences*, 35(6), 723-736. doi: 10.1007/s00376-017-7137-8
- Liu, Y., Chen, F., Warner, T. and Basara, J. (2006). Verification of a Mesoscale Data-Assimilation and Forecasting System for the Oklahoma City Area during the Joint Urban 2003 Field Project. *Journal of Applied Meteorology and Climatology*, 45(7), 912-929. doi: 10.1175/jam2383.1
- Loughner, C. P., Allen, D. J., Zhang, D.-L., Pickering, K. E., Dickerson, R. R. and Landry, L. (2012). Roles of Urban Tree Canopy and Buildings in Urban Heat Island Effects: Parameterization and Preliminary Results. *Journal of Applied Meteorology and Climatology*, 51(10), 1775-1793. doi: 10.1175/jamc-d-11-0228.1
- Matzarakis, A., Rutz, F. and Mayer, H. (2007). Modelling radiation fluxes in simple and complex environments—application of the RayMan model. *International Journal of Biometeorology*, 51(4), 323-334. doi: 10.1007/s00484-006-0061-8

- Matzarakis, A., Rutz, F. and Mayer, H. (2010). Modelling radiation fluxes in simple and complex environments: basics of the RayMan model. *International Journal of Biometeorology*, 54(2), 131-139. doi: 10.1007/s00484-009-0261-0
- McMahon, E. T. and Benedict, M. (2000). Green infrastructure. *Planning Commissioners Journal*, 37(4), 4-7.
- Melbourne (Vic.) Council (2011). Urban forest strategy: making a great city greener: 2012-2032. City of Melbourn, Australia.
- https://books.google.com.bd/books/about/Urban_Forest_Strategy.html?id=jo0PMwEACAAJ&redir_esc=y
- Middel, A., Häb, K., Brazel, A. J., Martin, C. A. and Guhathakurta, S. (2014). Impact of urban form and design on mid-afternoon microclimate in Phoenix Local Climate Zones. *Landscape and Urban Planning*, 122, 16-28. doi: <https://doi.org/10.1016/j.landurbplan.2013.11.004>
- Mirzaei, P. A. and Haghghat, F. (2010). Approaches to study Urban Heat Island – Abilities and limitations. *Building and Environment*, 45(10), 2192-2201. doi: <https://doi.org/10.1016/j.buildenv.2010.04.001>
- Morris, K. I., Chan, A., Morris, K. J. K., Ooi, M. C. G., Oozeer, M. Y., Abakr, Y. A., . . . Al-Qrimli, H. F. (2017). Impact of urbanization level on the interactions of urban area, the urban climate, and human thermal comfort. *Applied Geography*, 79, 50-72. doi: <https://doi.org/10.1016/j.apgeog.2016.12.007>
- Nairn, J. R. and Fawcett, R. G. (2013). *Defining heatwaves: heatwave defined as a heat-impact event servicing all community and business sectors in Australia*: Centre for Australian Weather and Climate Research.
- Nicholls, N. and Larsen, S. (2011). Impact of drought on temperature extremes in Melbourne, Australia. *Australian Meteorological and Oceanographic Journal*, 61(2), 113-116.
- Nicholls, N., Skinner, C., Loughnan, M. and Tapper, N. (2008). A simple heat alert system for Melbourne, Australia. *International Journal of Biometeorology*, 52(5), 375-384. doi: 10.1007/s00484-007-0132-5

- Ohashi, Y., Genchi, Y., Kondo, H., Kikegawa, Y., Yoshikado, H. and Hirano, Y. (2007). Influence of Air-Conditioning Waste Heat on Air Temperature in Tokyo during Summer: Numerical Experiments Using an Urban Canopy Model Coupled with a Building Energy Model. *Journal of Applied Meteorology and Climatology*, 46(1), 66-81. doi: 10.1175/jam2441.1
- Oliveira, S., Andrade, H. and Vaz, T. (2011). The cooling effect of green spaces as a contribution to the mitigation of urban heat: A case study in Lisbon. *Building and Environment*, 46(11), 2186-2194. doi: <https://doi.org/10.1016/j.buildenv.2011.04.034>
- Papangelis, G., Tombrou, M., Dandou, A. and Kontos, T. (2012). An urban “green planning” approach utilizing the Weather Research and Forecasting (WRF) modeling system. A case study of Athens, Greece. *Landscape and Urban Planning*, 105(1), 174-183. doi: <https://doi.org/10.1016/j.landurbplan.2011.12.014>
- Park, M., Hagishima, A., Tanimoto, J. and Narita, K.-i. (2012). Effect of urban vegetation on outdoor thermal environment: Field measurement at a scale model site. *Building and Environment*, 56, 38-46. doi: <https://doi.org/10.1016/j.buildenv.2012.02.015>
- Redon, E.C., Lemonsu, A., Masson, V., Morille, B., Musy, M. (2017). Implementation of street trees within the solar radiative exchange parameterization of TEB in SURFEX v8.0. *Geoscientific Model Development* 10, 385–411. <https://doi.org/10.5194/gmd-10-385-2017>
- Perkins-Kirkpatrick, S. E., White, C. J., Alexander, L. V., Argüeso, D., Boschat, G., Cowan, T., . . . Purich, A. (2016). Natural hazards in Australia: heatwaves. *Climatic Change*, 139(1), 101-114. doi: 10.1007/s10584-016-1650-0
- Rey, J. M. (1999). Modelling potential evapotranspiration of potential vegetation. *Ecological Modelling*, 123(2-3), 141-159.
- Rizwan, A. M., Dennis, L. Y. C. and Liu, C. (2008). A review on the generation, determination and mitigation of Urban Heat Island. *Journal of Environmental Sciences*, 20(1), 120-128. doi: [https://doi.org/10.1016/S1001-0742\(08\)60019-4](https://doi.org/10.1016/S1001-0742(08)60019-4)
- Sharma, A., Conry, P., Fernando, H. J. S., Alan, F. H., Hellmann, J. J. and Chen, F. (2016). Green and cool roofs to mitigate urban heat island effects in the Chicago metropolitan

- area: evaluation with a regional climate model. *Environmental Research Letters*, 11(6), 064004.
- Sharma, A., Fernando, H. J. S., Hamlet, A. F., Hellmann, J. J., Barlage, M. and Chen, F. (2017). Urban meteorological modeling using WRF: a sensitivity study. *International Journal of Climatology*, 37(4), 1885-1900. doi: doi:10.1002/joc.4819
- Shashua-Bar, L. and Hoffman, M. E. (2000). Vegetation as a climatic component in the design of an urban street: An empirical model for predicting the cooling effect of urban green areas with trees. *Energy and Buildings*, 31(3), 221-235. doi: [https://doi.org/10.1016/S0378-7788\(99\)00018-3](https://doi.org/10.1016/S0378-7788(99)00018-3)
- Shashua-Bar, L., Potchter, O., Bitan, A., Boltansky, D. and Yaakov, Y. (2010). Microclimate modelling of street tree species effects within the varied urban morphology in the Mediterranean city of Tel Aviv, Israel. *International Journal of Climatology*, 30(1), 44-57. doi: doi:10.1002/joc.1869
- Skamarock, W., Klemp, J., Dudhia, J., Gill, D., Barker, D., Duda, M., . . . Powers, J. (2008). A description of the advanced research WRF version 3. NCAR Technical Note, NCAR/TN\2013475? STR, 123 pp.
- Tanaka, K. and Hashimoto, S. (2006). Plant canopy effects on soil thermal and hydrological properties and soil respiration. *Ecological Modelling*, 196(1-2), 32-44.
- Theeuwes, N. E., Solcerová, A. and Steeneveld, G. J. (2013). Modeling the influence of open water surfaces on the summertime temperature and thermal comfort in the city. *Journal of Geophysical Research: Atmospheres*, 118(16), 8881-8896. doi: doi:10.1002/jgrd.50704
- Thompson, G., Field, P. R., Rasmussen, R. M. and Hall, W. D. (2008). Explicit Forecasts of Winter Precipitation Using an Improved Bulk Microphysics Scheme. Part II: Implementation of a New Snow Parameterization. *Monthly Weather Review*, 136(12), 5095-5115. doi: 10.1175/2008mwr2387.1
- Vatani, J., Golbabaee, F., Dehghan, S. F. and Yousefi, A. (2016). Applicability of Universal Thermal Climate Index (UTCI) in occupational heat stress assessment: a case study in brick industries. *Industrial Health*, 54(1), 14-19. doi: 10.2486/indhealth.2015-0069

- Victorian Auditor General's Office (2014). Heatwave Management: Reducing the Risk to Public Health. Report tabled in State Parliament 14 October 2014 <https://www.audit.vic.gov.au/sites/default/files/2017-07/20141014-Heatwave-Management.pdf>
- Wang, Z. H., Bou-Zeid, E. and Smith, J. A. (2013). A coupled energy transport and hydrological model for urban canopies evaluated using a wireless sensor network. *Q. J. R. Meteorol. Soc.*, 139, 1643–1657, doi:Doi 10.1002/Qj.2032.
- Yu, C. and Hien, W. N. (2006). Thermal benefits of city parks. *Energy and Buildings*, 38(2), 105-120. doi: <https://doi.org/10.1016/j.enbuild.2005.04.003>
- Zhao, L., Oppenheimer, M., Zhu, Q., Baldwin, J. W., Ebi, K. L., Bou-Zeid, E., and Liu, X. (2018). Interactions between urban heat islands and heat waves. *Environmental Research Letters*, 13(3), 034003.
- Žuvela-Aloise, M., Koch, R., Buchholz, S. and Früh, B. (2016). Modelling the potential of green and blue infrastructure to reduce urban heat load in the city of Vienna. *Climatic Change*, 135(3), 425-438. doi: 10.1007/s10584-016-1596-2

Chapter 8

General Discussion and Conclusions

8.1 General Discussion

The aims of this thesis were as follows:

1. Evaluation of the performance of the WRF model to simulate heatwave events over the city of Melbourne
2. Evaluation of the effectiveness of green and cool roofs in mitigating UHI effects during heatwave event in the city of Melbourne
3. Evaluation of the impacts of future urbanization on UHI effects during heatwave events in the city of Melbourne
4. Evaluation of the effectiveness of MF, MFAG and MSAG in mitigating UHI effects during heatwave event in the city of Melbourne

Chapter 4 presented the sensitivity study that was carried out to obtain the best WRF model physical parameterization options for simulating the UHI during heatwaves in Melbourne. A series of simulations were conducted using a total 27 WRF configurations including three PBL schemes (MYJ, ACM2, and QNSE), three MP schemes (WDM5, WSM6 and Thompson), and three SW (Dudhia, RRTMG, Goddard) and LW (RRTM, RRTMG, Goddard) radiation schemes. Additionally, simulations were conducted to examine the role of the SLUCM and two LSMs (Noah-MP and CLM4) in simulating the UHI and heatwave events. All simulations showed that the WRF model was able to

accurately simulate various atmospheric variables including temperature, wind speed and relative humidity over the Melbourne region. Different evaluation metrics showed that no particular WRF model configuration showed the best performance in simulating all different atmospheric variables for all heatwave events for all evaluation metrics. Similar findings have been obtained by previous studies Stegehuis et al. (2015) and Evans et al. (2012) who reported that no single configuration of the multi-physics ensemble showed the best performance in simulating all atmospheric variables for all cases. Based on statistical measures, it was therefore difficult to identify a consistently best performing WRF ensemble member as different metrics showed preferences for some particular physics options across all four events. Hence, the best selection was made based on the aggregated performance. The results from the sensitivity study confirmed that, the configuration consisting of the MYJ PBL scheme, RRTMG SW and LW radiation schemes and Thompson MP scheme showed the best performance as compared to other WRF configurations, and this configuration was therefore adopted for the rest of the thesis. The combination included the QNSE PBL scheme, Dudhia shortwave RRTM longwave radiation schemes, and WSM6 MP scheme should not be used for Melbourne region. The choice of PBL and LSM schemes had the largest influence on the UHI and heatwave simulations. The results of sensitivity analyses of the WRF model provided an improved understanding of how different physics options responded including different driving mechanisms in simulating different atmospheric variables during heatwaves, and this will be useful to the wider research community.

In chapter 5, the potential of cool roofs and green roofs in reducing UHI effects during one of the most severe heatwave events in southeast Australia was examined. The green and cool roofs practices were very effective in minimizing UHI effects in the city of

Melbourne during the heatwave event. Cool roofs reflected the incoming solar radiation, and consequently, decreased the sensible heat flux and reduced UHI effects. Green roofs provided heat transfer benefits via evapotranspiration. The green roofs and cool roofs modified the surface energy balance by reducing sensible heat flux, consequently, and reduced the UHI effects and the influence extended up to 2.5 km within the boundary layer. The decrease in sensible flux due to the green and cool roofs reduced vertical mixing and the PBL height, and consequently, reduced the air temperature. However, the changes in wind speed and relative humidity were not substantial in the lower boundary layer during the day. It was shown that the green roof approach had a limitation particularly in the early morning because of slightly increased UHI effects. The reduction in UHI varied linearly with the increasing green roof fractions, but slightly non-linear with the increasing albedo fractions of cool roofs. Both green and cool roofs showed higher UHI reductions in high-density urban area (centre of the city) as compared low-density urban area (suburb). Increased soil moisture did not have a substantial impact in reducing UHI effects, but soil moisture deficit on green roofs intensified the UHI during both the day and night. In addition, green and cool roofs largely improved HTC at the roof surface level but this effect was much lower at near surface (2 m). However, green and cool roofs showed potential in reducing thermal stress during the day when the worst thermal stress occurred. Cool roofs showed more effectiveness in reducing UHI and improving HTC as compared to green roofs. Although other studies showed that advection of moisture from rural to urban areas influenced the urban boundary layer (Li et al., 2014; Sharma et al., 2016), this was not the case for this study. Instead this thesis showed that connective rolls played important role in influencing the urban boundary layer because of heated urban surface during severe the heatwave.

In chapter 6, the potential impacts of future urban expansion on the UHI during heatwaves were examined. The future urban expansion strategy was examined based on the Plan Melbourne 2050 urban expansion strategy. Urban expansion altered the surface energy balance by substantially increasing storage heat and decreasing latent heat flux because of impervious urban surfaces. Higher thermal conductivity of urban surfaces and lack of vegetation and soil moisture in urban areas played leading role in increasing storage heat and reducing latent heat. The increased storage heat was key driver in increasing UHI_2 and UHI_{sk} effects during the night. Urban expansion substantially increased the daily minimum temperature as compared to mean and maximum daily temperatures. Urban expansion substantially increased the minimum temperature due to mainly increased storage heat. In addition, the reduction of wind speed was another important driver in intensifying UHI_2 and UHI_{sk} effects beyond the expanded urban areas. Furthermore, urban expansion did not substantially affect the HTC over existing and expanded urban areas.

Chapter 7 evaluated the potential of vegetated patches such as MF, MFAG and MSAG as GI practices in mitigating UHI effects during one of the most severe heatwave events. The future urban expansion based on Plan Melbourne 2050 (chapter 6) was included with the existing urban extent. Then different vegetated patches as GI practices were implemented into urban areas and their effectiveness in reducing urban temperatures were quantified. The higher percentages of vegetated patches/GI practices in urban areas increased the cooling effect, and consequently, reduced UHI effects between evening and early morning. The intensity of UHI decreased when the GI fractions increased and there was a non-linear relationship between reductions of UHI and increasing fractions of GI. The maximum cooling effect was obtained in the center of the city. Implementation of GI

practices in urban areas substantially altered the surface energy balance by decreasing the storage heat and increasing latent heat during the day. The lower storage heat in urban areas during the day was the main driver in reducing UHI effects during the night. The storage heat was reduced during the day as the higher fractions of urban areas were replaced by vegetated surfaces. MF and MFAG showed higher cooling effect as compared to MSAG since MF and MFAG stored a lower storage heat during the day. The higher shade factor and LAI of vegetated patches/GI practices as compared urban surfaces would have led to even less radiation reaching the ground surface during the day and leading to lower storage heat. There were no substantial reductions of the UHI during the day as there was no substantial reductions in SH flux. However, the cooling benefits were localized and varied both temporally and spatially. MFAG was more effective in reducing UHI effects followed by MF and MSAG. The MSAG showed a warming effect during the day due to SH flux because of lower LAI and shade factor as compared to MF and MFAG. Lower LAI would have allowed more solar radiation to reach the surface, and given the very dry soil conditions during the heatwave, more solar radiation reaching the surface would have enhanced SH, and consequently led to a slight warming effect. Therefore, the use of MFAG and MF were more effective in mitigating UHI effects. In addition, GI scenarios did not substantially change the wind direction but resulted in small reductions in wind speed, which intensified the cooling effects in the center of the city by the stagnation of cooler air as a result of GI implementation.

8.2 Conclusions

The WRF model is an effective modelling tool to investigate the effectiveness of different UHI mitigation strategies and impacts of urban expansion on the UHI during heatwaves. The city of Melbourne is already experiencing substantial UHI effects and these effects will increase in future due to urban expansion. Green and cool roofs showed potential in mitigating UHI effects and improving HTC particularly during the day while implementation of vegetated patches was effective during the night. Therefore, the combination of green/cool roofs with different vegetated patches would be optimal and effective mitigation strategies in mitigating UHI effects and improving HTC during both the day and night. Additionally, these combined mitigation strategies can provide some other benefits such as maintain diverse ecosystem, reducing air pollution, spaces for recreation activities.

8.3 Recommendations for Future Research

Finally, a number of important research questions and gaps for further study have arisen from this thesis. The following research gaps are recommended for future study:

1. The WRF model is sensitive to different physical parameterizations and this thesis used the default urban parameterization in the SLUCM model. Therefore, the sensitivity of the model to different urban parameterizations is recommended for future studies, to investigate if results are consistent when different parameterizations are used. There are other two UCM options available in the WRF model such as BEM and BEP. The sensitivity of the WRF model to BEM and BEP should also be investigated in future studies.

2. This thesis examined the impacts of future urban expansion on the UHI and effectiveness of UHI mitigation strategies during heatwaves without considering the effects of future climate change. Therefore, further studies should be carried out including the effect of future climate change.
3. The effectiveness of green and cool roofs examined based on current urban scenarios. Further investigation can be conducted for future urban expansion scenarios considering the effects of future climate change. There is also scope to investigate the potential of cool roads and walls (whitening surface/increasing albedo) in reducing UHI effects.
4. Although GI offers a number of vegetation types, the thesis only evaluates the effectiveness of green roofs, MF, MFAG and MSAG. Further GI practices such as green walls can be assessed using other modelling tools or introducing new parameterization scheme in the WRF model.
5. This study examined the role of green and cool roofs, and MF, MFAG and MSAG separately. Future studies should examine the combined implementation of these strategies to investigate the maximum possible benefits during both the day and night, and any possible interactions between the different strategies.

References

- Ahmad, S. and Hashim, N. M. (2007). Effects of soil moisture on urban heat island occurrences: case of Selangor, Malaysia. *Humanity & Social Sciences Journal*, 2(2), 132-138.
- Akbari, H. (2008). Evolution of cool-roof standards in the United States. *Advances in Building Energy Research*, 2 (1), 1-32.
- Akbari, H., Pomerantz, M. and Taha, H. (2001). Cool surfaces and shade trees to reduce energy use and improve air quality in urban areas. *Solar Energy*, 70(3), 295-310.
- Arakawa, A. (2004). The cumulus parameterization problem: Past, present, and future. *Journal of Climate*, 17(13), 2493-2525.
- Argüeso, D., Evans, J. P., Fita, L. and Bormann, K. J. (2014). Temperature response to future urbanization and climate change. *Climate dynamics*, 42(7-8), 2183-2199.
- Argüeso, D., Hidalgo-Muñoz, J. M., Gámiz-Fortis, S. R., Esteban-Parra, M. J. and Castro-Díez, Y. (2012). Evaluation of WRF mean and extreme precipitation over Spain: present climate (1970–99). *Journal of Climate*, 25(14), 4883-4897.
- Arnfield, A. J. (2003). Two decades of urban climate research: a review of turbulence, exchanges of energy and water, and the urban heat island. *International journal of climatology*, 23(1), 1-26.
- Atkinson, B. (2003). Numerical modelling of urban heat-island intensity. *Boundary-layer meteorology*, 109(3), 285-310.

- Australian Bureau of Statistics (2011). Main Features, 3218.0 - Regional Population Growth, Australia. Available from: <http://www.abs.gov.au/ausstats/abs@.nsf/Products/3218.0~2011~Main+Features~Main+Features?OpenDocument>
- Authority Greater London (2008). Living Roofs and Walls: Technical Report Supporting London Plan Policy. *London, UK*.
- Baker, L. A., Brazel, A. J., Selover, N., Martin, C., McIntyre, N., Steiner, F. R., Musacchio, L. (2002). Urbanization and warming of Phoenix (Arizona, USA): Impacts, feedbacks and mitigation. *Urban ecosystems*, 6(3), 183-203.
- Banting, D., Doshi, H., Li, J. and Missios, P. (2005). Report on the environmental benefits and costs of green roof technology for the city of Toronto.
- Baumüller, J., Baumüller, N. (2011). Climate change adaptation strategies in German regions and cities: a review. European Conference on Applications of Meteorology, EMS Annual Meeting, 12-16 September, viewed 3 March 2012: <http://www.presentations.copernicus.org/EMS2011-706_presentation.pdf>.
- Berry, R., Livesley, S. J. and Aye, L. (2013). Tree canopy shade impacts on solar irradiance received by building walls and their surface temperature. *Building and Environment*, 69, 91-100.
- Bornstein, R. and Lin, Q. (2000). Urban heat islands and summertime convective thunderstorms in Atlanta: Three case studies. *Atmospheric Environment*, 34(3), 507-516.

- Boschat, G., Pezza, A., Simmonds, I., Perkins, S., Cowan, T. and Purich, A. (2015). Large scale and sub-regional connections in the lead up to summer heat wave and extreme rainfall events in eastern Australia. *Climate dynamics*, 44(7-8), 1823-1840.
- Bowler, D. E., Buyung-Ali, L., Knight, T. M. and Pullin, A. S. (2010). Urban greening to cool towns and cities: A systematic review of the empirical evidence. *Landscape and Urban Planning*, 97(3), 147-155.
- Ca, V. T., Asaeda, T. and Abu, E. M. (1998). Reductions in air conditioning energy caused by a nearby park. *Energy and Buildings*, 29(1), 83-92.
- Cao, X., Onishi, A., Chen, J. and Imura, H. (2010). Quantifying the cool island intensity of urban parks using ASTER and IKONOS data. *Landscape and Urban Planning*, 96(4), 224-231.
- Chandler, T. (1965). *The Climate of London*, Hutchinson & Co. Ltd., London, 1965.
- Chen, F. and Dudhia, J. (2001). Coupling an advanced land surface–hydrology model with the Penn State–NCAR MM5 modeling system. Part II: Preliminary model validation. *Monthly weather review*, 129(4), 587-604.
- Chen, F., Kusaka, H., Bornstein, R., Ching, J., Grimmond, C., Grossman-Clarke, S., Miao, S. (2011). The integrated WRF/urban modelling system: development, evaluation, and applications to urban environmental problems. *International journal of climatology*, 31(2), 273-288.
- Chen, L. and Frauenfeld, O. W. (2016). Impacts of urbanization on future climate in China. *Climate dynamics*, 47(1-2), 345-357.

- Cheng, C. K. and Chan, J. C. (2012). Impacts of land use changes and synoptic forcing on the seasonal climate over the Pearl River Delta of China. *Atmospheric Environment*, 60, 25-36.
- Christen, A. and Vogt, R. (2004). Energy and radiation balance of a central European city. *International journal of climatology*, 24(11), 1395-1421.
- Coates, L., Haynes, K., O'Brien, J., McAneney, J. and De Oliveira, F. D. (2014). Exploring 167 years of vulnerability: An examination of extreme heat events in Australia 1844–2010. *Environmental Science & Policy*, 42, 33-44.
- Collier, C. G. (2006). The impact of urban areas on weather. *Quarterly Journal of the Royal Meteorological Society*, 132(614), 1-25.
- Coughlan, M. (1983). A comparative climatology of blocking action in the two hemispheres. *Aust. Meteor. Mag.*, 31, 3-13.
- Coutts, A. M., Beringer, J. and Tapper, N. J. (2007). Impact of increasing urban density on local climate: spatial and temporal variations in the surface energy balance in Melbourne, Australia. *Journal of Applied Meteorology and Climatology*, 46(4), 477-493.
- Coutts, A. M., Beringer, J. and Tapper, N. J. (2008). Investigating the climatic impact of urban planning strategies through the use of regional climate modelling: a case study for Melbourne, Australia. *International Journal of Climatology: A Journal of the Royal Meteorological Society*, 28(14), 1943-1957.
- Coutts, A. M., White, E. C., Tapper, N. J., Beringer, J. and Livesley, S. J. (2016). Temperature and human thermal comfort effects of street trees across three

- contrasting street canyon environments. *Theoretical and applied climatology*, 124(1-2), 55-68.
- Cowan, T., Purich, A., Perkins, S., Pezza, A., Bosch, G. and Sadler, K. (2014). More frequent, longer, and hotter heat waves for Australia in the twenty-first century. *Journal of Climate*, 27(15), 5851-5871.
- Craig, K. and Bornstein, R. (2001). *Urbanisation of numerical meso-scale models*. Paper presented at the workshop on urban boundary layer parameterisations.
- Dee, D. P., Uppala, S. M., Simmons, A., Berrisford, P., Poli, P., Kobayashi, S., . . . Bauer, D. P. (2011). The ERA-Interim reanalysis: Configuration and performance of the data assimilation system. *Quarterly Journal of the Royal Meteorological Society*, 137(656), 553-597.
- Department of Human Services (2009). January 2009 Heatwave in Victoria: an Assessment of Health Impacts, Victorian Government www.health.vic.gov.au
[http://docs.health.vic.gov.au/docs/doc/F7EEA4050981101ACA257AD80074AE8B/\\$FILE/heat_health_impact_rpt_Vic2009.pdf](http://docs.health.vic.gov.au/docs/doc/F7EEA4050981101ACA257AD80074AE8B/$FILE/heat_health_impact_rpt_Vic2009.pdf)
- Dudhia, J. (2014). A history of mesoscale model development. *Asia-Pacific Journal of Atmospheric Sciences*, 50(1), 121-131.
- Easterling, D. R., Horton, B., Jones, P. D., Peterson, T. C., Karl, T. R., Parker, D. E., . . . Jamason, P. (1997). Maximum and minimum temperature trends for the globe. *Science*, 277(5324), 364-367.
- Eliasson, I. (1996). Urban nocturnal temperatures, street geometry and land use. *Atmospheric Environment*, 30(3), 379-392.

- Englart, J. (2015). Heatwaves and Victoria's Heat Health Alert Warning System. (4 January 2015) Climate Action Moreland blog, viewed 9 February 2015. <http://climateactionmoreland.org/2015/01/04/heatwaves-and-victorias-heat-health-alert-warning-system/>
- Evans, J. P., Ekström, M. and Ji, F. (2012). Evaluating the performance of a WRF physics ensemble over South-East Australia. *Climate dynamics*, 39(6), 1241-1258.
- Fahmy, M. and Sharples, S. (2009). On the development of an urban passive thermal comfort system in Cairo, Egypt. *Building and Environment*, 44(9), 1907-1916.
- Fallmann, J., Emeis, S. and Suppan, P. (2014). Mitigation of urban heat stress—a modelling case study for the area of Stuttgart. *DIE ERDE—Journal of the Geographical Society of Berlin*, 144(3-4), 202-216.
- Fintikakis, N., Gaitani, N., Santamouris, M., Assimakopoulos, M., Assimakopoulos, D., Fintikaki, M., . . . Katopodi, K. (2011). Bioclimatic design of open public spaces in the historic centre of Tirana, Albania. *Sustainable Cities and Society*, 1(1), 54-62.
- Foster, J., Lowe, A. and Winkelman, S. (2011). The value of green infrastructure for urban climate adaptation. *Center for Clean Air Policy*, 750, 1-52.
- Gago, E. J., J., R., R., P.-T. and Javier, G. (2013). *The city and urban heat islands: A review of strategies to mitigate adverse effects* (Vol. 25).
- Gallo, K. P., Owen, T. W., Easterling, D. R. and Jamason, P. F. (1999). Temperature trends of the US historical climatology network based on satellite-designated land use/land cover. *Journal of Climate*, 12(5), 1344-1348.

- Gartland, L. (2008). Heat islands. London: Sterling VA,: 215 p.
- Gedzelman, S., Austin, S., Cermak, R., Stefano, N., Partridge, S., Quesenberry, S. and Robinson, D. (2003). Mesoscale aspects of the urban heat island around New York City. *Theoretical and applied climatology*, 75(1-2), 29-42.
- Georgescu, M., Miguez-Macho, G., Steyaert, L. and Weaver, C. (2009). Climatic effects of 30 years of landscape change over the Greater Phoenix, Arizona, region: 1. Surface energy budget changes. *Journal of Geophysical Research: Atmospheres*, 114(D5).
- Georgi, N. J. and Zafiriadis, K. (2006). The impact of park trees on microclimate in urban areas. *Urban ecosystems*, 9(3), 195-209.
- Gesch, D. B., Verdin, K. L. and Greenlee, S. K. (1999). New land surface digital elevation model covers the Earth. *EOS, Transactions American Geophysical Union*, 80(6), 69-70.
- Golden, J. S. and Kaloush, K. E. (2006). Mesoscale and microscale evaluation of surface pavement impacts on the urban heat island effects. *The international journal of pavement engineering*, 7(1), 37-52.
- Grell, G. A., Dudhia, J. and Stauffer, D. R. (1994). A description of the fifth-generation Penn State/NCAR Mesoscale Model (MM5).
- Grossman-Clarke, S., Liu, Y., Zehnder, J. A. and Fast, J. D. (2008). Simulations of the urban planetary boundary layer in an arid metropolitan area. *Journal of Applied Meteorology and Climatology*, 47(3), 752-768.

- Grossman-Clarke, S., Zehnder, J. A., Loridan, T. and Grimmond, C. S. B. (2010). Contribution of land use changes to near-surface air temperatures during recent summer extreme heat events in the Phoenix metropolitan area. *Journal of Applied Meteorology and Climatology*, 49(8), 1649-1664.
- Gunawardena, K. R., Wells, M. J. and Kershaw, T. (2017). Utilising green and bluespace to mitigate urban heat island intensity. *Science of The Total Environment*, 584-585, 1040-1055. doi: <https://doi.org/10.1016/j.scitotenv.2017.01.158>
- Grunstein, R. (2013). Too hot to sleep? Here' s why. *The Conversation* (8 January 2013) Viewed 23 March 2014. <http://theconversation.com/too-hot-to-sleep-heres-why-11492>
- Hamdi, R. and Schayes, G. (2005). Validation of the Martilli's urban boundary layer scheme with measurements from two mid-latitude European cities. *Atmospheric Chemistry and Physics Discussions*, 5(4), 4257-4289.
- He, J., Liu, J., Zhuang, D., Zhang, W. and Liu, M. (2007). Assessing the effect of land use/land cover change on the change of urban heat island intensity. *Theoretical and applied climatology*, 90(3-4), 217-226.
- Heisler, G. M., Grimmond, S., Grant, R. H. and Souch, C. (1994). Investigation of the Influence of Chicago's Urban Forests on Wind and Air Temperature Within Residential Neighborhoods. *Chicago's Urban Forest Ecosystem: Results of the Chicago Urban Forest Climate Project*, 19.
- Howard, L. (1833). The climate of London, vols. I–III. *London: Harvey and Dorton*.

- Hoyano, A. (1988). Climatological uses of plants for solar control and the effects on the thermal environment of a building. *Energy and Buildings*, 11(1-3), 181-199.
- Hu, X.-M., Nielsen-Gammon, J. W. and Zhang, F. (2010). Evaluation of three planetary boundary layer schemes in the WRF model. *Journal of Applied Meteorology and Climatology*, 49(9), 1831-1844.
- Hutchinson, M. F., McKenney, D. W., Lawrence, K., Pedlar, J. H., Hopkinson, R. F., Milewska, E. and Papadopol, P. (2009). Development and testing of Canada-wide interpolated spatial models of daily minimum–maximum temperature and precipitation for 1961–2003. *Journal of Applied Meteorology and Climatology*, 48(4), 725-741.
- IPCC (2012). Managing the Risks of Extreme Events and Disasters to Advance Climate Change Adaptation. . A Special Report of Working Groups I and II of the Intergovernmental Panel on Climate Change. Field, C.B., Barros, V., Stocker, T.F., Qin, D., Dokken, D.J., Ebi, K.L.,Mastrandrea, M.D., Mach, K.J., Plattner, G-K., Allen, 100 S.K.,Tignor, M. and Midgley, P.M. (eds.). Cambridge University Press, Cambridge, UK, and New York, NY, USA, 582pp. http://www.ipcc.ch/publications_and_data/publications_and_data_reports.shtml#SREX.
- Jackson, T. L., Feddema, J. J., Oleson, K. W., Bonan, G. B. and Bauer, J. T. (2010). Parameterization of urban characteristics for global climate modeling. *Annals of the Association of American Geographers*, 100(4), 848-865.

- Jáuregui, E. (2005). Possible impact of urbanization on the thermal climate of some large cities in México. *Atmósfera*, 18(4), 249-252.
- Jin, M. and Shepherd, J. M. (2005). Inclusion of urban landscape in a climate model: How can satellite data help? *Bulletin of the American meteorological Society*, 86(5), 681-690.
- Kala, J., Andrys, J., Lyons, T. J., Foster, I. J. and Evans, B. J. (2015). Sensitivity of WRF to driving data and physics options on a seasonal time-scale for the southwest of Western Australia. *Climate dynamics*, 44(3-4), 633-659.
- Kalnay, E. and Cai, M. (2003). Impact of urbanization and land-use change on climate. *Nature*, 423(6939), 528.
- Keating, A. and Handmer, J. (2013). Future potential losses from extremes under climate change: the case of Victoria, Australia. *VCCCAR Project: Framing Adaptation in the Victorian Context, Working Paper*.
- Klaić, Z. B., Nitis, T., Kos, I. and Moussiopoulos, N. (2002). Modification of the local winds due to hypothetical urbanization of the Zagreb surroundings. *Meteorology and Atmospheric Physics*, 79(1-2), 1-12.
- Kusaka, H., Chen, F. and Tewari, M. (2006). *Impact of using the urban canopy model on the simulation of the heat island of Tokyo*. Paper presented at the Extended Abstracts, Sixth Symp. on the Urban Environment, Atlanta, GA, Amer. Meteor. Soc. J.
- Kusaka, H., Chen, F., Tewari, M., Dudhia, J., Gill, D. O., Duda, M. G., . . . Miya, Y. (2012). Numerical simulation of urban heat island effect by the WRF model with

- 4-km grid increment: An inter-comparison study between the urban canopy model and slab model. *Journal of the Meteorological Society of Japan. Ser. II*, 90, 33-45.
- Kusaka, H. and Kimura, F. (2004). Coupling a single-layer urban canopy model with a simple atmospheric model: Impact on urban heat island simulation for an idealized case. *Journal of the Meteorological Society of Japan. Ser. II*, 82(1), 67-80.
- Kusaka, H., Kondo, H., Kikegawa, Y. and Kimura, F. (2001). A simple single-layer urban canopy model for atmospheric models: Comparison with multi-layer and slab models. *Boundary-layer meteorology*, 101(3), 329-358.
- Lamprey, B., Barron, E. and Pollard, D. (2005). Impacts of agriculture and urbanization on the climate of the Northeastern United States. *Global and Planetary Change*, 49(3-4), 203-221.
- Lee, H.-Y. (1993). An application of NOAA AVHRR thermal data to the study of urban heat islands. *Atmospheric Environment. Part B. Urban Atmosphere*, 27(1), 1-13.
- Lee, H., Holst, J. and Mayer, H. (2013). Modification of human-biometeorologically significant radiant flux densities by shading as local method to mitigate heat stress in summer within urban street canyons. *Advances in Meteorology*, 2013.
- Levinson, R., Berdahl, P., Berhe, A. A. and Akbari, H. (2005). Effects of soiling and cleaning on the reflectance and solar heat gain of a light-colored roofing membrane. *Atmospheric Environment*, 39(40), 7807-7824.
- Li, D. and Bou-Zeid, E. (2013). Synergistic Interactions between Urban Heat Islands and Heat Waves: The Impact in Cities Is Larger than the Sum of Its Parts. *Journal of*

Applied Meteorology and Climatology, 52(9), 2051-2064. doi: 10.1175/jamc-d-13-02.1

Li, D., Bou-Zeid, E. and Oppenheimer, M. (2014). The effectiveness of cool and green roofs as urban heat island mitigation strategies. *Environmental Research Letters*, 9(5), 055002.

Li, D., Sun, T., Liu, M., Yang, L., Wang, L. and Gao, Z. (2015). Contrasting responses of urban and rural surface energy budgets to heat waves explain synergies between urban heat islands and heat waves. *Environmental Research Letters*, 10(5), 054009.

Lim, K.-S. S. and Hong, S.-Y. (2010). Development of an effective double-moment cloud microphysics scheme with prognostic cloud condensation nuclei (CCN) for weather and climate models. *Monthly weather review*, 138(5), 1587-1612.

Lin, B.-S. and Lin, Y.-J. (2010). Cooling effect of shade trees with different characteristics in a subtropical urban park. *HortScience*, 45(1), 83-86.

Lin, C.-Y., Chen, F., Huang, J., Chen, W.-C., Liou, Y.-A., Chen, W.-N. and Liu, S.-C. (2008). Urban heat island effect and its impact on boundary layer development and land–sea circulation over northern Taiwan. *Atmospheric Environment*, 42(22), 5635-5649.

Liu, X., Tian, G., Feng, J., Ma, B., Wang, J. and Kong, L. (2018). Modeling the Warming Impact of Urban Land Expansion on Hot Weather Using the Weather Research and Forecasting Model: A Case Study of Beijing, China. *Advances in Atmospheric Sciences*, 35(6), 723-736.

- Liverpool City Council (2012). Liverpool City Council green infrastructure strategy, Liverpool City Council, Liverpool, viewed 3 March 2012: <<http://www.greeninfrastructurenw.co.uk/liverpool/>>.
- Lowry, W. P. (1998). Urban effects on precipitation amount. *Progress in Physical Geography*, 22(4), 477-520.
- Manfred, K., Marco, S., Friedrich, W. G., Michael, L., Vera, L. d. A. P. and Sergio, T. (2002). Green roofs in temperate climates and in the hot-humid tropics—far beyond the aesthetics. *Environmental management and health*, 13(4), 382-391.
- Manley, G. (1958). On the frequency of snowfall in metropolitan England. *Quarterly Journal of the Royal Meteorological Society*, 84(359), 70-72.
- Marshall, A., Hudson, D., Wheeler, M., Alves, O., Hendon, H., Pook, M. and Risbey, J. (2014). Intra-seasonal drivers of extreme heat over Australia in observations and POAMA-2. *Climate dynamics*, 43(7-8), 1915-1937.
- Martilli, A., Clappier, A. and Rotach, M. W. (2002). An urban surface exchange parameterisation for mesoscale models. *Boundary-layer meteorology*, 104(2), 261-304.
- Masson, V. (2006). Urban surface modeling and the meso-scale impact of cities. *Theoretical and applied climatology*, 84(1-3), 35-45.
- McPherson, G., Simpson, J. R., Peper, P. J., Maco, S. E. and Xiao, Q. (2005). Municipal forest benefits and costs in five US cities. *Journal of forestry*, 103(8), 411-416.

- Mellon, M. T., Jakosky, B. M., Kieffer, H. H. and Christensen, P. R. (2000). High-resolution thermal inertia mapping from the Mars global surveyor thermal emission spectrometer. *Icarus*, 148(2), 437-455.
- Mesinger, F. and Arakawa, A. (1976). Numerical methods used in atmospheric models.
- Morini, E., Touchaei, A. G., Castellani, B., Rossi, F. and Cotana, F. (2016). The impact of albedo increase to mitigate the urban heat island in Terni (Italy) using the WRF model. *Sustainability*, 8(10), 999.
- Morris, C. and Simmonds, I. (2000). Associations between varying magnitudes of the urban heat island and the synoptic climatology in Melbourne, Australia. *International Journal of Climatology: A Journal of the Royal Meteorological Society*, 20(15), 1931-1954.
- Morris, C., Simmonds, I. and Plummer, N. (2001). Quantification of the influences of wind and cloud on the nocturnal urban heat island of a large city. *Journal of applied meteorology*, 40(2), 169-182.
- Morris, K. I., Chan, A., Morris, K. J. K., Ooi, M. C., Oozeer, M. Y., Abakr, Y. A., Al-Qrimli, H. F. (2017). Impact of urbanization level on the interactions of urban area, the urban climate, and human thermal comfort. *Applied geography*, 79, 50-72.
- Myrup, L. O. (1969). A numerical model of the urban heat island. *Journal of applied meteorology*, 8(6), 908-918.
- Nairn, J. and Fawcett, R. (2011). Defining heatwaves: heatwave defined as a heat-impact event servicing all. *Europe*, 220, 224.

- Nicholls, N., Skinner, C., Loughnan, M. and Tapper, N. (2008). A simple heat alert system for Melbourne, Australia. *International journal of biometeorology*, 52(5), 375-384.
- Oberndorfer, E., Lundholm, J., Bass, B., Coffman, R. R., Doshi, H., Dunnett, N., Rowe, B. (2007). Green roofs as urban ecosystems: ecological structures, functions, and services. *BioScience*, 57(10), 823-833.
- Oke, R. (1997). Urban climate and global environmental change. *Applied climatology*, 273-287.
- Oke, T. (1987). Boundary layer climates. 2nd. *Methuen*, 289p, 548.
- Oke, T. R. (1982). The energetic basis of the urban heat island. *Quarterly Journal of the Royal Meteorological Society*, 108(455), 1-24.
- Ooka, R. (2007). Recent development of assessment tools for urban climate and heat-island investigation especially based on experiences in Japan. *International Journal of Climatology: A Journal of the Royal Meteorological Society*, 27(14), 1919-1930.
- Parker, J. (1983). The effectiveness of vegetation on residential cooling. *Passive Solar Journal*, 2(2), 123-132.
- Pearlmutter, D., Bitan, A. and Berliner, P. (1999). Microclimatic analysis of “compact” urban canyons in an arid zone. *Atmospheric Environment*, 33(24-25), 4143-4150.

- Perkins, S. E. (2015). A review on the scientific understanding of heatwaves—Their measurement, driving mechanisms, and changes at the global scale. *Atmospheric Research*, 164, 242-267.
- Pezza, A. B., Van Rensch, P. and Cai, W. (2012). Severe heat waves in Southern Australia: synoptic climatology and large scale connections. *Climate dynamics*, 38(1-2), 209-224.
- Philandras, C., Metaxas, D. and Nastos, P. T. (1999). Climate variability and urbanization in Athens. *Theoretical and applied climatology*, 63(1-2), 65-72.
- Pino, D., de Arellano, J. V.-G., Comeron, A. and Rocadenbosch, F. (2004). The boundary layer growth in an urban area. *Science of The Total Environment*, 334, 207-213.
- Piringer, M., Grimmond, C., Joffre, S., Mestayer, P., Middleton, D., Rotach, M., Guilloteau, E. (2002). Investigating the surface energy balance in urban areas—recent advances and future needs. *Water, Air and Soil Pollution: Focus*, 2(5-6), 1-16.
- Population Reference Bureau (2005). World Population Data Sheet. Population Reference Bureau.
- Rankin, D. (1959). Mortality associated with heat wave conditions in the Melbourne Metropolitan area, January and February 1959. *Australian Meteorological Magazine*, 26, 96-98.
- Rauscher, S. A., Ringler, T. D., Skamarock, W. C. and Mirin, A. A. (2013). Exploring a global multiresolution modeling approach using aquaplanet simulations. *Journal of Climate*, 26(8), 2432-2452.

- Razzaghmanesh, M., Beecham, S. and Salemi, T. (2016). The role of green roofs in mitigating Urban Heat Island effects in the metropolitan area of Adelaide, South Australia. *Urban Forestry & Urban Greening*, 15, 89-102.
- Razzaghmanesh, M. and Razzaghmanesh, M. (2017). Thermal performance investigation of a living wall in a dry climate of Australia. *Building and Environment*, 112, 45-62.
- Reeves, J., Foelz, C., Grace, P., Best, P., Marcussen, T., Mushtaq, S., Ahmed, I. (2010). *Impacts and adaptation response of infrastructure and communities to heatwaves: the southern Australian experience of 2009*: National Climate Change Adaptation Research Facility.
- Rizwan, A. M., Dennis, L. Y. and Chunho, L. (2008). A review on the generation, determination and mitigation of Urban Heat Island. *Journal of Environmental Sciences*, 20(1), 120-128.
- Robine, J.-M., Cheung, S. L. K., Le Roy, S., Van Oyen, H., Griffiths, C., Michel, J.-P. and Herrmann, F. R. (2008). Death toll exceeded 70,000 in Europe during the summer of 2003. *Comptes rendus biologiques*, 331(2), 171-178.
- Romero, H., Ihl, M., Rivera, A., Zalazar, P. and Azocar, P. (1999). Rapid urban growth, land-use changes and air pollution in Santiago, Chile. *Atmospheric Environment*, 33(24-25), 4039-4047.
- Rosenfeld, A. H., Akbari, H., Bretz, S., Fishman, B. L., Kurn, D. M., Sailor, D. and Taha, H. (1995). Mitigation of urban heat islands: materials, utility programs, updates. *Energy and Buildings*, 22(3), 255-265.

- Rosenfeld, A. H., Akbari, H., Romm, J. J. and Pomerantz, M. (1998). Cool communities: strategies for heat island mitigation and smog reduction. *Energy and Buildings*, 28(1), 51-62.
- Rosenzweig, C., Solecki, W. and Slosberg, R. (2006). Mitigating New York City's heat island effect with urban forestry, living roofs and light surfaces. New York City Regional Heat Island Initiative, *Final Report 06-06 New York State Energy Research and Development Authority*.
- Sailor, D. J. (1995). Simulated urban climate response to modifications in surface albedo and vegetative cover. *Journal of applied meteorology*, 34(7), 1694-1704.
- Sailor, D. J. and Dietsch, N. (2007). The urban heat island mitigation impact screening tool (MIST). *Environmental Modelling & Software*, 22(10), 1529-1541.
- Santamouris, M., Synnefa, A. and Karlessi, T. (2011). Using advanced cool materials in the urban built environment to mitigate heat islands and improve thermal comfort conditions. *Solar Energy*, 85(12), 3085-3102.
- Santamouris, M., Xirafi, F., Gaitani, N., Spanou, A., Saliari, M. and Vassilakopoulou, K. (2012). Improving the microclimate in a dense urban area using experimental and theoretical techniques-The case of Marousi, Athens. *International Journal of Ventilation*, 11(1), 1-16.
- Seth, A. and Giorgi, F. (1998). The effects of domain choice on summer precipitation simulation and sensitivity in a regional climate model. *Journal of Climate*, 11(10), 2698-2712.

- Sharma, A., Conry, P., Fernando, H., Hamlet, A. F., Hellmann, J. and Chen, F. (2016). Green and cool roofs to mitigate urban heat island effects in the Chicago metropolitan area: Evaluation with a regional climate model. *Environmental Research Letters*, 11(6), 064004.
- Shashua-Bar, L. and Hoffman, M. E. (2000). Vegetation as a climatic component in the design of an urban street: An empirical model for predicting the cooling effect of urban green areas with trees. *Energy and Buildings*, 31(3), 221-235.
- Shepherd, J. M. (2005). A review of current investigations of urban-induced rainfall and recommendations for the future. *Earth Interactions*, 9(12), 1-27.
- Sherwood, S. C. and Huber, M. (2010). An adaptability limit to climate change due to heat stress. *Proceedings of the National Academy of Sciences*, 107(21), 9552-9555.
- Skamarock, W., Klemp, J., Dudhia, J., Gill, D., Barker, D., Duda, M., Powers, J. (2008). A description of the advanced research WRF version 3. NCAR Technical Note, NCAR/TN\u2013475 STR, 123 pp.
- Skamarock, W. C., Klemp, J. B., Dudhia, J., Gill, D. O., Barker, D. M., Wang, W. and Powers, J. G. (2005). A description of the advanced research WRF version 2: National Center For Atmospheric Research Boulder Co Mesoscale and Microscale Meteorology Div.
- Smith, K. R. and Roebber, P. J. (2011). Green roof mitigation potential for a proxy future climate scenario in Chicago, Illinois. *Journal of Applied Meteorology and Climatology*, 50(3), 507-522.

- Solecki, W., Rosenzweig, C., Parshall, L., Pope, G., Clark, M., Cox, J. and Wiencke, M. (2005). *Mitigation of the heat island effect in urban New Jersey* (Vol. 6).
- Souch, C. and Souch, C. (1993). The effect of trees on summertime below canopy urban climates: a case study Bloomington, Indiana. *Journal of Arboriculture*, 19(5), 303-312.
- Spronken-Smith, R. A., Oke, T. R. and Lowry, W. P. (2000). Advection and the surface energy balance across an irrigated urban park. *International journal of climatology*, 20(9), 1033-1047.
- Steffen, W. L., Hughes, L. and Perkins, S. (2014). *Heatwaves: hotter, longer, more often*: Climate Council.
- Stegehuis, A., Vautard, R., Ciais, P., Teuling, A., Miralles, D. and Wild, M. (2015). An observation-constrained multi-physics WRF ensemble for simulating European mega heat waves. *Geoscientific Model Development*, 8(7), 2285-2298.
- Susca, T. (2012). Enhancement of life cycle assessment (LCA) methodology to include the effect of surface albedo on climate change: Comparing black and white roofs. *Environmental pollution*, 163, 48-54.
- Synnefa, A., Dandou, A., Santamouris, M., Tombrou, M. and Soulakellis, N. (2008). On the use of cool materials as a heat island mitigation strategy. *Journal of Applied Meteorology and Climatology*, 47(11), 2846-2856.
- Synnefa, A., Karlessi, T., Gaitani, N., Santamouris, M., Assimakopoulos, D. and Papakatsikas, C. (2011). Experimental testing of cool colored thin layer asphalt

- and estimation of its potential to improve the urban microclimate. *Building and Environment*, 46(1), 38-44.
- Synnefa, A., M, S. and I, L. (2006). A study of the thermal performance of reflective coatings for the urban environment. *Solar Energy*, 80(8), 968-981.
- Taha, H. (1996). Modeling impacts of increased urban vegetation on ozone air quality in the South Coast Air Basin. *Atmospheric Environment*, 30(20), 3423-3430.
- Takebayashi, H. and Moriyama, M. (2009). Study on the urban heat island mitigation effect achieved by converting to grass-covered parking. *Solar Energy*, 83(8), 1211-1223.
- Thompson, G., Field, P. R., Rasmussen, R. M. and Hall, W. D. (2008). Explicit forecasts of winter precipitation using an improved bulk microphysics scheme. Part II: Implementation of a new snow parameterization. *Monthly weather review*, 136(12), 5095-5115.
- Torok, S. J., Morris, C. J., Skinner, C. and Plummer, N. (2001). Urban heat island features of southeast Australian towns. *Australian Meteorological Magazine*, 50(1), 1-13.
- Touchaei, A. G., Akbari, H. and Tessum, C. W. (2016). Effect of increasing urban albedo on meteorology and air quality of Montreal (Canada)—Episodic simulation of heat wave in 2005. *Atmospheric Environment*, 132, 188-206.
- Tumanov, S., Stan-Sion, A., Lupu, A., Soci, C. and Oprea, C. (1999). Influences of the city of Bucharest on weather and climate parameters. *Atmospheric Environment*, 33(24-25), 4173-4183.

Unger, J., Sümeghy, Z. and Zoboki, J. (2001). Temperature cross-section features in an urban area. *Atmospheric Research*, 58(2), 117-127.

USEPA (2008). Reducing Urban Heat Islands: Compendium of Strategies: Green Roofs. Available from: <http://www.epa.gov/heatisld/resources/pdf/GreenRoofsCompendium.pdf>.

Victorian Auditor General's Office (2014). Heatwave Management: Reducing the Risk to Public Health. Report tabled in State Parliament 14 October 2014 <https://www.audit.vic.gov.au/sites/default/files/2017-07/20141014-Heatwave-Management.pdf>

Victorian Department of Human Services (2009). January 2009 heatwave in Victoria: an assessment of health impacts, by Services, Victorian Department of Human Services, Melbourne. viewed 3 March 2018. <https://www2.health.vic.gov.au/about/publications/researchandreports/January-2009-Heatwave-in-Victoria-an-Assessment-of-Health-Impacts>

Voogt, J. A. and Oke, T. R. (2003). Thermal remote sensing of urban climates. *Remote sensing of environment*, 86(3), 370-384.

Walko, R. L., Band, L. E., Baron, J., Kittel, T. G., Lammers, R., Lee, T. J., Tague, C. (2000). Coupled atmosphere–biophysics–hydrology models for environmental modeling. *Journal of applied meteorology*, 39(6), 931-944.

Wong, N. H., Chen, Y., Ong, C. L. and Sia, A. (2003). Investigation of thermal benefits of rooftop garden in the tropical environment. *Building and Environment*, 38(2), 261-270.

- Wong, N. H. and Yu, C. (2005). *Study of green areas and urban heat island in a tropical city* (Vol. 29).
- Yaghoobian, N., Kleissl, J. and Krayenhoff, E. S. (2010). Modeling the thermal effects of artificial turf on the urban environment. *Journal of Applied Meteorology and Climatology*, 49(3), 332-345.
- Yang, J., Wang, Z.-H., Chen, F., Miao, S., Tewari, M., Voogt, J. A. and Myint, S. (2015). Enhancing hydrologic modelling in the coupled weather research and forecasting–urban modelling system. *Boundary-layer meteorology*, 155(1), 87-109.
- Yang, L., Niyogi, D., Tewari, M., Aliaga, D., Chen, F., Tian, F. and Ni, G. (2016). Contrasting impacts of urban forms on the future thermal environment: example of Beijing metropolitan area. *Environmental Research Letters*, 11(3), 034018.
- Yu, C. and Hien, W. N. (2006). Thermal benefits of city parks. *Energy and Buildings*, 38(2), 105-120.
- Zhou, Y. and Shepherd, J. M. (2010). Atlanta’s urban heat island under extreme heat conditions and potential mitigation strategies. *Natural Hazards*, 52(3), 639-668.